# PHOSPHORUS-CONTAINING POLYMERS, THEIR BLENDS, AND HYBRID NANOCOMPOSITES WITH POLY(HYDROXY ETHER), METAL CHLORIDES, AND SILICA COLLOIDS

by

Sheng Wang

Dissertation submitted to the Faculty of the

Virginia Polytechnic Institute and State University

in partial fulfillment of the requirements for the degree of

doctor of philosophy

in

Chemistry

APPROVED:

Dr. James E. McGrath, Chairman

Dr. David G. I. Kingston

Dr. Gary L. Long

Dr. Judy S. Riffle

Dr. James P. Wightman

March 06, 2000

Blacksburg, Virginia

Keywords: Poly(arylene ether), Phosphonyl, Miscibility, Polymer Blend, Hydrogen Bonding, Vinyl Ester, Nanocomposites

# PHOSPHORUS-CONTAINING POLYMERS, THEIR BLENDS, AND HYBRID NANOCOMPOSITES WITH POLY(HYDROXY ETHERS), METAL CHLORIDES, AND SILICA COLLOIDS

by

Sheng Wang
Dr. James E. McGrath, Committee Chairman
Chemistry

(Abstract)

Phosphorus-containing high performance polymers have been extensively studied during the last 10 years. These materials are of interest for a variety of optical and fire resistant properties, as well as for their ability to complex with the inorganic salts. This dissertation has focused on the nature of the phosphonyl group interactions with hydroxyl containing polymers, such as the poly(hydroxy ether)s. These may be considered linear models of epoxy resins and are also closely related to dimethacrylate (vinyl ester) matrix resins that are important for composite systems. It has been shown that bisphenol A poly(arylene ether phosphine oxide/sulfone) homo- or statistical copolymers are miscible with a bisphenol A-epichlorohydrin based poly(hydroxy ethers) (PHE), as shown by dynamic mechanical analysis (DMA) and differential scanning calorimetry (DSC), infrared spectroscopy and , solid state cross polarization-magic angle spinning nuclear magnetic resonance (CP-MAS). These measurements illustrate the strong hydrogen bonding between the phosphonyl groups of the copolymers and the pendent hydroxyl groups of the PHE as the miscibility inducing mechanism. Complete miscibility at all blend compositions was achieved with as little as 20 mole% of phosphine oxide units in the poly(arylene ether) copolymer. Replacement of the bisphenol A moiety by other diphenols, such as hydroquinone, hexafluorobisphenol A and biphenol did not significantly affect blend miscibilities. Miscible polymer blends with PHE were also made by blending poly(arylene thioether phosphine oxide), and fully cyclized phosphine oxide containing polyimides based on (prepared from 2,2'-bis[4-(3,4-dicarboxyphenoxy)phenyl]propane dianhydride (BPADA) and bis(*m*-aminophenyl) methyl phosphine oxide (DAMPO)) or bis(*m*-aminophenyl) phenyl phosphine oxide).

Additional research has focused on the influence of these materials on the property

characteristics of vinyl ester matrix resins and has shown that the concentration of phosphonyl groups controls the homogeneity of both oligomers and the resulting networks. Scanning electron microscopy (SEM), transmission electron microscopy (TEM), and fracture toughness measurements further confirmed the qualitative observations.

Metal salts, such as $CoCl_2$ and $CuCl_2$ had earlier been demonstrated to form complexes/nanocomposites with phosphorus-containing poly(arylene ethers). It has been possible to prepare transparent films with 100 mol% of metal chlorides, based upon the phosphonyl groups. The films are transparent, unlike the opaque polysulfone control systems. FTIR results suggested the formation of inorganic salt and polymer complexes at low concentrations. TEM showed homogeneous morphology at low concentrations and excellent dispersion even at high mole % of salts. Cobalt materials reinforce the basic poly(arylene ether)s to provide higher modulus values and influence positively the char yield generated after TGA experiments in air. The cobalt salt/BPADA-DAMPO polyimide composites also yield transparent films, implying very small dimensions.

Silica-polymer nanocomposites were also produced by mixing commercial silica colloid/N,N-dimethylacetamide (DMAc) fine dispersions (~ 12 nm) with bisphenol A poly(arylene ether phenyl phosphine oxide). The dry films produced by solution casting are transparent and silica colloids are evenly dispersed (~ 12 nm) into the polymer matrix as shown by TEM. These nanocomposites increased char yield compared with the polymer control, suggesting their fire retardant character. In comparison, the silica/polysulfone hybrid films prepared by the same methods were opaque and the char yield was not improved. This different phase behavior has been explained to be due to the hydrogen bonding between phosphonyl groups and silanol hydroxyl groups on the surface of the nanosilica.

ACKNOWLEDGEMENTS

I would like to take this opportunity to express my gratitude to my research advisor, Dr. James E. McGrath, for his guidance, inspiration and encouragement throughout the work. Throughout my education at Virginia Tech have I benefited not only from his profound knowledge, enormous enthusiasm, and keen insight in polymer science and technology but also his wonderful personality. I would also like to sincerely thank my committee members Dr. D. G. I. Kingston, Dr. G. Long, Dr. J. S. Riffle, Dr. J. P. Wightman for their knowledge and advice. Special thanks to Dr. J. S. Riffle for providing me an opportunity to take her course entitled Communication Skills and Methods of Presentation and always helping me improve my presentation skills. Special gratitude is due to Dr. A. R. Shultz for his guidance and discussions. He has also greatly helped me in the preparation of manuscripts, both with regard to language and techniques.

I would also like to acknowledge the invaluable assistance of Mr. Frank Cromer (SEM and XPS), Mr. Tom Glass (NMR), and Mr. Steve McCartney (TEM).

Many thanks go to my former and present colleagues at Virginia Tech for their assistance. I deeply appreciate the help from Drs. Isaac Farr, Qing Ji, Yongning Liu, Sue Mecham, M. Sankarapandian, H. K. Shobha, Biao Tan, Charles Tchatchoua, Feng Wang, Lance Wang, Jim Yang, and Hong Zhuang. I also enjoyed working and discussing with my fellow graduate students Debi Dunson, Nazan Gunduz, Mike Hickner, William Harris, Jeff Mecham, and Dave Polk. Special thanks to Dr. Hong Zhuang for her generous help whenever I needed it.

Special thanks are due to our secretarial group, Laurie Good, Esther Brann and Millie Ryan for their help over the years.

I would like to thank my high school chemistry teachers, Mr. Yuanyu Li and Mr. Hanmin Xie for initiating my interest in chemistry, and my M. S. advisor Prof. Guanghua Xie for nurturing my interest in polymer science.

Finally, I would like to thank my family. My parents, Mr. Shuhuan Wang and Ms. Taozhi Liu installed in me the value of perseverance and of being responsible. My brother Shengbin

and sister Qiaoping are always a source of love and help. My cousin Ms. Ailing Xia and her family always helped me make crucial decisions during difficult times. They act not only as my relatives but also good friends. Many thanks are due to my mother-in-law, Prof. Yinlan Hou, for her help in taking care of my daughter, which makes it possible for me to focus on my Ph.D. study. My wife Xinxin and my daughter Wendi are always my source of energy and love. Their encouragement and patience has enabled me to pursue my career through the successful completion of this thesis.

# Table of Contents

# List of Tables

# List of Schemes

# List of Figures

List of Abbreviations

| | |
|---|---|
| APTEOS | (3-aminopropyl)triethoxysilane |
| BFPMPO | Bis(4-fluorophenyl)methyl phosphine oxide |
| BFPPO | Bis(4-fluorophenyl)phenyl phosphine oxide |
| BHPA | 4,4′-bis(4-hydroxyphenyl)-pentanoic acid |
| BP | biphenol |
| BP-PEPO | Biphenol poly(arylene ether phenyl phosphine oxide) |
| BPA | Bisphenol A |
| BPA-PEPO | Bisphenol A poly(arylene ether phenyl phosphine oxide) |
| CHP | 1-cyclohexyl-2-pyrrolidinone |
| BPADA | 2,2'-bis[4-(3,4-dicarboxyphenoxy)phenyl]propane dianhydride (BPADA) |
| BPADA-DAMPO | Polyimide prepared from BPADA and DAMPO |
| BPADA-DAPPO | Polyimide prepared from BPADA and DAPPO |
| BPADA-*m*-PDA | Polyimide prepared from BPADA and *m*-PDA |
| DAMPO | Bis(*m*-aminophenyl)methyl phosphine oxide |
| DAPPO | Bis(*m*-aminophenyl)phenyl phosphine oxide |
| DCC | N-dicylcohexylcarbodiimide |
| DCDPS | 4,4′-dichlorodiphenyl sulfone |
| DFDPS | 4,4′-difluorodiphenyl sulfone |
| DMAc | N,N-dimethylacetamide |
| DMF | N,N-dimethylformamide |
| DMSO | Dimethyl sulfoxide |
| DPS | Diphenyl sulfone |
| EMA | ethyl methacrylate |
| ERL-4221® (ECHMECHC) | 3,4-epoxycyclohexylmethyl-3,4-epoxycyclohexyl carboxylate |
| HFBPA | Hexafluorobisphenol A |
| HFBPA-PEPO | Hexafluorobisphenol A poly(arylene ether phenyl phosphine oxide) |
| HQ | Hydroquinone |
| IPN | Interpenetrating network |
| LCST | Lower critical solution temperature |
| UCST | Upper critical solution temperature |
| NMP | N-methyl pyrrolidone (NMP) |
| PAMAM | Poly(aminoamine) |

| | |
|---|---|
| *m*-PDA | Meta-phenylene diamine |
| PAPO | Poly(4,4′-diphenylphenylphosphine oxide) |
| PcM | Metallophthalocyanine |
| *m*-PDA | Meta-phenylene diamine |
| PEOx | Poly(ethyl oxazoline) |
| PDMAc | Poly(N,N-dimethylacrylamide) |
| PDMS | Polydimethylsiloxane |
| PEGDA | Poly(ethylene glycol) |
| PEO | Poly(ethylene oxide) |
| PEPO | Poly(arylene ether phosphine oxide) |
| PI | Polyisoprene |
| PMDA | Pyromellitic dianhydride |
| PMMA | Poly(methyl methacrylate) |
| PS | Polystyrene |
| PSVBDEP | Poly(styrene-*stat*-4-vinyl benzenephosphonic acid diester) |
| PVC | Poly(vinyl chloride) |
| PVPh | Poly(*p*-vinylphenol) or poly(4-hydroxyl styrene) |
| SS-PTPO | Thiodithiophenol poly(arylene thioether phenyl phosphine oxide) |
| TEA | Triethylamine |
| TEOS | Tetraethoxysilane |
| TEP | Triethyl phosphate |
| Udel® | Bisphenol A polysufone |
| Ultem® | Polyimide based on BPADA-*m*-PDA |
| VE | Vinyl ester |
| Victrex® | Poly(ether sulfone) |

# 1 Literature Review

## *1.1 Synthesis and Characterization of Poly(arylene ether sulfone)s*

### 1.1.1 Introduction

Poly(arylene ethers)s are a family of high performance engineering thermoplastic materials with high glass transition temperature, high thermal stability, good mechanical properties, and excellent resistance to hydrolysis and oxidation.[1,2,3,4,5,6,7,8,9,10,11] Their outstanding properties have resulted in several important commercial sulfone or ketone containing products, such as bisphenol A polysulfone, Udel® (BP-Amoco); poly(ether sulfone), Victrex® (ICI); poly(arylene ether ether ketone) (PEEK), Victrex® PEEK (ICI); poly(arylene ether ketone) (PEK), Stilan® (Raychem Corporation); and poly(arylene ether ketone ether ketone ketone) (PEKEKK), Ultrapek® (BASF), shown in Scheme 1.1.1.

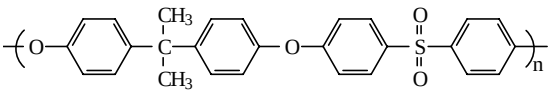

Udel®

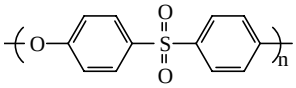

Victrex®

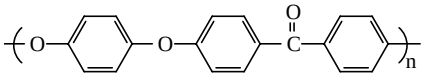

[1] (a) Cotter, R. J. *Engineering Plastics: Handbook of Polyarylethers* Gordan and Breach Publishers: Basel, Switzerland, **1995**.
[2] Clagett, D.C. in *Encyclopedia of Polymer Science and Engineering*, Mark, H. F.; Bikales, N. M.; Overberger, C. G.; Menges, G., Ed. John Wiley & Sons: New York, **1986**, Vol. 6. pp 94.
[3] Johnson, R. N. in *Encyclopedia of Polymer Science and Technology*, Bikales, N. M., Ed. John Wiley & Sons: New York, **1969**.
[4] (a) Johnson, R. N.; Farnham, A. G.; Clendinning, R. A.; Hale, W. F.; Merriam, C. L. *J. Polym Sci., Polym. Chem. Ed*. **1967**, *5*, 2375; (b) Farnham, A. G.; Robeson, L. M.; McGrath, J. E. *J. Appl. Polym. Sci*., *Appl. Poly. Symp*. **1975**, *26*, 373.
[5] Johnson, R. N.; Farnham, A. G. *U.S. Pat*. **1979**, 4,175,175, to Union Carbide Corp.
[6] Atwood, T. E.; Dawson, P. C.; Freeman, J. L.; Hoy, L. R. J.; Rose, J. B.; Staniland, P. A. *Polymer* **1981**, *22*, 1096.
[7] (a) Viswanathan, R.; Johnson, B. C.; McGrath, J. E. *Polymer* **1984**, *25*, 1927; (b) Viswanathan, R. *Ph.D. Thesis*, Virginia Polytechnic Institute and State University: Blacksburg, Virginia, **1981**.
[8] Hergenrother, P. E.; Jensen, B. J.; Havens, S. J. *Polymer* **1988**, *29*,357.
[9] Searly, O. B.; Pfeifer, R. H. *Polym. Eng. Sci*. **1985**, *25*, 474.
[10] Rao, V. L. *J. Macromol. Sci*., *Rev. Macromol. Chem. Phys*. **1999**, *C39*, 655.
[11] Riley, D. J.; Gungor, A.; Srinivasan, S.; Sankarapandian, M.; Tchatchoua, C.; Muggli, M. W.; Ward, T.; C.; McGrath, J. E.; Kashiwagi, T. *Polym. Eng. Sci*. **1997**, *37*, 1501.

Victrex PEEK®

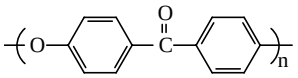

Stilan®

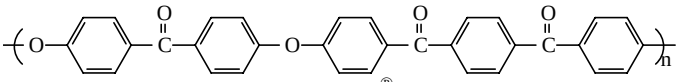

Ultrapek®

Scheme 1.1.1 Examples of commercial poly(arylene ether)s

A generalized structure of the poly(arylene ether)s can be represented as in Scheme 1.1.2.

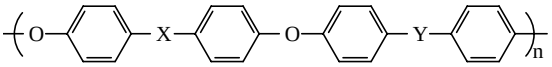

Scheme 1.1.2 A generic representation of poly(arylene ether) backbone structure.

Accordingly, wide variety of high performance polymeric materials have been synthesized by incorporating other thermally stable moieties such as sulfone, ketone, or aryl or alkyl phosphine oxide in addition to the ether linkage in poly(arylene ether)s.[12]

The research in this area has been focused on the synthesis of poly(arylene ether sulfone)s via new approaches, modification of the polymers, and synthesis of new polymers with functional groups or with novel properties. This part of review will survey some general synthesis approaches, new polymers with novel applications, and the properties of these polymers.

### 1.1.2 General Approaches for the Synthesis of Poly(arylene ether sulfone)s

The general approaches for the synthesis of poly(arylene ether)s include electrophilic aromatic substitution, nucleophilic aromatic substitution and metal catalyzed coupling reactions.

#### *1.1.2.1 Friedel-Crafts Sulfonylation Reaction Step (Condensation) Polymerization*

##### 1.1.2.1.1 Mechanism for Friedel-Crafts Sulfonylation and Acylation

The sulfonylation mechanism involves a two-stage reaction, as shown in Scheme 1.1.3. The sulfonylium cation $ArSO_2^+$ attacks the carbon on the aromatic nucleus to generate an intermediate complex, which subsequently decomposes to afford the final product by eliminating a proton. It is postulated that the effective sulfonylating agent is the sulfonylium

[12] Riley, D. J.; Gungor, S. A.; Srinivasan, S.; Sankarapandian, M.; Tchatchoua, C.; Muggli, M. W.; Ward, T.; C.;

salt generated by action of the Lewis-acid catalyst on the sulfonyl halide.[13]

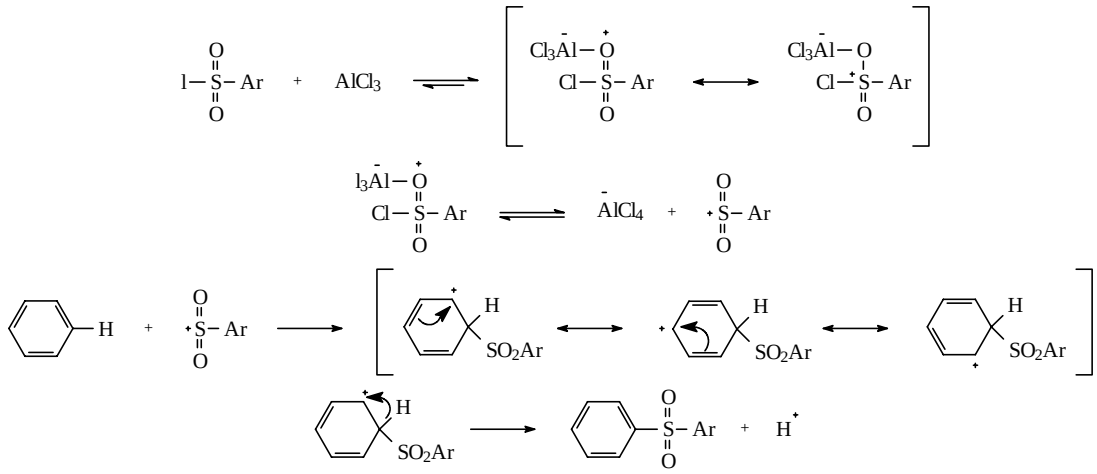

Scheme 1.1.3 Sulfonylation Mechanism

The synthesis of sulfones included electrophilic substitution, specifically, Friedel-Crafts catalysis by $AlCl_3$, $FeCl_3$, $SbCl_5$, $AlBr_3$ and $BF_3$, etc., which are efficient catalysts for the sulfonylation by arenesulfonyl halides.[14,15,16,17]

### 1.1.2.1.2 Poly(arylene ether sulfone) Synthesis via Friedel-Crafts Sulfonylation

Earlier synthesis of polysulfones included electrophilic aromatic substitution. Traditionally, this reaction requires high catalyst-concentrations. However, polysulfonylation to achieve high molecular weights can utilize elevated temperatures and low concentration of the Lewis acids. For example, arenesulfonyl chlorides react smoothly in the molten state at 120-140 ºC with aromatics in the presence of 1-5 mol % of $FeCl_3$ (or $SbCl_5$, $InCl_3$, iron (II) or iron (III) acetylacetonate (acetyacetone is 2,4-pentanedione) or $BiCl_3$), giving, in a few hours, the corresponding sulfones in high yields.[18,19]

Poly(arylene ether sulfone)s can be synthesized by two different polysulfonylation

---

McGrath, J. E.; Kashiwagi, T. *Polym. Eng. Sci*. **1997**, *37*, 1501.
[13] Olah, G. A. in *Friedel-Crafts Chemistry* Wiley: New York, **1973**, p488.
[14] Suter, C. M. in *The Organic Chemistry of Sulfur* Wiley: New York, **1944**, p673.
[15] Olah, G. A. in *Friedel-Crafts Chemistry* Wiley: New York, **1973**, p122.
[16] Cox, S. F.; Neill, K. G. (ICI Ltd.) *Aust. Pat.* **1962**, 242,187. (*Chem. Abstr*., **1965**, 63, 4208g.)
[17] Huismann, J. (I. G. Farbenind A. G.) *Ger. Pat*. **1941**, 701,954, (*Chem. Abstr*., **1942**, *36*, 987.)
[18] Jones, M. E. B.(ICI Ltd.), *Br. Pat*. **1965**, 979,111(*Chem Abstr*. **1965**, 62, 9065h)
[19] Jennings, B. E.; Jones, M. E. B.; Rose, J. B. *J. Polym. Sci*., *Part C* **1967**, *16*, 715.

reaction routes: condensation of AA and BB monomers[20] or self-condensation of AB monomer.[21] Scheme 1.1.4 shows two approaches.

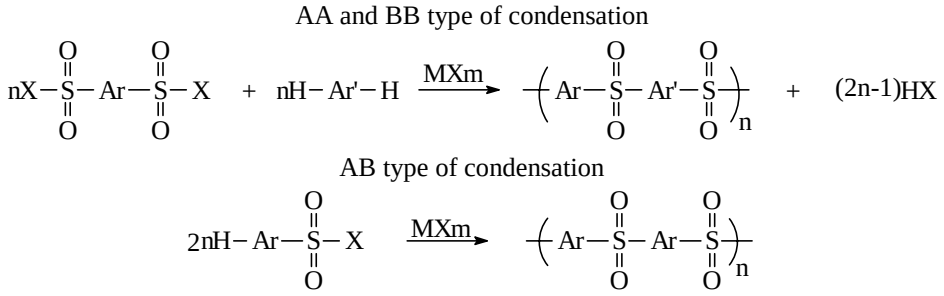


Scheme 1.1.4 Friedel-Crafts sulfonylation of AA-BB and AB types of polycondensations

In the AA-BB type of sulfonylation, two or more activated aromatic hydrogen atoms are commonly present in the reacting molecules. Therefore, this polycondensation process may result in different repeating units. Structural irregularities can occur due to possible sulfonylation at various ring-positions, disulfonylations on one aromatic nucleus, as well as side reactions directly promoted by the Friedel-Crafts catalyst.[22,23,24] When high amounts of catalyst are used, more than the theoretical amount of HCl is evolved, probably because of the attack of anhydrous metal halides on the aromatic nuclei, a known reaction for $FeCl_3$ and $AlCl_3$.[22,23] Indeed, polymers containing structures in Scheme 1.1.5 were proposed.[20]

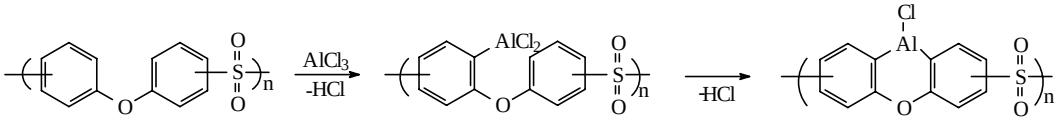


Scheme 1.1.5 Side reactions of polysulfonation by high catalyst-concentration.[20]

Generally, higher catalyst concentration leads to side reactions. An efficient approach to minimize the side reactions is to use the minimum amount of Friedel-Crafts catalyst (e.g. $FeCl_3$, 0.1-4 wt %). The reaction can be performed either in bulk or in solution using nitrobenzene, dimethyl sulfone, or chlorinated biphenyls, etc. as the reaction media.

Bulk polysulfonylation was initially performed in the molten state and the resulting solid low molecular weight polymer can be ground, followed by powder sintering at high

[20] Cohen, S. M.; Young, R. H. *J. Polym. Sci., Polym. Chem. Ed*. **1966**, *4*, 722.
[21] Cudby, M. E. A.; Feasey, R. G.; Gaskin, S.; Jones, M. E. B.; Rose, J. B. *J. Polym. Sci., Part C*. **1969**, *22*, 747.
[22] Kovacic, P.; Wu, C. *J. Org. Chem*. **1961**, *26*, 759, 762.
[23] Thomas, C. A. *Anhydrous Alumium Chloride in Organic Chemistry* Reinhold: New York, **1961**, p648.

temperature to produce high molecular weight. The final reaction temperatures were from 150 to 320 °C under nitrogen, and vacuum eventually was applied to remove HCl.[25,26] Since sulfonyl chlorides decompose above 250 °C via a radical mechanism, the best reaction temperature range was from 230 to 250 °C.[27] However, the polymers prepared by this approach were insoluble because of crosslinking side reactions.

In contrast to bulk polymerization, solution polymerization provided soluble polymers with high molecular weights, using low $FeCl_3$ concentration at 120-140 °C.[28] A major disadvantage of the above approaches is that all the metal-halide catalysts need to be removed, since the catalyst residue will deteriorate the thermal stability, electrical and other properties.

Electron-donating groups strongly activate sulfonylation at *ortho* or *para* positions, with *para* sulfonylation more favored due to less steric hindrance. Variables, such as highly reactive monomers, elevated reaction temperatures, high amounts of catalyst, etc. promote high conversion but may also result in structural irregularity and even crosslinking.

Self-polycondensation of monosulfonyl chlorides, A-B systems can demonstrate advantages compared with A-A, B-B polycondensation of dichlorosulfonyl compounds with suitable aromatics. The former stoichiometry is not affected by preferential vaporization. Therefore, self-polycondensation yields polymers with high molecular weight and regular structures. Since the sulfonyl group is a strong deactivating group for further sulfonylation, usually high reaction temperature is needed.

Sulfonic acid monomers can also be used to prepare poly(arylene ether sulfone)s, with typical catalysts being strong acids, such as $(CF_3CO)_2O$, polyphosphoric acid (PPA),[24] $MeSO_3H/P_2O_5$ mixture,[29] $CF_3SO_3H$.[30]

---

[24] Cohen, S. M.; Young, R. H. *J. Polym. Sci., Polym. Chem. Ed*. **1966**, *4*, 722.
[25] Jennings, B. E.; Jones, M. E. B.; Rose, J. B. *J. Polym. Sci., Part C* **1967**, *16*, 715.
[26] Cudby, M. E. A.; Feasey, R. G.; Jennings, B. E.; Jones, M. E. B.; Rose, J. B. *Polymer* **1965**, *6*, 589.
[27] Bain, P. J.; Blackman, E. J.; Cummings, W.; Hughes, S. A.; Lynch, E. R.; McCall, E. B.; Roberts, R. J. *Proc. Chem. Soc.*, London, **1962**, 86.
[28] Cudby, M. E. A.; Feasey, R. G.; Jennings, B. E.; Jones, M. E. B.; Rose, J. B. *Polymer* **1965**, *6*, 589.
[29] Ueda, M. (Idemitsu Kosan Co.) *Jpn. Pat*. **1985**, 85,228,541 (*Chem. Abstr*., **1986**, *104*, 187100).
[30] Rose, J. B. (ICI plc) *Eur. Pat. Appl*. **1982**, 49,070 (*Chem. Abstr*. **1982**, *97*, 6999).

### *1.1.2.2 Nucleophilic Substitution Reaction Step(Condensation) Polymerization*

#### 1.1.2.2.1 Mechanism for Nucleophilic Aromatic Substitution

The most practical method for the preparation of poly(arylene ether sulfone)s employs nucleophilic aromatic substitution ($S_NAr$).[4,5] Although nucleophilic substitution can occur via four principal mechanisms,[31] the most important mechanism utilized for the synthesis of poly(arylene ether sulfone)s has been $S_NAr$, in which activating groups are present on the aromatic ring (Scheme 1.1.6).

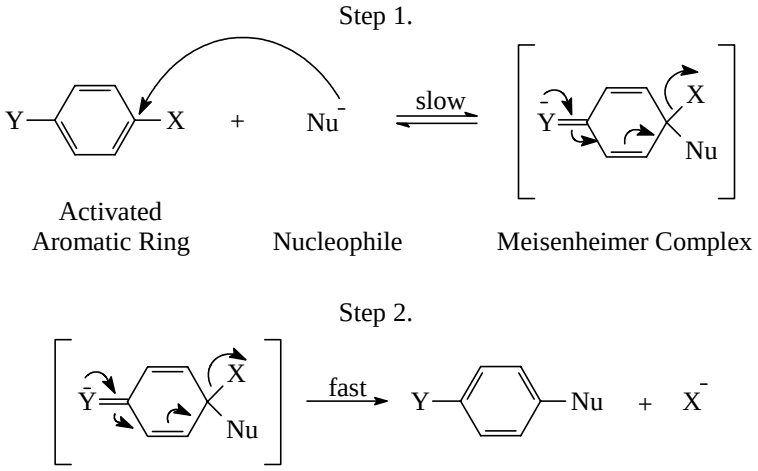


Y = Activating or electron withdrawing group
X = Leaving group
Nu = Attacking nucleophilic anion

Scheme 1.1.6 Nucleophilic aromatic substitution mechanism for the synthesis of poly(arylene ether sulfone)s.

In the first step, the nucleophile attacks the carbon atom of the activated C-X bond, resulting in a resonance stabilized intermediate, often termed a Meisenheimer complex.[32] The second step involves the departure of the leaving group. The first step is generally the rate-determining step. The proposed mechanism can be supported by the isolation of Meisenheimer salts. Investigating the effects of the leaving group on the reaction rate provided further evidence for this mechanism. In spite of the strength of the carbon-fluorine bond, the order of reactivity for the halogens was found to be F >> Cl > Br > I, suggesting the rate determining step does not involve the departure of the leaving group. Therefore, the

[31] March, J. in *Advanced Organic Chemistry: Reactions, Mechanisms, and Structure* 4th ed. Johns Wiley & Sons **1994**, p641.
[32] Meisenheimer, J. *Liebigs Ann. Chem.* **1902**, *323*, 205.

observed order of reactivity can be explained by the better stabilization of the Meisenheimer intermediate by the highly electronegative fluorine through inductive electron withdrawing effects. Furthermore, the carbon directly attached to the fluorine will be more electrophilic and, consequently, more susceptible to nucleophilic attack.

Many factors, such as the strength of the activating group, the nucleophilicity of the attacking nucleophile, the electronegativity of the leaving group, the reaction conditions, the nature of the solvent determines the kinetics of the $S_NAr$ reaction. Some major activating groups, such as

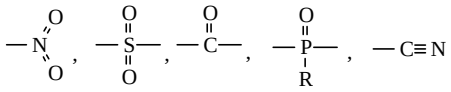

in the *ortho* and *para* positions of the leaving groups accelerate the nucleophilic substitution since they strongly stabilize Meisenheimer intermediate. On the contrary, electron-donating groups such as amine or methoxy decrease the stability of Meisenheimer intermediate, thus hindering the substitution.

The reaction rate increases with increasing the strength of the nucleophile. The overall approximate order of nucleophilicity is $ArS^- > RO^- > R_2NH > ArO^- > OH^- > ArNH_2 > NH_3 > I^- > Br^- > Cl^- > H_2O > ROH$.[33]

Since the decomposition of the Meisenheimer intermediate is not the rate-determining step, the trends for the leaving groups are quite different from common nucleophilic substitution. The leaving group trends for $S_NAr$ substitutions were reported to have the following order: $F^- > NO_2^- > {}^-SOPh > Cl^- > Br^- \sim I^- > {}^-OAr > {}^-OR > SR$.[34,35]

### 1.1.2.2.2 Poly(arylene ether Sulfone)s Synthesis via $S_NAr$ Reaction.

The $S_NAr$ reactions were first successfully used in the synthesis of high molecular weight poly(arylene ether)s first by Johnson *et al.*[4,5] This reaction represents a good example for poly(ether sulfone)s in general, either in laboratory or industrial-scale preparations. In this procedure, the bisphenol A and sodium hydroxide with an exact mole ratio of 1:2 were dissolved into DMSO/chlorobenzene. The bisphenol A was converted into disodium

[33] Bunnett, J. F.; Zahler, R. E. *Chem. Rev.* **1951**, *49*, 273.
[34] Miller, J. A. in *Aromatic Nuceophilic Substitution* Elsevier: London, **1968**, p61.

bisphenolate A and water was removed by azeotropic distillation. After the formation of the anhydrous disodium bisphenolate A, an equal molar amount of 4,4′-dichlorodiphenyl sulfone (DCDPS) was added in chlorobenzene under anhydrous conditions and the temperature was increased to 160 °C for over 1 hour to afford high molecular weights. Chlorobenzene is added to the viscous polymer solution during cooling, since it is a solvent at room temperature and facilitates precipitation of the salts (Scheme 1.1.7).

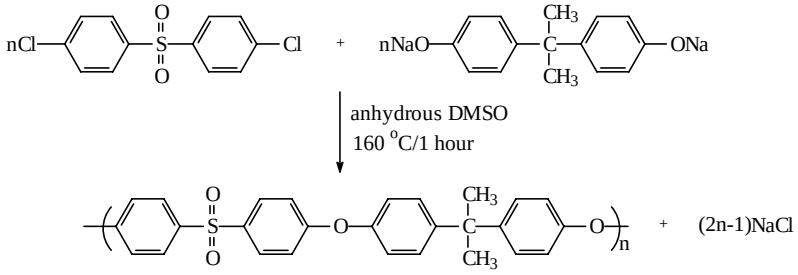


Scheme 1.1.7 Typical nucleophilic synthesis of bisphenol A polysulfone.[4,5]

As mentioned before, 4,4′-difluorodiphenyl sulfone (DFDPS) is much more reactive, but its application is limited because of economics. It can be prepared by the melt reaction of KF with DCDPS. The mechanism and kinetics of polyetherification have been investigated in detail for the polymerization of AA-BB monomers[4,5,36,37] and AB monomers.[38,39] Although the polymerizations of AA-BB and AB monomers have an identical mechanism, the halogen and phenoxide anion deactivate each other, in (halophenylsulfonyl)phenoxides and thus have self-polyetherification tates which are comparatively much lower than those of the corresponding two-component polycondensation. The reactivity of the activated halides can be estimated by measuring $^{1}H$, $^{13}C$ and $^{19}F$ NMR chemical shifts. The nucleophilic substitution reaction only proceeds in the halides with *ortho* or *para* positions substituted by strong electron-withdrawing group. Therefore, $^{1}H$ NMR chemical shift data from the protons *ortho* or *para* to the electron-withdrawing group can be used to determine the reactivity of the monomer indirectly.[40] $^{13}C$ NMR and $^{19}F$ NMR can be used to probe the chemical shift at the actual site of nucleophilic reaction. In general, lower chemical shifts correlate with lower monomer

[35] Beck, J. R. *Tetrahedron* **1978**, 34, 2057.
[36] Shultze, S. R.; Baron, A. L. *Adv. Chem. Ser.* **1969**, *96*, 692.
[37] Attwood, T. E.; Newton, A. B.; Rose, J. B. *Br. Polym. J.* **1972**, *4*, 391.
[38] Attwood, T. E.; Barr, D. A.; King, T.; Newton, A. B.; Rose, J. B. *Polymer* **1977**, *18*, 359.
[39] Newton, A. B.; Rose, J. B. *Polymer* **1972**, *13*, 465.
[40] Hedrick, J. L.; Labadie, J. W. *Macromolecules* **1990**, *23*, 1561.

reactivity. Carter reported that a compound may be appropriate for nucleophilic displacement if the $^{13}C$ chemical shift of an activated fluoride ranges from 164.5 to 166.2 *ppm* in $CDCl_3$.[41]

Preparing bisphenolates by using strong base is often feasible, and the phenolate readily reacts with activated dihalides (DCDPS or DFDPS) at high temperature to yield high molecular weight in a short period of time.

However, many salts such as the hydroquinone or biphenol salt are so insoluble that they do not work well. Furthermore, a stoichiometric amount of base used for the reaction is critical to obtain high molecular weight polymers. Moreover, the strong base may undesirably hydrolyze the dihalides to afford deactivated diphenolates which upset the stoichiometry. Clendinning *et al.* reported that potassium carbonate or bicarbonate could be used in these reactions instead of corresponding hydroxides.[42] McGrath and coworkers were the first to systematically study the use of the weak base $K_2CO_3$ instead of strong base to obtain phenolate salts.[7,43,44] $K_2CO_3$ was found to be better than $Na_2CO_3$ due to its relative stronger basicity and higher solubility in the reaction medium. The proposed mechanism for this method is shown in Scheme 1.1.8. This approach makes it fairly easy to control the molecular weights and the end groups. An additional advantage is that the precise amount of weak base is not extremely critical for achieving high molecular weight, as long as it is in excess. The kinetics of these reactions are slower than the strong base method.

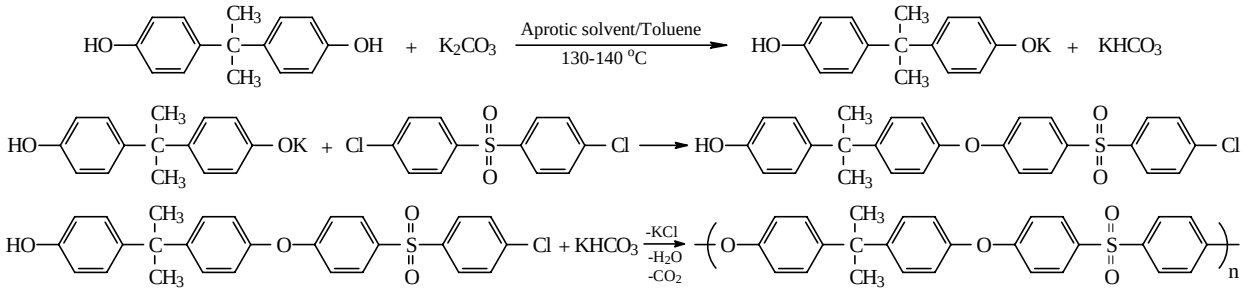


Scheme 1.1.8 Proposed mechanism for the synthesis of poly(arylene ether sulfone) via the potassium carbonate process.[7]

Aprotic polar solvents have to be used for several reasons. They are often good solvents

[41] Carter, K. R. *Polym. Mater. Sci. Eng.* **1993**, *69*, 432.
[42] Clendining, R. A.; Farnham, A. G.; Zutty, N. L.; Priest, D. C. *Canadian Patent* **1970**, *847 963*. Union Carbide Corp.
[43] Hedrick, J. L.; Mohanty, D. K.; Johnson, B. C.; Viswanathan, R.; Hinkley, J. A.; McGrath, J. E. *J. Polym. Sci., Polym. Chem.* **1986**, *23*, 287.
[44] Hedrick, J. L.; Dumais, J. J.; Jelinski, L. W.; Patsiga, R. A.; McGrath, J. E. *J. Polym. Sci., Polym. Chem.* **1987**, *25*,

for both monomers (including phenolates) and amorphous polymers. In addition, they can also stabilize the Meisenheimer intermediates. Common aprotic polar solvents, such as dimethyl sulfoxide (DMSO), N,N-dimethyl acetamide (DMAc), N,N-dimethyl formamide (DMF), N-methyl pyrrolidone (NMP), cyclohexylpyrrolidone (CHP) can be used. Under some circumstances, very high reaction temperature and boiling point solvents, such as sulfolane, diphenyl sulfone (DPS) have to be used due to the poor reactivity of the monomers or poor solubility of the resulting, possibly semi-crystalline polymers, as in the PEEK systems.

The choice of solvent is not trivial and generally, the reaction medium must be a good solvent for both monomers and polymer product. In addition, to obtain high molecular weight, water needs to be removed from the system to avoid hydrolyzing the activated substrate, since hydrolysis reduces the reaction rate and upsets the stoichiometry of the monomers.[44,52,45]

The reaction generated easily oxidizable alkali phenates. Thus, the polymerization must be carried out in an inert atmosphere. The sodium and potassium salts of the bisphenol are used because they are more soluble in polar aprotic solvents.

Other salts, especially fluoride salts, (eg. KF) can be used to perform nucleophilic substitution. As is well known, halides, and particularly the fluoride anions, are rather powerful Lewis bases and can exert a catalytic effect on aromatic nucleophilic substitutions in dipolar aprotic solvents. Phenols can be alkylated in the presence of KF (or CsF) absorbed on Celite[46,47] or $Et_4NF$.[48] Taking advantage of this reaction, halophenols and dihalides with bisphenols have been successfully polymerized in sulfolane at 220-280 °C by using KF as the base.

While most of the polymers have been synthesized by solution polymerization through nucleophilic substitution, Kricheldorf *et al.* showed that melt or solvent free polymerization can be achieved by reacting bis(trimethylsilyl ether)s of various bisphenols with bis(4-

---

2289.
[45] Johnson, R. N.; Farnham, A. G. *J. Polym. Sci., Polym. Chem.* **1967**, *5*, 2415.
[46] Ando, T.; Yamawaki, J.; Kawate, *Chem. Lett.* **1979**, *45*.
[47] Ando, T.; Yamawaki, J.; Kawate, T.; Sumi, S.; Hanfusda, T. *Bull. Chem. Soc. Jpn.* **1982**, *55*, 2504.
[48] Miller, J. M.; So, K. H.; Clark, J. H. *Can. J. Chem.* **1979**, *57*, 1887.

fluorophenyl) sulfone (Scheme 1.1.9).[49] This idea came from well-known reactions on trimethylsilyl ethers, esters, etc., that were performed with fluoride-catalyzed desilylation in the presence of KF, CsF or $(C_4H_9)_4NF$.[50,51] Silylation followed by distillation is an efficient method for purifying many bisphenols, aminophenols and diamines. The product can be directly processed without further purification since the highly volatile fluorotrimethylsilane is the only by-product and the catalytic amount of CsF does not deteriorate the mechanical properties of the final products. In addition, the removal of the volatile fluorotrimethylsilane by-product further drives the reaction to yield high molecular weight. No halogen substituted diphenols can be used, since the exchange reaction may occur.[52]

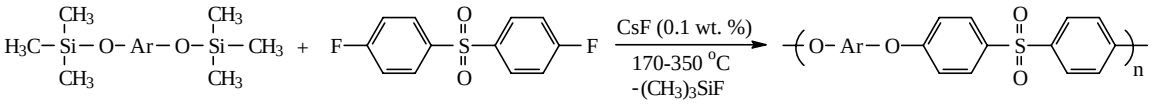


Scheme 1.1.9 Synthesis of poly(arylene ether sulfone)s via silyl ether displacement

A proposed mechanism for silyl ether displacement is shown in Scheme 1.1.10. In the first step, the fluoride anion converts the trimethyl siloxy group into a phenolate salt. In the following step, the phenolate anion attacks the activated fluoro-monomer to generate an ether bond. The amount of catalyst required is about 0.1-0.3 mole%. Catalyst type and concentration is crucial for this reaction.

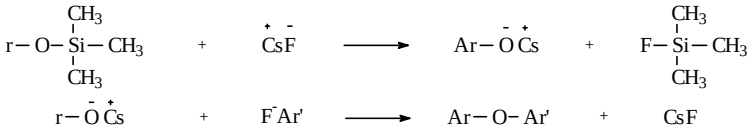

Scheme 1.1.10 Reaction mechanism of silyl ether displacement

Unfortunately, the method is only suitable for fluorinated systems such as DFDPS. Using chloro-monomers generally affords low molecular weight, because a weak base like KF or CsF is needed and DCDPS is not reactive enough under these reaction conditions. However, the activated dichloro-compounds can be successfully polymerized in NMP in the presence of equimolar amounts of $K_2CO_3$.[53]

[49] Kricheldorf, H. R.; Bier, G. *J. Polym. Sci. Polym. Chem. Ed.* **1983**, *21*, 2283.
[50] Corey, E. J.; Snider, B. B. *J. Am. Chem. Soc.* **1972**, *94*, 2549.
[51] Fieser, M. *Reagents for Organic Synthesis* Wiley: New York, **1982**, Vol 10, p81, 325, 378.
[52] Kricheldorf, H. R.; Delius, U.; Tonnes, K. U. *New Polym. Mater.* **1988**, *1*, 127.
[53] Kricheldorf, H. R.; Jahnke, P. *Makromol. Chem.* **1990**, *191*, 2027.

### *1.1.2.3 Other Approaches for the Synthesis of Polysulfones*

In addition to nucleophilic and electrophilic substitution reactions, other reactions have also been used to prepare poly(arylene ether sulfone)s with special structures which otherwise could not be prepared. The following paragraph briefly reviews these reactions.

#### 1.1.2.3.1 The Ullman Reaction

The Ullman reaction has long been known as a method for the synthesis of aromatic ethers by the reaction of a phenol with an aromatic halide in the presence of a copper compound as a catalyst. It is a variation on the nucleophilic substitution reaction in that it is a phenolic salt that reacts with the halide. The advantage in the synthesis of poly(arylene ether)s lies in the fact that the synthesis uses nonactivated aromatic halides, thus providing a way of obtaining structures not available by the conventional nucleophilic route. The ease of halogen displacement was found to be the reverse of that observed for nucleophilic substitution reaction, that is, I>Br>Cl>>F. The solvent of choice for these reactions is benzophenone with a cuprous chloride-pyridine complex as a catalyst; bromine compounds are the favored reactants.[4b,54,55,56] Poor reproducibility, the need for brominated monomers, and the difficulty of removing copper salts are major disadvantages of this reaction.

#### 1.1.2.3.2 The Nickel Coupling Reaction

A relatively new approach for preparing poly(arylene ether sulfone)s involves the formation of an aromatic carbon-carbon bond by coupling halogenated aromatic compounds with $Ni^0$.[57] Thus, polymers with biphenyl units can be made without starting with a biphenyl compound. Unlike the Ullman reaction, the nickel coupling reaction works well with chloro-compounds and the reaction conditions are much milder. The reaction is carried out in an aprotic solvent at 60 to 80 °C.[58,59] A zero valent nickel-triphenylphosphine complex was used as the catalyst prepared from nickel chloride and zinc metal. Both nonactivated and activated halides could be used.

---

[54] Farnham, A. G.; Johnson, R. N. *U. S. Patent* **1967**, 3, 332 909.
[55] Jurek, M. J.; McGrath, J. E. *Polym. Prepr., ACS*, **1987**, 28(1), 180.
[56] Burgoyne, Jr., W. F.; Robeson, L. M.; Vrtis, R. N. *U.S. Pat.* **1997**, 5,658,994.
[57] Colon, I.; Kwiatokowski, G. T. *J. Polym. Sci., Polym. Chem.* **1990**, *28*, 367.
[58] Colon, I.; Maresca, L. M.; Kwiatkowski, G. T. *U. S. Patent* **1991**, 4, 263 466.
[59] Havelka, P. A.; Sheares, V. V. *Macromolecules* **1999**, *32*, 6418.

### 1.1.3 Poly(arylene sulfide sulfone) and poly(arylene ether sulfide sulfone)s

Polysulfonation of self-polycondensation of 4-(phenylthio)benzenesulfonyl chloride was also used to prepare poly(arylene sulfide sulfone)s.[60,61] Condensation of diphenyl sulfide with 4,4´-oxydibenzylsulfonic acid or 4,4´-thiodibenesulfonic acid[62] or by polyetherification of polycondensation of DCDPS with 4,4´-dihydroxydiphenol sulfide.[63]

Condensation of an activated aromatic halide with either an alkali metal thiophenoxide or an alkali metal sulfide is performed under the same experimental condensations as used for polyetherification (Scheme 1.1.11).[64]

Bis(haloaryl) sulfones can indeed be polycondensed with dialkali metal bisthiophenoxides as in equation,[65,66,67] and alkali metal (haloarylsulfonyl)thiophenoxides also work.[68] In some cases, the polymerization of (haloarylsulfononyl)thiophenol can be promoted by KF.[69,70] Bis(haloaryl) sulfones may also be polycondensed with alkali metal sulfides in the presence of $CH_3COOLi$ or heterocyclic amines,[71] as in equation, or additionally, copolycondensed with dihalobenzenes.[72]

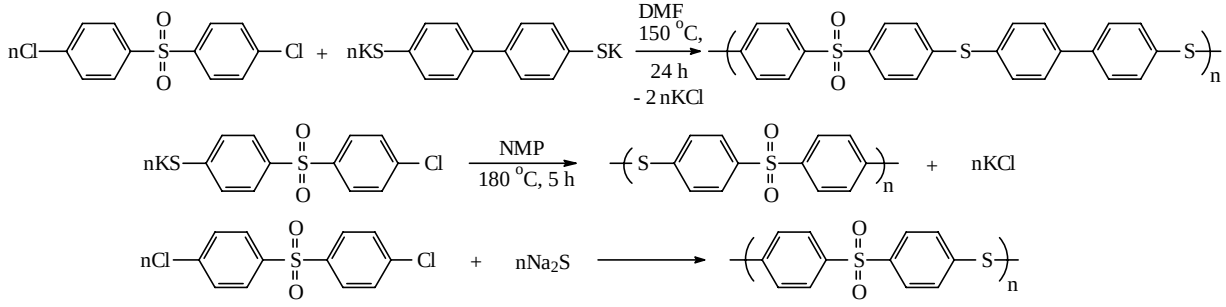


Scheme 1.1.11 Some examples of synthesis of poly(arylene thioether sulfone)s

---

[60] Cudby, M. E. A.; Feasey, R. G.; Jennings, B. E.; Jones, M. E. B.; Jones, J. B. *Polymer* **1965**, *5*, 589.
[61] ICI Ltd., *Belg. Pat.* **1964**, *639 634* (*Chem. Astr*., **1965**, *63*, 700f)
[62] Cohen, S. M.; Young, R. H. Jr. (Monsanto Co.), *US Pat.* **1968**, *3418277* (*Chem. Abstr*., **1969**, *70*, 48045.)
[63] Johnson, R. N.; Farnham, A. G.; Clendinning, R. A.; Hale, W. F.; Merriam, C. N. *J. Polym. Sci. Polym. Chem. Ed.* **1967**, *5*, 2375.
[64] Sandler, S. R.; Karo, W. *Polymer Syntheses* Academic Press New York, **1980**, *Vol. 3*, p98.
[65] Kreuchunas, A. *US Pat*. **1958**, 2822351 (Chem. Abstr., 1958, 52, 7778b).
[66] Baron, A. L.; Blank, D. R. *Makromol. Chem.* **1970**, *140*, 83.
[67] Gabler, R. (Inventa, A. G.) *Ger. Pat*. **1970**, *2009323* (*Chem. Abstr*. **1958**, *52*, 7778b).
[68] Feasey, R. G. (ICI Ltd.) *US Pat*. **1974**, *3819582*, (*Chem. Abstr.* **1975**, *82*, 157207.)
[69] Feasey, R. G.; Rose, J. B. (ICI Ltd.) *Ger Pat.* **1972**, *2156343* (*Chem. Abstr.* **1972**, *77*, 75774)
[70] Fortuin, M. S. (ICI Ltd.) *Br. Pat.* **1974**, *1369 217* (*Chem. Abstr.* **1975**, *82*, 98741.)
[71] Campbell, R. W. (Phillips Petroleum Co.), *Ger. Pat* **1977**, 2726862 (*Chem. Abstr*. **1978**, *88*, 137178); *US Pat*. 1978, 4070349 (Chem. Abstr. 1978, 89, 25071); *US Pat*. **1978**, 4125535 (*Chem. Abstr*. **1979**, *90*, 55528).
[72] Idel, K.; Ostlinning, E.; Koch, W.; Heitz, W. (Bayer A. G.) *Ger. Pat* **1984**, *3312254* (*Chem. Abstr.*, **1985**, *102* , 25584).

Recently, Liu *et al.* used DCDPS to prepare bis(mercaptophenyl) sulfone (DTPS) by hydrolysis.[73] DTPS can be used to react with DCDPS in a dipolar aprotic solvent with $K_2CO_3$ as the weak base and high molecular weight can be obtained due to higher reactivity of thiophenol compared with its phenol counterpart, and is similar to that reported by Viswanathan *et al.* for the preparation of bisphenol A polysulfone.[4]

### 1.1.4 Control of Molecular Weight and/or Endgroups

Control of molecular weight is very important, because the molecular weight needs to be high enough to afford polymers with good mechanical properties and to be low enough to have good processibility. Generally, by upsetting the mole ratio of the two monomers, one can easily control the molecular weight. Under some circumstances, the reactive endgroups may significantly deteriorate the polymer stability. One way to minimize the problem is to use a monofunctional monomer as a comonomer to endcap the polymer chain. Thus, it is known that end capped Udel can be prepared by bubbling methyl chloride into phenolate reactive systems.

End-capping the polymer chain with functional groups is also a very useful approach to prepare reactive oligomers for generating some block copolymers or modifying polymer networks. Polysulfones were prepared with different terminal functional groups, such as carboxyl,[74,75,76,77] amine,[78,79] hydroxyl[80], and phenylethynyl[81,82] chain ends. Amino-terminated poly(arylene ether sulfone)s or poly(arylene ether ketone)s were synthesized and used to modify epoxies.[83,84,85] Noshay *et al.* used phenol terminated Udel to prepare multi-block copolymers with functional polydimethylsiloxane.

---

[73] Liu, Y. N.; Geibel, J.; Riffle, J. S.; McGrath, J. E. *Polymer* **2000** (in press); Liu, Y. N. *Ph.D Thesis* Virginia Tech: Blacksburg, VA, **1998**.
[74] Waehamad, W.; Cooper, K. L.; McGrath, J. E. *Polym. Prepr.* **1989**, *30 (2)*, 441.
[75] Cooper, K. L.; Waehamad, W.; Huang, H.; Chen, D.; Wilkes, G. L.; McGrath, J. E. *Polym. Prepr., ACS* **1989**, *464*.
[76] VPI &SU PHD Dissertations of a) Lambert, J. M. **1986**; b) Cooper, K. L. **1991**; Waehamad, W. **1991**.
[77] Wan, I-Y.; Srinivasan, R.; McGrath, J. E. *Polym. Prepr.* **1992**, 33(2), 223.
[78] Lyle, G. D.; Jurek, M. J.; Mohanty, D. K.; Wu, S. D.; Hedrick, J. C.; McGrath, J. E. *Polym. Prepr., ACS* **1987**, *28(1)*, 77.
[79] Jurek, M. J.; McGrath, J. E. *Polymer* **1989**, *30*, 1552.
[80] Lyle, G. D.; Senger, J. S.; Chen, D. H.; Kilic, S.; Wu, S. D.; Mohanty, D. K.; McGrath, J. E. *Polymer* **1989**, *30*, 978.
[81] Mecham, S. *Ph.D. Thesis Virginia Tech*: Blacksburg, VA, **1997**.
[82] Ayamba, A.; Mecham, S.; McGrath, J. E. *Polymer* **2000**, in press.
[83] Mohanty, D. K.; Lowery, R. C.; Lyle, G. D.; McGrath, J. E. *Int. SAMPE Symp.* **1987**, *32*, 408.
[84] Mohanty, D. K.; Senger, J. S.; Smith, C. D.; McGrath, J. E. *Int. SAMPE Symp.* **1988**, *33*, 970.
[85] Bennett, G. S.; Farris, J. *J. Polym. Sci., Polym. Chem. Ed.* **1994**, *32*,73.

Mandal et al reported poly(sulfone)s end-capped with metal containing phthalocyanines (PcM), as shown in Scheme 1.1.12.[86]

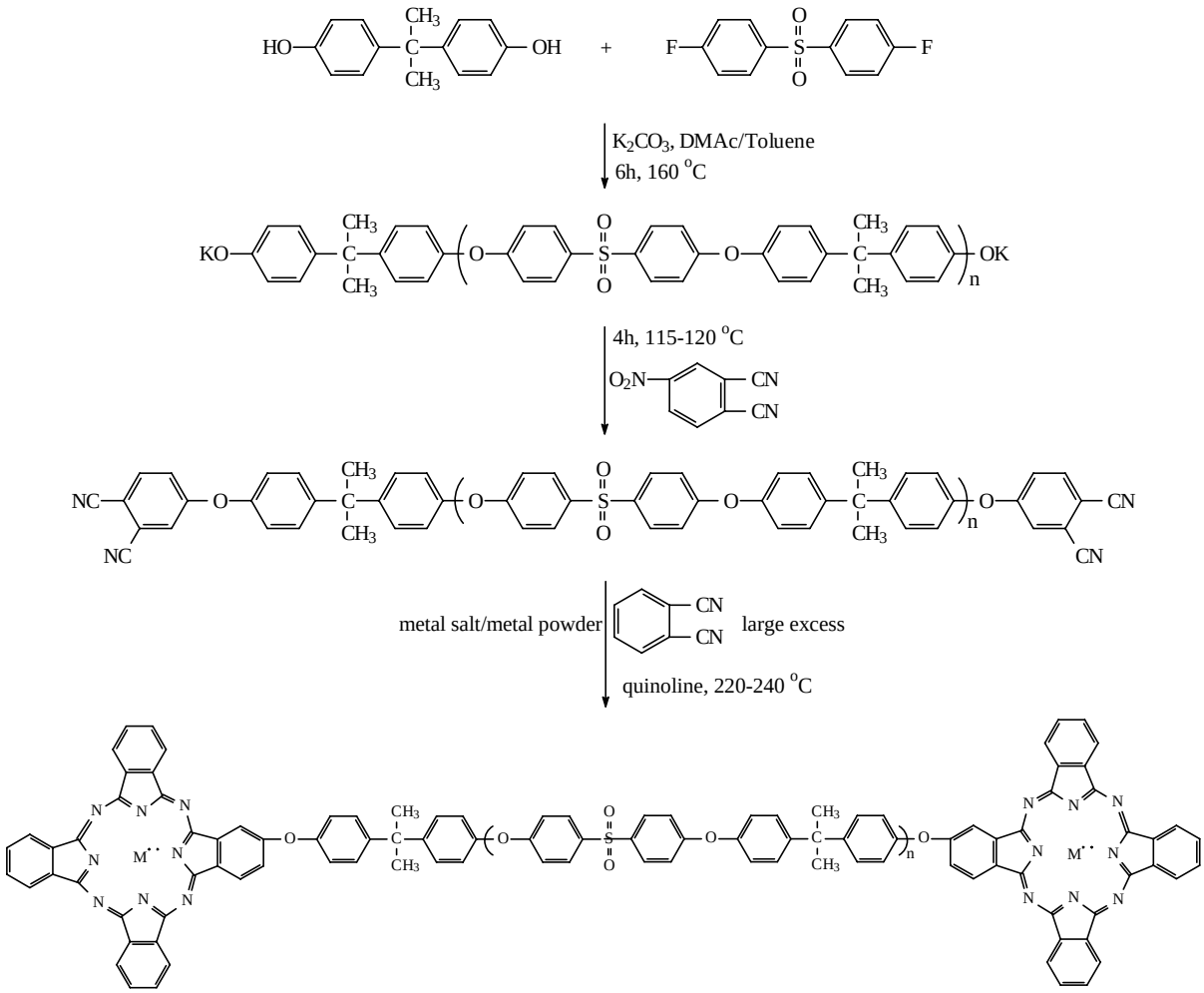


Scheme 1.1.12 Synthesis of metallophthalocyanine end-capped polymer.

The polymers were soluble in common organic solvents. $T_g$ was increased probably due to the stacking of PcM moieties. In addition, annealing the polymers afforded a melting endotherm due to crystallization. Again, this may be due to the stacking of PcM rings.

### 1.1.5 Modification of Poly(arylene ether sulfone)s

One objective of modifying poly(arylene ether)s was to alter their chemical nature to some degree without sacrificing their excellent physical and other properties. Functionalized polysulfones may find many applications as membrane materials. These materials may be used as gas separation membranes or membrances for water desalination. In addition,

[86] Mandal, H.; Hay, A. S. *J. Macromol. Sci., Pure Appl. Chem.* **1998**, *A35*, 1979.

functionalized polymers can be further modified to generate graft copolymers or used to modify the networks. Recent advances in fuel cells require higher performance proton exchange membranes, which has motivated research on sulfonated high performance polymers. Generally, there are two methods to functionalize polymers. One is to chemically modify the preformed polymer. Another is to use a functionalized monomer to prepare the polymer via direct polymerization.

#### *1.1.5.1 Modification of Polymers*

Introducing amino groups onto the phenylene rings comprising poly(phenylene ether sulfone) chains was reported by Conningham *et al.* by carrying out nitration/reduction procedures on preformed PES.[87] However, side reactions can occur in nitration/reduction procedures due to the attack of nitronium ion at carbon-to-sulfur chain linkages as previously suggested by Schofield *et al.*[88]

Questin may have been the first to sulfonate poly(arylene ether sulfone).[89] In this patent, it was demonstrated that the bisphenol A polysulfone could be sulfonated by chlorosulfonic acid to produce a sulfonated poly(arylene ether sulfone), which was used for desalination via reverse osmosis. However, the chlorosulfonic acid may be capable of cleaving the bisphenol A polysulfone partially at the isopropylidene link, or that it might undergo branching and crosslinking reactions by converting the intermediate sulfonic acid group into a partially branched or crosslinked sulfone unit. An alternative route was employed to sulfonate bisphenol A polysulfone. In this approach, a complex of $SO_3$ and triethyl phosphate (TEP) with a mole ratio of 2:1 was used to sulfonate the polymer at room temperature.[90,91] This mild sulfonation treatment could minimize or even eliminate possible side reactions.

Chloromethylation was also carried out to modify the polysulfone for preparing membrane materials.[92]

Recently, Guiver *et al.* reported a quantitative and regiospecific method for attaching

---

[87] Conningham, P.; Roach, R. J.; Rose, J. B.; McGrail, P.T. *Polymer* **1992**, *33*, 3951.
[88] Schofield, K. *Aromatic Nitration* Cambridge Press: Cambridge, England, **1980**, p209.
[89] Quentin , J. P. *Sulfonated Polyarylether Sulfones*, US 3,709,841. Rhone-Poulenc, January 9, **1973**.
[90] Noshay, A.; Robeson, L. M. *J. Appl. Polym. Sci.* **1976**, *20*, 1885.
[91] Johnson, B. C.; Yilgor, I.; Tran, C.; Iqbal, M.; Wightman, J. P.; Lloyd, D. R.; McGrath, J. E. *J. Polym. Sci., Polym. Chem. Ed.* **1984**, *22*, 721.

azide groups onto the aromatic rings of polysulfone and poly(aryl sulfone).[93] Polysulfones were activated either on the *ortho*-sulfone sites or the *ortho*-ether sites by direct lithiation or bromination-lithiation. The lithiated intermediates were claimed to be quantitatively converted to azides by treatment with tosyl azides. Azides are thermally and photochemically labile groups capable of being transformed readily into a number of other useful derivatives.

Modifying polymers is very convenient and relatively inexpensive. However, control of sulfonation is very difficult since the sulfonation occurs on the activated ring, which may deteriorates thermal stability of the polymer. The extent of sulfonation is also hard to control and side reactions may occur.

### *1.1.5.2 Modification of Monomers*

Modification of monomers is a fundamentally different approach from modification of polymer in that modification of monomer makes feasible control of the molecular structures. Both diphenols and dihalides can be modified to incorporate functional groups or new monomers containing functional groups can be synthesized with similar structures as their counterparts.

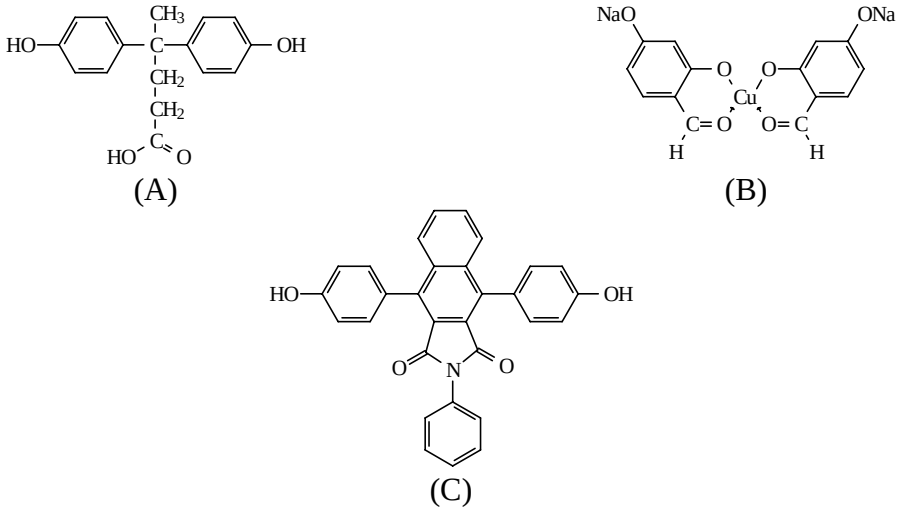


Scheme 1.1.13 Structures of modified biphenols

BHPA (A), copper-chelate monomer (B), and (C) 3,8-bis(4-hydroxyphenyl)-N-phenyl-1,2-naphthalimide.

[92] Daly, W. H. *J. Macromol. Sci., Chem.* **1985**, *A22*, 713.
[93] Guiver, M. D.; Robertson, G. P. *Macromolecules* **1995**, *28*, 294.

Using 4, 4-bis(4-hydroxyphenyl)-pentanoic acid (BHPA)[94,95] as comonomer, some polysulfones with pendant carboxylic groups were successfully synthesized.[96,97] Scheme 1.1.13 (A) shows the structure of BHPA. The functional groups can be used for the preparation of graft copolymers. A new monomer containing copper (II) was also used to synthesize the electrically conductive polysulfone (Scheme 1.1.13 (B)).[98,99]

Hay *et al.* reported a bisphenolic monomer, 3,8-bis(4-hydroxyphenyl)-N-phenyl-1,2-naphthalimide (Scheme 1.1.13 (C) as well as its corresponding poly(N-phenyl imido aryl ether sulfone) via transimidization reactions with hydrazine monohydrate, aliphatic amines, and an amino acid.[100] These polysulfones with reactive functional groups can be used to prepare graft copolymers or polymer networks by thermal curing.

The monomers could be nitrated and then reduced to amine functionalized monomers (Scheme 1.1.14).[101] This approach was used to nitrate 4,4′-dichlorodiphenyl sulfone (DCDPS) or bis-4-fluorophenyl phenyl phosphine oxide.[102] These monomers were used to copolymerize with some other activated dihalides as the comonomers.

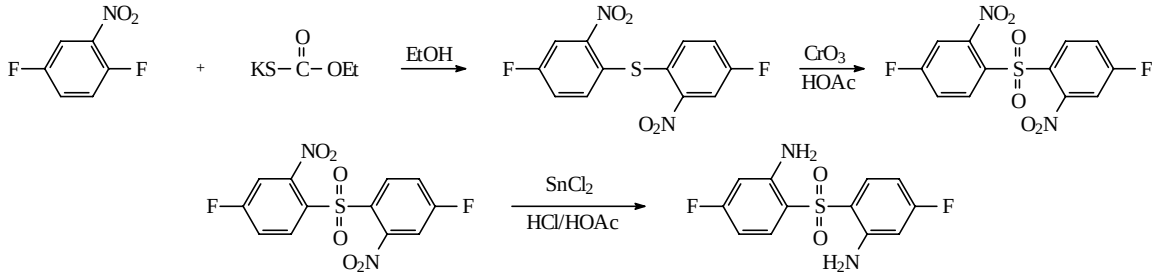


Scheme 1.1.14 Synthetic route for the synthesis of amino-DFDPS

Ueda et al reported the sulfonation of the activated dihalide DCDPS (Scheme 1.1.15).[103] This work makes it possible to synthesize sulfonated poly(arylene ether sulfone) with well-

[94] Bader, A. R.; Kontowicz, A. D. *J. Am. Chem. Soc.* **1954**, *76*, 4465.
[95] Mikroyannidis, J. A. *Eur. Polym. J.* **1985**, *21*, 1031.
[96] Esser, I. C. H. M.; Parsons, I. *Polymer* **1993**, *34*, 2836.
[97] Koch, T.; Ritter, H. *Macromol. Chem. Phys.* **1994**, *195*, 1709.
[98] Butuc, E.; Cozan, V.; Giurgiu, I.; Mihalache, I.; Ni, Y.; Ding, M. *J. Macromol. Sci., Pure Appl. Chem.* **1994**, *A31*, 219.
[99] Rusu, M.; Airinei, A.; Butuc, E.; Rusus, G. G.; Baban, C.; Rusu, G. I. *J. Macromol. Sci., Phys.* **1998**, *B37*, 73.
[100] Herbert, C. G.; Hay, A. S. *J. Polym. Sci., Chem. Ed.* **1997**, *35*, 1095.
[101] Bottino, F. A.; Mamo, A.; Recca, A.; Brady, J.; Street, A. C.; McGrail, P. T. *Polymer* **1993**, *34*, 2901.
[102] Park, S. J.; Lyle, G. D.; Mercier, R.; McGrath, J. E. *Polymer* **1993**, *34*, 885; Park, S. J. *Ph. D. Thesis* Virgnia Tech, Blacksburg, VA, **1992**.
[103] Ueda, M.; Toyota, H.; Ouchi, T.; Sugiyama, J.; Yonetake, K.; Masuko, T.; Teramoto *J. Polym. Sci., Polym. Chem.* Ed. **1993**, *31*, 853.

controlled structures. This monomer was used as a comonomer of DCDPS to react with bisphenol A and high molecular weight bisphenol A based copolymers with up to 30 mol% sulfonation were achieved. Biphenol based copolymers with up to 60 mol% sulfonation were recently reported by Wang *et al.*[104]

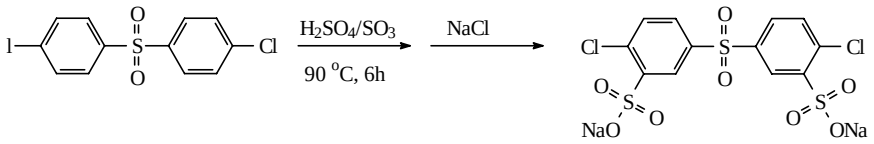


Scheme 1.1.15 Synthesis route for sulfonated DCDPS

### 1.1.6 Poly(arylene ether sulfone) Mechanical Behavior

Polysulfones haven been widely used as engineering thermoplastics due to their good mechanical properties and thermal stability, which depend on their unique structures. In the polysulfone main chain, the bond energy of an aliphatic carbon-oxygen ether linkage (84.0 kcal/mol) is slightly higher than that of the carbon-carbon counterpart (83.1 kcal/mol). Aromatic ether linkages (Ar-O-Ar) are stabilized through resonance, as is illustrated in Scheme 1.1.16 for diphenyl ether.[105]

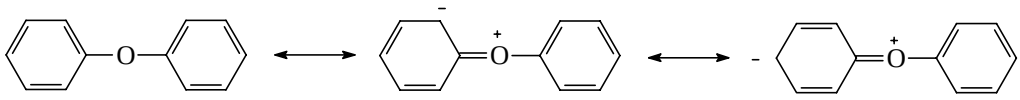

Scheme 1.1.16 Resonance stabilization in aryl ethers

The aryl C-O-C linkage has a lower rotation barrier, lower excluded volume, and decreased Van der Waals interaction forces compared to the C-C bond. Therefore, the backbone containing C-O-C linkage is highly flexible. In addition, the low barrier to rotation about the aromatic ether bond provides a mechanism for energy dispersion which is believed to be the principal reason for the toughness or impact resistance observed for these materials.[106,107,108]

Robeson *et al.* studied the secondary loss transitions of a series of poly(arylene ether)s

---

[104] Wang, F.; Ji, Q.; Harrison, W., Mecham, J.; Formato, R.; Kovar, R.; Osenar, P.; McGrath, J. E. *Polym. Prepr.*, ACS **2000**, *41(1)*, 237.
[105] Patai, S. in *The Chemistry of the Ether Linkage* Interscience: London, **1967**.
[106] Robeson, L. M.; Farnham, A. G.; McGrath, J. E. in *Molecular Basis of Transitions and Relaxations*, Boyer, R. F.; Meier, D.,J., Eds.; Gordon: New York, **1978**; pp 405-425.
[107] Dumais, J. J.; Cholli, A. L.; Jelinski, L. W.; Hedrick, J. L.; McGrath, J. E. *Macromolecules* **1986**, *19*, 1884.
[108] Yee, A. F.; Smith, S. A. *Macromolecules* **1981**, *14*, 54.

using a torsion pendulum.[106] They found that the secondary loss transitions are closely related with the segmental motion of the aryl ether bonds. The secondary loss transitions due to the interactions between the sulfonyl groups and water molecules are not dependent on the structure of the polymers. Dumais et al studied the β-relaxation in poly(arylene ether sulfone)s by deuterium NMR.[107] The results suggested that the primary mode of motion of the aromatic rings in these polymers is 180° phenyl ring flips with a broad distribution of characteristic frequencies (ca. $10^2$-$10^7$ $s^{-1}$). Addition of antiplasticizers decreases the phenyl ring flipping rate.

Table 1.1.1 Thermal Transitions of Poly(arylene ether sulfone)s and Related Polymers

| Structure | $T_g$ (°C) | $T_m$ (°C) | References |
|---|---|---|---|
| 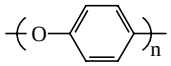 | 110 | 285 | [109] |
| 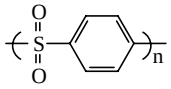 | 350 | >520, >580 | [110,111] |
| 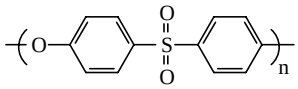 | 223-230 | - | [112,113] |
| 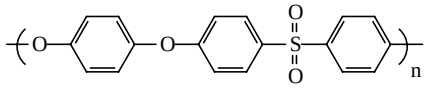 | 217 | - | [44] |
| 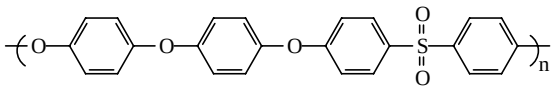 | 180 | - | [114] |
| 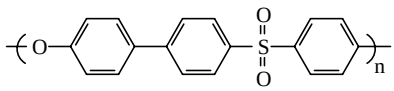 | 265 | - | [113] |
| 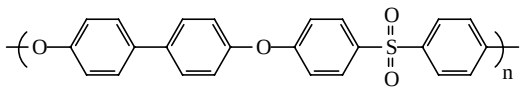 | 232 | - | [44] |
| 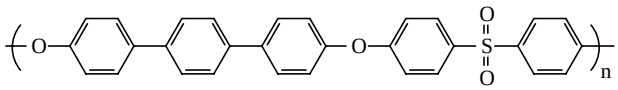 | 251 | 389 | [115] |
| 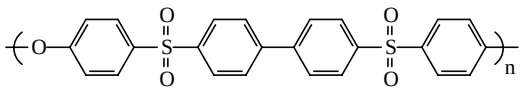 | 280-290 | 395 | [112,113,116] |

Polysulfone can be amorphous or crystalline, depending on the main chain structure. Most of the polysulfones are amorphous because of the kink structure of the sulfone group. However, some polysulfones have more rigid, regular structures and thus they can be crystallized. The amorphous polymers are generally soluble in chlorinated solvents and aprotic dipolar solvents, which makes them processible in solution. The electron-withdrawing character and polarity of these groups are important factors in determining the stiffness of the

[109] Harris, J. E.; Robeson, L. M. *J. Polym. Sci*., *Polym. Phys. Ed*. **1987**, *25*, 311.
[110] Colquhoun, H. M.; MacKenzie, P. D.; McGrail, P. T.; Nield, E. *Preprint of the International Conference on Polymers for Composites*, Solihull, Dec 2-4, **1987**.
[111] Inventa, A. G. *Br. Pat*. 1234008.
[112] White, D. M.; Cooper, G. D. in *Encyclopedia of Chemical Technology*, 3rd ed.; Mark, H. F;, Othmer, D. F.; Overberger, C. G.; Seaborg, G. T. Eds. Wiley: New York, **1982**, Vol. 18; p23.
[113] Rose, J. B. *Polymer* **1974**, *15*, 456.
[114] Rose, J. B. *Chem. Ind.* **1968**, 461.
[115] Staniland, p. A. *Bull. Soc. Chim. Belg*. **1989**, *98*, 667.
[116] Attwood, T. E.; King, T.; Leslie, V. J.; Rose, J. B. *Polymer* **1977**, *18*, 369.

chain and its ability to crystallize.[117]

Poly(arylene ether sulfone)s have high $T_g$ due to their very high chain rigidity, although $T_g$ various with changing chain structures. Generally, the ether linkage decreases $T_g$ and the phenyl linkage increases the $T_g$, since they affect the rigidity in an opposite direction. Sulfone linkages increase the $T_g$ because of their rigidity and polarity that may increase the intermolecular interactions. Increasing the molecular symmetry also increases the $T_g$. Indeed, the $T_g$ and $T_m$ can be tuned to the applications by tailoring the main chain structures.

Table 1.1.1 shows the effect of the structure on the $T_g$ and $T_m$.[103] Poly(arylene ether sulfone)s generally have high fracture toughness and impact strength. Structural symmetry plays a very important role in determining the toughness. High symmetry and high rigidity also increase the Young's modulus.

[117] Calier, V.; Devaux, J.; Legras, R.; McGrail, P. T. *Macromolecules* **1992**, *25*, 6646.

## 1.2 Polyimides

Polyimides are a class of polymers known for their high temperature stability, favorable dielectric properties, and chemical resistance. They have found applications in the composites and microelectronic industries. Some polyimides have been commercialized, among them Kapton® (made by DuPont) and Ultem® (made by GE) are the most important ones (Scheme 1.2.1).

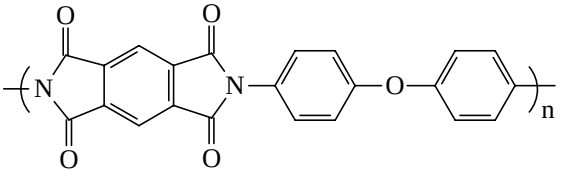

Kapton®

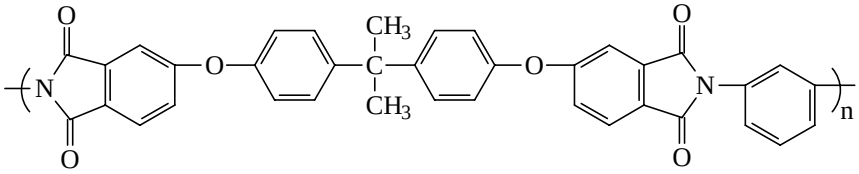

Ultem®

Scheme 1.2.1 Structures of some commercial polyimides

The nomenclature of polyimides is quite complicated. The IUPAC name can be used for polyimides, but for convenience, the common name and the name according to their starting monomers are still widely used.[118]

Although the first synthesis of an aromatic polyimide was carried out in 1908,[119] it was not until the late 1950s that high molecular weight polymers were prepared.[120,121,122] Even today the preparation mechanisms are still not well understood.

Some comprehensive reviews can be found in books and reviews.[123,124,125,126] This part of

[118] IUPC Macrom. Chem. Div. (IV) Commission on Macromolecular Nomenclature *Macromolecules* **1997**, *30*, 7356.
[119] Bogert, T. M.; Renshaw *J. Am. Chem. Soc.* **1908**, *30*, 1140.
[120] E. I. du Pont de Nemours & Co. *French Pat.* **1960**, 1239491.
[121] Edwards, W. M. *U.S. Pats.* **1965**, 3179614 and 31179634; *Brit. Pat.* **1959**, 898651.
[122] Endrey, A. L. U. *S. Pats.* **1965**, 3179631 and 3179633; *Can. Pat. 1963*, 659328.
[123] *Polyimides* Wilson, D.; Stenzenberger, H. D.; Hergenrother, P. M. Ed. Blackie &Son Ltd. Chapman & Hall: New York, **1990**.
[124] *Polyimides: Fundamentals and Applications* Ghosh, M. K.; Mittal, K. L. Ed. Marcel Dekker, Inc., **1996**.

review will deal with the basic synthesis and characterization aspects of polyimides.

### 1.2.1 Synthesis of Polyimides

Designing a proper approach for the synthesis of polyimides is dependent on the nature of the final polymer structures. The polymerization can be fulfilled either in solution or melt.

#### *1.2.1.1 Classical Two-step Method via Poly(amic acid)s*

The pioneering work at DuPont Co. on the synthesis of high molecular weight polyimide resulted in a classic two-step approach.[120] This method has been used to synthesize insoluble and infusible aromatic polyimides. Scheme 1.2.2 shows the approach for preparing commercial Kapton® polyimide.[127,128] This conventional method includes two steps: in the first step, the poly(amic acid) is formed; the following step involves the imidization of poly(amic acid).

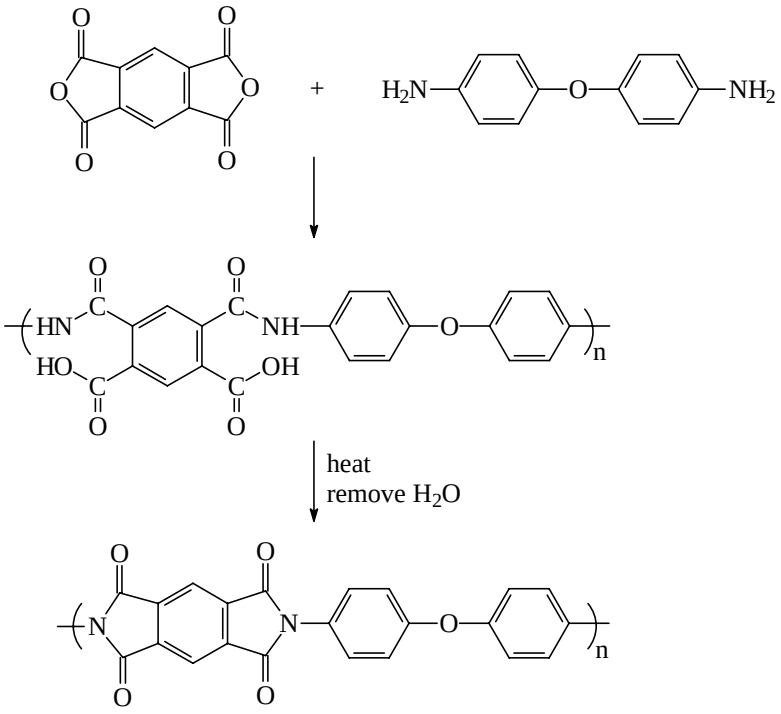


Scheme 1.2.2 Preparation of Kapton® polyimide (simplified)

[125] Sillion, B. in *Comprehensive Polymer Science* **1989**, Vol. 5, p499.
[126] McGrath, J. E.; Dunson, D. L.; Mecham, S. J.; Hedrick, J. L. *Adv. Polym. Sci*. **1999**, *140*, 61.
[127] Sroog, C. E.; Endrey, A. L.; Abramo, S. V.; Edwards, C. E.; Olivier, K. L. *J. Polym. Sci.* **1965**, *3*, 1373.
[128] Sroog, C. E. *Prog. Polym. Sci*. **1991**, *16*, 561.

#### 1.2.1.1.1 Formation of Poly(amic acid)s

The poly(amic acid) can be easily obtained by reacting a dianhydride and a diamine in a dry aprotic dipolar solvent at no higher than ambient temperatures because this reaction is reversibly exothermic.[129] The diamine should have moderate nucleophility in order to promote attacking the carbonyl group, without forming a salt with carboxyl group. An optimal $pK_b$ value was suggested to be in the range of 4.5-6.[130] Incorporating electron-withdrawing group into the dianhydride increases the reaction rate due to the increase of the electrophilicity of the carbonyl group. While the structures of both the diamine and the dianhydride may influence the rate of the formation of poly(amic acid), recent studies by Kim *et al.* showed that the structure variations of diamine play a more significant effect.[131]

The reaction medium also plays a very important role on the formation of poly(amic acid). The widely used solvents are the aprotic dipolar solvents, such as dimethylformamide (DMF), dimethylacetamide (DMAc), N-methylpyrrolidone (NMP), and dimethyl sulfoxide (DMSO). It was surmised that the strong hydrogen bonding interactions between poly(amic acid) and the solvents drive the equilibrium to poly(amic acid). The assumption was supported by the reaction rate of phthalic anhydride and 4-phenoxyaniline in different reaction solvents. The order of reaction rate was shown in the order of THF < acetonitrile < DMAc.[132] Riffle and coworkers found, however, that the rate order is THF>>NMP.[133]

Although the major reaction is the formation poly(amic acid), some side reaction may also occur, as shown in Table 1.2.1.[134] Small amounts of dianhydride may hydrolyze in the presence of water that may come as a by-product of the imidization or as an impurity of reaction medium. It is well known that water can gradually degrade the poly(amic acid).[135] To avoid degradation and hydrolyzation, poly(amic acid) should be kept at low temperature and free of moisture.

---

[129] Harris, F. W. in *Polyimides* Wilson, D.; Stenzenberger, H. D.; Hergenrother, P. M. Ed. Blackie & Son Ltd.: Glasgow and London, **1990**.
[130] Hodgkin, J. H. *J. Polym. Sci., Polym. Chem. Ed.* **1976**, *14*, 409.
[131] Kim, Y. J.; Glass, T. E.; Lyle, G. D.; McGrath, J. E. *Macromolecules* **1993**, *26*, 1344.
[132] Solomin, V. A.; Kalnins, K.; Kudryavtsev, V. V.; Koton, M. M. *Dokl. Akad. Nauk USSR (Engl. Transl.)* **1977**, *237*, 693.
[133] Facinelli, J. V.; Gardner, S. L.; Dong, L.; Sensenich, C. L.; Davis, R. M.; Riffle, J. S. *Macromolecules* **1996**, *29*, 7342.
[134] Volksen, W. *Adv. Polym. Sci.* **1994**, *117*, 111.
[135] Frost, L. W.; Kesse, I. *J. Appl. Polym. Sci.* **1964**, *8*, 1039.

Table 1.2.1 Major Reaction Pathways Involved in Poly(amic acid) Synthesis[135]

| Reactions Related to the Formation of Poly(amic acid) | Reaction Type | Rate Constant |
|---|---|---|
| 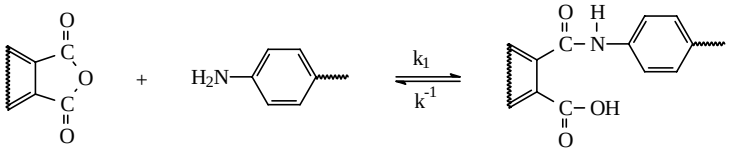 | Propagation ($k_1$) | 0.1-0.5 |
| | Depropagation ($k_{-1}$) | $10^{-5}$-$10^{-6}$ |
| 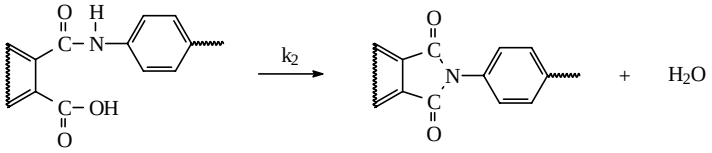 | Spontaneous Imidization ($k_2$) | $10^{-8}$-$10^{-9}$ |
| 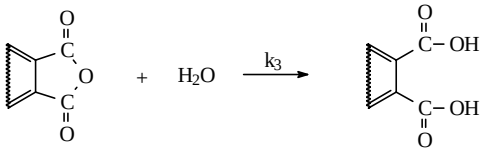 | Hydrolysis ($k_3$) | $10^{-1}$-$10^{-2}$ |
| 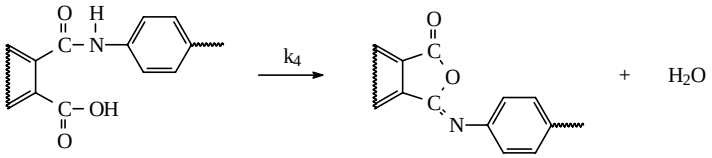 | Isoimide Formation ($k_4$) | N/A |
| 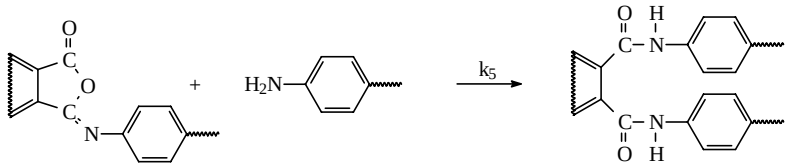 | Diamide Formation($k_5$) | N/A |
| 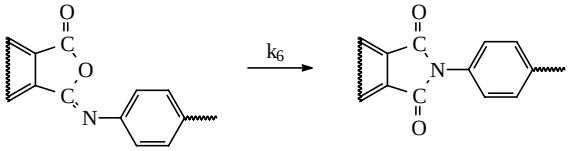 | Isomerization($k_6$) | N/A |

*Rate constants were estimated for a typical polymerization at ca. 10 wt.% concentration, i.e. 0.5 M.

### 1.2.1.1.2 Imidization of Poly(amic acid)

Imidization can be achieved by various approaches such as thermal imidization, chemical imidization, solution imidization. Different imidization approaches can be adopted according to the nature and the applications of the final products.

- **Thermal Imidization of Poly(amic acid)s**

The first pathway for cyclization of the amic acid moiety into imide involves gradual heating of poly(amic acid) up to 250-350 °C. During this process, the solvent can be removed and water evolves as a by-product. Two possible mechanisms were proposed as shown in Scheme1.2.3.[136] Experimental results showed extremely small amide dissociation constants.

[136] Harris, F. W. in *Polyimides* Wilson, D.; Stenzenberger, H. D.; Hergenrother, P. M. Ed. Blackie & Son Ltd.:

Furthermore, addition of acid increased the imidization rate.[130,137,138] These results supported mechanism 1 (Scheme 1.2.3).[136]

Mechanism 1.

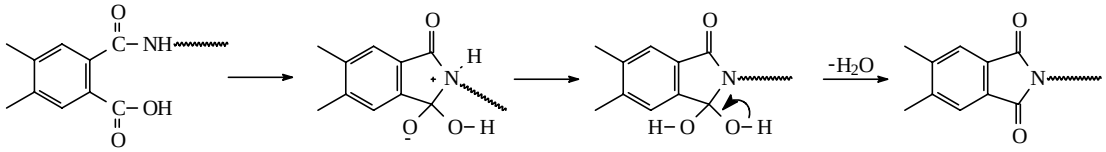

Mechanism 2.

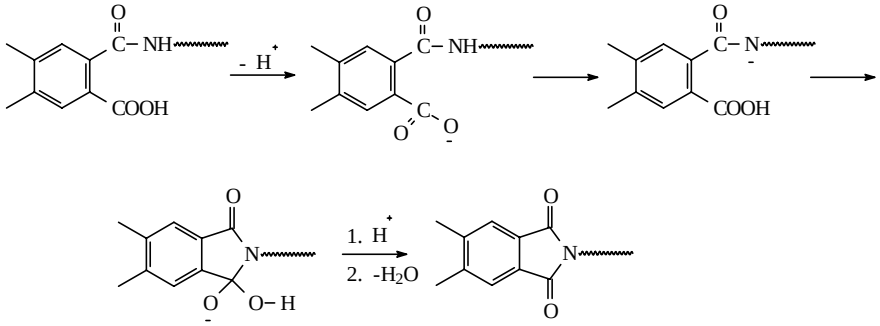

Scheme 1.2.3 Possible imide formation mechanisms[136]

Thermal imidization is widely used for preparing thin films, coatings, fibers, and powders since the solvent and by-product can be easily removed without generating voids and defects. Carefully choosing the imidization procedure may eliminate cracks caused by shrinkage stress.

Thermal imidization may not lead to 100% conversion, because increasing the heating temperature above 300 °C may lead to the "kinetic interruption" effect. Partially reversible decrease of molecular weight at the early stage of imidization was observed due to the depolymerization reaction. Direct evidence was the observation of the temporary appearance of the anhydride carbonyl absorption band near 1860 $cm^{-1}$ between 100-250 °C.[139,140,141]

---

Glasgow and London, **1990**.

[137] Lavrov, S. V.; Ardashnikov, A. Y.; Kardash, I. Y.; Pravednikov, A. N. *Polym. Sci. USSR (Engl. Transl.)* **1977**, *19*, 1212.

[138] Lavrov, S. V.; Talankina, O. B.; Vorob'yev, V. D.; Izyumnikov, A. L.; Kardash, I. Y.; Pravednikov, A. N. *Polym. Sci.USSR (Engl. Transl.)* **1980**, *22*, 2069.

[139] Fjare, D. E.; Roginski, R. T. in *Advances in Polyimide Science and Technology* Feger, C.; Khojasteh, M. M.; Htoo, M. S. Ed. Technomic, Lancaster, PA **1993**, p326.

[140] Dine-Hart, R. A.; Wright, W. W. *J. Appl. Polym. Sci.* **1967**, *11*, 609.

[141] Laius, L. A.; Tsapovetskii in *Polimides: Synthesis, Characterization and Applications* Mittal, K. L. Ed. Vol. 1 Plenum, New York, **1984**.

Further evidence was provided by measuring the molecular weight of soluble polyimide at different thermal imidization stages.[142] Other side reactions may include some form of crosslinking.[143]

- **Chemical imidization of poly(amic acid)s**

Chemical imidization of amic acid involves the use of a chemical dehydrating agent to promote ring closure reactions within a temperature ranged from 20 to 80 °C. Commonly used dehydrating reagents are acid anhydrides, such as acetic, propionic, *n*-butyric, benzoic anhydrides, etc. in aprotic polar solvents or in the presence of tertiary amines. Commonly used amine catalysts include trialkylamines, pyridine, lutidine, N-methylmorpholine. Both soluble and insoluble polyimides can be prepared by this method.[144,145]

Many factors, such as dehydrating agents, types of monomers, reaction temperatures, may affect the molecular weight of the final polymer. Kinetic study of chemical imidization process led to a proposed mechanism (Scheme 1.2.4).[132,146]

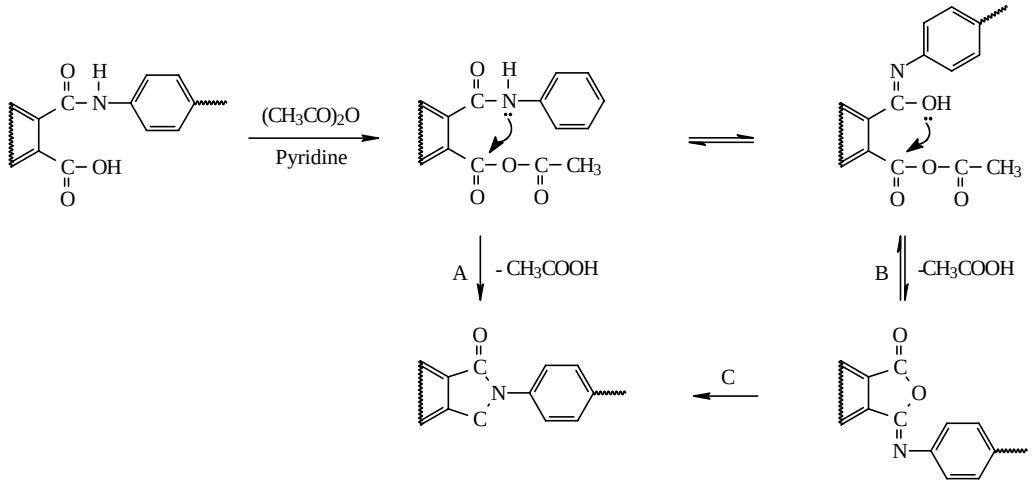


Scheme 1.2.4 Mechanism involved in chemical dehydration of amic acid

The poly(amic acid) reacts with acetic anhydride to yield a mixed anhydride intermediate. The amide tautomer cyclizes to afford the thermally favored imide. The mixed anhydride can further tautomerize from the amide to the iminol form, which generates the kinetically

[142] Young, P.R.; Davis, J. R.; Chang, A. C.; Richardson, J. N. *J. Polym. Sci., Polym. Chem. Ed.* **1990**, *28*, 3107.
[143] Snyder, R. W.; Thomson, B.; Bartges, B.; Czerniwski, D.; Painter, P. C. *Macromolecules* **1989**, *22*, 4166.
[144] Vinogradova, S. V.; Vygodskii, Ya. S.; Vorob'ev, V. D.; Churochkina, N. A.; Chudina, L. I.; Spirina, T. N.; Korshak, V. V. *Polym. Sci. USSR (Eng. Transl.)* **1974**, *16*, 584.
[145] Ranney, M. W. in *Polyimide Manufacture* Noyes Data Corp, Park Ridge, NJ **1971**.
[146] Koton, M. M.; Kudryavtsev, V. V.; Zubkov, V. A.; Yakimanskii, A. V.; Meleshko, T. K.; Bogorad, N. N. *Polym.*

favored isoimide form. Isoimide form may further convert to thermally stable polyimide. The reaction can be promoted by tertiary amine.

The major advantage of this approach over thermally induced process is that the degree of polymerization remains constant since no obvious depolymerization occurs during imidization process. The disadvantages include additional expenses and complicated process.

- **Solution imidization of poly(amic acid)s**

Solid state thermal imidization often affords polyimides that are insoluble, infusible and thus are intractable. High temperature solution imidization may minimize this problem. Cyclodehydrations are fulfilled in high boiling point solvent at 160-200 °C in the presence of an azeotropic solvent. In contrast to bulk polymerization, this process can be performed at much lower temperature. Therefore, degradation and other side reactions may be prevented.

By means of 2D-$^{1}$HNMR, Kim *et al.* demonstrated that the poly(amic acid) chains cleaved to form o-dicarboxylic acids and amine endgroups as water liberated from the reaction caused initial hydrolysis of partially imidized poly(amic acid)s.[130] As the reaction proceeded, the endgroups recombined or the chains "healed" to form polyimides resulting in an increase in molecular weight. The same phenomenon is believed to occur in bulk thermal imidization.

Preparation of high molecular weight poly(amic acid)s is not necessary in this procedure. Although imidization still proceeds via amic acid intermediate, the concentration of amic acid is very low during the polymerization because of its short lifetime at high temperature due to rapid imidization, or conversion to amine and anhydride.

Polyimides may also be prepared in one pot. After the formation of poly(amic acid)s, they can be directly imidized in solvent at high temperature.[130] Commonly used solvents include aprotic amides, nitrobenzene, benzonitrile, $\alpha$-chloronaphthalene, *o*-dichlorobenzene, trichlorobenzene, and phenolic solvents, e.g. *m*-cresol and chlorophenols. Toluene, *o*-dichlorobenzene, 1-cyclohexyl-2-pyrrolidinone (CHP) are widely used as the azeotropic cosolvents to remove water from the reaction system.

The amic acid can be fully imidized by the one-pot high temperature solution synthesis.

---

*Sci. USSR (Engl. Transl.)* **1984**, *26*, 2839.

Neither amic acid nor isoimide type has been detected in the final products. This may lead to polyimide with different mechanical properties compared with their counterpart made by conventional two-step technique.[147,148] In addition, some sterically or electronically hindered monomers can still yield high molecular weight polyimides that would otherwise be hard to successfully polymerize via a two-step route.

#### *1.2.1.2 Polyimides from Diester-Acids and Diamines (Ester-Acid Route)*

In the ester-acid synthesis route, the dianhydride readily reacts with alcohol to afford ester-acid. Subsequently, the diamine is added into the ester-acid solution to yield desirable poly(amic acid) and polyimide.[149,150]

In this process, the dianhydride is refluxed in the presence of excess amounts of alcohol, e.g., ethanol. Some weak organic bases, e.g., triethylamine (TEA), have been observed to significantly increase the reaction rate because these bases act as an acid acceptor. Evaporating excess amount of alcohol afforded the desirable diester diacid, which can react with a diamine in the solution. Again, an aprotic solvent is needed for stabilizing poly(amic acid). The poly(amic acid) can be imidized by either thermal or high temperature solution approach.

Earlier it was surmised that the conversion of ester acids into amic acids was achieved by nucleophilic substitution. Recent investigations, however, have found that the ester acid was converted into anhydride at elevated temperature in situ.[151,152,153] The generated anhydride readily reacts with the amine under the reaction conditions.

The major advantage of this approach is its tolerance with water. Residual water in the solvent does not significantly affect the molecular weight.

#### *1.2.1.3 Polyimide via Amine-Imide Exchange Reaction (Transimidization)*

In 1945, Spring *et al.* reported preparing N-alkyl imides by exchange reaction of an imide

[147] Harris, F. W.; Hsu, S. L-C. *High Perform. Polym.* **1989**, *1*, 3.
[148] Oishi, Y.; Ishida, M.; Kakimoto, M.; *et al. J. Polym. Sci. Polym. Chem.* **1992**, *30*, 1027.
[149] Moy, T. M.; DePorter, C. D.; McGrath, J. E. *Polymer* **1993**, *34*, 819.
[150] Johnston, J. C.; Meador; M. A. B.; Alston, W. B. *J. Polym. Sci., Polym. Chem. Ed.* **1987**, *25*, 2175.
[151] Moy, T. M.; DePorter, C. D.; McGrath, J. E. *Polymer* **1993**, *34*, 819.
[152] Moy, T. M. *Ph.D. Dissertation*, Virginia Tech: Blacksburg, VA, **1993**.
[153] Johnston, J. C.; Meador, M. A. B.; Alston, W. B. *J. Polym. Sci., Polym. Chem.* **1987**, *25*, 2175.

(phthalimide) with an alkyl amine (methylamine).[154] However, use of this reaction was due in 1960's to DuPont[155] and Imai *et al.*[156] Scheme 1.2.5 showed some examples of polyimides prepared by this approach.

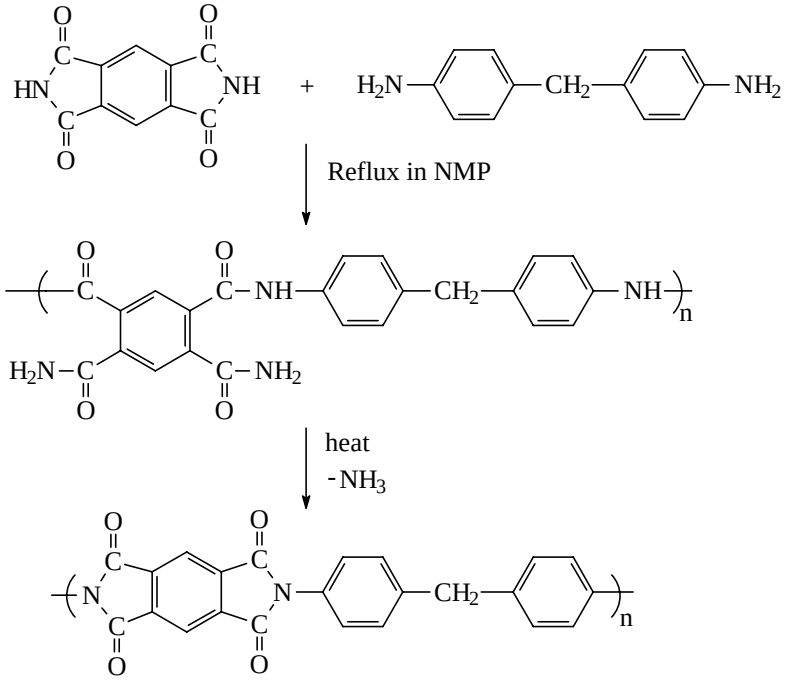


(a)

[154] Spring, F. S.; Wood, J. C. *J. Chem. Soc.* **1945**, *625*.
[155] Neth. Pat. Appl. To DuPont **1965**, *61413552*.
[156] Imai, Y. *J. Polym. Sci*., *Polym. Chem. Ed*. **1970**, *8*, 555.

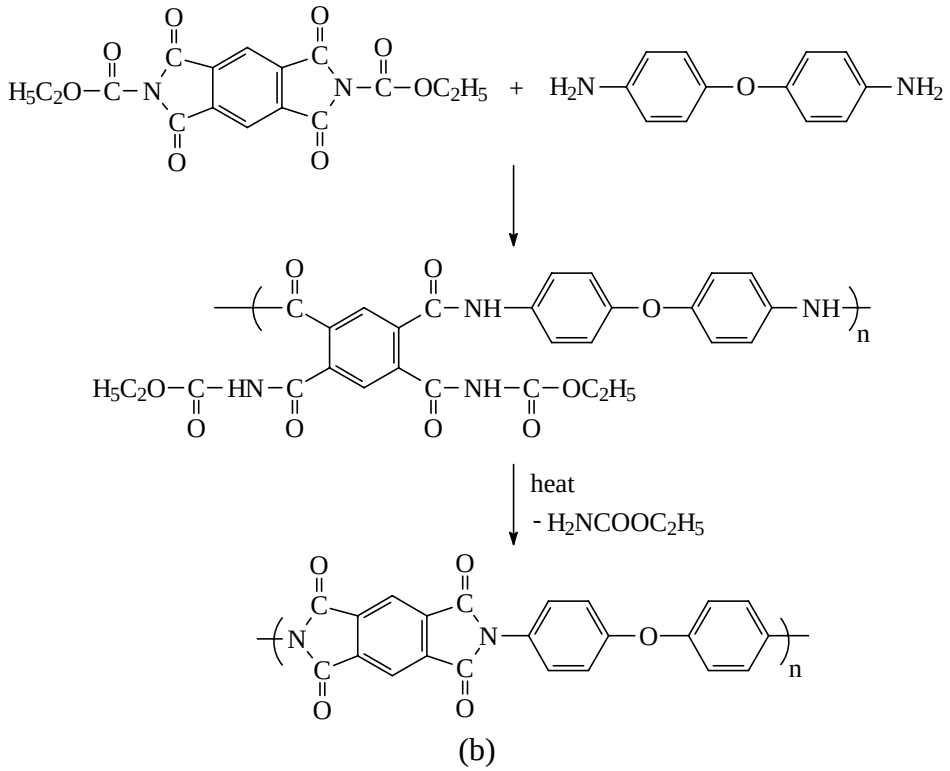


(b)

Scheme 1.2.5 Preparation of polyimides via amine-imide exchange reaction (transimidization)

The amine used for exchange reaction needs to be more basic or nucleophilic than its counterpart to be exchanged. Utilizing this approach, Rogers *et al.* successfully prepared perfectly alternating polyimide-poly(dimethyl siloxane) (PI-PDMS) block copolymers.[157] The imide oligomers endcapped with 2-aminopyrimidine were allowed to react with aminopropyl terminated PDMS in chlorobenzene. High molecular weight and fully imidized polymers can be prepared within 2 h at temperatures of 60-110 °C.

### *1.2.1.4 Polyimides from Dianhydrides and Diisocyanates*

Phthalic anhydride was known to react with aromatic and aliphatic isocyanates to give N-aryl and N-alkylphalimides.[158] This reaction was also used to successfully synthesize polyimides with the development of polyimide synthesis. The reaction is believed to experience a seven-member ring intermediate that immediately yields polyimide with the evolution of $CO_2$ in the absence of catalysts (Scheme 1.2.6).[159]

[157] Rogers, M. E.; Glass, T. E.; Mecham, S. J.; Rodrigues, D.; Wilkes, G. L.; McGrath, J. E. *J. Polym. Sci., Polym. Chem. Ed.* **1994**, *32*, 2663.
[158] Hurd, C. D.; Prapas, A. G. *J. Org. Chem.* **1959**, *24*, 388.
[159] Meyers, R. A. *Polym. Prepr., ACS* **1969**, *10 (1)*, 186.

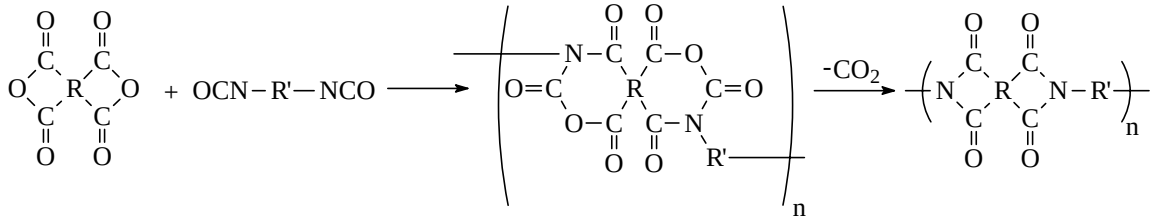

Scheme 1.2.6 Mechanism of polyimides from dianhydrides and diisocyanates

The aliphatic isocyanates react much faster than their aromatic counterpart. The reaction can be further accelerated by adding catalysts, such as tertiary amines, alkali metal alcoholate, metal lactamate, water, and alcohols. Addition of catalytic water promotes the formation of amine, which reacts with dianhydride to generate polyimide. However, adding water may also lead to the hydrolysis of the isocyanate.[160] Polyimide foams can be prepared by taking the advantage of the evolution of $CO_2$.

### *1.2.1.5 Polyimides via Polyisoimide Precursors*

Polyisoimides are significantly more soluble and possess lower melt viscosities and $T_g$ than their polyimide counterparts, probably due to their lower symmetry and structural irregularity.[161] Utilizing this property made it possible to prepare rigid polyimides though soluble and processible polyisoimide precusors.[162]

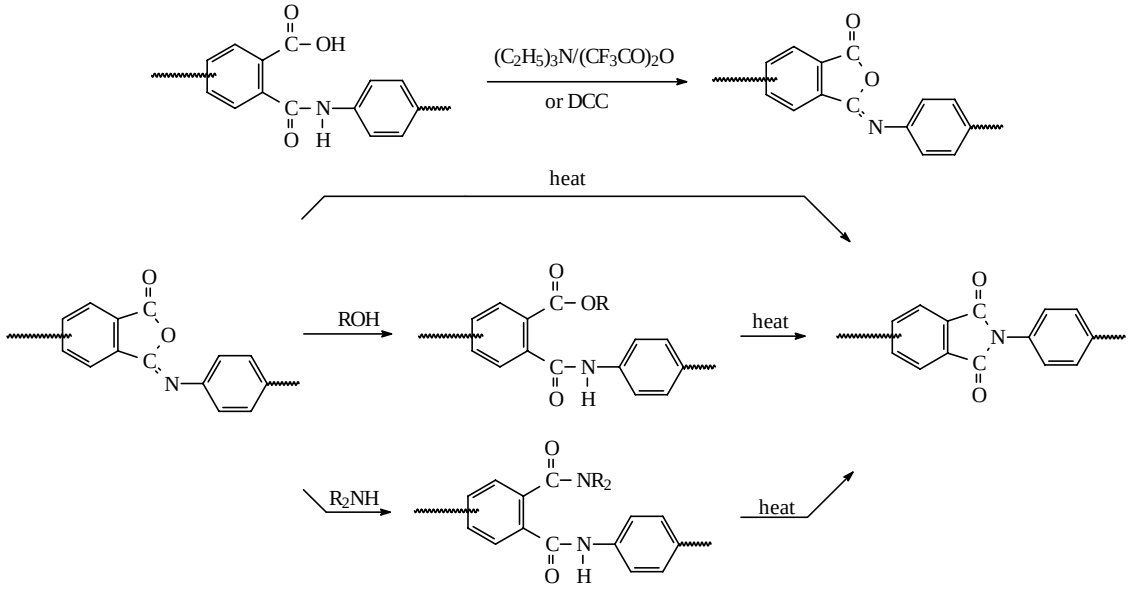

[160] Carleton, P. S.; Farrissey, W. J. Jr.; Rose, J. S. *J. Appl. Polym. Sci.* **1972**, *16*, 2893.
[161] Mochizuki, A.; Teranishi, T.; Ueda, M. *Polym. J.* **1994**, *26*, 315.
[162] Wallace, J. S.; Arnold, F. E.; Tan, L. S. *Polym. Prepr., ACS* **1987**, *28 (2)*, 316.

Scheme 1.2.7 Polyimides via polyisoimides precursors

Poly(amic acid)s can be easily converted into polyisoimides in the presence of dehydrating agent, such as trifluoroacetic anhydride, in conjunction with triethylamine. N-dicylcohexylcarbodiimide (DCC) and acetyl chloride were reported to give high yield.[163] Polyisoimides can be converted into corresponding polyimides either by thermal treatment (> 250 °C), or by reacting with alcohols followed by thermal treatment,[164] or by reacting with amines followed by thermal treatment (Scheme 1.2.7).[165]

### *1.2.1.6 Polyimides from Tetracarboxylic Acids and Diamines*

Aromatic-aliphatic polyimides can hardly be prepared by traditional approaches, because the aliphatic diamines are more basic compared with aromatic amines and tend to react with dianhydrides to yield salt rather than generate poly(amic acid)s. However, an approach similar to the synthesis of nylon can be adopted to prepare this kind of polyimide. Typically, the salts can be thermally imidized at temperature above 200 °C under high pressure (Scheme 1.2.8). No poly(amic acid) form was detected during the reaction process, suggesting the formation of poly(amic acid) and the imidization take place simultaneously with imidization as the rate determining step.[166]

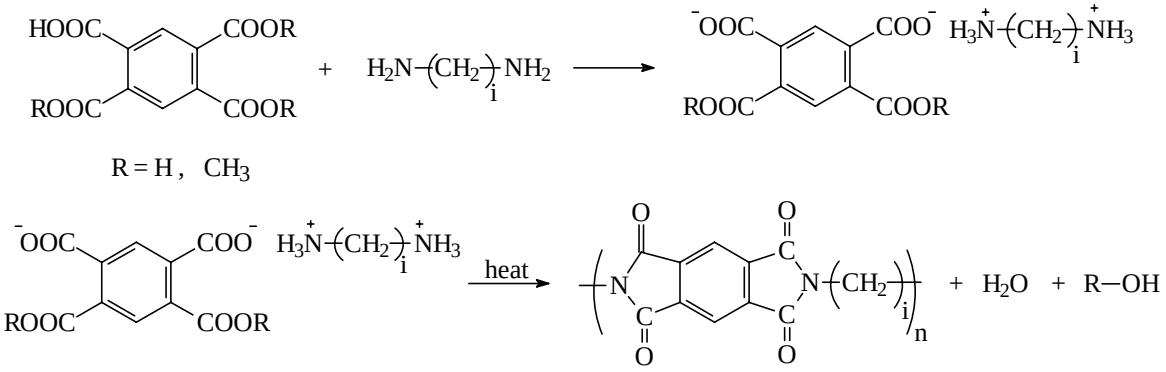


Scheme 1.2.8 Polyimide from tetracarboxylic acid-amine salt

The major advantage of using tetracarboxylic acids in this one-step melt polymerization includes low melt viscosities in the initial stage. In addition, tetracarboxylic acids are quite stable and easy to purify. Many tetracarboxylic acids can be recrystallized from hot water.

---

[163] Angelo, R. J.; Golike, R. C.; Tatum, W.; Kreuz, J. A. in *Advances in Polyimide Science and Technology* Weber, W. D. and Gupta, M. R. Ed. Plast. Eng.: Brookfield, CT, **1985**, p67.
[164] Tan, L.; Arnold, F. E. *Polym. Prepr., ACS* **1988**, *29 (2)*, 316.
[165] Delvigis, P.; Hsu, L. C.; Serafini, T. T. *J. Polym. Sci., Part C* **1970**, *8*, 29.

### *1.2.1.7 One-pot Procedure Utilizing Thioanhydrides*

Oishi *et al.* reported a new method to prepare soluble polyimides.[167] They used a bulky diamine, 4,4´-diaminotriphenylamine in conjunction with thioanhydride analogs of BTDA, PMDA, DSDA and BPDA. Polyimides were prepared in NMP at 140 °C in a nitrogen atmosphere (Scheme 1.2.9).

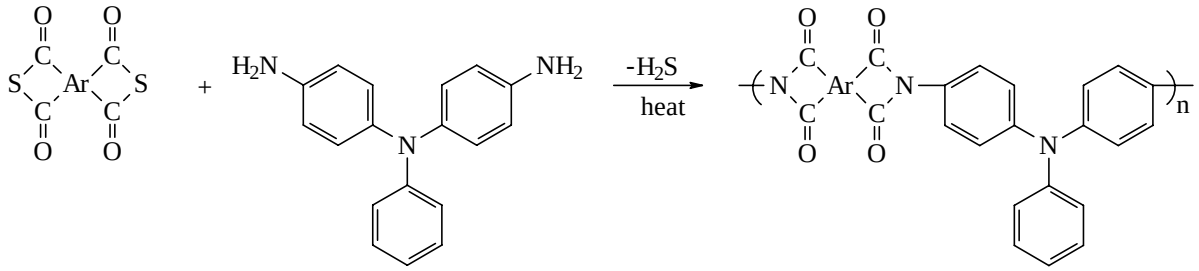


Scheme 1.2.9 Polyimide synthesis utilizing thioanhydrides as monomers. Ar can be any central aromatic unit commonly found in conventional dianhydrides

The polyimides prepared by this approach were slightly more soluble compared with their counterparts by the standard two-stage procedure with thermal imidization. However, when the films were heated above 300 °C, they became less soluble and essentially the same as their counterparts. Elimination of the morphology differences and the further reaction among the reactive end-groups at high temperatures may be responsible for the results.

Instead of water, only volatile $H_2S$ evolves. Therefore, the effect of water in this approach is eliminated. However, the toxicity of $H_2S$ by-product limits its applications.

### *1.2.1.8 Indirect Synthesis*

Polyimides can be prepared indirectly from small molecular imides without forming or breaking imide bonds, provided that the small molecular imides have some active groups that can be used to polymerize. A couple of routes have been developed to prepare polyimides based on some well-known reactions. It is expected that some other reactions, e.g. Heck reaction, Stille reaction, may also be used for this purpose, as long as the reactions are tolerable to imide groups and the conversion can be achieved in 100% yield. The major advantage for these series reactions is that no crucible imidization conditions are required.

---

[166] Sato, M. in *Handbook of Thermoplastics* Olabisi, O. Ed. Marcel Dekker: New York, **1997**, p665.
[167] Oishi, Y.; Ishida, M.; Kakimoto, M-A.; Imai, Y.; Kurosaki, T. *J. Polym. Sci., Polym. Chem. Ed.* **1992**, *193*, 1509.

Thus, a lot of side reactions related to imidization reaction can be prevented.

### 1.2.1.8.1 Polyimides via Nucleophilic Substitution Reaction

Similar to the synthesis of poly(arylene ether sulfone)s[4,5,6,7] by aromatic nucleophilic substitution of bishalo- and bisnitro- groups, poly(ether imide)s were also prepared by substituting aromatic halo- and nitro-groups on the bishaloimide[168,169] or bisnitroimides[170,171] rings since these groups are also strongly activated by imide groups toward nucleophilic substitution reaction. Scheme 1.2.10 (A) shows the synthesis of poly(ether imide)s by nucleophilic substitution.

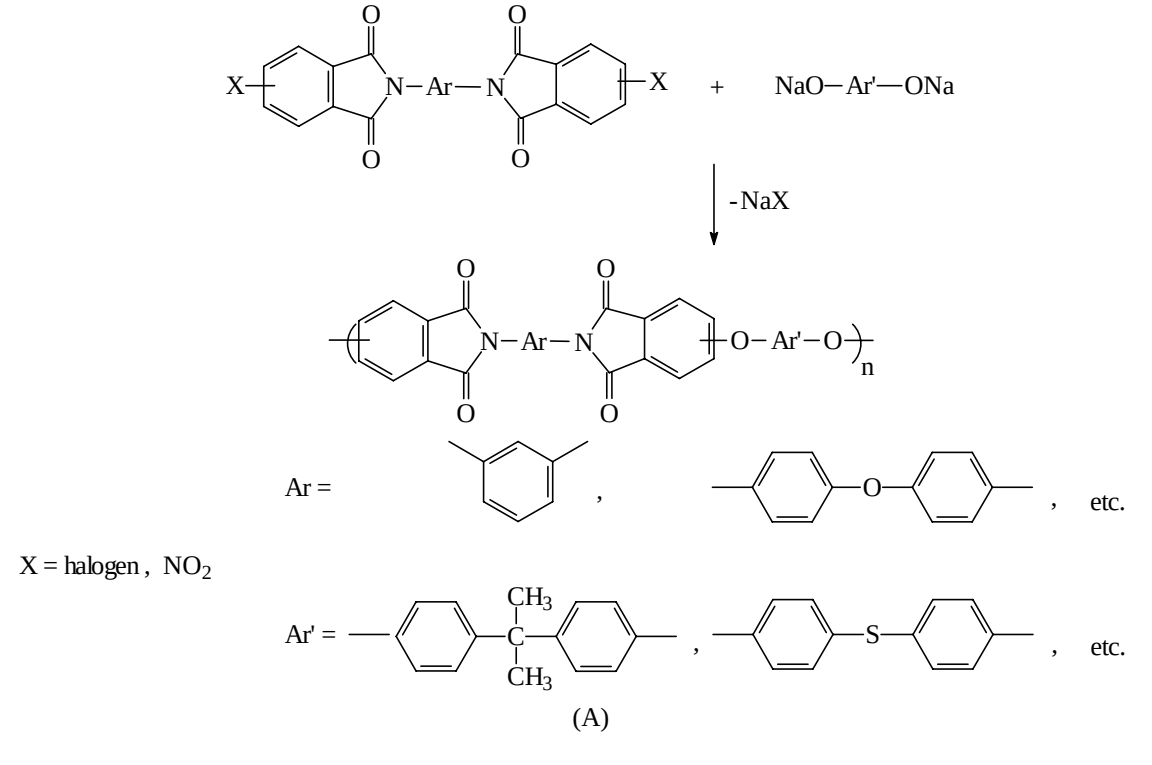


(A)

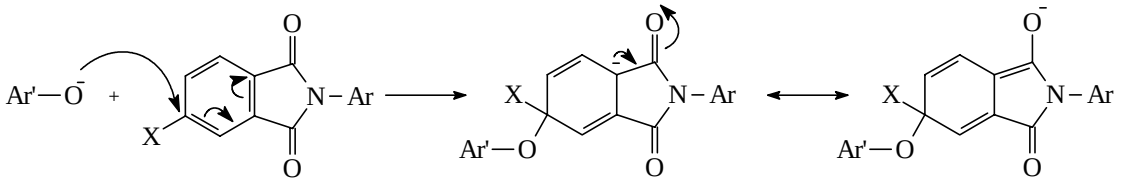

(B)

[168] Wirth, J. G.; Health, D. R. *U.S. Patent 3786364* to General Electric Co. **1974**.
[169] Williams, F. J. *U.S. Patent 3847869* to General Electric Co. **1974**.
[170] Wirth, J. G.; Health, D. R. *U.S. Patent 3838097* to General Electric Co. **1974**.
[171] Takekoshi, T.; Wirth, J. G.; Health, D. R.; Kochanowski, J. E.; Manello, J. S.; Webber, M. J. *J. Polym. Sci., Polym. Chem. Ed*. **1980**, *18*, 3069.

Scheme 1.2.10 Synthesis of polyimides by nucleophilic aromatic substitution (A) and delocalization of negative charge in Meisenheimer transition state in imide system (B).[172]

Halo- and nitro-substituted imides are more reactive than the corresponding sulfones and ketones due to their stronger electron withdrawing ability. The Meisenheimer type transition state is well stabilized by the effective delocalization of the negative charge as shown in Scheme 1.2.10 (B).[172]

This approach is fast and some typical side reactions in polyimide synthesis can be avoided since no amic acid and imidization steps are involved. However, $NaNO_2$ may be basic enough to degrade the imide at the carbonyl group.

#### 1.2.1.8.2 Polyimides via Addition Reactions

Bisimide monomers or oligomers with unsaturated C=C bonds, such as maleiimide, acetylene, and xylene groups, may go through Diels-Alder reaction with bisdienes, e.g. biscyclopentadienes, bisfurans.[173] Another approach is using poly(bismaleiimidediamine)s Michael addition.[174]

#### 1.2.1.8.3 Palladium-Catalyzed Coupling Utilizing Imide-Containing Monomers

Palladium-catalyzed coupling reaction used for the synthesis of polyimides is a new approach. Helmer-Metzmann *et al.* introduced palladium-catalyzed coupling reaction into the polyimide synthesis.[175] The approach is shown in Scheme 1.2.11.

[172] Takekoshi, T. in *Polyimides* Wilson, D.; Stenzenberger, H. D.; Hergenrother, P. M. eds. P38. Blackie & Son Ltd.: Glassgow and London, **1990**.
[173] Alhakimi, G.; Klemm, E. *J. Polym. Sci. Polym. Chem.* **1995**, *33*, 767.
[174] Laurienzo, P.; Malinconico, M.; Perenze, Z.; Segre, A. L. *Macromol. Chem. Phys*. **1994**, *195*, 3057.
[175] Helmer-Metzmann, F.; Rehahn, M.; Schmitz, L.; Ballauff, M.; Wegner, G. *Makromol. Chem.* **1992**, *193*, 1847.

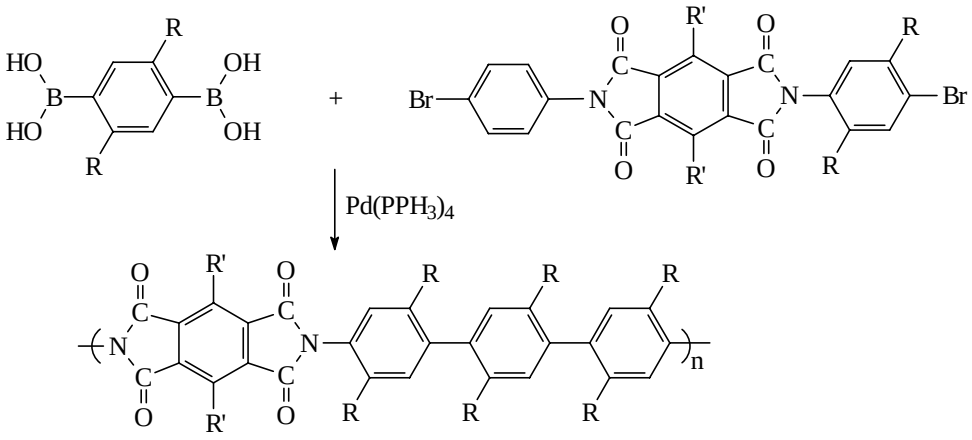


Scheme 1.2.11 Palladium-catalyzed coupling reaction. R is n-dodecyl; R′ can be H, phenyl, phenoxy or cresoxy. Nucleophilic substitution at R' sites with azo dyes can also be accomplished

The reaction was performed in a heterogeneous mixture of toluene and 2 M aqueous sodium carbonate at a 50:50 (v/v) ratio using tetrakis(triphenylphosphine)-palladium ($Pd(Ph_3)_4$) as the catalyst under refluxing for 48 h. The number average molecular weights of the prepared polyimides were around 20,000 measured by membrane osmometry. The obtained polymers were also soluble in chloroform and dichlorobenzene. Substitution on the phenyl ring of diimide (for example, R´=phenyl) significantly increased the molecular weight due to increased polymer solubility in the reaction medium.[176]

Another approach of coupling was also reported by Perry *et al.* In this approach, a palladium-mediated carbonylation and condensation of diiodo monomers and aromatic diamines were used.[177,178,179] As an example, tetraiodobenzene was reacted with aromatic diamines under CO pressure of approximately 95 *psi* and in the presence of a palladium catalyst (bis(triphenylphosphine) palladium (II) chloride) at 115 °C as shown in Scheme 1.2.12. High molecular weight polymers could be prepared. This route has the advantage of making fully imidized polymers without using hydrolytically sensitive monomers.

[176] Schmitz, L.; Rehahn, M. Ballauff, M. *Polymer* **1993**, *34*, 646.
[177] Perry, R. J.; Turner, S. R.; Blevins, R. W. *Macromolecules* **1994**, *27*, 4058.
[178] Perry, R. J.; Turner, S. R.; Blevins, R. W. *Macromolecules* **1993**, *26*, 1509.
[179] Perry, R. J.; Turner, S. R. *J. Macromol. Sci., Chem.* **1991**, *A28*, 1213.

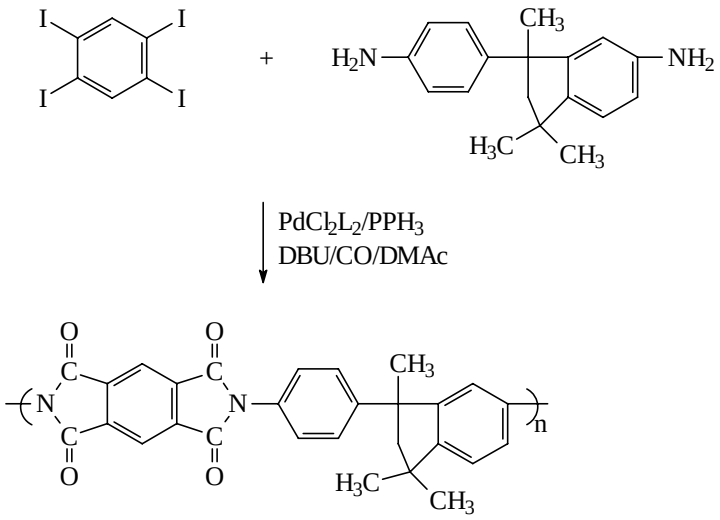


Scheme 1.2.12 Palladium-catalyzed route to polyimides

### 1.2.2 Solution and Melt Processibility

The rigid chains of polyimides may increase several types of chain-chain interactions. Packing interactions, such as crystallinity, are major factors in determining polyimide properties. Most polyimides are semicrystalline polymers with very high $T_g$ and $T_m$. The crystals generally have extremely high melting temperatures and can function as physical crosslinks in a system, leading to desirable thermal and mechanical properties.[180] Some polyimides with intermediate $T_m$ can be processed in melt. Unfortunately, many of them are usually not quite soluble in common organic solvents or not melt processible due their too strong intermolecular interactions, high crystallinity, and $T_m$. The strong interchain interactions further increase the insolubility and infusibility. Therefore, processing polyimides is not a trivial issue. Usually, polyimides have to be processed before imidization. As a consequence, processing polyimides is generally carried out from poly(amic acid) solutions that are cast into films, spun into fibers or coated onto the composite reinforcement materials, and then subjected to rigorous thermal treatment to convert the polymeric acid to polyimide. Several inherent problems may exist. The undesirable water and volatiles are released during thermal treatment. Therefore, the voids and stresses may develop and are hard to avoid. In addition, substantial shrinkage may occur as a more coil-like poly(amic acid)

[180] (a) Srinivas, S.; Graham, M.; Brink, M. H.; Gargner, S.; Davis, R. M.; McGrath, J. E.; Wilkes, G. L. *Polym. Eng. Sci*. **1996**, *36*, 1928; (b) Srinivas, S.; Caputo, F. E.; Graham, M.; Gradner, S.; Davis, R. M.; McGrath, J. E.; Wilkes, G. L. *Macromolecules* **1997**, *30*, 1012; (c) Ratta, V.; Stancik, E. J.; Ayambem, A.; Pavatareddy, H.; McGrath, J. E.;

contracts into a more rod-like polyimide. Shrinkage may also generate stresses in the final product. One way to alleviate the problem is to synthesize soluble polyimides since soluble polyimides can be imidized in solution and further processed in solution.[181,182]

To increase the solubility, one has to decrease the structural symmetry. This includes introducing angular or flexible linkages into the backbone; introducing kinked linkages (*meta*- and *ortho*-catenations) or unsymmetrical and cardo (loop) structures; incorporating large polar or nonpolar pendent bulky groups along the polymer backbones; and disrupting the symmetry of polymer chains by copolymerization.[183,184,185] Introducing irregularity could decrease the interchain interactions.

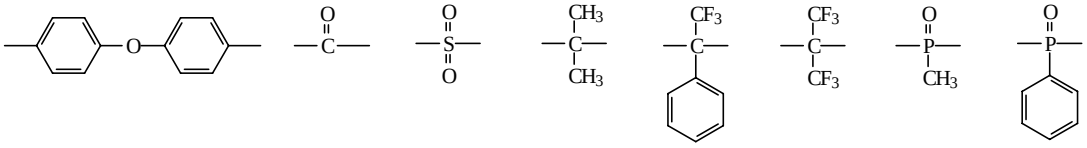

Scheme 1.2.13 Some commonly used flexible or angular units

Some commonly used flexible or angular units were shown in Scheme 1.2.13.[186,187,188,189,190,191]

### 1.2.3 Thermosetting Polyimides

A subset family of polyimides, the thermosetting polyimides are very important. Oligomeric polyimides containing the moieties shown in Scheme 1.2.14 can be thermally cured. Oligomeric polyimides can be processed in common organic solvents and cured at high temperatures without voids or defects because no volatile molecules evolve during the curing process. Furthermore, the cured polyimides are solvent resistant due to their high

---

Wilkes, G. L. *Polymer* **1999**, *40*, 1889.
[181] St. Clair, T. L. *Polyimides* Wilson, D.; Stenzenberger, H. D.; Hergenrother, P. M. Ed. Blackie, New York, **1989**, P58
[182] Huang, S. J.; Hoyt, A. E. *Trends Polym. Sci*. **1995**, *3*, 262.
[183] Rhee, S. B.; Park, J-W.; Moon, B. S.; Chang, J. Y. *Macromolecules* **1993**, *26*, 404.
[184] Arnold, C. A.; Summers, J. D.; Chen, Y. P.; Bott, R. H.; Chen, D.; McGrath, J. E. *Polymer* **1989**, *30*, 986.
[185] Arnold, C. A.; Summers, J. D.; McGrath, J. E. *Polym. Eng. Sci.* **1989**, *29*, 1413.
[186] Moy, T. M.; DePorter, C. D.; McGrath, J. E. *Polymer* **1993**, *34*, 819.
[187] Hergenrother, P. M.; Havens, S. J. *J. Polym. Sci., Polym. Chem. Ed.* **1989**, *27*, 1161.
[188] Hergenrother, P. M.; Beltz, M. W.; Havens, S. J. *J. Polym. Sci., Polym. Chem. Ed.* **1991**, *29*, 1483.
[189] Hougham, G.; Tesoro, G.; Shaw, J. *Macromolecules* **1994**, *27*, 3642.
[190] Brink, M. H.; Brandom, D. K.; Wilkes, G. L.; McGrath, J. E. *Polymer* **1994**, *35*, 5018.
[191] Rogers, M. E.; Brink, M. H.; McGrath, J. E.; Brennan, A. *Polymer* **1993**, *34*, 849.

crosslink density. In addition, unfavorable polymer chain orientation due to the relative chain rigidity can be avoided during processing, which is especially important for electronic packaging materials because of the requirement of isotropic properties. Some widely used crosslinking functional groups are shown in Scheme 1.2.14.[192,193,194]

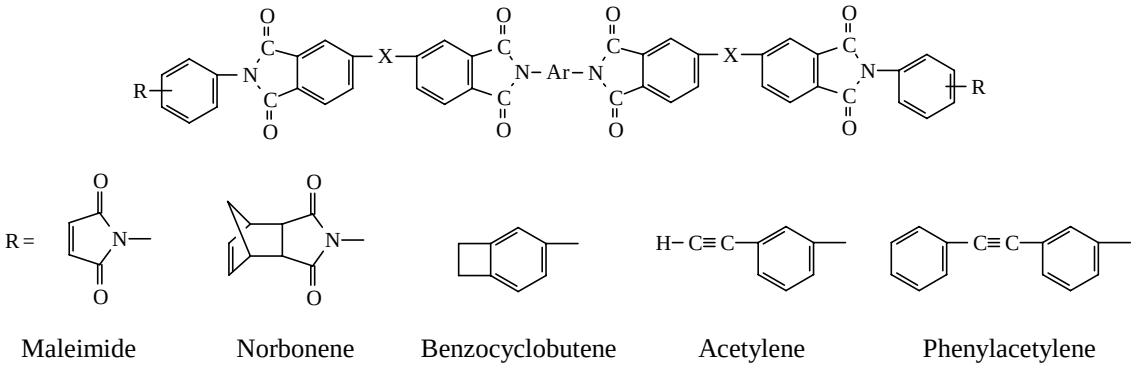


Scheme 1.2.14 Chemical structures of thermosetting polyimides

### 1.2.4 Polyimides Applications

Due to their excellent properties, polyimides are widely used for gas separation, electronic packaging, adhesives, among others.

#### *1.2.4.1 Gas Separation*

As gas separation membrane, the material should exhibit excellent mechanical properties, both good permeability and selectivity. Several factors contribute to the separation of gases by polyimides. These include total free volume; distribution of free volume; intersegmental resistance to chain motion; intrasegmental resistance to chain motions.[195] Generally, increasing the free volume increases gas solubility (gas permeation), but polymers with good permeability have bad selectivity.[196] Fortunately, most polyimides possess very good mechanical properties and the structure of the polyimide can be tailored to get medium permeability and selectivity.[197] Incorporating poly(dimethyl siloxane) into the polyimide main

[192] Stenzenberger, H. D. *Adv. in Polym. Sci*. **1994**, *117*, 165.
[193] Stenzenberger, H. D. in *Polyimides* Wilson, D.; Stenzenberger, H. D.; Hergenrother, P. M., Eds., Blackie & Son Ltd.: Glassgow and London, **1990**, p79.
[194] Pater, H. *SAMPE J*. **1994**, *30*, 29.
[195] Coleman, M. R.; Koros, W. J. *J. Polym. Sci., Polym. Chem. Ed*. **1994**, *32*, 1915.
[196] Robeson, L. M.; Burgoyne, W. F.; Kangsam, M.; Savoca, A. C.; Tien, C. F. *Polymer* **1994**, *35*, 4970.
[197] Farr, I.V.; McGrath, J. E., *et al. J. Polym. Sci., Polym. Chem*. **2000** (in press)

chain may further improve both the permeability and the selectivity.[198]

### *1.2.4.2 Electronic Packaging*

Electronic packaging materials require low dielectric constant over a wide range of frequencies, thermal stability, adequate glass transition temperatures, chemical resistance, low coefficient expansion (CTE), low modulus, high elongation at break, good adhesion to metals and other substrates.[199] Polyimides have many excellent properties. Incorporating fluoro-atoms into the polyimides may significantly lower the dielectric constants. Crosslinked fluorinated polyimides have generated great interest, since they are solvent resistant in addition to all the advantages of linear polyimides.[200] The processibility is also improved due the low viscosities of the polyimide oligomers. Finally, anisotropic properties due to the orientation of the polymers during processing can be avoided.

### *1.2.4.3 Proton Exchange Membranes and Nonlinear Optical Materials*

With the deterioration of the environment, new fuels are required to substitute the present gas for the transportation industry. Fuel cells have developed great interest recently, because the only product is environmentally friendly water. The currently used proton exchange membrane is a perfluorinated polyolefin copolymer, Nafion®, a DuPont product. However, this material is very expensive and its conductivity decreases at high temperature (> 80 °C). Sulfonated polyimides have aroused interest because of their good mechanical properties and thermal stability. They may also retain high conductivity at high temperature due to their ability to hold water. Like sulfonated poly(arylene ether sulfone)s, polyimides can be prepared by both modifying the polyimides and incorporating sulfonated monomers.[201,202,203,204] Obviously, by using sulfonated monomers one can better control both the chain structure and the extent of sulfonation.

Over the past decades, organic materials having nonlinear optical (NLO) response have

---

[198] McGrath, J. E.; Dunson, D. L.; Mecham, S. J.; Hedrick, J. L. *Adv. Polym. Sci*. **1999**, *140*, 61.
[199] Miller, R. D. *Science* **1999**, *286*, 41.
[200] Dunson, D. L.; Sankarapandian, M.; Glass, T. E.; Oyama, H.; Farr, I. V.; McGrath, J. E. *Polym. Prepr*., *ACS* **1998**, *39(2)*, 796.
[201] Pak, Y. S.; Xu, G. *Solid. State Ionics* **1993**, *67*, 165.
[202] Zhang, Y.; Litt, M.; Savinell, R. F.; Wainright, J. S. *Polym. Prepr*., *ACS* **1999**, *40(2)*, 480.
[203] Vallejo, E.; Pourcelly, G.; Gavach, C.; Mercier, R.; Pineri, M. *J. Membr. Sci*. **1999**, *160*, 127.
[204] Gunduz, N.; McGrath, J. E. *Polym. Prepr*., *ACS* **2000**, *41(1)*, 182.

been widely noted for their good mechanical properties and processibility.[205,206,207,208] It is known that larger NLO responses and a higher thermal stability in dipole orientation are two key requirements in the development of second-order NLO materials for practical applications. The polyimide backbones were chosen because of their high glass transition temperatures, which are needed to fix the dipole orientation of the NLO chromophores induced by an external electric field. Research in this area has focused on incorporating thermally stable chromophore with large NLO responses into high $T_g$ polyimides while reasonably retaining high $T_g$, good thermal stability, and mechanical properties.[191,209]

#### *1.2.4.4 Polymeric Adhesives*

Most of polyimides have very high $T_g$, good mechanical properties. They also have very good adhesion ability because of their strong molecular interactions with some other materials. Crosslinked polyimides can further increase the solvent resistance.[210]

[205] Williams, D. J. *Nonliear Optical Properties of Organic and Polymeric Materials* ACS Symp. Ser. No. 233, ACS: Washinton, D.C., **1983**.
[206] Verbiest, T.; Burland, D. M.; Jurich, M. C.; Lee, Y. U.; Miller, R. D.; Volksen, W. *Science* **1995**, *268*, 1604.
[207] Fu, C. Y. S.; Lackritz, H. S.; Priddy, D. B., Jr.; McGrath, J. E. *Macromolecules* **1996**, *29*, 3470.
[208] Saadeh, H.; Charavi, A. G.; Yu, D.; Yu, L. *Macromolecules* **1997**, *30*, 5403.
[209] Chen, J. P.; Labarthe, L., F.; Natansohn, A.; Rochon, P. *Macromolecules* **1999**, *32*, 8572.
[210] Zhuang, H.; Sankarapandian, M.; Ji. Q.; McGrath, J. E. *J. Adhesion* **1999**, *71*, 231.

## *1.3* *Phosphorus-Containing Polymers*

### 1.3.1 Introduction

Phosphorus-containing polymers are a relatively new family compared with many other polymers. They have aroused wide interest, mainly due to their excellent fire resistance and good mechanical properties. In addition, the phosphonyl kink group may disrupt the symmetry of the molecules. Thus, many high performance phosphorus-containing polymers are amorphous and soluble in common organic solvents that may otherwise be crystalline.

Many phosphorus-containing polymers have been synthesized. These include poly(styrenephosphonate diethyl ester),[211] poly(4-vinylbenzenephosphonic acid diethyl ester),[212] polyphosphazines,[213] polyphosphonites,[214] polyphosphonate,[215,216,217] poly(phosphorus amide),[218,219] polyimides,[220, 221] poly(arylene ether),[11,222,223] polyamide,[224] polycarbonate,[225] polyester,[226] polyurethane,[227] epoxies,[228,229] etc. Among them, phosphorus-containing high performance polymers are the most important ones both due to good their thermal and chemical stability, excellent mechanical properties, very good fire retardancy. These include poly(arylene ether)s, and polyimides, epoxy, cyanate, etc.

---

[211] Cabasso, I.; Jagur-Gradzinski, J.; Vofsi, D. *J. Appl. Polym. Sci*. **1974**, *18*, 1969, 2137.
[212] Hartmann, H.; Hipler, U.-C.; Carlsohn, H. *Acta Poly*. **1980**, *31*, 700.
[213] Allcock, H. R. *Inorganic and Organometallic Polymers*, ACS Symposium Series No. 360. ACS, Washington, D. C. **1988**.
[214] Steininger, E.; Sander, M. *Kunststoffe 1964*, *54*, 507.
[215] Millich, F.; Lambring, L. L. *J. Polym. Sci. Polym.* Chem. **1980**, *18*, 2155.
[216] Imal, Y.; Sato, N.; Ueda, M. *Makromol. Chem. Rapis Comm*. 1980, 1, 419.
[217] Kim, K. S. *J. Appl. Polym. Sci.* **1983**, *28*, 1119.
[218] Coover, H. W.; McConnell, R. L.; Shearer, N. H. *Ind. Eng. Chem.* **1960**, *52*, 412.
[219] Carraher, C. E. Jr.; Winthers, D. *J. Polym. Sci., Polym. Chem. Ed*. **1969**, *7*, 2417.
[220] Varma, I. K.; Rao, B. S. *J. Appl. Polym. Sci.* **1983**, *28*, 2805.
[221] Tan, B.; Tchatchoua, C. N.; Dong, L. *Polym. Advan. Technol*. **1998**, *9*, 84.
[222] Hashimoto, S.; Furukawa, I.; Ueyama, K. *J. Macromol. Sci.-Chem.* **1977**, *A11(12)*, 2617.
[223] Smith, C. D.; Grubbs, H.; Webster, H. F.; Gungör, Wightman, J. P.; McGrath, J. E. *High Perform. Polym.* **1991**, *4*, 211.
[224] Wan, I. *Ph.D. Dissertation*, Virginia Polytechnic Institute and State University, Blacksburg, VA, **1995**.
[225] Knauss, D. *Ph.D. Dissertation*, Virginia Polytechnic Institute and State University, Blacksburg, VA, **1995**.
[226] Sato, M.; Tada, Y.; Yorkoyama, M. *Eur. Polym. J.* **1980**, *16*, 671.
[227] Ji, Q.; Muggli M.; Wang, F.; Ward, T.C.; Burns, G.; Sorathia, U.; McGrath, J. E. *Polym. Prepr*., *ACS Polym. Prepr*. **1997**, *213(2)*, 120.
[228] Senear, A. E.; Valient, W.; Wirth, J. *J. Org. Chem*. **1960**, *25*, 2001.
[229] Fenimore, C. P.; Martin, F. J. *Mod. Plast.* **1966**, *44*, 141.

### 1.3.2 Poly(arylene ether phosphine oxide)s

Poly(arylene ether phosphine oxide) (PEPO) was first reported by Hashimoto *et al.*[230] However, only low molecular weight PEPOs were obtained by reacting bis(4-chlorophenyl)phenyl phosphine oxide with bisphenols in various aprotic dipolar solvents utilizing sodium hydroxide as the base. This is because the electron-withdrawing ability of phosphonyl group is not as strong as sulfonyl. Later, Smith *et al.* prepared high molecular weight PEPOs using bis(4-fluorophenyl)phenyl phosphine oxide instead of bis(4-chlorophenyl)phenyl phosphine oxide.[222] Riley *et al.* extended this work and many structural units, such as carbonyl, sulfonyl, etc. were successfully incorporated into the polymer main chain.[11] These polymers are thermally stable, amorphous with high $T_g$s, and show very high decomposition temperatures. Thermogravimetric analysis showed high char yield both in nitrogen and in air. Cone calorimetry measurements showed their lower heat release rate compared to polysulfones with similar structures, indicating their potential application as fire retardant materials. It is also noted that they are optically clear and colorless with much higher refractive index than polycarbonate (n=1.58), suggesting their potential application as optic lenses. Very recently, McGrath and coworkers successfully synthesized a bisphenol A based PEPO by melt polymerization[231] via a silyl ether displacement similar to the synthesis of polysulfone by Kricheldorf *et al.*[50] This approach does not require the removal of catalyst and avoids using solvent as the reaction medium and the resulting polymer can be directly melt processed.

Phosphine oxide containing polymers can be chemically modified by reducing the phosphonyl group to phosphine using phenylsilane as the reducing agent.[232] The phosphine group can react with halocompounds and phosphonium salts can be generated.[233] This kind of polyelectrolyte was employed to prepare nonlinear optical (NLO) materials.[11,234]

Poly(4,4'-diphenylphenylphosphine oxide) (PAPO) was synthesized by nickel-catalyzed

---

[230] Hashimoto, S.; Furukawa, I.; Ueyama, K. *J. Macromol. Sci. Chem.* **1977**, *A11*, 2167.
[231] (a) McGrath, J. E.; Mecham, S. J.; Hickner, M. A.; Wang, S.; Shoba, H. B.; Oishi, Y.; Sankarapandian, M. *Polym. Prepr., ACS* **1999**, *40(2)*, 1291; (b) Mecham, S. J.; Hickner, M. A.; Sankarapandian, M.; Grieco, L. M.; McGrath, J. E. *SAMPE* **1999**, *16*.
[232] Ghassemi, H.; McGrath, J. E. *Polymer* **1997**, *38*, 3139.
[233] Ghassemi, H.; Riley, D. J.; Curtis, M.; Bonaplata, E.; McGrath, J. E. *Appl. Organomet. Chem.* **1998**, *12*, 781.
[234] Riley, D. J. *PHD Thesis* Virginia Tech: Blacksburg, Vierginia, **1997**.

coupling polymerization. Ghassemi and McGrath reported preparing PAPO using bis(4-chlorophenyl)phenyl phosphine oxide catalyzed by a mixture of $NiCl_2$, 2,2'-bipyridine, zinc powder, and triphenyl phosphine in a nitrogen atmosphere.[232] The polymer developed a deep red color once the phosphine oxide groups in the polymer were reduced to phosphine using phenylsilane.

### 1.3.3 Phosphorus-Containing Polyimides

As is known, many polyimides are semicrystalline with high $T_m$. Therefore, they possess poor processiblity. Incorporating phosphonyl group into polyimide backbones may remarkably depress their $T_m$ and increase their solubility in common organic solvents. The result is that many phosphorus-containing polyimides can be prepared by solution imidization. The polyimides containing phosphine oxide moiety can be achieved either by using phosphorus containing diamines, or phosphorus-containing dianhydride, or both. One other way is to modify prepared polyimides. This can be achieved via phosphorylation by esterification of their hydroxyl groups with diphenylphosphoryl chloride.[235]

Some commonly used phosphorus containing monomers are shown in Scheme 1.3.1.[236]

Diamines

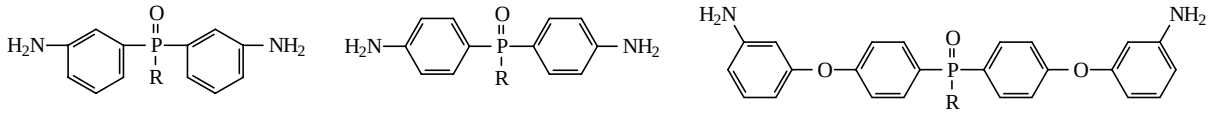

Dianhydride

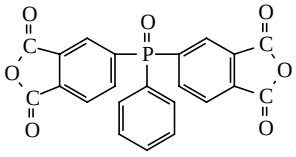

Scheme 1.3.1 Some common phosphorus-containing monomers used to prepare polyimides

### 1.3.4 Phosphorus-containing Epoxies

Generally, the monomers used for preparing polyimides and phosphonate diamine can be also used to cure epoxy resin in order to increase the fire resistance.[237,238] An alternative way

[235] Chang, T. C.; Wu, K. H.; Chiu, Y. S. *Polym. Degrad. Stab*. **1999**, *63*, 103.
[236] Lin, Y.-N.; Joardar, S.; McGrath, J. E. *Polym. Prepr. ACS* **1993**, *34*, 515.
[237] (a) Tchatchoua, C. N. *Ph.D. Thesis* Virginia Tech: Blacksburg, Virginia, **2000**; (b) Park, Y. R.; Yoon, T. H.; Yuck, J. I.; Lee, S. G. *Polymer-Korea* **1998**, *22*, 901.
[238] Liu, Y. L.; Hsiue, G. H.; Chiu, Y. S. *J. Polym. Sci., Polym. Chem. Ed.* **1997**, *35*, 565.

is to prepare phosphorus containing epoxy resin.[239] Phosphorus containing aryl cyanate ester monomers were successfully prepared by Abed, *et al.* The cured network exhibited better short time thermal stability at high temperatures.[240]

### 1.3.5 Other Aspects of Phosphorus-containing Polymers

In recent years, the discovery of the hydrogen bonding between phosphonyl and hydroxyl groups has sparked new interest in preparing some new phosphorus containing polymers, since the hydrogen bonding interaction can promote polymer-polymer miscibility and improve the surface properties. [241,242,243,244,245,246]

As is well known, polysiloxanes are used as medical materials. However, their hydrophobicity limits their applications. Incorporating pendant phosphonate ester groups into polysiloxane chain may impart various unique properties, since the polar phosphonyl group can interact with biological and metal surfaces.[247] Lin *et al.* reported a method to synthesize poly(phosphonosiloxane).[248] Hydrosilylation of vinylbenzyl chloride (VBC) with a poly(methylhydrosiloxane) or its cyclic monomer followed by phosphonylation with triethyl phosphite afforded stable phosphonosiloxanes.

Recently, Mandal and Hay prepared polycylic phosphonate resins by reacting *p*-substituted phenol-formaldehyde resins with excess phosphonic dichlorides under dilute conditions in a polar aprotic solution.[249] The phosphorus-containing units were incorporated into the commercial polycarbonate by ring-opening polymerization simultaneously with a transesterification reaction with commercial polycarbonates. The crosslinked product was found to have considerably higher char yield than that of the linear polycarbonates by thermogravimetric analysis.

---

[239] (a) McGrath, J. E. *et al.* to be published; (b) Liu, Y.L.; Hsiue, G. H.; Chiu, Y. S.; Jeng, R. J.; Perng, L. H. *J. Appl. Polym. Sci*. **1996**, *61*, 613.
[240] Abed, J. C.; Mercier, R.; McGrath, J. E. *J. Polym. Sci., Polym. Chem. Ed*. **1997**, *35*, 977.
[241] Sun, J.; Cabasso, I. *J. Polym. Sci., Polym. Chem. Ed*. **1989**, *27*, 3985.
[242] Zhuang, H.; Pearce, E.; Kwei, T. K. *Macromolecules* **1994**, *27*, 6398.
[243] Srinivasan, S.; Kagumba, L.; Riley, D. J.; McGrath, J. E. *Macromol. Symp*. **1997**, 122, 95.
[244] Wang, S.; Ji, Q.; Tchatchoua, C. N.; Shultz, A. R. *J. Polym. Sci., Polym. Phys. Ed*. **1999**, 37, 1849.
[245] Wang, S.; Wang, J.; Ji, Q.; Shultz, A. R.; Ward, T. C.; McGrath, J. E. *Polym. Prepr., ACS* **1998**, *39(2)*, 384.
[246] Wang, S.; Glass, T. E.; Zhuang, H.; Sankarapandian, M.; Ji, Q.; Shultz, A. R.; McGrath, J. E. *Polym. Prepr., ACS* **1999**, *40(2)*, 744.
[247] Cabasso, I.; Suresh, S. *J. Biomed. Mater.Res*. **1990**, *24*, 705.
[248] Lin, S.; Cabasso, I. *J. Polym. Sci., Polym. Chem. Ed*. **1999**, 37, 4043.
[249] Mandal, H.; Hay, A. S. *J. Polym. Sci., Polym. Chem. Ed*. **1998**, *36*, 1911.

## *1.4 Flame Resistance in Polymeric Materials*

Polymeric materials have penetrated into every aspect of our routine life. They have been widely used as adhesives, aircraft interiors, and electronic components.[250] Polymeric materials have been used as very important units in building materials, which require fire retardancy.

### 1.4.1 Methods for Testing Flammability

As a consequence of the complicated nature and poor reproducibility of fire, many techniques have been employed for estimating the flammability of polymeric materials, depending upon the importance of different fire properties.[251] Examples of these properties are: easy of ignition, flame spread, rate of heat release, fire endurance, ease of extinction, smoke release and toxic gas evolution.

Char formation is important to flame retardancy because the carbonaceous char formed during degradation on top of a polymer can protect the underlying polymer from exposing to the flame.[252] Figure 1.4.1 illustrates a proposed mechanism for char formation.[253]

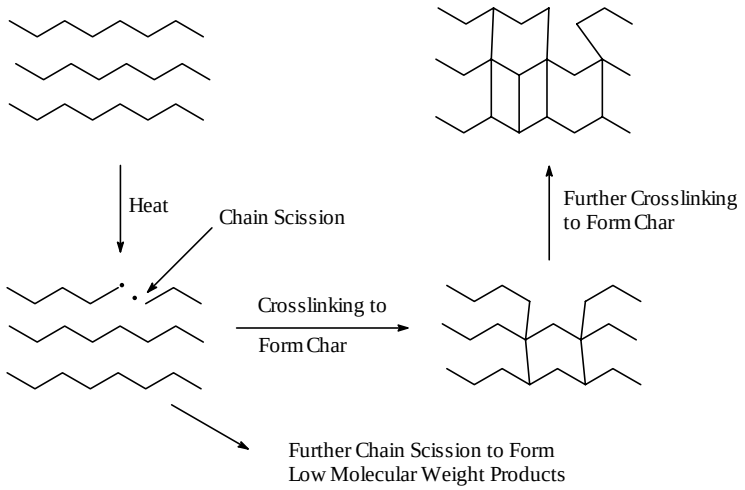


Figure 1.4.1 Possible mechanism for char formation[253]

This mechanism proposed a three-step process. In the initial stage, the polymer is degraded via chain scission. In the following step, the degraded polymer would either further decompose to yield volatiles through chain scission or crosslink. The final step involves

[250] Hergenrother, P. M. *Angew. Chem. Int. Ed.* **1990**, *29*.
[251] Nelson, G. L. in *Fire and Polymers II*, ACS Symposium Series **1995**, 599, 1.
[252] Carty, P. in *Polymeric Materials Encyclopedia* Salamon, J. C. Ed. in Chief, CRC Press: New York, **1996**, p2422.
[253] *Improved Fire- and Smoke-Resistant Materials for Commercial Aircraft Interiors* in National Research Council Publication NMAB-4772, National Academy Press: Washington, D.C., **1995**.

generating crosslinked char through further crosslinking. This mechanism helped to explain the reason for the formation of graphitic structures on the surface of many highly aromatic polymers.

Dynamic thermogravimetric analysis (TGA) has been extensively used to determine char yield. A few researchers have used other methods for determining char and qualitative results were obtained.[254,255] The relationship between the char yield and the fire retardancy is not well understood. High char yield does not necessarily mean better fire retardant.

A very convenient and reproducible test is the limiting oxygen index (LOI) (ASTM-D-2683) technique, which is widely used for laboratory test. The LOI value is the minimum amount of oxygen in a mixture of oxygen and nitrogen that will just support flaming combustion of a top ignited specimen. The higher the LOI value, the less flammable the material. It is also a measure of ease of extinction. LOI is the standard test for rigid plastics, fabrics, and films. It has also been run on powders and liquids. LOI has been taken as an ignition test by some researchers. However, the ignition parameters are not rigidly controlled and the sample needs to burn for at least 3 minutes after sustained ignition under the oxygen amount.

In the mid-1970s, Van Krevelen clearly established the correlation between LOI values and the amount of char a polymer forms when it burns.[256]

In practice, a real fire does not have the high concentration of oxygen involved with the LOI test. Recently, several novel techniques have been developed for measuring a range of properties under more practical burning conditions. The most widely used method is using the cone calorimeter to determine fire behavior (ASTM E1354) (Figure 1.4.2). This apparatus comprises an electrical heater in the form of a truncated cone, capable of generating a wide range of fire intensities with heat fluxes of up to 100 $kW/m^2$. This enables the pyrolysis profile of the polymeric materials to be obtained. Many important fire parameters can be simultaneously determined. These parameters include ignition time, total and maximum rates of heat release, heat of combustion, mass loses, $CO_2$, CO and smoke concentrations. The

[254] Kroenke, W. J. *J. Appl. Polym. Sci.* 1981, 26, 1167.
[255] Carty, P.; White, S. *Fire and Materials* **1994**, *18*, 151.
[256] Van Krevelen, D. W. *Polymer* **1975**, *16*, 615.

maximum rate of heat release is taken as the most important measurable parameter concerned with fire hazards and fire scenarios, since it controls the rate of burning, the rate of mass loss and the ignition of the surrounding environment.[257]

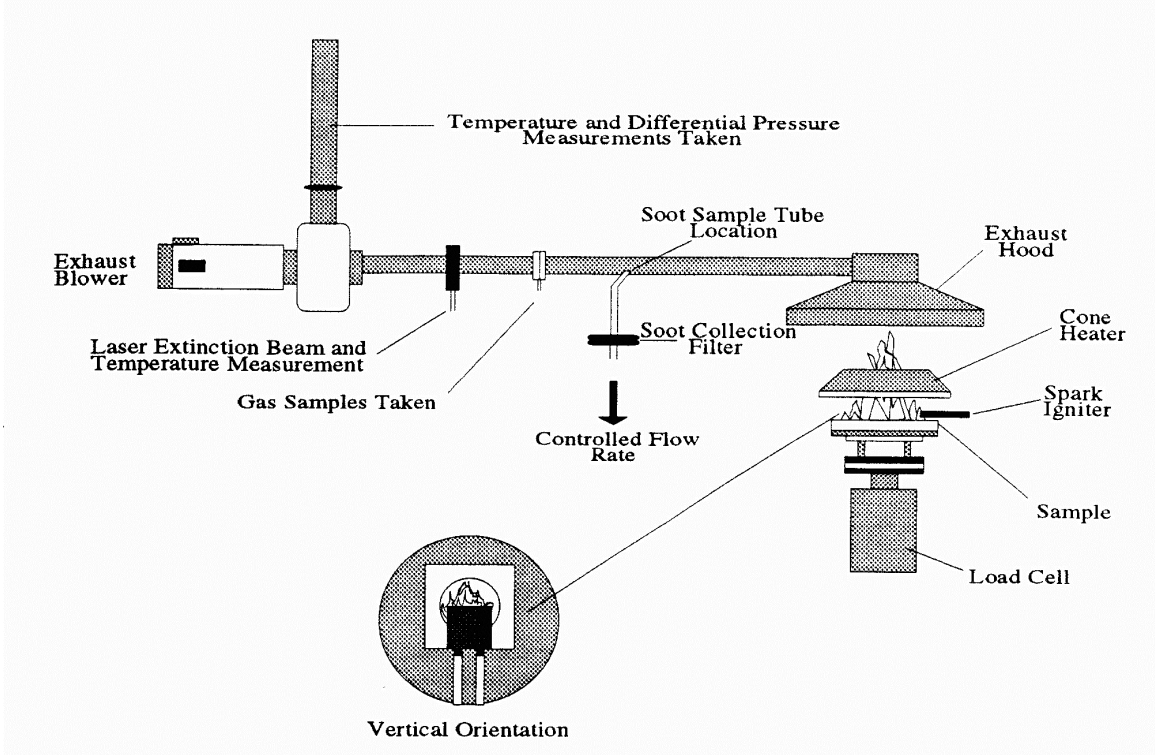


Figure 1.4.2 A cone calorimeter

One example of cone calorimetric measurements results is shown in Figure 1.4.3. The triarylphosphine oxide containing nylon 66 copolymers demonstrated much lower heat release rates than did the control 66, suggesting that the phosphine oxide group greatly reduced the flammability of the polymer.[257]

[257] Wan, I-Y; McGrath, J. E.; Kashiwagi, T. in *Fire and Polymers II, ACS Symposium Series* **1995**, *599*, 29.

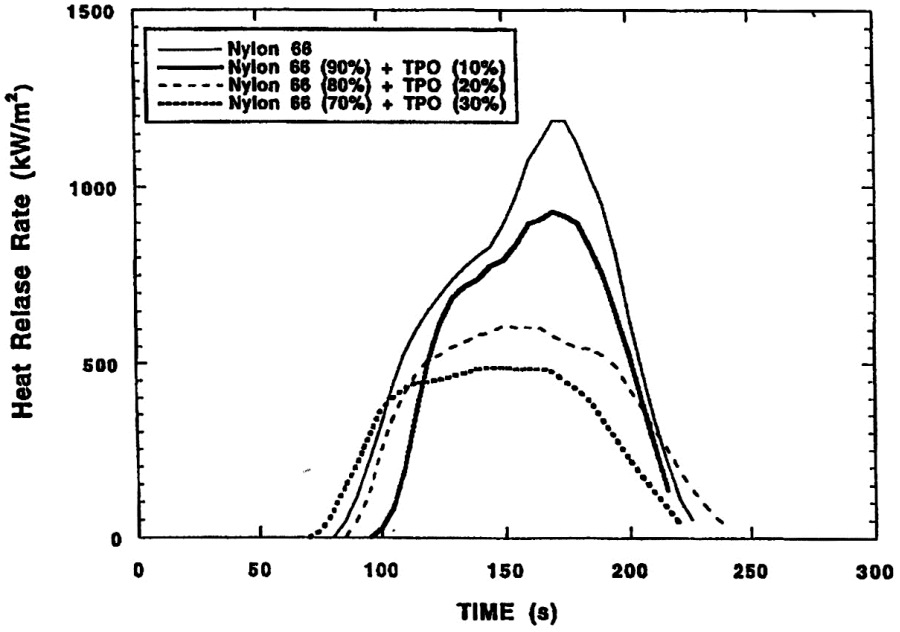


Figure 1.4.3 Heat release rate of triarylphosphine oxide containing nylon 66 copolymers

### 1.4.2 Combustion Cycle of Polymeric Materials

Some polymers have been found to be fire retardant. These include some halogen-containing polymer, such as polyvinyl chloride (PVC), poly(tetrafluoroethylene) (Teflon), and phenol based resins, such as phenolic or novalac resins. Most polymers, however, are not fire retardant.

Improving the polymer fire resistance is highly desirable for the safety of human beings and the properties. In addition, the environmental quality may also be improved. As a goal to improve the fire retardancy of the polymers, understanding of the combustion cycle is critical, because the mechanism provides us some clues to prevent the fire.

The combustion of a polymeric material is a very complicated process involving a series of interrelated and/or independent stages occurring in the condensed phase and the gas phase, and at the interface between the two phases.[258] The most important step in burning of a polymer is the fuel production stage. In this step, an external heat source increases the polymer temperature, resulting in breaking chemical bonds and generating volatile fragments.

[258] Aseeva, R. M.; Zaikov, G. E. *Adv..Polym. Sci.* **1985**, *70*, 171.

These fragments diffuse into the surrounding air to afford a flammable mixture and combustion is initiated when this mixture reaches the ignition concentration and temperature. Flaming combustion continues provided that the exothermic gas phase combustion reactions generate sufficient heat energy feeding back to the condensed phase. The feeding back heat may further decompose the polymer thus producing more fuel. Therefore, the combustion cycle is maintained. Figure 1.4.4 showed the schematic of the combustion cycle.[259]

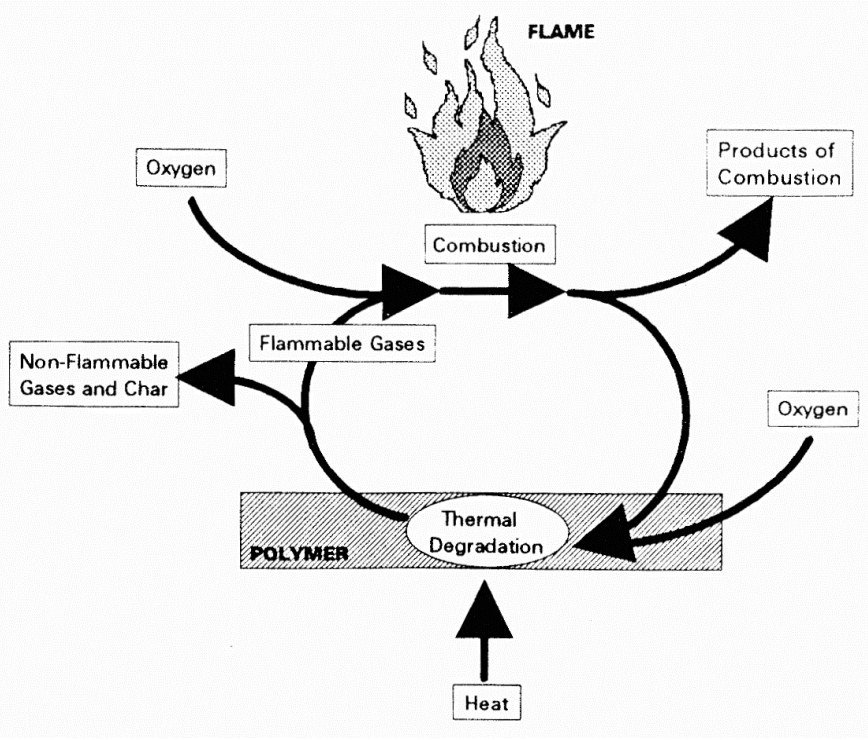


Figure 1.4.4 Schematic of the combustion cycle[259]

### 1.4.3 Approaches to Improve the Fire Resistance of Polymeric Materials

To stop the combustion, one needs to interrupt the burning cycle. Several approaches have been utilized for this purpose, which include changing the thermal decomposition temperature and mechanism of the polymer, quenching the flame, reducing the feed back heat to the decomposing polymers, covering the surface of the polymer with nonflammable materials.

What the polymer chemists and the materials scientists can contribute is physically blending flame retardant additives or synthesizing new polymers with flame retardant

[259] Ebdon, J. R.; Jones, M. S. in *Polymeric Materials Encyclopedia* Salamon, Ed. in Chief. CRC Press: New York,

structures.

### *1.4.3.1 Physical Blending*

Physically blending flame retardant additives into polymer matrix is a widely used method. Usually, the additives contain at least one of the following elements, or structures: halogen, sulfur, phosphorus, some phenolic compounds, some metal oxides. For example, $Sb_2O_3$ in combination with brominated aromatics were used to improve the fire retardancy.[260,261,262] Various phosphorus-containing compounds were also used for the same purpose.[263,264,265] Compared with halogen-hydrocarbon additives, phosphorus containing compounds emit less toxic volatiles during burning.

Aluminum trihydrate (ATH) is a widely used inorganic flame retardant with a well understood inhibition mechanism.[266] ATH loses water of hydration when heated over 250 °C. Since the strongly endothermic dehydration reaction consumes much thermal and radiant energy from the flame, the rate of the substrate pyrolysis is significantly decreased. Also, the released water vapor acts as an inert diluent and cools the flame, reducing the effective heat flux to the surface of the substrate. The alumina residue itself acts as a coating on the surface of the substrate and isolates the flame. Unfortunately, large amounts of ATH must be used to get the efficient flame retardancy, and excess ATH may deteriorate the mechanical properties of the polymer.

A flame retardant additive interferes with one or more of the steps of the combustion cycle, which includes heating of the polymeric materials, its subsequent degradation and the further combustion of the volatile that may be generated. Blending additives with the polymer matrix is relatively easy and inexpensive. However, under most circumstances, the introduction of additives may deteriorate the physical properties of the polymer. In addition,

---

**1996**, p2397.
[260] Kuryla, W. C.; Papa, A. J. *Flame Retardancy of Polymeric Materials Vol. 4*, Marcel Dekker, Inc.: New Rork, **1978**.
[261] Hawkins, W. L. *Polymer Stabilization* Wiley-Interscience, New York, **1972**.
[262] *Fire Safety Spects of Polymeric Materials* Vol. I, Technomic Publishing Co. Inc.: Connecticut, **1997**.
[263] Lyons, J. W. in *The Chemistry and Uses of Fire Retardants* Wiley, New York, **1970**.
[264] Kuryla, W. C.; Papa, A. J. *Flame Retardancy of Polymeric Materials* Vol. 1-5, Marcel Dekker, Inc.: New York, **1979**.
[265] Weil, E. D. in *Handbook of Organophosphorus Chemistry*, R. Engel, Ed. Chapter 14, Marcel Dekker, Inc.: New York, **1992**.
[266] Gann, R. G.; Dipert, R. A.; Drews, M. J. in *Encyclopedia of Polymer Science and Engineering* Vol. 7, p161 John Wiley & Sons, New York, **1988**.

the additives may penetrate to the surface due to aging, which may further degrade the properties of the materials.[267]

### *1.4.3.2 Synthesis Approach*

The deterioration of physical properties due to the incorporation of additive can be prevented by introducing some fire retardant moieties such as halogen, sulfur, phosphorus, into the polymer backbone. This has been realized for polyolefins[268] and epoxies[269,270] and the resulting materials afforded both high char yield and high limiting oxygen index (LOI). The disadvantages with halogen based flame retardants are the evolution of toxic gases such as HX upon combustion. Also, incorporating sulfur into the polymer cannot avoid the evolution of toxic $SO_2$ and $SO_3$.

Incorporation of phosphorus into the polymer backbone is a very efficient approach due to the good fire retardant of the phosphorus containing compound and lower amount of toxic gas emitting. Phosphorus containing poly(arylene ether)s were shown to have low heat release rate.[11] Their self-extinguishing characteristics endorsed them fire resistance. However, these materials are relatively expensive.

One other approach is to incorporate poly(dimethyl siloxane) (PDMS) oligomers into the polymers.[271] Similarly, polyimide-siloxane copolymers wherein the imide portion was derived from a phosphine oxide comonomer showed excellent fire resistance.[272] However, incorporating PDMS deteriorates both the physical and chemical properties.

---

[267] Clough, R. L. *J. Polym. Sci., Polym. Chem. Ed*. **1983**, *21*, 767.
[268] Van Krevelen, D. W. *Polymer* **1975**, *16*, 615.
[269] Nelson, G. L. Ed. *Fire and Polymers II*, ACS, Washington, D. C. **1995**.
[270] Yang, C.; Lee, T. *J. Appl. Polym. Sci.* **1987**, *34*, 2733.
[271] Wang, L. F.; Ji, Q.; McGrath, J. E. *Polymer* **2000**,
[272] Wescott, J. M.; Yoon, T. H.; Rodrigues, D.; Kiefer, L.; Wilkes, G. L.; McGrath, J. E. *J. Macromol. Sci. Chem.* **1994**, *A31*, 1071.

## 1.5 Polymer Blends

### 1.5.1 Introduction

The development of new technology requires more advanced polymeric materials. Since relatively few new polymers with novel properties are available due to the experimental difficulties or economic reasons, making new polymeric materials by blending the available polymers is always attractive to both industrial and academic researchers. The properties of the polymer blends can be tailored to the application by varying the components and their compositions. Many excellent books and reviews described the preparation and characterization of polymer blends.[273,274,275,276,277,278,279] This review, however, will focus on the hydrogen bonded polymer blend systems, especially those blends referred to bisphenol A poly(hydroxy ether), polysulfones, polyimides, and phosphorus-containing polymer blends.

### 1.5.2 Basic Theory for Polymer Blends

#### *1.5.2.1 Flory-Huggins Mean-Field Theory*

When two polymers are mixed, the original Flory-Huggins mean-field theory[280,281,282,283] could be used to describe the polymer mixtures.[284,285]

$$\Delta G_m = RT\left(n_A \ln \phi_A + n_B \ln \phi_B + N\chi_{AB}\phi_A\phi_B\right) \qquad \text{Equation 1.5.1}$$

[273] Paul, D. R.; Newman, S. *Polymer Blends Vol. I-II* Academic Press: New York, **1978**.
[274] Olabisi, O.; Robeson, L. M.; Shaw, M. *Polymer-Polymer Miscibility* Academic Press: New York, **1979**.
[275] Coleman, M. M.; Graf, J.; Painter, C. P. *Specific Interactions and the Miscibility of Polymer Blends* Technomic Publishing Company, Inc.: Lancaster, PA, **1991**.
[276] MacKnight, W. J.; Karasz, F. E. in *Comprehensive Polymer Science*, *Vol. 7*., Pergamon Press: Oxford, **1989**, p111.
[277] Katime, I. A.; Iturbe, C. C. in . in *Polymeric Materials Encyclopedia* Salamon, J. C. Ed. in Chief, CRC Press: New York, **1996**
[278] Jiang, M.; Li M.; Xiang, M. L.; Zhou, H. ***Polymer Synthesis Polymer-Polymer Complexation*** in *Adv. Polym. Sci*. **1999**, *146*, 121.
[279] Paul, D. R.; Bucknall, C. *Polymer Blends Vol. I. Formulation*, *Vol. II. Performance* John Wiley & Sons, Inc.: New York **2000**.
[280] Flory, P. J. *J. Chem. Phys*. **1941**, *9*, 660.
[281] Flory, P. J. *J. Chem. Phys*. **1942**, *10*, 51.
[282] Huggins, M. L. *J. Chem. Phys.* **1941**, *9*, 440.
[283] Huggins, M. L. *Ann. N. Y. Acad. Sci*. **1942**, *43*, 1.
[284] Scott, R. L. *J. Chem. Phys*. **1949**, *17*, 279.
[285] Tompa, H. *Trans. Faraday Soc.* **1949**, *45*, 1142.

with

$$\phi_A = \frac{n_A N_A}{n_A N_A + n_B N_B} \qquad \text{Equation 1.5.2}$$

$$N = n_A N_A + n_B N_B$$

$$\phi_A + \phi_B = 1$$

where $\Delta G_m$ is the Gibbs free energy of mixing, R = gas constant, $T$ = absolute temperature, $N_A$ = degree of polymerization of polymer A, $N_B$ = degree of polymerization of polymer B, $n_A$ = number of moles of polymerization of polymer A, $n_B$ = number of moles of polymerization of polymer B, $\phi_A$ = lattice volume fractions occupied by A, $\phi_B$ = lattice volume fractions occupied by B, $\chi_{AB}$ = binary interaction parameter, defined by $\frac{z\Delta w_{AB}}{RT}$, where $z$ = lattice coordination number and $\Delta w_{AB}$ =interchange energy.

Free energy in molar sites

$$\Delta G_m\big|_{site} = RT\left(\frac{\phi_A}{N_A}\ln\phi_A + \frac{\phi_B}{N_B}\ln\phi_B + \chi_{AB}\phi_A\phi_B\right) \qquad \text{Equation 1.5.3}$$

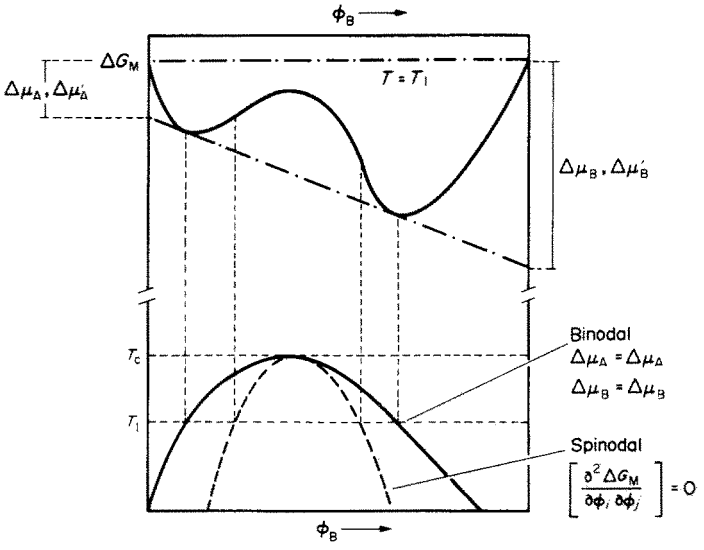


Figure 1.5.1 Composition dependence of $\Delta G_m$ at a temperature with the miscibility gap

(note: $\mu_i = \frac{\partial G_m}{\partial \phi_i}$ )[276]

Figure 1.5.1 showed the composition dependence of at a temperature within the

miscibility gap.[276] A miscible polymer blend was defined as one that satisfies the thermodynamic criteria for a single-phase system. As a specific case, a A-B binary polymer blend will afford a single-phase mixture at constant temperature and pressure, if

$$\frac{\partial^2 \Delta G_m}{\partial \phi_A^2} > 0 \qquad \text{Equation 1.5.4}$$

As is well known, spinodal and binodal curves are defined by $\frac{\partial^2 \Delta G_m}{\partial \phi_A^2} = 0$, and $\frac{\partial \Delta G_m}{\partial \phi_A} = 0$, respectively. Therefore, the critical conditions in such a system will exist when

$$\frac{\partial^2 \Delta G_m}{\partial \phi_A^2} = \frac{\partial^3 \Delta G_m}{\partial \phi_A^3} = 0 \qquad \text{Equation 1.5.5}$$

From the above equation, one has

$$\frac{\partial^2 \Delta G_m}{\partial \phi_A^2} = RT\left(\frac{1}{N_A \phi_A} + \frac{1}{N_B \phi_B} - 2\chi_{AB}\right) = 0 \qquad \text{Equation 1.5.6}$$

Therefore,

$$(\chi_{AB})_{sp} = \frac{1}{2} \cdot \left(\frac{1}{N_A \phi_A} + \frac{1}{N_B \phi_B}\right) \qquad \text{Equation 1.5.7}$$

The critical point always corresponds to the minimum value of $(\chi_{AB})_{sp}$ on the spinodal curve.

$$\frac{\partial (\chi_{AB})_{sp}}{\partial \phi_A} = \frac{1}{2} \cdot \left(-\frac{1}{N_A {\phi_A}^2} + \frac{1}{N_B (1-\phi_A)^2}\right) = 0 \qquad \text{Equation 1.5.8}$$

with $\phi_A = (\phi_A)_C$, The critical values can be also obtained by solving Equation 1.5.8.

$$(\phi_A)_c = \frac{\sqrt{N_B}}{\sqrt{N_A} + \sqrt{N_B}} \qquad \text{Equation 1.5.9}$$

$$(\chi_{AB})_c = \frac{1}{2} \cdot \left(\frac{1}{\sqrt{N_A}} + \frac{1}{\sqrt{N_B}}\right)^2 \qquad \text{Equation 1.5.10}$$

Generally, $\chi_{AB}$ is temperature dependent and can be expressed as

$$\chi_{AB} = \frac{X_{AB}}{T} + B(T) \qquad \text{Equation 1.5.11}$$

where $X_{AB}$ is the interaction parameter, $B(T)$ is a "free volume" term and is always positive.

From this equation, the miscible polymer blend requires a small positive or a negative $X_{AB}$ value. The negative value can be obtained by introducing specific interaction between two polymer components, such as dipole-dipole, hydrogen-bonding, charge-transfer, coulomb, and acid-base interaction or copolymer effect.

Considering the polydispersity of polymer Koningsveld developed a more comprehensive equation.[286]

### *1.5.2.2 Phase Diagram*

Figure 1.5.2 shows schematic representations of various types of phase diagrams for polymer mixtures.[276] Figure 1.5.2 (a) represented a typical upper critical solution temperature (UCST) behavior. Increasing temperature promotes the miscibility. In contrast to UCST, increasing temperature results in phase separation for lower solution temperature (LCST) behavior (Figure 1.5.2 (b)). In some cases, UCST and LCST behaviors coexist (Figure 1.5.2 (c)). It is possible for the UCST to merge with the LCST, producing an 'hour glass' type of diagram, as shown in Figure 1.5.2 (d). The 'hour glass' diagram has no temperature region for which a single phase exists over the entire composition range. This type of behavior can be represented by compatible blends. The UCST can lie above the LCST, generating a 'closed loop' phase diagram (Figure 1.5.2 (e)). In some cases, the UCST may be below the glass transition temperature ($T_g$) and the LCST may lie above the decomposition temperature. Determining phase diagram like Figure 1.5.2 (d) is experimentally difficult. Shaw developed an ingenious method based on light scattering for determining miscibility limits of components of incompatible blends.[287] No example for Figure 1.5.2 (e) has been detected. Although the equation-of-state theory would not predict such phase behavior based on homopolymer, it is still not clear for copolymers. Except for the problems mentioned above, some other factors may also affect the determination of phase diagram. These include the

[286] Koningsveld, R.; Kleintjens, L. A.; Schoffeleers, H. M. *Pure Appl. Chem*. **1974**, *39*, 1.
[287] Shaw, M. T. *Polym. Eng. Sci*. **1984**, *25*, 373.

effect of polydispersity and the difficulty in attaining an equilibrium state due to the high viscosities.

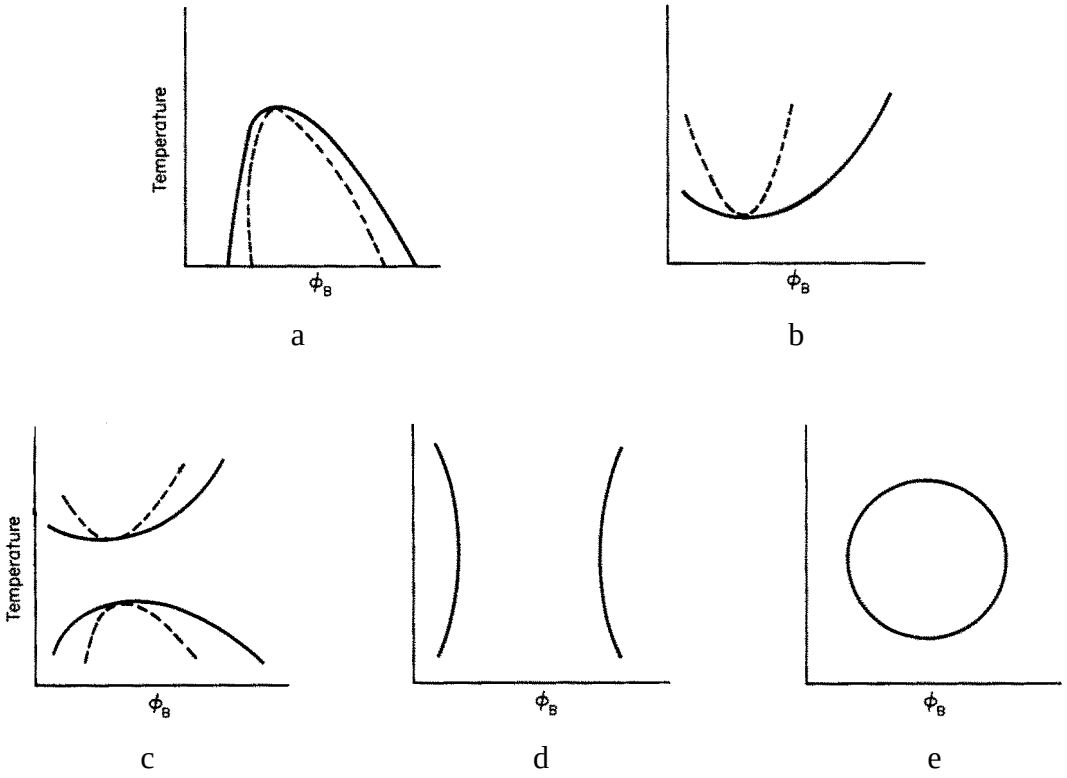


Figure 1.5.2 Schematic phase diagrams for polymer-polymer blend. Solid lines represent bimodal lines while broken lines represent spinodal lines: (a) a phase diagram of the UCST type; (b) a phase diagram of the LCST type; (c) a phase diagram in which both a UCST and an LCST occur; (d) an 'hourglass" phase diagram; and (e) a phase diagram in which the UCST occurs above the LCST.[276]

As an example, the more detailed phase diagram for LCST behavior is shown in Figure 1.5.3.[276] Annealing experiments can be carried out at various temperatures above the LCST, which is within the miscibility gap or the region in which phase decomposition will take place. If this process is allowed to reach an equilibrium state, two phases with compositions corresponding to those governed by the location of the bimodal boundary. If the phase separation process is interrupted before an equilibrium can be established, quite different morphologies would result, depending on whether the phase diagram occurs in the spinodal region or the bimodal region.

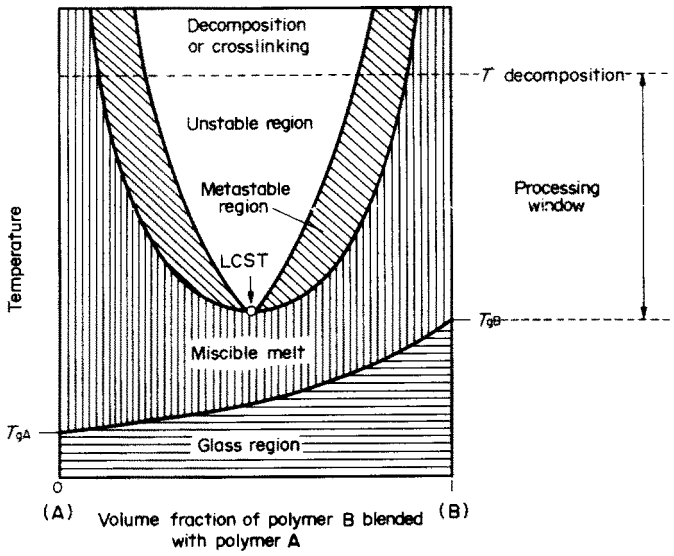


Figure 1.5.3 A schematic phase diagram for a polymer-polymer blend of the LCST type[276]

### *1.5.2.3 Spinodal Decomposition vs Nucleation and Growth*

In the spinodal decomposition, two phases with a type of interconnecting network morphology coexist. Within the composition range bounded by the spinodal boundary, the curvature of $\Delta G_m$, $\frac{\partial^2 \Delta G_m}{\partial \phi_B^2}$ is negative, and hence any small fluctuation in composition will cause a decrease in $\Delta G_m$ and therefore tend towards phase separation (uphill route) (Figure 1.5.4).[276] The decomposition follows spinodal phase separation.

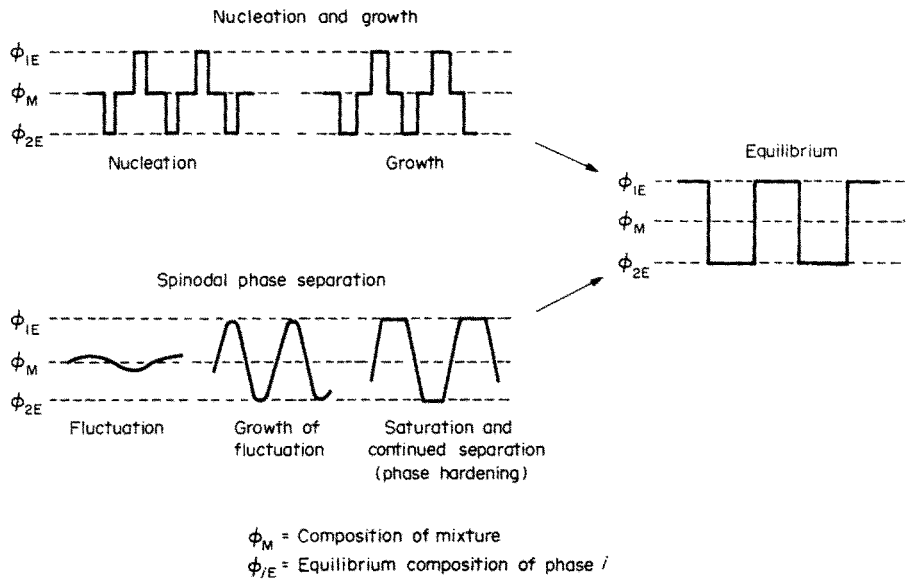


Figure 1.5.4 Modes of phase separation in miscible blends[276]

In the region between the spinodal and bimodal, $\frac{\partial^2 \Delta G_m}{\partial \phi_B^2}$ is positive, shown in Figure 1.5.1. Any small composition fluctuations in this region result in unfavorable free energy changes. The phase separation happens only when relatively large composition fluctuations are present (downhill route) (Figure 1.5.4).[276] The decomposition mechanism follows nucleation and growth.

### 1.5.3 Methods for Determining the Miscibilities of Polymer Blends

The criteria for the miscibility include the optical clarity and mechanical properties; glass transition temperature; melting point.[288]

Films or molded objects made from two mutually miscible or compatible polymers are optically clear and have good mechanical integrity. On the contrary, incompatible polymers are usually translucent or opaque and have inferior mechanical integrity. The critical domain size required for film transparency in a microheterogeneous blend was reported to be approximately 1000 Å.[289] The major limitation for this criterion is that it can not be used to judge the miscibility of two polymers with equal refractive indices. For the very thin films of

[288] MacKnight, W. J.; Karasz, F. E.; Fried, J. R. in *Polymer Blends Vol. I-II*, Paul, D. R.; Newman, S. Ed. Academic Press: New York, **1978**.
[289] Rose, S. L. *Polym. Eng. Sci*. **1967**, 7, 115.

the immiscible polymer blends, light may encounter only one of the two phases, so the films are transparent. The polymer phase having dimensions smaller than the wavelength of visible light may also lead to transparent films. Films consisting of two layers as a result of phase separation during casting may be transparent.[290] In addition, polymer blends with decent amounts of crystallinity cannot be judged by these criteria due to the light scattering of small crystals.

$T_g$ criteria have been taken as the most unambiguous criterion of polymer compatibility. A miscible polymer blend generally shows a single $T_g$ intermediate between those corresponding to the two component polymers. Using these criteria requires sufficient $T_g$ differences of two components. Single glass transition temperature criteria may not be used since $T_g$ may be suppressed or apparently absent in blends of one or more crystalline polymers. For certain polymers with well-defined crystalline-amorphous regions, both a melting endotherm and a glass transition may be detected by calorimetric methods. The crystallinity may be determined by the relation[291]

$$x = \frac{\Delta Q_f}{\Delta H_f} \approx 1 - \frac{\Delta C_p^{obsd}}{\Delta C_p{}^a} \qquad \text{Equation 1.5.12}$$

where $\Delta H_f$ and $\Delta Q_f$ are the heat of fusion of the completely crystalline polymer and the heat of fusion measured for the semicrystalline sample, respectively. $\Delta C_p^{obsd}$ is the observed height of the glass transition and $\Delta C_p^a$ is the change in heat capacity at $T_g$ for a totally amorphous sample.

Many attempts have been made to correlate the observed $T_g$ with blend composition as is frequently done with random copolymers. Fox equation is the simplest equation used to predict the $T_g$-composition dependences.[292] Other equations include Kelley-Bueche,[293] Gordon-Taylor,[294] Gibbs-Dimarzio,[295] Känig,[296] Kwei[297] expressions.

---

[290] Krause, S. *J. Maromol. Sci., Rev. Macromol. Chem*. **1972**, 7, 251.
[291] Karasz, F. E.; Bair, H. E.; O'Reilly, J. M. *J. Phys. Chem.* **1965**, *69*, 2657.
[292] Fox, T. G. *Bull. Amer. Phys. Soc*. **1956**, *1*, 123.
[293] Kelley, F. N.; Bueche, F. *J. Polym. Sci*. **1961**, *50*, 549.
[294] Gordon, M.; Taylor, J. S. *J. Appl. Chem*. **1952**, *2*, 493.
[295] Gibbs, J.; Dimarzio, E. *J. Polym. Sci*. **1959**, *40*, 121.

Many methods have been employed to determine the $T_g$. Common methods used to measure the $T_g$ include differential scanning calorimetry (DSC), dynamic mechanical analysis (DMA), dielectric measurements, dilatometry.

DSC measurements can be performed very fast and require only small amount of samples, typically 5-30 mg. Samples can be melted or annealed in-situ and thus accurate control of thermal history is available. Further advantage comes from quantitative determination of the composition of unknown multiple-phase or compatible blends by measuring $T_g$s and their height in transition.[298]

DMA is another widely used method to determine the $T_g$. The $T_g$ of the blend is defined as the temperature corresponding to the maximum in G´´ or tanδ at the main relaxation, which marks the onset of main segmental mobility corresponding to the glass transition. This method requires samples in the form of film or fiber. Secondary relaxations in miscible polymer blends were reported to be broadened, and the maxima of component polymers may overlap with consequent interpretative difficulties.[299]

Dielectric techniques in the study of polymer blends have been limited, in comparison with DSC and DMA. This is in part due to the greater experimental difficulties and the lack of sensitivity of dielectric measurements to the blends of nonpolar polymers. A wide and continuous range of frequencies can be readily used so that it permits the dynamic dielectric constants or tanδ to be determined either as a function of temperature over many frequencies or as a function of frequency at selected temperatures.[300]

Dilatometry is an earlier method[301] and has been infrequently used due to the speed and versatility requirements.

Some crystalline-amorphous polymer blends are miscible. These miscible polymer blends share three characteristics. The two polymers are thought to be miscible in the molten state. As the blends are cooled from the melt, crystallization may occur for the crystalline

---

[296] Känig, G. *Kolloid Z.* **1963**, *190*, 1.
[297] Kwei, T. K. *J. Poly. Sci., Polym. Lett. Ed.***1984**, *22*, 307.
[298] Bair, H. E. *Polym. Sci. Eng*. **1970**, *10*, 247.
[299] Zakrzewski, G. A. *Polymer* **1973**, *14*, 347.
[300] Wetton, R. E.; MacKnight, W. J.; Fried, J. R.; Karasz, F. E. *Macromolecules* **1978**, *11*, 158.
[301] Boyer, R. F.; Spencer, R. S. *J. Appl. Phys*. **1944**, *15*, 398.

components, but the total degree of crystallinity of the blend decreases rapidly with increasing the second, amorphous component. Substantial depression of the crystalline melt temperature $T_m$ is a third characteristic feature as a result of the diluent effect of the amorphous component. Early attempts have been made to fit the observed melting point depression to the well-known equation of Flory for polymer-diluent systems.[302,303,304]

$$\frac{1}{T_m} - \frac{1}{T_m^{\,o}} = \frac{R}{\Delta H_u} \cdot \frac{V_u}{V_1}(\phi_1 - \chi\phi_1^{\,2}) \qquad \text{Equation 1.5.13}$$

where $R$ is the ideal gas constant, $\Delta H_u$ is the heat of the unit of pure crystalline component, $\phi_1$ is the volume fraction of the diluent, $V_u$ and $V_1$ are the molar volumes of the polymer unit and diluent, respectively. $\chi$ is the polymer-dileunt interaction parameter, and $T_m$ and $T_m^{\,0}$ are the observed and equilibrium ($T_m^{\,0} = \frac{\Delta H_u}{\Delta S_u}$) melting temperatures.

A more appropriate equation for polymeric diluent systems was derived by Nishi and Wang et al[305] from Scott's equation.[306]

$$T_m^{\,0} - T_m = -T_m^{\,0}\left(\frac{V_{2u}}{\Delta H_{2u}}\right)B\phi_1^{\,2} \qquad \text{Equation 1.5.14}$$

with

$$B = RT\frac{\chi}{V_1} \qquad \text{Equation 1.5.15}$$

The morphologies of the polymer blends can be studied by microscopy, small angle X-ray scattering (SAXS), wide angle x-ray scattering (WAXS). The melting point can be determined by DSC.

### 1.5.4 Hydrogen Bonding Induced Miscible Polymer Blends

As is mentioned before, specific interactions or copolymer effect is the driving force for

[302] Flory, P. J. *J. Chem. Phys*. **1949**, *17*, 223.
[303] Mandelkern, L.; Garrett, P. R.; Flory, P. J. *J. Am. Chem. Soc*. **1952**, *74*, 3939.
[304] Mandelkern, L. *Chem. Rev*. **1956**, *56*, 903.
[305] Nishi, T.; Wang, T. T. *Macromolecules* **1975**, *8*, 909.
[306] Scott, R. L. *J. Chem. Phys*. **1949**, *17*, 279.

the miscibility in addition to small increase of entropy changes. Among those types of specific interactions, hydrogen bonding is the most important one in miscible polymer blend systems. In order to further discuss the hydrogen bonding in polymer blends, it is necessary to briefly summarize some aspect of hydrogen bonding in small molecules.

#### *1.5.4.1 Hydrogen Bonding in Small Molecule Systems*

Hydrogen bonding has been widely accepted as having a ubiquitous influence in gaseous, liquid, solid-state chemistry and in organisms. However, the definition of hydrogen bonding is not quite clear. It is believed that hydrogen bonding is a donor-accept or interaction specifically involving hydrogen atoms. Hydrogen bonds are formed when the electronegativity, as defined by Pauling,[307] of A relative to H in an A-H covalent bond is such as to withdraw electrons and leave the proton partially unshielded. To interact with this donor A-H bond, the acceptor B must have lone-pair electrons or polarizable π electrons. However, understanding the electronic nature of the hydrogen bond appears to be more elusive than for covalent and ionic bonds and Van der Waals forces, since the term hydrogen bond applies to a wide range of interactions from very strong hydrogen bonds resembling covalent bonds to very weak hydrogen bonds close to van der Waals forces. The majority of hydrogen bonds are distributed between these two extremes. The first text devoted entirely to hydrogen bonding was *The Hydrogen Bond* by Pimental and McClellan.[308] In this book, the definition of a hydrogen bond was made more general, as follows: "A hydrogen bond exists between the functional group, A-H, and an atom or a group of atoms, B, in the same or different molecules when (a) there is evidence of bond formation (association or chelation), (b) there is evidence that this new bond linking A-H and B specifically involves a hydrogen atom already bonded to A". This pragmatic definition satisfied all investigators at that time, since each experimentalist can answer the question *what is a hydrogen bond?* with reference to his particular method of investigation without considering the different sensitivities of the methods and observational time-scale.

With this phenomenological definition, researchers from different areas could make their contribution to the understanding of this specific interaction. For example, infrared, Raman

[307] Pauling, L. *The Nature of the Chemical Bond* Cornell University Press: Ithaca, NY, **1939**.
[308] Pimental, G. C.; McClellan, A. L. *The Hydrogen Bond* Freeman: San Francisco, **1960**.

and microwave spectroscopists define hydrogen bonds with respect to their effect on the vibrational motions of the bonds immediately involved. NMR spectroscopists observe the chemical shift caused by the change in the electronic environment around the proton. The diffractionists detect characteristics of the bond lengths and bond angles associated with hydrogen bonding. Thermodynamicists measure hydrogen bond energies and theoreticians calculate them and determine the configurations associated with the energy minima. All of the above measurements and calculations make it possible to provide criteria for the different types of hydrogen bond shown in Table 1.5.1. [309]

Table 1.5.1 Properties of Strong, Moderate, and Weak Hydrogen Bonds[309]

| | Strong | Moderate | Weak |
|---|---|---|---|
| A-H---B interaction | mostly covalent | mostly electrostatic | electrostatic |
| Bond lengths | A-H ≈ H---B | A-H < H --- B | A-H << H---B |
| H---B (Å) | ~1.2 - 1.5 | ~ 1.5 - 2.2 | 2.2 - 3.2 |
| A---B (Å) | 2.2 - 2.5 | 2.5 - 3.2 | 3.2 - 4.0 |
| Bond angles (°) | 175 - 180 | 130 - 180 | 90 - 150 |
| Bond energy (kcal/mol)[a] | 14-40 | 4 - 15 | < 4 |
| Relative IR $\nu_s$ vibration shift ($cm^{-1}$)[b] | 25 % | 10 - 25% | < 10 % |
| H1 chemical shift downfield (ppm) | 14-22 | < 14 | — |
| Examples | Gas-phase dimers with strong acids or strong bases<br>Acid salts<br>Proton sponges<br>Pseudohydrates<br>HF complexes | Acids<br>Alcohols<br>Phenols<br>Hydrates<br>All biological molecules | Gas phase dimers with weak acids or weak bases<br>Minor components of 3-cnter bonds<br>C-H---O/N bonds<br>O/N-H---π bonds |

[a]Suggested by Emsley[310]
[b]Observed *vs.* relative to $\nu_s$ for a nonhydrogen bonded X-H

[309] Jeffrey, G. A. *An Introduction to Hydrogen Bonding* Oxford University Press **1997**.
[310] Emsley, J. *Chem. Soc. Rev.* **1980**, *9*, 91.

Table 1.5.2 Functional Groups That Form Hydrogen Bonds[309]

| | |
|---|---|
| Strong hydrogen bonds | |
| Donors and acceptors | |
| $[F\text{-}\cdots H\text{-}\cdots F]^-$ | Symmetrical hydrogen bifluoride ion |
| $[H-F-H]_n^-$ | Anionic in fluoride HF adducts |
| $[O-H\cdots O^-]$ | Organic hydrogen anions, hydrogen phosphates and sulfates, hydrogen carboxylate ions |
| $[\overset{+}{O}-H\cdots O]$ | Hydroxonium ions, pseudo hydrates |
| $[\overset{+}{N}-H\cdots N]$ | Proton sponges |
| $[N-H\cdots \overset{-}{N}]$ | |
| Moderate hydrogen bonds | |
| Donors and acceptors | |
| $O-H$, $P-O-H$, $H-O_w-H$ | Water, hydrates, alcohols, carboxylic acids, phenols, carbohydrates, oligo- and polysaccharides, nucleosides, nucleotides, nucleic acids |
| 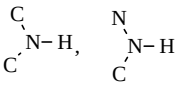 | Secondary amines, amides, carbamates, hydrazides, purines, pyrimidines, barbiturates, nucleosides, nucleotides, peptides, proteins (main chain and side chain) |
| Donors only | |
| $\overset{+}{N}(H_3)H$ | Ammonium salts |
| $-\overset{+}{N}(H_2)H$ | Zwitterion amino acids |
|  | |
| $S-H$ | Cysteine |
|  | Proteins (side chain, nucleic acids (low PH) |
| $C-N(H)H$ | Primary amines, pyrimidines, purines, barbiturates |
| Acceptors only | |
|  | Ethers, carbohydrates, oligo- and polysaccharides (ring and glycosidic oxygens) |
|  | Carboxylates, zwitterions amino acids |
|  | Carboxylic acids, ketones, esters, N-oxides, pyrimidines, purines, nucleosides, nucleotides, nucleic acids, peptides, proteins (main chain) |
| $\overset{-}{X}=O$ | Oxyanions, nitrates, chlorates, sulfates, phopshates |
|  | Tertiary amines |
|  | Purines, pyrimidines, barbiturates, nucleosides, nucleotides, nucleic acids |
| $N=O$ | Aromatic nitro compounds |
| $-S-$ | Methionine |
| Weak hydrogen bonds | |
| Donors | |
| $C-H$, $Si-H$ (?) | |
| Acceptors | |
| $C\equiv C$,  , $F-C$ (?) | |

Hydrogen bond energies range from about 15 to 40 kcal/mol for strong bonds, to 4-15

kcal/mol for moderate bonds and 1-4 kcal/mol for weak bonds. These are evidence of a wider range of interatomic interactions than is observed for covalent or ionic bonds or Van der Waals forces. Moderate and weak hydrogen bonds have a wide spread of hydrogen bond lengths and angles when observed in the crystalline state where there is a compromise with other packing forces due to their soft interactions with stretching and bending force constant of an order of magnitude less than for covalent bonds. The functional groups that from hydrogen bonds are tabulated in Table 1.5.2.[309]

### *1.5.4.2 Hydrogen Bonding Induced Miscible Polymer Blends*

Although hydrogen bonding plays an important role in the crystal structures of polymers such as nylons, our major interest is in the formation of hydrogen bonding between polymers. The formation of the hydrogen bonding between "unlike" groups is the driving force for forming miscible polymer blends. At least one of the components of the blend (A-H form) can form hydrogen bonding by self-associating. If the other component does not self-associate, it should have a functional group capable of forming a hydrogen bond with the A-H group of the self-associating polymer.

Coleman *et al* modified the Flory-Huggins equation by adding the hydrogen bonding term.

$$\Delta G_m\big|_{site} = RT\left(\frac{\phi_A}{N_A}\ln\phi_A + \frac{\phi_B}{N_B}\ln\phi_B + \chi_{AB}\phi_A\phi_B + \Delta G_H\right) \qquad \text{Equation 1.5.16}$$

where $\Delta G_H$ term accounts for the free energy changes that are a result of specific interactions.

The hydrogen bonding interaction in the polymer blends is quite similar as in the small molecules. The general proton donators are polymers containing hydroxyl or NH groups, although under some circumstances some polymers, such as poly(vinyl chloride) (PVC),[311] poly(vinyl difluoride) ($PVF_2$),[312] also act as proton donors. The general proton acceptors are polymer containing carbonyl, phosphonyl, ether bond oxygen, etc. The hydrogen bonding interaction may significantly improve the miscisbility of the polymer blends. When the

[311] Varnell, D. F.; Moskala, E. J.; Painter, P. C.; Coleman, M. M.
[312] Galin, M. *Makromol. Chem.* **1987**, *188*, 1391.

interactions between donors and acceptors are particularly intense and acquire a cooperative character they could form polymer-polymer complexes also called inter-polymers.[313,314] These materials can be obtained by mixing the homopolymer solutions. The complexes may precipitate very rapidly with a composition of simple stoichiometries (1:1 or 1:2) of repetitive units of the employed homopolymers. Many factors, such as temperature, concentration, and solvent, may affect the formation of the complexes. Some solvents may compete in the formation of hydrogen bonding between the polymers and thus prevent the forming polymer complex. This could be solved by solution casting the films. Most of the polymer-polymer complexes involve carboxylic polyacids [or other polymers with strong acid character like poly(4-vinylphenol)] and polymer with a strong basic character.

Two very important factors govern the polymer miscibility. One factor is the strength of the hydrogen bonding. The hydrogen bonding interactions in blends are not always capable of balancing the dispersive contributions when they are significantly unfavorable. The more similar the solubility parameters of the implicated polymers, the easier the miscibility of the blends. Another is the pronounced directional character of hydrogen bonds. The spatial disposition of the groups involved in both polymers and the presence or absence of esteric impediments are of great importance. This was proved by the observation that poly(4-vinylpyridine) was miscible with poly(enamino nitrile)[315] and poly(vinyl acetate-*co*-vinyl alcohol)[316] but not with poly(2-vinylpyridine).

#### *1.5.4.3 Detection and Characterization of Hydrogen Bonding in Blends*

The most widely used methods for detecting and characterizing hydrogen bonding interactions are spectroscopic methods. Among the spectroscopic methods, IR is the most extensively used method, although fluorescence and nuclear magnetic resonance studies have been carried out.

- **IR Spectroscopy**

Generally, the spectral modes corresponding to typical donor or acceptor groups are remarkably affected by hydrogen bonding in the form of band shift and intensity change. The

[313] Bekturov, E. A.; Bimendina, L. A. *Adv. Polym. Sci*. **1981**, *41*, 99.
[314] Tsuchida, E. A.; Abe, K. *Adv. Polym. Sci*. **1982**, *45*, 1.
[315] Moore, J. A.; Kim, J-H. *Macromolecules* **1992**, *25*, 1427.
[316] Cesteros, L. C.; Meaurio, E.; Katime, I. *Macromolecules* **1993**, *26*, 2323.

widely studied bands include O-H stretching vibration, N-H stretching vibration, carbonyl stretching vibration.

The O-H stretching band is interesting for the detection of hydrogen bonding in blends involving polyols and polyacids. This spectral mode in nonassociated form is placed at 3630 $cm^{-1}$ for hydroxyl groups in secondary alcohols and at 3530 $cm^{-1}$ for hydroxyl groups in carboxylic acids. This band shifts to lower frequencies when forming part of hydrogen bonding, increasing the intensity and the width of the band. This behavior has been attributed the decrease of the force constant of the covalent bond which has the H donor. In fact, the spectral shift from the position corresponding to a non-bonded hydroxyl group could be considered an indication of the strength of hydrogen bonding.[317] When the polyols and polyacids establish hydrogen bonds with a second component of the blend, the new distribution of interactions becomes evident by a change in the form of the hydroxyl stretching band. We can observe shifts of the maxima of these wide bands to higher or lower wave number, depending on the strength of the hydrogen bonds formed in the mixture. Hydrogen bonds within the blend that are stronger than those in the pure polymer shift bands towards lower wave number and vice versa. Examples of shifts to higher frequencies can be found in poly(ε-caprolactone)/PHE[318] and poly(4-vinylphenol) (P4VPh)/poly(2-vinylpyridine) (P2Vpy).[319] Examples of shifts to lower frequencies can be found in many polymer blend systems with strong hydrogen bonding.

The N-H stretching band is also sensitive to hydrogen bonding and occurs in blends involving polyamides,[320] polyurethanes,[321] or polybenzimidazoles.[322,323] In these systems the non-associated N-H groups are found close to 3400 $cm^{-1}$, while those associated by hydrogen bonding are placed at lower frequencies, at approximately 3300 $cm^{-1}$ for polyamides and polyurethanes, and at 3145 $cm^{-1}$ for polybenzimidazole. Relatively few systems were investigated.

---

[317] Purcell, K. F.; Drago, R. S. *J. Am. Chem. Soc*. **1968**, *89*, 2874.
[318] Coleman, M. M.; Moskala, E. J. *Polymer***1983**, *24*, 251..
[319] Lee, J. Y.; Painter, P. C.; Coleman, M. M. *Macromolecules* **1988**, *21*, 346.
[320] Bhagwagar, D. E. *et al. J. Polym. Sci., Polym. Phys*. **1991**, *29*, 1547.
[321] Coleman, M. M. et al *Macromolecules* **1988**, *21*, 59.
[322] Musto, P.; Karasz, F. E.; MacKnight, W. J. *Macromolecules* **1991**, *24*, 4762.
[323] Musto, P. *et al. Polymer* **1991**, *32*, 3.

The carbonyl group is a typical proton acceptor for hydrogen bonding and is present in many of the most interesting commercial polymers. Their spectral stretching modes are particularly sensitive to the formation of hydrogen bonds. As in the spectral modes previously cited, the formation of hydrogen bonds leads to weak the C=O band that produces a band displacement to lower frequencies. However, in the case of carbonyl stretching bands, the high mass of the oxygen atom and the great rigidity of the bond lead to a new band less sensitive to other spectral interference, which permits not only a very precise identification of associated and non-associated groups, but also their quantification. Thus, qualitative and quantitative analyses of hydrogen bonding in polymer blends are carried out on this band. This has been used to quantitatively analyze the hydrogen bonding interaction in PMMA/P4VPh,[324] PVP/PHE[325] and others.

Certainly, the band shift correlates with the change of the energy due to the hydrogen bonding. However, quantitatively correlating the band shift with the change of the energy due to the hydrogen bonding is not a trivial issue. Some tried to correlated the relationship between A-H infrared stretching frequencies $\nu_{A-H}$ and hydrogen bonding energies, or the relationship between $\nu_{A-H}$ and A---B bond distances. A relationship between A – H infrared stretching frequencies $\nu_{A-H}$ and hydrogen bond energies was proposed by Badger *et al.*[326,327] The absence of this reliable value for hydrogen bond energies hampered the development of this relationship. Bellamy *et al.* observed linear relationships between the relative changes in A – H stretching frequencies for a variety of donor-acceptor combinations.[328] Each line has a different slope. Measurements by Drago, *et al.* also indicated that approximately linear relationships existed but were different for different acid-base combinations.[329,330] Interest in this important correlation seems to have had an early and possibly premature death.

Similar relationships between $\nu_{A-H}$ and the A---B bond distances were

[324] Moskala, E. J. *et al*. *Macromolecules* **1984**, *17*, 1671.
[325] Martinez de Ilarduya, A.; Iruin, J. J.; Fernandez-Berridi, M. J. *Macromolecules* **1995**, *28*, 3707.
[326] Badger, R. M.; Bauer, S. H. *J. Chem. Phys.* **1937**, *5*, 839.
[327] Badger, R. M. *J. Chem. Phys*. **1940**, *8*, 288.
[328] Bellamy, L. J.; Pace, R. J. *Spectrochim Acta* **1969**, *25A*, 319.
[329] Purcell, K. F.; Drago, R. S. *J. Am. Chem. Soc*. **1967**, *89*, 2874.
[330] Drago, R. S.; Vogel, G. C.; Needham, T. E. *J. Am. Chem. Soc*. **1971**, *93*, 6014.

observed.[331,332,333,334,335] These relationships have been pursued with much enthusiasm up to the present time, The earlier data gave promise of a definite $\nu_s$ *vs* A---B or A-H algebraic relationship. A number of such relationships were suggested in the references.[336,337] Unfortunately, no such relationships have been established due to the experimental difficulties.

- **NMR Spectroscopy**

NMR spectroscopy measures the degree to which the proton is shielded by its electronic environmental in terms of proton chemical shifts. These shifts provide evidence of hydrogen bonding in liquid and solution and their magnitude is quantitatively proportional to the strength of the hydrogen bond. The more recent development of solid-state spectroscopy has prompted a greater interest in the application to hydrogen bonding. This is certainly because the results can be correlated with those of crystal structure analyses. In the absence of the tumbling of molecules in the liquid state and in solution, the dipolar interactions between like nuclei in solids make the NMR spectra very broad, so much so that they cannot be resolved. This problem is overcome by mechanical macroscopic spinning, known as magic angle (54°44′) spinning. A method is called cross-polarization magic angle spinning (CP-MAS). This technique has been widely used in investigating the hydrogen bonding in polymeric materials, because the chemical shift of the functional groups related to hydrogen bonding can be directly observed. In addition, the $T_{1\rho}$ can be measured by this method. Therefore, the domain size of the material can be derived.[338]

Other spectroscopic techniques have been employed for miscibility assessment, mainly fluorescence. The extent of energy transfer and excimer formation, as monitored by the fluorescence of the excited state present, depends on the degree of mixing in the blend. This technique requires that the components of the blend contain chromophoric structure active in

[331] Rundle, R. E.; Parasol, M. *J. Chem. Phys.* **1952**, *20*, 1487.
[332] Lord, R. C.; Merrifield, R. E. *J. Chem. Phys*. **1953**, *21*, 166.
[333] Nakamoto, K. M.; Margolis, M.; Rundel, R. E. *J. Am. Chem. Soc.* **1955**, *77*, 6480.
[334] Ratajczak, H.; Orville-Thomas, W. J. *Molecular Interactions Vol. I* Ratajczak, H.; Orville-Thomas, W. J. Eds. New York: John Wiley & Sons **1980**.
[335] Novak, A. *Structure and Bonding* 18: 177. Springer-Verlag **1974**.
[336] Pimental, G. C.; Sederholm, C. H. *J. Chem. Phys*. **1956**, *24*, 639.
[337] Bellamy, L. J.; Owens, A. J. *Spectrochim Acta* **1969**, *25A*, 329.
[338] McBrierty, V. J.; Packer, K. J. *Nuclear Magnetic Resonance in Solid Polymers* Cambridge Press: Cambridge, **1993**.

the ultraviolet, or they must be modified with appropriate groups.[339,340]

#### *1.5.4.4 Bisphenol A Poly(hydroxy ether) Based Polymer Blends*

Bisphenol A poly(hydroxy ether) has pedant hydroxyl groups which act as both proton-donating and proton-accepting groups. Therefore, it was found to be miscible with a number of polymers.

So far, it has been shown to be miscible with poly(ε-caprolactone),[341] poly(butylene terephthalate),[342] a cylcohexane-dimethanol-based polyester,[343] a polyester-based polyurethane,[344] poly(ethylene adipate),[345] and poly(butylene adipate), poly(ethylene oxide),[346,347] poly(methyl methacrylate),[348] bisphenol A poly(arylene ether phenyl phosphine oxide),[229] phosphorus-containing polyimides.[231] All of the polymer blend systems have been found to be miscible within the entire composition region. Table 1.5.3 listed the typical polymers that are miscible with phenoxy.

[339] Morawetz, H.; Amrani, F. *Macromolecules* **1978**, *11*, 281.
[340] Geller, G.; Frank, C. W. *Macromolecules* **1983**, *16*, 1448.
[341] Brode, G. L.; Koleske, J. V. *J. Macromol. Sci. Chem.* **1972**, *6*, 1109.
[342] Robeson, L. M.; Furtek, A. B. *J. Appl. Polym. Sci*. **1979**, *23*, 645.
[343] Seefried, C. G. Jr.; Koleske, J. V.; Critchfield, F. E. *Polym. Eng. Sci*. **1976**, *16*, 771.
[344] Paul, D. R.; Barlow, J. W. *J. Macromol. Sci. Rev. Mcromol. Chem*. **1980**, *C18*, 109.
[345] Smith, K. L.; Winslow, A. E.; Petersen, D. E. *Ind. Eng. Chem*. **1959**, *51*, 1361.
[346] Osada, Y.; Sata, M. *J. Polym. Sci., Polym. Lett. Ed*. **1976**, *14*, 129.
[347] Robeson, L. M.; Hale, W. F.; Merriam, C. N. *Macromolecules* **1981**, *14*, 1644.
[348] Chiou, J. S.; Paul, D. R. *J. Appl. Polym. Sci*. **1991**, *42*, 79.

Table 1.5.3 Structures of Some Typical Polymers Miscible with PHE

Carbonyl oxygen as proton acceptor[348,353,355, 341]

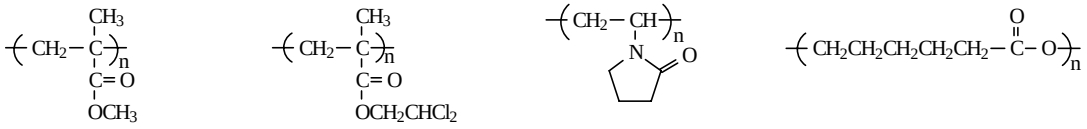

Phosphonyl oxygen as proton acceptor[244]

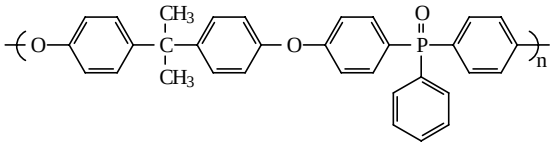

Ether oxygen as proton acceptor[347]

Tertiary amine as proton acceptor[370]

Carbonyl oxygen as the major proton acceptor[362,363]

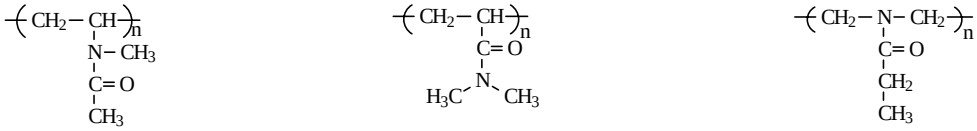

Not clarified proton acceptor[366,367]

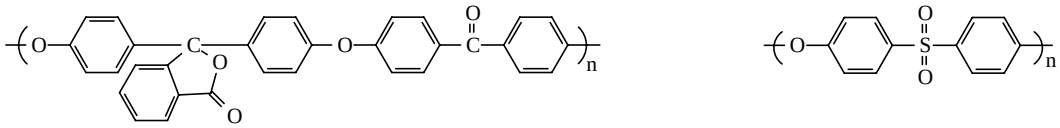

Among the vinyl polymers, poly(methyl methacrylate) (PMMA) is miscible with PHE in the entire composition range. IR results showed that the band due to the hydroxyl stretching vibration shifts to higher wave number.[349] This polymer blend system showed a lower critical solution temperature phase behavior.[348] The results suggest weaker hydrogen bonding between two components compared with the self-association of hydroxyl groups. Raman spectroscopic studies showed the shift of carbonyl group in the miscible PMMA/PHE blends,

[349] Soh, Y. S. *J. Appl. Polym. Sci.* **1992**, *45*, 8131.

providing further evidence for the hydrogen bonding between two components.[350] In addition, the mixing condition also affects the miscibility. Miscible blends were obtained only at temperatures well above $T_g$.[351] The tacticity of PMMA may also affect its miscibility with PHE.[352] A similar polymer, poly(2,2-dichloroethyl methacrylate) (PDCEMA) is also miscible with PHE.[353] However, the copolymer P(DCEMA-stat-MMA) has an immiscible window. Poly(ethyl methacrylate) is sheer immiscible with PHE.[354] The accessibility of carbonyl group for hydrogen bonding and the dissimilarity of the solubility parameters may be responsible the immiscibility. Further understanding these phenomena is highly required.

The miscibility of poly(vinylpyrrolidone) (PVP) and PHE has been widely studied.[355,356,357] The experimental results showed only single $T_g$s of polymer blends with much higher values than additive value. Analysis of FTIR spectra showed that the stretching vibration of OH (self-associated hydroxyl group) and carbonyl group shifted down to lower wave number about 150 $cm^{-1}$ and 30 $cm^{-1}$, respectively. These results suggested strong hydrogen bonding interactions. Solid state $^{13}C$ NMR showed that the chemical shift of carbonyl carbon shifted downfield by 1.6 ppm, further indicating the hydrogen bonding interactions. In addition, the calculated values of the association constant and enthalpy imply that the blend system PVP/PHE can be classified as high-level specific interactions in comparison with other polymer blends. Furthermore, $T_{1\rho}(H)$ measurements indicated that the blends were homogeneous on the scale of 40-50 Å.

The phosphonyl group is quite similar to the carbonyl group. Recently, McGrath and coworkers found that phosphorus-containing poly(arylene ether)s were miscible with PHE.[243,244] The blends showed a single $T_g$, increasing with increasing the weight fraction of poly(arylene ether)s. The stretching vibration of both self-associated hydroxyl and phosphonyl groups shifted down to lower wav enumber with about 150 $cm^{-1}$, and 25 $cm^{-1}$, respectively. The CP-MAS $^{31}P$ NMR showed the shift of phosphorus chemical shift.

---

[350] Ward, Y.; Mi, Y. *Polymer* **1999**, *40*, 2465.
[351] Erro, R.; Gaztelumendi, M.; Nazabal, J. *J. Appl. Polym. Sci.* **1992**, *45*, 339.
[352] Alberdi, M.; Espi, E.; Fernandezberridi, M. J.; Iruin, J. J. *Polym. J.* **1994**, *26*, 1037.
[353] Goh, S. H.; Lee, S. Y. Low, S. M. *Macromolecules* **1994**, *27*, 6736.
[354] Erro, R.; Gaztelumendi, M.; Nazabal, J. *J. Appl. Polym. Sci.* **1999**, *74*, 1539.
[355] Eguiazable, J. I.; Iruin, J. J.; Cortazer; Guzman, G. M. *Makromol. Chem.* **1984**, *185*, 1761.
[356] Martinez de Ilarduya, A.; Iruin, J. J.; Fernandez-Berridi, M. J. *Macromolecules* **1995**, *28*, 3707.
[357] Zheng S.; Guo, Q.; Mi, Y. *J. Polym. Sci., Polym. Phys.* **1998**, *36*, 2291.

Ether bond oxygen atom acts proton acceptor. Representative polymers miscible with PHE are poly(vinyl methyl ether) (PVME) and poly(ethylene oxide) (PEO). The $T_g$ values of the polymer blend were higher than predicted by Fox equation. The miscibility of PVME/PHE was reported by Iruin and coworkers.[358] This group also estimated the $\chi$ parameter of PVME/PHE by inverse gas-chromatography.[359] PEO is a crystalline polymer and its miscibility with PHE will be discussed later.

Hydroxyl containing polymers have structures similar to that of PHE and thus are expected to be miscible with PHE. Wu *et al.* reported that phenolic resin was miscible with phenoxy resin.[360] This can be expected due to the intermolecular hydrogen bondings between two components. Unfortunately, it is hard to differentiate self-association and intermolecular interactions. Epoxy resins are also miscible with PHE. Furthermore, some crosslinked epoxy resins are still miscible with PHE. This was demonstrated by Quo in crosslinked blends of epoxy cured with 4,4′-diaminodiphenylmethane (DDM) or aliphatic anhydrides, i.e. maleic anhydride (MA) and hexahydrophthalic anhydride (HHPA).[361] DSC showed a single $T_g$ and scanning electron microscopy (SEM) showed homogenous morphologies.

Poly(N-methyl-N-vinylacetatamide) (PMVAc), poly(N,N-dimethylacrylamide) (PDMA), and poly(ethyl oxazoline) were found to be miscible with PHE.[362,363] All of these polymers are tertiary amide polymers and the amide group is a proton acceptor. Therefore, both the carbonyl oxygen and the tertiary amide nitrogen can form hydrogen bonding with the hydroxyl group of PHE. Studies from model compounds showed that the association favors the former.[364,365] The polymer blends showed a single $T_g$, indicating complete miscibility of two components over the entire composition range. FTIR showed the band due to the carbonyl stretching vibration shifted from 1640 $cm^{-1}$ to 1609 $cm^{-1}$. $^{13}C$ CP-MAS NMR also showed the shift of carbonyl carbon and broadening of the peak, suggesting the formation of hydrogen bond. Spin-lattice relaxation times in both the laboratory and the rotating frame

[358] Uriarte, C.; Eguiazabal, J. I.; Llanos, M.; Iribarren, J. I.; Iruin, J. J. *Macromolecules* **1987**, *20*, 3038.
[359] Etxeberria, A.; Uriarte, C.; Fernandezberridi; M. J.; Iruin, J. J. *Polymer* **1994**, *35*, 2128.
[360] Wu, H-D.; Ma, C-C.; Chu, P. P. *Polymer* **1997**, *38*, 3419.
[361] Guo, Q. *Polymer* **1995**, *36*, 4753.
[362] Dai, J.; Goh, S. H.; Lee, S. Y.; Siow, K. S. *Polymer* **1996**, *37*, 3259.
[363] Lau, C.; Zheng S.; Zhong, Z.; Mi, Y. *Macromolecules* **1998**, *31*, 7291.
[364] Schmulbach, C. D.; Drago, R. S. *J. Phys. Chem.* **1960**, *64*, 1956.
[365] Bull, W. E.; Madan, S. K.; Willis, J. E. *Inorg. Chem.* **1963**, *2*, 303.

determined by high resolution solid state $^{13}C$ NMR spectroscopy reveal that the spin-diffusion among all protons in the blends average out the whole relaxation process, suggesting that the blends are intimately mixed on the scale of 10-15 Å.

Two of the high performance polymers were reported to be miscible with PHE. Some examples are phenolphthalein poly(ether ether ketone) (PEK-C),[366] poly(ether sulfone).[367,368,369] Their blends with PHE showed a single $T_g$. The band attributed to the stretching vibration of inter-component hydrogen bonded hydroxyl group shifted to higher frequencies in comparison with the hydrogen bonded self-associated OH groups. Detailed studies of PES/PHE showed a LCST around 185 °C. All of these results indicated that only weak hydrogen bonding exists in these polymer blends. Furthermore, the hydrogen bonding interactions between hydroxyl group and ether oxygen or sulfonyl group/carbonyl group may exist simultaneously. Only the band shift due to the hydrogen bonded hydroxyl stretching vibration was reported. None of the papers reported which one plays the main role for the hydrogen bonding. Further fundamental understanding of the hydrogen bonding interactions is needed.

The nitrogen atom has nonpair electrons that can act as proton acceptors to form hydrogen bond with hydroxyl group. Both poly(2-vinylpyridine) (P2VPy) and poly(4-vinylpyridine) (P4Vpy) are miscible with PHE. However, the blends showed a different $T_g$-composition.[370] The P4VPy/PHE showed a larger interaction constant while the $T_g$-composition diagram of P2Vpy/PHE indicated a stronger interaction in the later polymer blend. The reason is still not unknown.

Very few crystalline polymers have been reported to be miscible with PHE. Compared with amorphous polymer/PHE blends, crystalline polymer/PHE blends are much more complicated, since melting and crystallization process is involved in preparation and characterization polymer blends. Two widely studied crystalline polymers miscible with PHE are PEO and poly(caprolactone) (PCL). Poly(ethylene oxide) (PEO) was found to be miscible

[366] Guo, Q.; Huang, J.; Chen T. *Polym. Bull.* **1988**, *20*, 517.
[367] Singh, V. B.; Walsh, D. J. *J. Macromol. Sci. Phys.* 1986, B25, 65.
[368] Reimers, M. J.; Barbari, T. A. *J. Polym. Sci., Polym. Phys.* 1994, 32, 131.
[369] Sun, Z.; An, L.; Jiang Z.; Ma, R.; Wu, Z. *J. Macromol. Sci. Phys.* **1999**, *B38*, 67.
[370] Martinez de Ilarduya, A.; Eguiburu, J. L.; Espi, E.; Iruin, J. J.; Fernandez-Berridi, M. J. *Makromol. Chem.* **1993**,

with PHE over the entire composition range. Blending PEO with PHE results in the melting depression, because the interaction of hydroxyl group and ether oxygen disrupts the regularity of the crystals. The hydrogen bonded hydroxyl mode is observed to shift to lower frequencies as a function of PEO concentration.[371] This implied that the hydrogen bonding interaction between the phenoxy hydroxyl and PEO is stronger than the corresponding self-associated hydrogen bonding in pure phenoxy. Further detailed studied were reported by Iriarte, *et al.*[372] The $T_{1\rho}$ was determined by CP-MAS $^{13}C$ NMR. Mixing volumes have resulted in a negative excess volume of mixing, suggesting the existence of strong intermolecular interaction between the blend components. They also observed a positive excess heat capacity in a 50/50 blend. The $\chi$ was measured by inverse gas chromatography (IGC).

Other polymers reported to be miscible with PHE include PEA, PBA, and polyurethanes. Very few papers deal with PHE with PEA or PBA. The reason may be due to the less theoretical interest or few potential applications. Polyurethane/PHE blends, however, are of great interest, mainly because of their biocompatible characters. Research in this are focuses on the surface properties.[373,374] No detailed studies on the bulk properties have been reported.

Brode *et al.* were the first one to prepare poly(ε-caprolactone) (PCL)/PHE miscible polymer blends.[322] Later Coleman, *et al.* studies specific interaction (hydrogen bonding) between two components by FTIR.[352] Their results showed that the amorphous carbonyl stretching vibration shifted from 1732 $cm^{-1}$ to 1718 $cm^{-1}$, indicating the hydrogen bonding interactions. However, the 3450 $cm^{-1}$ band due to the self-associated hydroxyl stretching vibration shifted to 3505 $cm^{-1}$. This was ascribed to the relatively weaker hydrogen bonding strength between hydroxyl and carbonyl compared with that of hydroxyl self-associated hydrogen bonding. The intermolecular hydrogen bonding between two components is enthalpically unfavorable, but the increase of entropy may be the driving force for the miscibility. The crystallization and the transition behavior were studied in detail by De Juana

---

*194*, 501.
[371] Coleman, M. M.; Moskala, E. J. *Polymer* **1983**, *24*, 251.
[372] Iriarte, M.; Espi, E.; Etxeberria, A.; Valero, M.; Fernandezberridi, M. J.; Iruin, J. J. *Macromolecules* **1991**, *24*, 5546.
[373] Wen, J.; Somorjai, G. *Macromolecules* **1997**, *30*, 7206.
[374] Chen, Z.; Ward, R.; Tian, Y.; Eppler, A. S.; Shen, Y. R.; Somorjai, G. A. *J. Phys. Chem. B* **1999**, *103*, 2935.

*et al.*[375,376,377,378] The single composition dependent $T_g$ was observed in this blend. Also, negative blend interaction parameters were calculated by analyzing the melting point depression or the data of IGC. The β-transition measurements by dynamic mechanical analysis (DMA) showed that the two polymers relax independently of each other in the blend, although the shift of PHE β-transition to lower temperatures as PCL concentration increases is a symptom of the influence of this polymer on the secondary relaxation of PHE.

#### *1.5.4.5 Poly(sulfone) Based Miscible Polymer Blends*

Very few miscible polymer blends have been reported. Poly(ether sulfone) was reported to be miscible with poly(ethylene oxide)[379,380]and PHE. However, only poly(ether sulfone)/poly(hydroxy ether) miscible blends were induced by hydrogen bonding interactions.[381] The blends showed a single, composition-dependent glass transition. Poly(ether sulfone) was reported to be partially miscible with an aramide (prepared from 4,4′-diamainodiphenyl ether and isophthaloyl chloride).[382] This polymer blend is thermodynamically unstable and annealing the obtained blend results in phase separation. The FTIR spectra of the blend films showed a blue shift, indicating dissociation of hydrogen bonding between amide groups. Since the dissociation is caused by dilution of aramide molecules, the larger value of the blue shift implies higher compatibility. In addition, the blue shift implies enthalpy loss relating to the dissociation of hydrogen bonding, and hence to the thermodynamic immiscibility of the binary systems. An interesting phenomenon is that the incorporation of poly(ether sulfone) increased the crystallization rate.

#### *1.5.4.6 Polyimide Based Miscible Polymer Blends*

Polyimides were found to be miscible with some other polyimides with different chain structure[383] and some polysulfones. However, very few reported the hydrogen bonding promoted miscible polymer blend. Ultem polyimide was reported to be miscible with

---

[375] De Juana, R.; Cortazar, M. *Macromolecules* **1993**, *26*, 1176.
[376] De Juana, R.; Hernandez, R.; Pena, J. J.; Santamaria, A.; Cortazar, M. *Macromolecules* **1994**, *27*, 6980.
[377] De Juana, R.; Etxeberria, A.; Cortazar, M.; Iruin, J. J. *Macromolecules* **1994**, *27*, 1395.
[378] De Juana, R.; Jauregui, A.; Calahorra, E.; Cortazar, M. *Polymer* **1996**, *37*, 3339.
[379] Dreezen G.; Fang Z.; Groeninckx G *Polymer* **1999**, *40*, 5907-5917.
[380] Dreezen G.; Mischenko N.; Koch M. H. J.; Reynaers, H.; Groeninckx *Macromolecules* **1999**, *32*, 4015.
[381] Reimers, M. J.; Barbari, T. A. *J. Polym. Sci., Polym. Phys.* **1994**, *32*, 131.
[382] (a) Nakata, S.; Kakimoto, M.; Imai, Y. *Polymer* **1991**, *33*, 3875; (b) Hayashi, H.; Hayashi, H.; Kakimoto, M.; Imai, Y. *Polymer* **1995**, *36*, 2797.

polyamides due to the interaction between the N-H of polyamides and the carbonyl of the polyimides.[384] FTIR showed a shift in OH stretching vibrations. Polyimides is also miscible with polybenzimidazole and other heterocyclic polymers containing N-H groups.[385,386,387] The stretching vibration bands of both carbonyl and N-H shifted to low frequency, suggesting hydrogen bonding interactions between N-H and carbonyl group of polyimides.

Nakata *et al.* studied the miscibility of polyimide (derived from 4,4'-oxydiamine and 3,3',4,4'-biphenyltetracarboxylic dianhydride) and polyamide ( prepared with 3,4'-oxydainiline and isophthaloyl chloride).[388] The results showed that two polymer components were miscible when heated above 300 °C. Composition-dependent upward frequency shifts by 60 $cm^{-1}$ in the N-H stretching band of the aramide due to dissociation of hydrogen bonding were observed, indicating enthalpy increase in the blend system. This result was explained according to Coleman and Painter's disorientational entropy change.[389] The enthalpy penalty due to the hydrogen bonding dissociation could be compensated by the increase of disorientational entropy.

#### *1.5.4.7 Phosphorus-Containing Polymer Based Polymer Blends*

Although phosphonate compounds were reported to have strong proton-accepting strength,[390] not until recently has much attention been paid to phosphorus-containing polymers. Table 1.5.4 shows some typical hydrogen-bonded polymer blend systems based on phosphorus containing polymers.

Cabasso and coworkers prepared miscible polymer blends of poly(4-vinyl benzenephosphonic acid diethyl ester) and cellulose acetate.[241] The driving force is the hydrogen bonding interaction between phosphonyl group and the hydroxyl group. This can be proved by the observation of the IR band shift of the phosphonyl stretching vibration, which shifts about 17 $cm^{-1}$. Zhuang *et al.* investigated the miscibility of poly(styrene-stat-4-vinyl benzenephosphonic acid diester) (PSVBDEP) and poly(*p*-vinylphenol) (PVPh).[242] The results

---

[383] Goodwin, A. A. *J. Appl. Polym. Sci*. **1999**, *72*, 543.
[384] Etxeberria, A.; Guezala, S.; Iruin, J. J.; De La Campa, J. G.; De Abajo, J. *J. Appl. Polym. Sci*. **1998**, *68*, 2141.
[385] Musto, P.; Karasz, F. E.; MacKnight, W. J. *Macromolecules* **1991**, *24*, 4762.
[386] Kao, Y-H.; Chen, L-W. *Mater. Chem. Phys.* **1997**, *47*, 51.
[387] Ahn, T-W.; Kim, M.; Choe, S. *Macromolecules* **1997**, *30*, 3369.
[388] Nakata, S.; Kakimoto, M.; Imai, Y. *Polym. J.* **1993**, *25*, 569.
[389] Painter, P. C.; Graf, J. F.; Coleman, M. M. *Macromolecules* **1991**, *24*, 5630.

showed that the copolymer with 7.5 mol % of VBDEP was miscible when the concentration of copolymer was higher than 60 wt.%. Mixing PSVBDEP with 13.3 mol % of VBDEP with PVPh resulted in coprecipitates in THF. FTIR showed a band shift of hydroxyl stretching vibration of phenol by 330-350 $cm^{-1}$ when of PVPh and VBDEP monomer. Hydrogen bonding interactions also led to a band shift of 34 $cm^{-1}$ of P=O group. Additional evidence for hydrogen bonding interaction was provided by the chemical shift of $^{31}P$ NMR. The shift ranged from 0.3 to 0.7 ppm for the polymer blends. McGrath and coworkers synthesized a series of phosphorus-containing poly(arylene ether)s,[11,222,223] polyimides,[224] among others. Recently studies showed that many of these polymers are miscible with bisphenol A poly(hydroxy ether), epoxy and dimethacrylates (vinyl ester) resins.[243,244,245,246] Table 1.5.4 summarizes some miscible systems.

Table 1.5.4 Phosphorus-Containing Polymers as Proton Acceptor and the Corresponding Polymers

| Proton acceptor[241,242,244,246] | Proton donator |
|---|---|
| 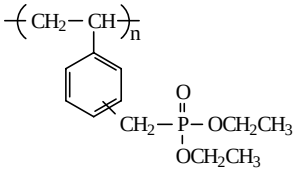 | 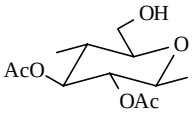 |
| 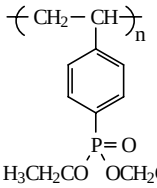 | 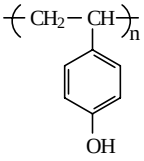 |
| 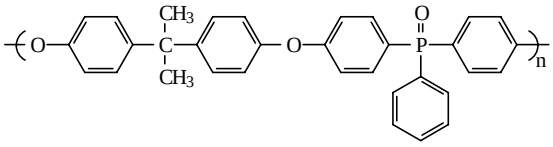 | 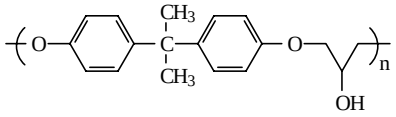 |
| 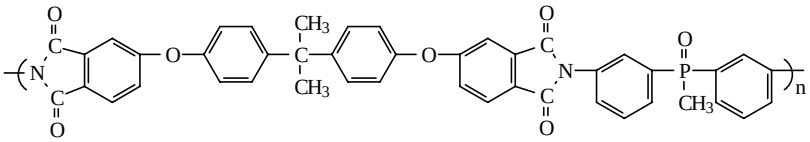 | 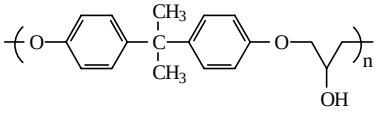 |

Hydrogen bonding interaction between phosphonyl and hydroxyl groups were shown to

[390] Joesten, M.; Schaad, L. *Hydrogen Bonding* Marcel Dekker, New York, **1974**, p332.

be the driving force for the miscibility. This can be supported by the band shift of hydroxyl stretching vibration to the lower wave number with about 150 $cm^{-1}$. Further evidence was provided by the chemical shift of $^{31}P$ CP-MAS. With the formation of hydrogen bond the peak shifts down to low field.

# 2 PHOSPHONYL/HYDROXYL HYDROGEN BONDING-INDUCED MISCIBILITY OF POLY(ARYLENE ETHER PHOSPHINE OXIDE/SULFONE) STATISTICAL COPOLYMERS WITH POLY(HYDROXY ETHER) (PHENOXY RESIN): SYNTHESIS AND CHARACTERIZATION

## *2.1 Introduction*

Polymer matrix composite materials can be designed to have very good mechanical properties.[391] Epoxy and dimethacrylate "vinyl ester" resins are widely used as crosslinked polymer matrix resins. However, some matrices exhibit marginal adhesion among the polymer matrix and reinforcing fibers. The adhesion can be improved by introducing an interphase material among the matrix and fibers. An interphase with a finite thickness has been shown to drastically alter the mechanical performance of various composite systems drastically.[392] It is proposed that an interphase material should be miscible with the polymer matrix and exhibit excellent adhesion to the fibers.

Miscible polymer blends often require some type of specific interaction between the two components to provide a negative enthalpy of mixing.[393] One very important specific interaction is hydrogen bonding, which may have bond energies of about 13-25 kJ/mole.[394] The formation of hydrogen bonds requires proton-donating groups, such as hydroxyl, carboxyl, amine, or amide groups and proton accepting groups such as carbonyl, ether, or hydroxyl group oxygen atoms or amine and heterocyclic compound nitrogen atoms. Examples of miscible blends fostered by such strong specific interactions include (1) phenoxy with poly(butylene/terephthalate),[395] with poly(2-vinylpyridine) and poly(4-

[391] *International Encyclopedia of Composites, Vol. 1-5*, Lee, S. M. Ed.; VCH: New York, 1990; Vols. 1-5.
[392] Lesko, J. J.; Swain, R. E.; Cartwright, J. M.; Chin, J. W.; Reifsnider, K. L.; Dillard, D. A.; Wightman, J. P. *J. Adhesion* **1994**, *45*, 43.
[393] Coleman, M. M.; Graf, J. F.; Painter, P. C. *Specific Interactions and the Miscibility of Polymer Blends* Technomic: Lancaster, PA, **1991**.
[394] Katime, I. A.; Iturbe, C. C. in *Polymeric Materials Encyclopedia* Salamone, J. C., Ed.; CRC Press: Boca Raton, FL, **1994**.
[395] (a) Robeson, L. M. *J. Polym. Sci., Polym. Lett. Ed.* **1978**, *16*, 261; (b) Olabisi, O.; Robeson, L.; Shaw, M. *Polymer-Polymer Miscibility* Academic Press: New York, **1979**.

vinylpyridine);[396] (2) poly(4-vinylphenol) with vinyl acetate,[397] poly(arylate)s,[398] or poly(vinyl pyrrolidone);[399] and (3) poly(benzimidazole) with polyimides or poly(bisphenol-A carbonate).[400] Hydrogen bonding is believed to be responsible for the miscibility of these polymer blends, as well as being crucial for the strengthening of polymer-polymer interfaces.[401]

Several aryl phosphine oxide containing poly(arylene ether)s have been reported to be tough thermoplastic fire retardant materials.[402] Introduction of the polar phosphonyl group into the polymer chain also allows the preparation of miscible blends with certain other polymers.

One major objective of this work was to develop an attractive interphase between a reinforcing fiber and a polymer matrix (e.g., epoxies and vinyl ester resins), as the mechanical properties of the composites can be strongly influenced by the interphase.[2] Because phenoxy resin [poly(hydroxy ether)] is a thermoplastic with a structure similar to those of epoxy and vinyl ester precursors of thermosetting polymer matrix composites, it should be an appropriate model polymer. Preliminary research showed that a bisphenol A poly(arylene ether phenyl phosphine oxide) with a $M_n$ of 20,000 g/mole was miscible with phenoxy resin.[403] FTIR showed a band shift of the phosphonyl group stretching mode, indicating specific interactions (hydrogen bonding) between the phosphonyl group of the poly(arylene ether phenyl phosphine oxide) and the hydroxyl group of the phenoxy resin repeat unit.[403] However, detailed studies of the magnitude of the band shift as a function of copolymer composition were not pursued. It was noted that bisphenol A based commercial poly(arylene ether sulfone) was not miscible with phenoxy resin. It is of interest from both a

---

[396] (a) de Ilarduya, A. M.; Eguiburu, J. L.; Espi, E.; Iruin, J. J.; Fernandez-Berridi, M. *Macromol. Chem.* **1993**, *194*, 501; (b) de Ilarduya, A. M.; Iruin, J. J.; Fernandez-Berridi, M. J. *Macromolecules* **1995**, *28*, 3707.
[397] Moskala, E. J. *Macromolecules* **1984,** *17*, 1671.
[398] Coleman, M. M.; Lichkus, A. M.; Painter, P. C. *Macromolecules* **1989**, *22*, 586.
[399] (a) Moskala, E. J.; Varnell, D. F.; Coleman, M. M. *Polymer* **1985**, *26*, 228; (b) Wang, L. F.; Pearce, E. M.; Kwei, T. K. *J. Polym. Sci., Polym. Phys. Ed.* **1991**, *29*, 619.
[400] (a) Musto, P.; Karasz, F. E.; MacKnight, W. J. *Macromolecules* **1991**, *24*, 4762; (b) Musto, P.; Wu, L.; Karasz, F. E.; MacKnight, W. J. *Polymer* **1991**, *32*, 3.
[401] Edgecombe, B. D.; Frechet, J. M.; Kramer, E. *J. Chem. Mater*. **1998**, *10*, 994.
[402] (a) Smith, C. D. *Ph.D. Dissertation* Virginia Polytechnic Institute and State University, **1991**; (b) Smith, C. D.; Grubbs, H. J.; Webster, H. F.; Gungor, A.; Wightman, J. P.; McGrath, J. E. *High Perform. Polym.* **1991**, *4*, 211; (c) Riley, D. J.; Gungor, S. A.; Srinivasan, S.; Sankarapandian, M.; Tchatchoua, C. N.; Muggli, M. W.; Ward, T. C.; McGrath, J. E.; Kashiwagi, T. *Polym. Eng. Sci.* **1997**, *37*, 1501.
[403] Srinivasan, S.; Kagumba, L.; Riley, D. J.; McGrath, J. E. *Macromol. Symp.* **1997**, *122*, 95.

scientific and technological point of view to improve miscibility by incorporation of phosphonyl groups into the poly(arylene ether sulfone) main chain. The present study has focused on further investigation of the miscibility of phenoxy resin with poly(arylene ether phosphine oxide)s and with poly(arylene ether phosphine oxide/sulfone) statistical copolymers as a function of the phosphine oxide content. The structures of poly(arylene ether phosphine oxide/sulfone) copolymer, phenoxy, epoxy and dimethacrylate ("vinyl ester") resin and related structures are shown in Scheme 2.1.1.

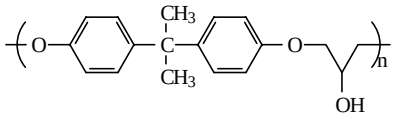

Phenoxy Resin

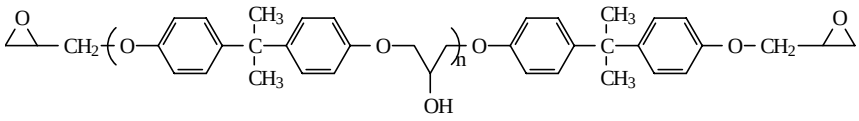

Epoxy Resin

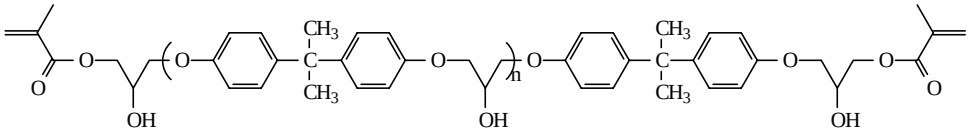

Vinyl Ester Resin

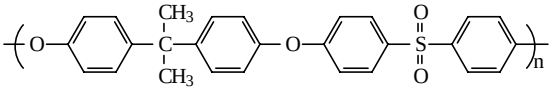

Bisphenol A poly(arylene ether sulfone)

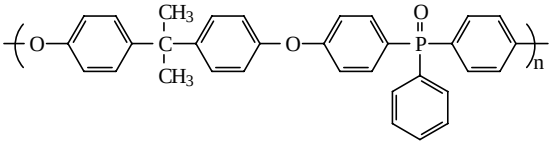

Bisphenol A poly(arylene ether phenyl phosphine oxide)

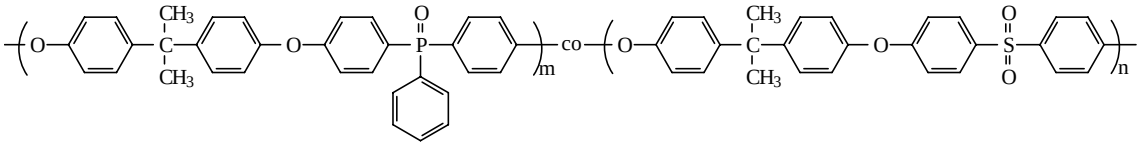

Bisphenol A poly(arylene ether phenyl phophine oxide/sulfone) Statistical Copolymers

Scheme 2.1.1 Structures of bisphenol A poly(arylene ether phenyl phosphine oxide/sulfone)s, phenoxy resin, and related systems.

## 2.2 Experimental

### 2.2.1 Materials

Materials included PAPHEN™ Phenoxy Resin PKHH™ with $M_n$ of about 20,000 g/mol (20K), (Phenoxy Associates, Inc., Rock Hill, SC), bisphenol A (Dow Chemical Company, Midland, MI), hydroquinone (Eastman Chemical Company, Kingsport, TN), and 4,4'-dichloro diphenyl sulfone (DCDPS) monomer (AMOCO Chemical Company). The 4,4'-bis(fluorophenyl) phenyl phosphine oxide (BFPPO) and 4,4'-bis(fluorophenyl) methyl phosphine oxide (BFPMPO) were synthesized in our laboratory.[12] All monomers were of high purity, as judged by melting behavior and H-NMR.

### 2.2.2 Synthesis of Bisphenol A Based Poly(Arylene Ether Phenyl Phosphine Oxide/Sulfone)

All of the polymers were synthesized via aromatic nucleophilic substitution reactions by using 1:1 stoichiometry and no monofunctional end-capping agents. Typically, a 250-mL, four-neck round-bottom flask equipped with an overhead stirrer, nitrogen inlet, and Dean-Stark trap with a reflux condenser was employed for all of the polymerizations. As an example, 0.03300 moles of bisphenol A were reacted with 0.03300moles of mixtures of BFPPO and DCDPS. The molar ratio of BFPPO/DCDPS was varied to achieve desired target compositions of the copolymer. A 15 mol % excess of potassium carbonate was also charged as the weak base for the nucleophilic reaction. A 70/30 volume ratio of dimethylacetamide/toluene (140 /60 mL) was used as the reaction medium. The reaction was initially performed at 135 °C reflux for 4 hours in a nitrogen atmosphere to dehydrate the system. Then most of the toluene was removed and the reaction temperature was kept at 160 °C for 16 h to achieve high molecular weight. The viscous liquid was allowed to cool to room temperature, diluted with more solvent, filtered, and acidified with acetic acid to protonate any phenolate end groups. The polymer was precipitated into methanol, redissolved in chloroform, again precipitated into methanol, filtered and dried in a vacuum oven at 150 °C for 24 h.

### 2.2.3 Synthesis of Hydroquinone Based Poly(Arylene Ether Phosphine Oxide/Sulfone) Copolymers

The procedure described above was also followed for hydroquinone based polymer

synthesis. By using hydroquinone in place of bisphenol A, various mixtures of BFPPO and DCDPS, or BFPMPO and DCDPS, were used to prepare copolymers with desired target compositions.

### 2.2.4 Preparation of Polymer Blends

The poly(arylene ether) copolymers and phenoxy resin were separately dissolved in chloroform as 7.5 wt% solutions. These solutions were then mixed to achieve the desired compositions. The polymer mixtures were isolated by precipitating the co-solutions in methanol, and the precipitates were dried in a vacuum oven for 24 hours at 150 °C. Films for FTIR measurements were prepared by casting blend solutions onto glass slides or salt plates and vacuum oven and drying in a vacuum oven in a similar manner. The films used for dynamic mechanical analysis (DMA) measurements were obtained by melt pressing the precipitates between metal plates for about 3 min at temperatures ranging from 160 °C for the phenoxy resin to 260 °C for the poly(arylene ether phenyl phosphine oxide). The melt-pressed samples were allowed to cool to ambient temperature between the metal plates.

### 2.2.5 Characterization

Intrinsic viscosities of the homopolymers and copolymers were measured in chloroform at 25 °C. Gel Permeation Chromatography (GPC) measurements were performed at 60 °C in a Waters 150C instrument to characterize the molecular weights and molecular weight distributions of the poly(arylene ether phosphine oxide)s and phenoxy resin. N-methyl pyrrolidone (NMP) containing 0.02M phosphorus pentoxide was the solvent. A differential refractive index detector and a Viscotek differential viscometer connected in parallel permitted calculation of absolute molecular weights and molecular weight distributions by application of the universal calibration principle.

FTIR measurements utilized a Nicolet Impact 400 instrument at a resolution of 2 $cm^{-1}$ with an average of 256 scans. FTIR measurements at various temperatures were performed after the samples were allowed to approach equilibrium for 5 minutes.

The $T_g$ of the poly(arylene ether phosphine oxide/sulfone)/phenoxy resin blends was measured with a Perkin-Elmer DSC-7 differential scanning calorimeter at a heating rate of 10 °C/min. All the results reported in this article were obtained during a second heat after

cooling from 250 °C. The midpoint temperature of the specific heat transition during the second heat was taken as the value of $T_g$.

A Perkin-Elmer DMA-7e instrument was employed for dynamic mechanical analysis (DMA) measurements in an extension mode at 1 Hz frequency and a heating rate of 5 °C/min.

## 2.3 Results and Discussion

The compositions, molecular weights, and intrinsic viscosities for four bisphenol A based polymers and for the phenoxy resin are shown in Table 2.3.1. The compositions, molecular weights, and intrinsic viscosities of hydroquinone based homopolymers and copolymers are shown in Table 2.3.2. The results confirm that high molecular weight homopolymer and copolymers were obtained under the chosen reaction conditions. The $T_g$ BA-Px/PHE blends are presented in Table 2.3.3. The blend variables include both the weight percentage of the poly(arylene ether) and the poly(arylene ether) composition.

Table 2.3.1 GPC and Intrinsic Viscosity Characterization of Bisphenol A Based Poly(arylene ether phenyl phosphine oxide/sulfone) Homo- and Copolymers and Phenoxy Resin

| | BFPPO:DCDPS | GPC | | | [η] (dl/g)[(b)] | [η] (dl/g) |
|---|---|---|---|---|---|---|
| Sample[(a)] | (mol %) | $M_n*10^{-3}$ | $M_w*10^{-3}$ | $M_w/M_n$ | NMP (60°C) | $CHCl_3$ (25°C) |
| BA-P100 | 100/0 | 39 | 74 | 1.9 | 0.43 | 0.42 |
| BA-P50 | 50/50 | 70 | 159 | 2.3 | 0.76 | 0.73 |
| BA-P20 | 20/80 | 44 | 85 | 1.9 | 0.51 | 0.62 |
| BA-P10 | 10/90 | 39 | 67 | 1.7 | 0.43 | 0.55 |
| Phenoxy | - | 20 | 46 | 2.3 | 0.38 | - |

[a] BA, bisphenol A; P-represents the mole percent of 4,4'-bis(fluorophenyl) phenylphosphine oxide used as the activated halide.
[b] From GPC/differential viscometric measurements

Table 2.3.2 GPC and Intrinsic Viscosity Characterization of Hydroquinone Based Poly(arylene ether phenyl or methyl phosphine oxide/sulfone) Homo- and Copolymers

| | BFPPO:DCDPS | GPC | | | [η] (dl/g)[(b)] | [η] (dl/g) |
|---|---|---|---|---|---|---|
| Sample | (mol %) | $M_n*10^{-3}$ | $M_w*10^{-3}$ | $M_w/M_n$ | NMP (60°C) | $CHCl_3$ (25°C) |
| HQ-BFPPO1[(a)] | 50/50 | 32 | 62 | 1.9 | 0.45 | 0.53 |
| HQ-BFPMPO1 | 100/0 | 48 | 74 | 1.8 | 0.63 | 0.85 |
| HQ-BFPMPO2 | 50/50 | 59 | 149 | 2.5 | 1.00 | 1.39 |

[a] HQ-BFPPO is

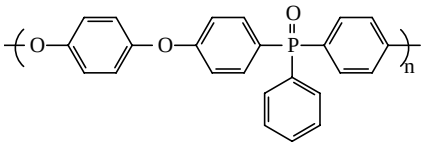

HQ-BFPMPO is

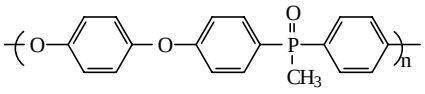

[b] From GPC/differential viscometric measurements

Table 2.3.3 Influence of Phosphine Oxide Concentration on the Composition Dependency of the Glass Transition Temperature (°C) for Various Polymer Blends

| Blend | Wt.% of BA-Px In the Blends | | | | | | |
|---|---|---|---|---|---|---|---|
| | 0 | 20 | 40 | 50 | 60 | 80 | 100 |
| | $T_g$ ($^oC$) | | | | | | |
| BA-P100/PHE | 93 | 123 | 145 | 153 | 163 | 182 | 200 |
| BA-P50/PHE | 93 | 121 | 138 | 149 | 159 | 180 | 204 |
| BA-P20/PHE | 93 | 106 | 120 | 129 | 141 | 161 | 186 |
| BA-P10/PHE | 93 | 99 | 102, 138 | 102, 140 | 140[a] | 160 | 183 |

[a] Very broad glass transition.

### 2.3.1 Hydrogen Bonding

FTIR has been widely used to study hydrogen bonding in polymer blends. The specific interaction (hydrogen bonding) generally affects the FTIR band widths and positions of the interacting groups.[393] Hydrogen bonding between phosponyl groups of poly(arylene ether phosphine oxide) and phenoxy resin hydroxyl groups has previously been measured from the shift of the phosphonyl group stretching vibration.[403] Further characterization of the specific interaction between phosphonyl groups of poly(arylene ether phosphine oxide) and hydroxyl groups of phenoxy resin was achieved by observation of the hydroxyl stretching region. In the present study the effect of copolymer composition and blend composition on the phosphonyl group and hydroxyl group stretching vibrations are examined by FTIR.

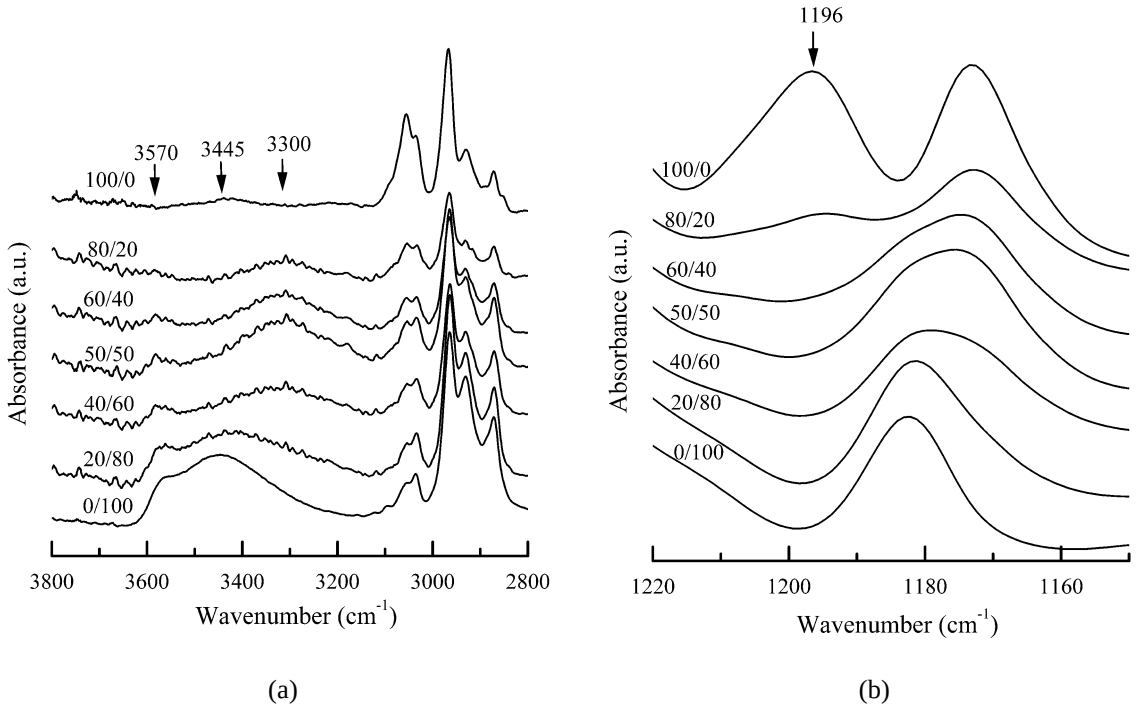


(a) (b)

Figure 2.3.1 FTIR spectra of BA-P100/phenoxy blends at various weight compositions recorded at room temperature in the hydroxyl stretching region (A) and in the phosphonyl stretching region (B).

Figure 2.3.1 shows typical infrared spectra of the BA-P100/PHE polymer blends recorded at room temperature in the hydroxyl [Figure 2.3.1(A)] and phosphonyl [Figure 2.3.1(B)] stretching regions. The spectrum of the phenoxy resin in the hydroxyl stretching region shows a small peak at 3570 $cm^{-1}$, attributed to free hydroxyl groups, with a major broad shoulder at about 3445 $cm^{-1}$ attributed to hydrogen-bonded OH dimers and multimers.[378] When the phenoxy was blended with sample BA-P100, the intensities of these two bands decreased significantly. The free hydroxyl group absorption peak wave number remains at 3570 $cm^{-1}$. However, an obvious band shift of the dimer and multimer hydroxyl stretching vibrations was observed with 20 wt % of BA-P100. A blend of 40 wt% of BA-P100 leads to a shift of the broad dimer and multimer OH group stretching vibration peak absorbance down to 3300 $cm^{-1}$. The stretching vibration of free phosphonyl groups in BA-P100 was observed at 1196 $cm^{-1}$(Figure 2.3.1B).[403] However, with the addition of 20 wt % phenoxy resin, the band shifted to 1194 $cm^{-1}$ and the relative intensity decreased significantly. Increased amounts of phenoxy resin leads to larger band shifts of the phosphonyl group absorbance peak. More critical analysis of the band shifts has been realized by subtraction of the spectra of phenoxy and BA-P100 from the spectrum of their blend. Thus, if there is no interaction

between the two components, the spectra of the blends should be the weight-averaged sum of the spectra of the two components. In contrast, interaction between the two components may lead to band shifts in the blends, as shown in Figure 2.3.2. The difference spectrum in Figure 2.3.2B showed that the stretching band of phosphonyl group shifts about 25 $cm^{-1}$. The shift of both hydrogen bonded hydroxyl group and phosphonyl group absorptions suggests a strong hydrogen bonding between the two groups. Although quantitative correlations are difficult in this region of the spectrum due to the effects of the associated environment, the results are consistent with reasonably strong hydrogen bonding.[404]

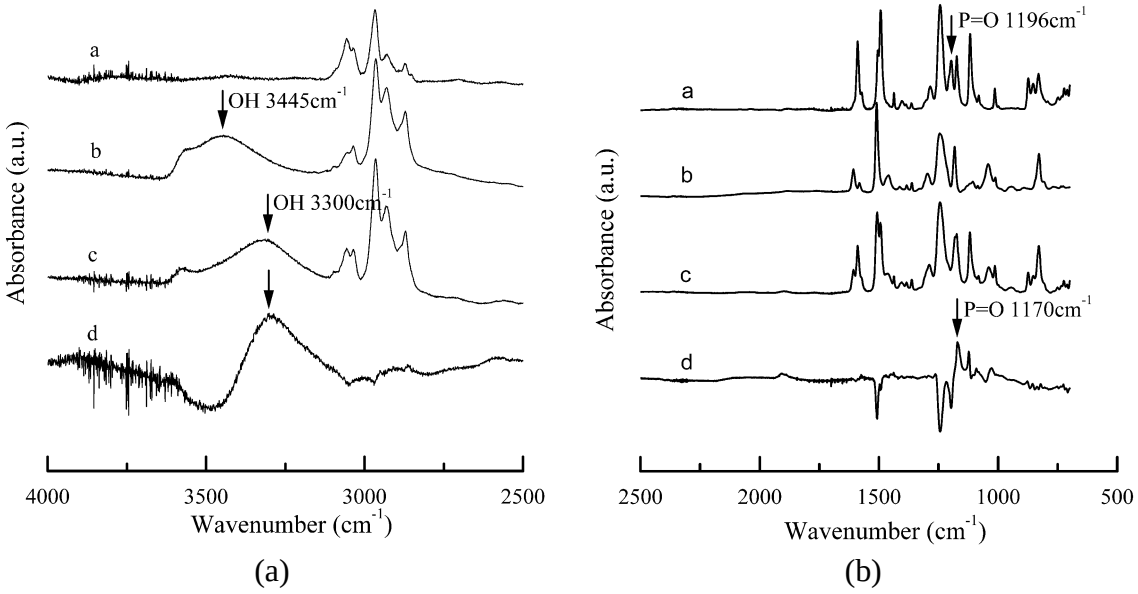


Figure 2.3.2 FTIR spectra of (a) BA-P100; (b) phenoxy; (c) 50/50 wt% blend; and (d) difference spectra of the blend and the components in the hydroxyl stretching region (A) and in the phosphonyl stretching region (B).

When the amount of phosphine oxide in the copolymer was reduced to 50 mole% strong hydrogen bonding of the phosphonyl group could still be observed in the polymer blends. In contrast to the BA-P100/PHE, very broad bands in the hydroxyl stretching vibration region were observed, as illustrated in Figure 2.3.3. Some self-associated hydrogen bonds remained in all the polymer blends within the studied composition region. Only with 80 wt % BA-P50 can one observe two separate hydroxyl stretching bands. Coleman *et al.* recently proposed a

[404] Yang, X.; Painter, P. C.; Coleman, M. M.; Pearce, E. M.; Kwei, T. K. *Macromolecules* **1992**, *25*, 2156.

concept of accessibility of functional groups that may aid understanding this phenomenon.[405] Because phosphonyl groups are randomly dispersed in the copolymer chains, not all of the hydroxyl groups can form intermolecular hydrogen bonding with phosphonyl groups, because of space accessibility limitations. High amounts of self-associated hydrogen bonding among hydroxyl groups leads to a high wave number, because not all the hydroxyl groups are readily available for the hydrogen bonding to phosphonyl groups. If the hydroxyl groups are strongly diluted by BA-P50, more hydroxyl groups have opportunities to form intermolecular hydrogen bondings. Meanwhile, hydrogen bonding between hydroxyl groups and phosphonyl groups shifts the band of hydroxyl group stretching vibrations to a lower wave number. Also, various environments of hydrogen bonding lead to different stretching frequencies. A combination of these three factors results in a fairly broad band of hydroxyl group stretching vibrations.

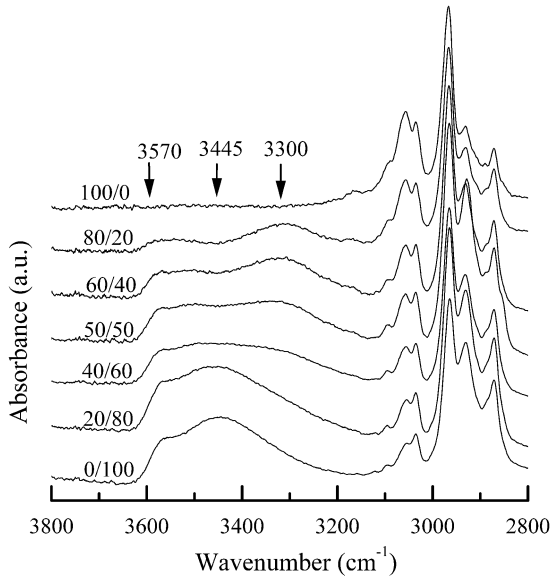


Figure 2.3.3 FTIR spectra of BA-P50/phenoxy blends at various weight compositions recorded at room temperature in the hydroxyl stretching region.

Figure 2.3.4 displays FTIR spectra in the hydroxyl stretching region of 50/50 weight composition blends of BA-Px/PHE with various compositions (x) of phosphine oxide in the copolymers. As expected, a decrease of the amount of phosphine oxide in the copolymer reduced the amount of hydrogen bonding between the two components. For BA-P20/PHE,

[405] Coleman, M. M.; Pehlert, G. J.; Painter, P. C. *Macromolecules* 1996, **29**, 6820.

the hydrogen bonding was barely observable for a 50/50 polymer blend. No hydrogen bonding between the hydroxyl and phosphonyl groups could be observed in the system of BA-P10/PHE within the sensitivity limit of the FTIR measurement.

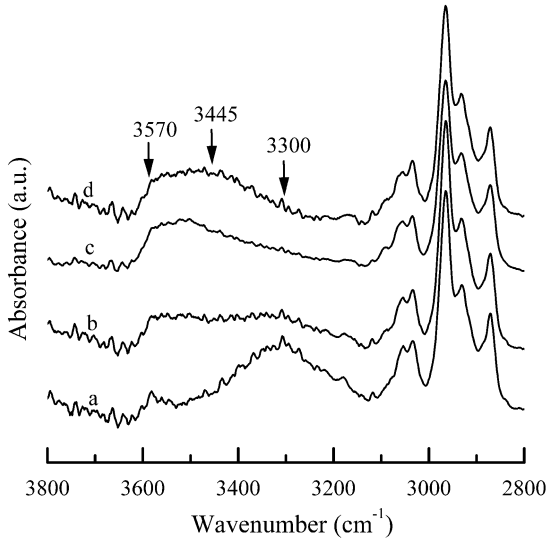


Figure 2.3.4 FTIR spectra recorded at room temperature in the hydroxyl stretching region for 50/50 BA-Px/PHE blends for various phosphonyl composition (x) in the copolymers. (a) BA-P100; (b) BA-P50; (c) BA-P20; (d) BA-P10.

To study qualitatively the strength of the hydrogen bonding, temperature measurements of the FTIR spectra were performed. Figure 2.3.5 shows the temperature dependency of hydrogen bonding of BA-P100/phenoxy (50/50). No significant change of intensity and shift of band were observed until 180 °C. When the temperature was raised to 230 °C, the band of OH stretching vibration shifted slightly and became broader. Its intensity decreased but still remained fairly strong. No significant band shift of the phosphonyl stretching vibration was observed. In contrast, the hydrogen-bonded hydroxyl groups were highly dissociated at 160 °C for the pure phenoxy control, as shown in Figure 2.3.6.

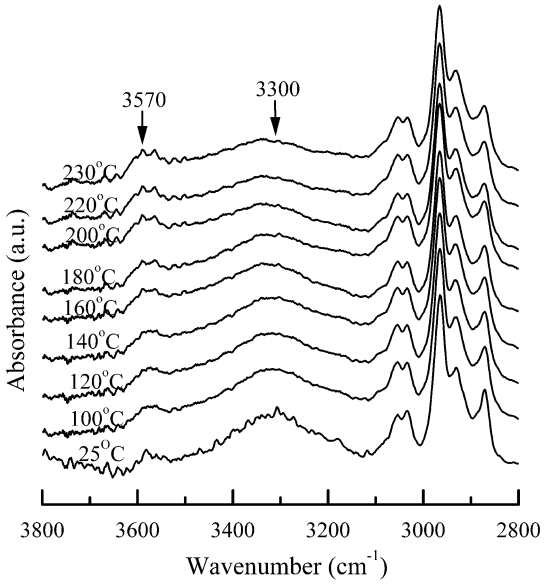


Figure 2.3.5 FTIR spectra of blend BA-P100/PHE 50/50 wt% in the hydroxyl stretching region recorded at various temperatures.

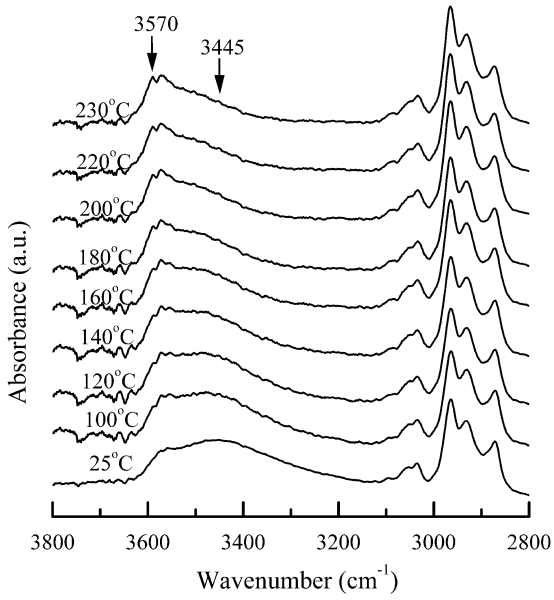


Figure 2.3.6 FTIR spectra of PHE in the hydroxyl stretching region recorded at various temperatures.

The temperature dependency of hydrogen bonding of BA-P50/phenoxy(50/50) showed a similar behavior as that of BA-P100/Phenoxy (50/50), as illustrated in Figure 2.3.7. However, when the temperature was raised to 180 °C, significant dissociation of the hydrogen-bonded OH group was observed. At 230 °C, the hydrogen bonding was sharply decreased. Although

the $T_g$ of the two polymer blends BA-P100/Phenoxy (50/50) and BA-P50/Phenoxy (50/50) are only slightly changed, the strength of the hydrogen bonding is quite different. This is due in part to the dissociation of self-associated hydroxyl groups. Although it is difficult to quantitatively analyze the data, we qualitatively conclude that the strength of hydrogen bonding between the hydroxyl groups and phosphonyl groups is higher than that of self-associated hydroxyl groups, which no doubt enhances miscibility.

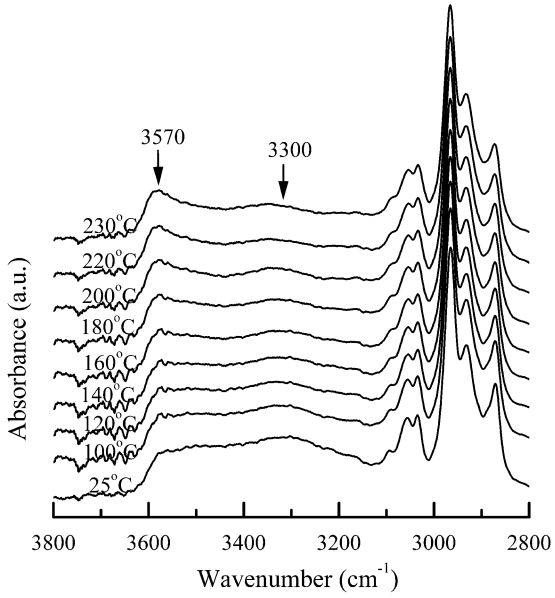


Figure 2.3.7 FTIR spectra of blend BA-P50/PHE 50/50 wt% in the hydroxyl stretching region recorded at various temperatures.

It has been suggested to the author that the phenoxy hydroxyl groups should also be able to hydrogen bond to the ether groups in the arylene ether homopolymers and copolymers of this study. This is a reasonable possibility. Such hydroxyl-ether group hydrogen bonding should be considerably weaker than hydroxyl-hydroxyl and hydroxyl-phosphonyl hydrogen bonding. In blends of phenoxy resin with poly(arylene ether)s the effect of such hydroxyl-ether group hydrogen bonding on miscibility is greatly mitigated by the fact that these groups are present in both polymers in the blends. The phenoxy resin arylene-oxygen-methylene structure and the poly(arylene ether)s arylene-oxygen-arylene structure should provide a slight difference in hydroxyl-ether hydrogen bonding strength.

### 2.3.2 Phase Behavior of Polymer Blends

A polymer blend that exhibits a sharp single $T_g$ may be considered to be a miscible blend.

Partially miscible or incompatible blends display two or more glass transition temperatures.[406,407] Poly(arylene ether phosphine oxide) homopolymer, and the poly(arylene ether phosphine oxide/sulfone) copolymers used for this study and phenoxy resin are amorphous materials. When a poly(arylene ether phosphine oxide/sulfone) copolymer having high phosphine oxide content with number average molecular weight of 20K was blended with phenoxy resin, the blends were found to be miscible, on the basis that solvent cast well dried films from these blend solutions were transparent and displayed a single $T_g$.[385] The miscible blends utilized phenoxy resin with poly(arylene ether phenyl phosphine oxide/sulfone) copolymers of high molecular weight. The films prepared by blending polymer BA-P100, PA-P50 with phenoxy were transparent. DSC shows a single $T_g$ for blends of high molecular weight phosphine oxide containing polymer and phenoxy resin, within the studied composition range from 20/80 to 80/20 weight ratio. From the previous FTIR analysis the miscibility was ascribed to hydrogen bonding. These results suggest that homogeneous polymer blends can be obtained with the component polymers even at high molecular weights.

When the amount of phosphine oxide in the copolymer was decreased to 20 mole %, DSC measurements still showed a single $T_g$ for the BA-P20/PHE blends, as illustrated in Figure 2.3.8. This is still presumed to be due to hydrogen bonding, although FTIR measurements do not show an obvious band shift. To further confirm the conclusions from the DSC results, the blend components as well as BA-P20/PHE blends in the whole composition range were subjected to dynamic mechanical analysis. Generally, the segmental motions responsible for mechanical loss peaks are considered to be related to smaller domains than those of the molecular processes responsible for the heat capacity discontinuity measured by DSC.[408,409] The temperature at a maximum of mechanical loss tangent (tan $\delta$) was taken as the $T_g$. These results for the BA-P20/PHE blends are shown in Figure 2.3.9; note that a single tan $\delta$ peak was observed for each blend. The $T_g$ of the blends, like those of the parent PHE and BA-P20, are sharp and increase monotonically with the BA-P20

[406] Olabisi, O.; Robeson, L.; Shaw, M. *Polymer-Polymer Miscibility* Academic Press: New York, **1979**.
[407] Paul, D. R.; Newman, S. *Polymer Blends* Academic Press: New York, **1978**, Vol. 1.
[408] Stoelting, J.; Karasz, F. E.; MacKnight, W. J. *Polym. Eng. Sci.* **1970**, *10*, 133.
[409] Shultz, A. R.; Beach, B. M. *Macromolecules* **1974**, *7*, 902.

concentration. No low-temperature transitions near the glass transition temperature of the phenoxy resin were observed, which again suggests that the blends are homogeneous.

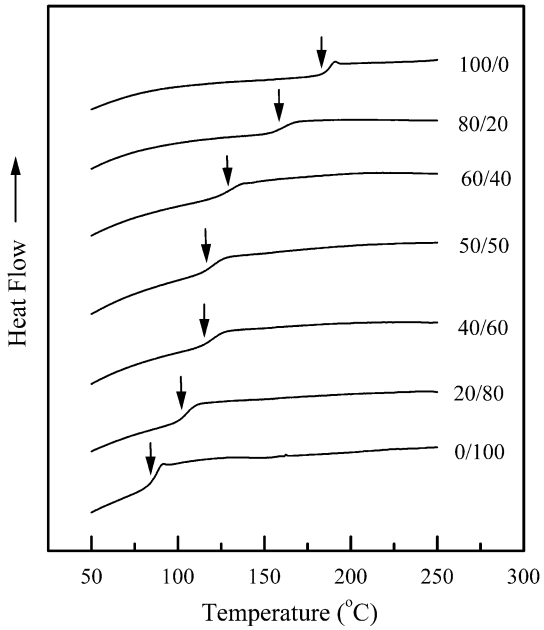


Figure 2.3.8 DSC thermograms of BA-P20/PHE blends at various weight compositions.

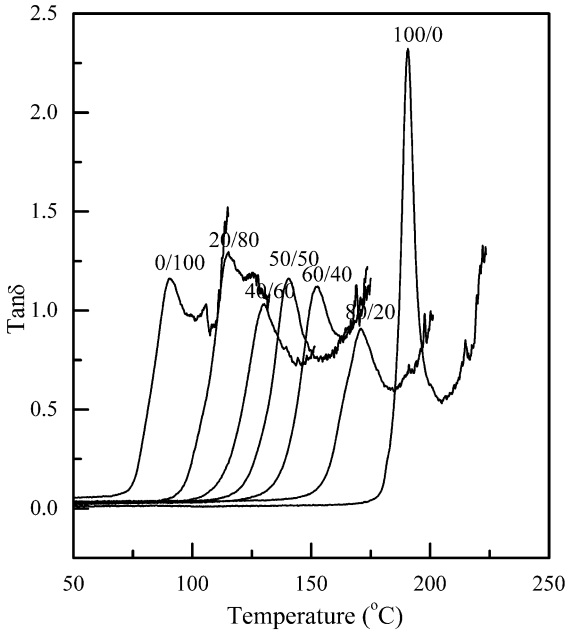


Figure 2.3.9 Mechanical loss tangents of BA-P20/PHE blends at various weight compositions.

The effect of annealing on the phase behavior of a blend of BA-P20 and PHE was studied

using a 50/50 (w/w) blend of BA-P20/PHE. The sample was quenched from 250 °C to 180 °C and further cooled to 70 °C at a rate of 0.13 °C/min; then, a DSC measurement was performed at a heating rate of 10 °C/min. Again, only a single glass transition was observed. This result showed that the high temperature annealing under the experimental conditions did not lead to a phase separation. One could reasonably expect a lower critical solution temperature (LCST) behavior for the hydrogen bonding blend system. However, if a LCST exists for the BA-P20/PHE blends, it is above the temperatures investigated.

One notes in Figure 2.3.10 that a decrease in the amount of phosphine oxide to 10 mol % in the copolymer resulted in DSC curves showing two $T_g$ of blends with 40/60, 50/50, and 60/40 BA-P10/PHE (w/w) compositions. However, blends of BA-P10/PHE with 20/80 and 80/20 blends still appear to be homogeneous. DMA measurements revealed rather broad tan δ transitions for the 40/60, 50/50, and 60/40 blends but single, well-defined peaks for the 20/80 and 80/20 blends, as shown in Figure 2.3.11. These results are consistent with the DSC data that showed partial miscibility in the intermediate blend compositions and miscibility for the 20/80 and 80/20 w/w blends. Stoelting *et al.* observed a similar phenomenon in a different system.[408] The partial miscibility behavior is ascribed to a compromise of the repulsion and the attraction between the two components. Because pure bisphenol A polysulfone is not miscible with phenoxy resin,[403] sulfone units do not promote miscibility with the phenoxy resin. Phosphonyl groups and hydroxyl groups provide hydrogen bonding and thus promote miscibility. The limited amount of hydrogen bonding between BA-P10 and PHE thus afforded only partial miscibility.

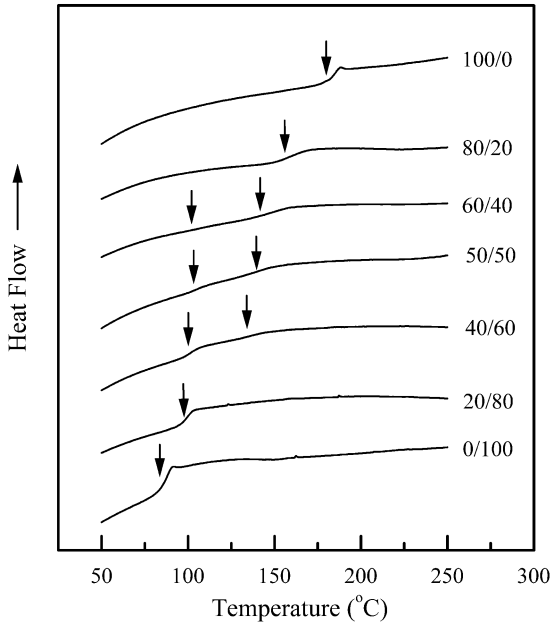


Figure 2.3.10 DSC thermogram of BA-P10/PHE blends at various weight compositions.

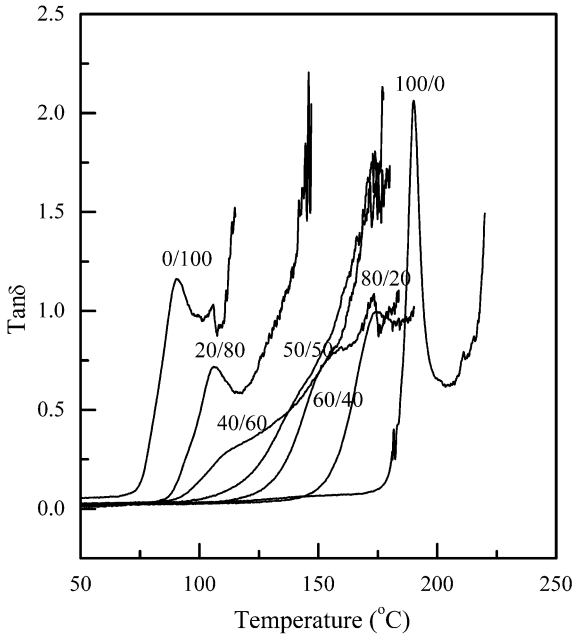


Figure 2.3.11 Mechanical loss tangent of BA-P10/PHE blends at various weight compositions.

In a 50/50 (w/w) blend of BA-P10/PHE annealed by the same procedure as BA-P20/PHE, the two $T_g$ were more distinct, but not shifted from those in the nonannealed blend as illustrated in Figure 2.3.12. Further study of the phase behaviors of blends of phenoxy resin

with copolymers having phosphine oxide unit concentrations slightly above 10 mole% could give a blend system with an observable LCST and phase boundaries in the vicinity of the LCST.

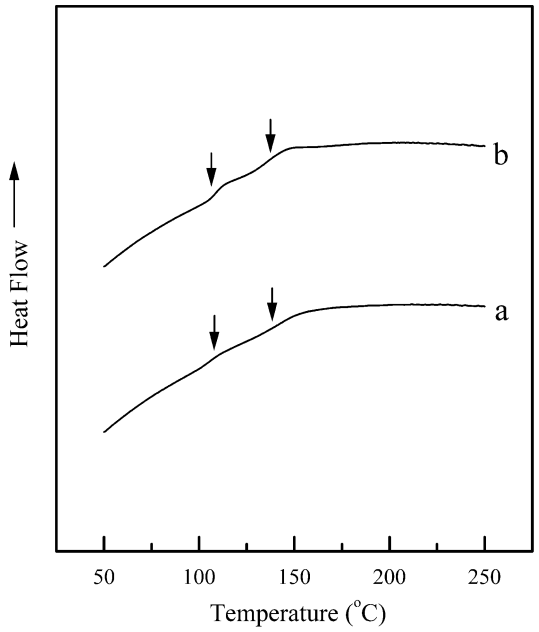


Figure 2.3.12 DSC thermogram of BA-P10/PHE blend at 50/50 wt% composition. (a) not annealed; (b) annealed.

### 2.3.3 Effect of the Copolymer Structure on the Miscibility

An obvious question is to what extent does the arylene ether portion of the polymer backbone structure affects the molecular interaction? To address this question, hydroquinone based poly(arylene ether phenyl phosphine oxide/sulfone) copolymers-phenoxy blends were also studied. Again, only a single transition behavior was observed. The hydroquinone poly(arylene ether methyl phosphine oxide) copolymer was blended with phenoxy resin and DSC results still showed a single $T_g$, as illustrated in Figure 2.3.13. These results indicate that the arylene ether portion of the backbone structure does not play a major role in the miscibility, at least in the case of hydroquinone *vs*. BA-based system.

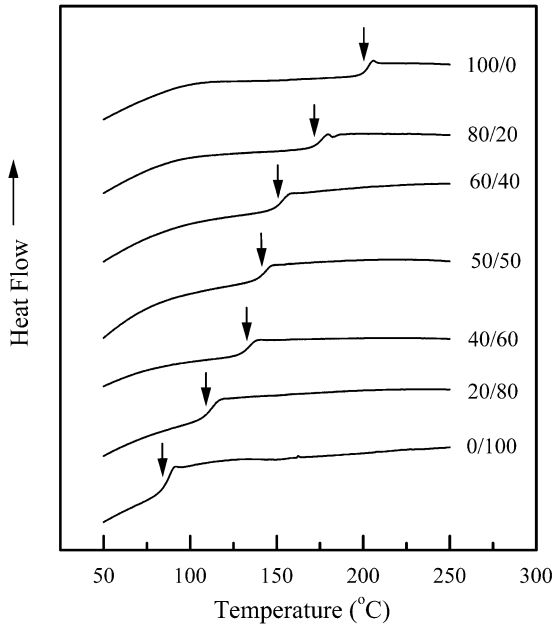


Figure 2.3.13 DSC thermogram of HQ-BFPMPO-2/PHE blends at various weight compositions.

### 2.3.4 Glass Transition Temperatures

One of the most important ways of characterizing miscible polymer blends is the determination of the composition dependencies of their glass transition temperatures, $T_g$s. Because our aim was to study the effect of the amount of phosphine oxide on the blend miscibilities, $T_g$ data (Table 2.3.3) were examined in the context of four existing blend $T_g$-weight fraction composition equations.

Three of these were derived on the bases of free volume additivity [Fox Equation 2.3.1][410], free volume additivity corrected for thermal expansion coefficient differences [Gordon-Taylor Equation 2.3.2],[411] or a psuedo-second-order thermodynamic transition combination of entropic changes in the constituent polymers at their respective $T_g$ [Couchman: Eq. 2.3.3].[412] The fourth equation [Kwei Eq. 2.3.4][413] is an empirical equation of the Gordon-Taylor form to which a term representing specific interaction contributions has been added. A recent derivation similar in protocol to that of Couchman, but from an

[410] T. G. Fox, *Bull. Am. Phys. Soc*. **1956**, *1*, 123.
[411] Gordon, M.; Taylor, J. S. *J. Appl. Chem.* **1952**, *2*, 493.
[412] Couchman, P. R. *Phys. Lett.* **1979**, *70A*, 155.
[413] Kwei, T. K. *J. Polymer Sci., Polymer Lett Ed.* **1984**, *22*, 307.

enthalpic approach and incorporating an enthalpy of mixing, has yielded an equation of the Kwei form expressed, however, in polymer unit mole fractions.[414]

Fox:
$$\frac{1}{T_{g_m}} = \frac{w_A}{T_{g_A}} + \frac{w_B}{T_{g_B}} \qquad \text{Equation 2.3.1}$$

Gordon-Taylor:
$$T_{g_m} = \frac{w_A T_{g_A} + k_{GT} w_B T_{g_B}}{w_A + k_{GT} w_B} \qquad \text{Equation 2.3.2}$$

Couchman:
$$\ln T_{g_m} = \frac{w_A \ln T_{g_A} + k_C w_B \ln T_{g_B}}{w_A + k_C w_B} \qquad \text{Equation 2.3.3}$$

Kwei:
$$T_{g_m} = \frac{w_A T_{g_A} + k_K w_B T_{g_B}}{w_A + k_K w_B} + q w_A w_B \qquad \text{Equation 2.3.4}$$

The Fox equation contains only the weight fraction compositions of the prepared blends and the experimentally determined glass transition temperatures of the constituent polymers. From the derivation of the Gordon-Taylor equation $k_{GT} = \frac{\alpha_{l_B} - \alpha_{g_B}}{\alpha_{l_A} - \alpha_{g_A}}$ is a compression constant involving the ratio of the thermal expansion coefficient changes of the constituent polymers at their respective glass transitions. The Couchman equation derivation gives $k_C = \frac{C_{l_B} - C_{g_B}}{C_{l_A} - C_{g_A}}$, the ratio of the specific heat increases of the constituent polymers at their respective $T_g$. The empirical Kwei equation, which has the form of the Gordon-Taylor equation plus an arbitrary "interaction contribution" term, could logically be applied by setting $k_K$ equal to the theoretical $k_{GT}$ and using $q$ as an adjustable parameter. In $T_g$ data analyses of the composition dependencies of miscible polymer blends, $k_{GT}$ and $k_C$ are often treated as adjustable, curve-fitting parameters that contain a combination of the individual constituent contributions and specific interaction contributions. Adopting such an empirical curve-fitting approach to the present $T_g$-$w$ data, we obtained the parameter values shown in Table 2.3.4. Rather than setting $k_K$ equal to the theoretical $k_{GT}$ as suggested earlier, we set $k_K$ equal to the theoretical $k_C$ in calculating the q values listed in Table 2.3.4. The increases in heat capacity at $T_g$ that were used in the theoretical Couchman $k_C$ and in the Kwei equation

[414] P. C. Painter, J. F. Graf, M. M. Coleman *Macromolecules* **1991**, *24*, 5630.

are 0.23 J/g•°C for the phosphine oxide-containing polymers and 0.41 J/g•°C for the phenoxy resin.

Table 2.3.4 Empirical Constants Determined for the $T_g$/Composition Equations of BA-P/PHE Blends

| Blend | $k_{GT}$ | $k_C$ | $q$ (°C) |
|---|---|---|---|
| BA-P100/PHE | 1.2 | 1.4 | 93 |
| BA-P50/PHE | 0.89 | 1.0 | 68 |
| BA-P20/PHE | 0.69 | 0.78 | 14 |

Figure 2.3.14 presents the observed glass transition temperatures of bisphenol A poly(arylene ether phosphine oxide/sulfone)/phenoxy resin blends plotted against the weight fraction of bisphenol A poly(arylene ether phosphine oxide/sulfone). The elevation of the blend $T_g$ relative to the Fox equation prediction (broken line) is greatest for the phosphine oxide homopolymer blends (BA-P100/PHE), decreases as the copolymer phosphine oxide content is decreased to 50 mol % (BA-P50/PHE), and becomes slightly negative as the phosphine oxide content is decreased to 20 mol %. These observations are consistent with a free volume decrease with resultant increased $T_g$ in the blends because of favorable (exothermal, densifying) phosphonyl/hydroxyl group interactions. Fitting of the data to the Gordon-Taylor equation (solid curves in Figure 2.3.14) by an adjustable $k_{GT}$ is fairly successful. Figure 2.3.15 indicates that the $k_{GT}$ values required for the best fits of the datasets increase linearly with increasing mol % phosphine oxide units in the copolymer. Because the compression constants for the three blend systems should not differ greatly, the rather marked increase of $k_{GT}$ with increase in phosphine oxide may reasonably be attributed to favorable (exothermal, densifying) interactions of the phosphonyl groups with the PHE hydroxyl groups. Such attribution of $k_{GT}$ association with specific interaction contributions in other blend systems has previously been proposed.[415]

[415] (a) Belorgey, M.; Prud'homme, R. E. *J. Polymer Sci., Polym. Phys. Ed.* **1982**, *20*, 191; (b) Belorgey, G.; Aubin, M.; Prud'homme, R. E. *Polymer* **1985**, *23*, 1051.

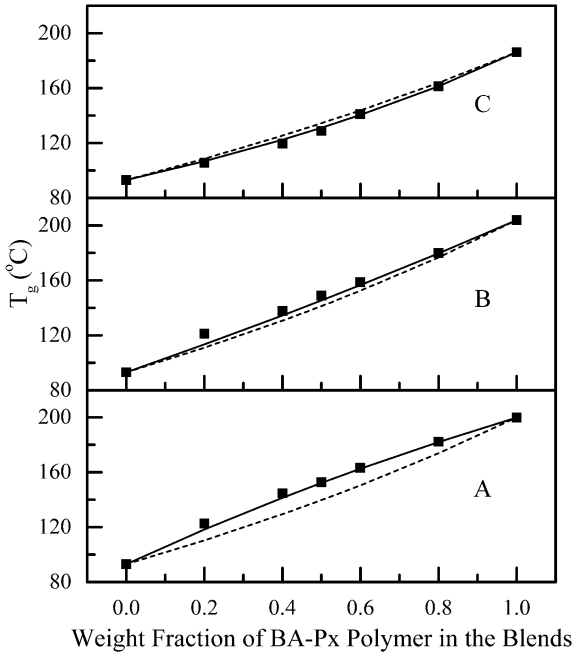


Figure 2.3.14 Fit of experimental $T_g$ *vs.* composition data to the curves predicted by the Fox equation (broken line) and the Gordon-Taylor equation with empirical adjusted $k_{GT}$(solid line). (A) BA-P100/phenoxy; (B) BA-P50/phenoxy; (C) BA-P20/phenoxy.

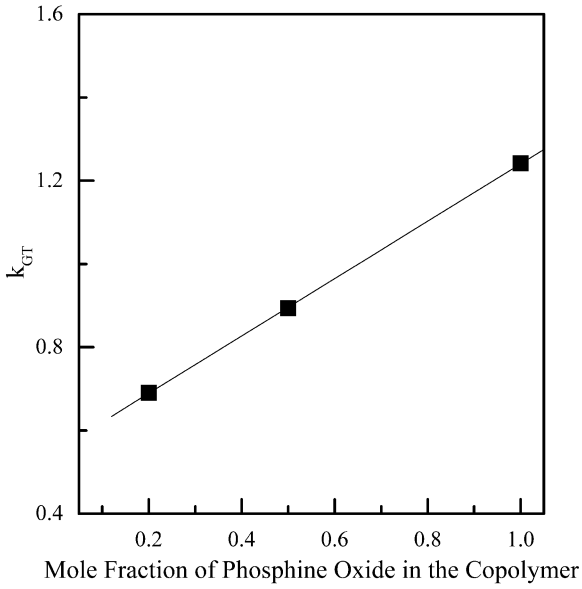


Figure 2.3.15 Effect of the amount of phosphine oxide in the copolymer on the $k_{GT}$ coefficient of the Gordon-Taylor equation.

Figure 2.3.16 presents the same blend glass transition temperature data which were presented in Figure 2.3.14. The broken-line curves correspond to the Couchman equation in

which $k_C$ values were calculated from the individual constituent polymer-specific heat changes at their glass transitions. The solid curves represent the fit by using adjustable $k_C$ values. The increased $T_g$ elevation, relative to the theoretical Couchman equation prediction, with increased phosphine oxide content is consistent with favorable (exothermal, densifying) phosphonyl/hydroxyl group interactions. Figure 2.3.17 presents the blend $T_g$ data, the $T_g$ values predicted by the theoretical Gordon-Taylor equation (with $k_{GT}=k_C$; broken-line curves), and the empirical Kwei equation fit (solid curves) of the data. Fitting the blend $T_g$ data by the Kwei equation with $q$ as an adjustable interaction parameter gives very good fits (solid curves) with q values increasing with increasing copolymer phosphine oxide content. The parameter $q$ is 14, 68, and 93 °C for blends containing 20 mole%, 50 mole%, and 100 mol %, respectively, phosphonyl units in the copolymer (Table 2.3.4). This trend of enhanced $T_g$ by the $qw_Aw_B$ term is definitely consistent with a favorable, hydrogen bonding interaction between the phosphonyl group of the copolymer and the hydroxyl group of the phenoxy resin.

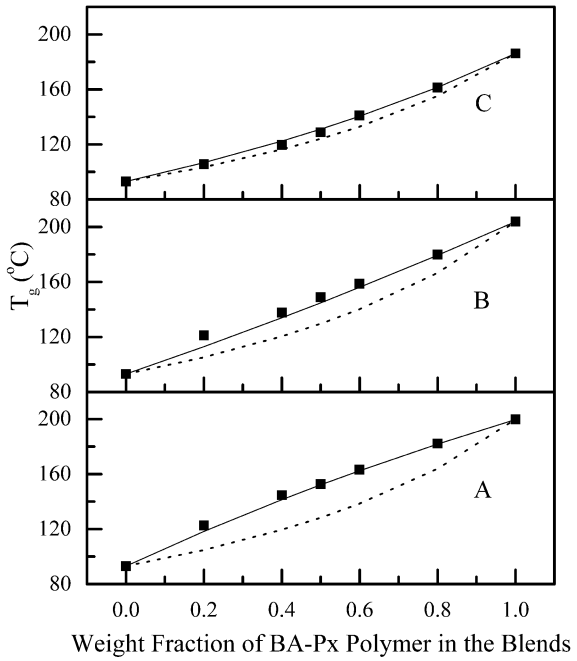


Figure 2.3.16 Fit of experimental $T_g$ values to those predicted by Couchman with $k_C$ as the ratio of the heat capacity increases of the components at their $T_g$s(broken line) and with empirical $k_C$ values (solid line). (A) BA-P100/phenoxy; (B) BA-P50/phenoxy; (C) BA-P20/phenoxy.

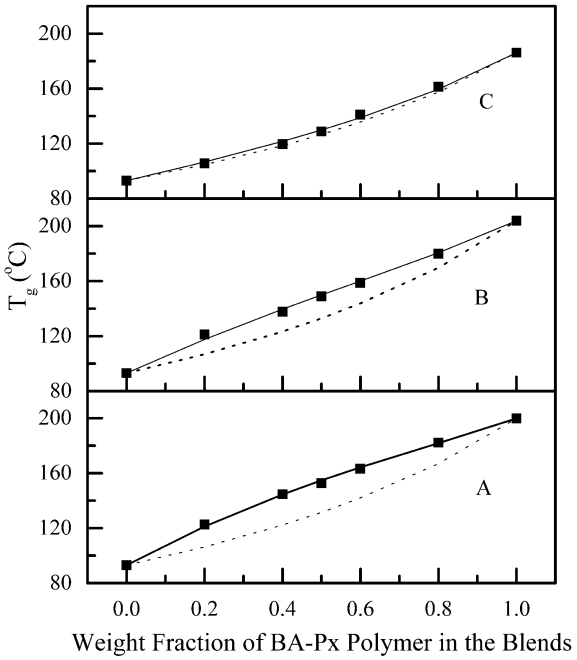


Figure 2.3.17 Fit of experimental $T_g$ values to those predicted by the Gordon-Taylor part term of the Kwei equation with $k_K=k_C$ (broken line) and the full form of Kwei equation (solid line). (A) BA-P100/phenoxy; (B) BA-P50/phenoxy; (C) BA-P20/phenoxy.

## *2.4 Conclusions*

High molecular weight tough, film forming amorphous poly(arylene ether phenyl phosphine oxide/sulfone) homopolymers and copolymers of various compositions have been successfully prepared. Blends prepared via solution mixing of these polymers with phenoxy resin exhibited specific interaction (hydrogen bonding) between the phosphonyl groups of the poly(arylene ether phosphine oxide) and hydroxyl groups of the phenoxy resin. This was confirmed by the observation of the band shift of the hydrogen-bonded hydroxyl group stretching mode from around 3445 $cm^{-1}$ to 3300 $cm^{-1}$ and of the phosphonyl group stretching mode from 1196 $cm^{-1}$ to 1170 $cm^{-1}$. The miscibility of the blends depends on the mole ratio of phosphine oxide to sulfone in the copolymer. Bisphenol A based copolymers from miscible blends with phenoxy resin even when the phosphine oxide monomer used to prepare copolymer is decreased to 20 mol %. However, a further decrease of the amount of phosphine oxide in the copolymer to 10 mol % results in multi-phase blends. These results provided good evidence of the importance of hydrogen bonding to the miscibility of the polymer

blends. Various empirical equations have been used to describe the composition dependency of $T_g$. The elevation of $T_g$ with increased phosphonyl group concentration can be attributed to the hydrogen bonding specific interaction between the copolymer phosphonyl groups and the phenoxy resin hydroxyl groups. Replacement of bisphenol A by hydroquinone in the copolymers did not significantly affect their miscibility with phenoxy resin, confirming the important role of phosphorus oxygen bond for this specific interaction. The study also provides evidence that these copolymers may be useful to provide interphase materials in several composite structures and in the important field of polymer blends.

# 3 On the Miscibility of Phosphorus-Containing Polymers and Bisphenol A Poly(hydroxy ether) Blends

## *3.1 Introduction*

Polymer blending has found many industrial applications, since this strategy can often generate relatively inexpensive materials with improved properties. Most polymer blends are heterogeneous (immiscible). From a thermodynamic point of view, mixing entropy increase is very small in polymer blends. Miscibility must be achieved by a favorable (negative) mixing enthalpy. Understanding the driving force for the miscibility and the stability of homogeneous polymer blends is of great interest from both academic and industrial points of view. This understanding has been crucial for the development of new materials, since only the miscible polymer blends are thermodynamically stable.[416,417,418,419] Hydrogen bonding is the most important specific interactions for promoting polymer miscibility.

The literature shows that bisphenol A poly(hydroxy ether) (PHE) is miscible with many polymers, because its pendant hydroxyl groups can act as both proton donators and acceptors. For example, it is miscible with poly(ε-caprolactone),[420] poly(butylene terephthalate),[421] a cyclohexane-dimethanol-based polyester,[422] a polyester-based polyurethane,[423] poly(ethylene adipate),[424] poly(butylene adipate), poly(ethylene oxide),[425] poly(vinyl ethyl ether),[407a] poly(methyl methacrylate),[426] poly(vinylpyrrolidone) (PVP),[427] phenolphthalein poly(ether

[416] Olabisi, O.; Robeson, L. M.; Shaw, M. T. *Polymer-Polymer Miscibility* Academic Press: New York, **1979**.
[417] (a) Paul, D. R.; Newman, S. *Polymer Blends Vol. I-II* Academic Press: New York, **1978**; (b) Paul, D. R.; Bucknall, C. *Polymer Blends Vol. I. Formulation, Vol. II. Performance* John Wiley & Sons, Inc.: New York **2000**.
[418] Coleman, M. M.; Graf, J. F.; Painter, P. C. *Specific Interactions and the Miscibility of Polymer Blends* Technomic: Lancaster, PA, **1991**.
[419] Utracki, L. A. *Polymer Alloy and Blends* Hanser Publishers: Munich, **1989**.
[420] Brode, G. L.; Koleske, J. V. *J. Macromol. Sci. Chem.* **1972**, *6*, 1109.
[421] Robeson, L. M.; Furtek, A. B. *J. Appl. Polym. Sci*. **1979**, *23*, 645.
[422] Seefried, C. G. Jr.; Koleske, J. V.; Critchfield, F. E. *Polym. Eng. Sci*. **1976**, *16*, 771.
[423] Paul, D. R.; Barlow, J. W. *J. Macromol. Sci. Rev. Macromol. Chem.* **1980**, *C18*, 109.
[424] Smith, K. L.; Winslow, A. E.; Petersen, D. E. *Ind. Eng. Chem.* **1959**, *51*, 1361.
[425] (a) Robeson, L. M.; Hale, W. F.; Merrian, C. N. *Macromolecules* **1980**, *14*, 1644; (b) Osada, Y.; Sata, M. *J. Polym. Sci., Polym. Lett. Ed*. **1976**, *14*, 129; (c) Coleman, M. M.; Moskala, E. J. *Polymer* **1983**, *24*, 251.
[426] (a) Chiou, J. S.; Paul, D. R. *J. Appl. Polym. Sci*. **1991**, *42*, 8131; (b) Soh, Y. S. *J. Appl. Polym. Sci*. **1992**, *45*, 8131; (c) Ward, Y.; Mi, Y. *Polymer* **1999**, *40*, 2465.
[427] (a) Eguiazable, J. I.; Iruin, J. J.; Cortazer; Guzman, G. M. *Makromol. Chem*. **1984**, *185*, 1761; (b) Martinez de Ilarduya, A.; Iruin, J. J.; Fernandez-Berridi, M. J. *Macromolecules* **1995**, *28*, 3707; (c) Zheng, S.; Guo, Q.; Mi, Y. *J.*

ether ketone),[428] poly(N-methyl-N-vinylacetamide) (PMVAc),[429] poly(N,N-dimethylacrylamide) (PDMAc),[429] poly(ethyl oxazoline) (PEOx),[429,430] poly(ether sulfone),[431] poly(arylene ether phenyl phosphine oxide),[432,433] and various epoxy resins.[434] All of the polymer blend systems were reported to be miscible over the entire composition region.

In recent years, the discovery of the extensive hydrogen bonding between phosphonyl and hydroxyl groups has sparked new interest in preparing some new phosphorus-containing polymers, since the hydrogen bonding interaction between hydroxyl group and phosphonyl group promotes polymer-polymer miscibility and improves the selected properties.[432,433,435,436,437]

Introducing interphase or sizing materials has been demonstrated to improve the mechanical properties of the composites.[438] In the past decade, many new phosphorus containing high performance polymers including poly(arylene ether)s,[439] poly(arylene thioether)s,[440] polyimides,[441] and cyanate resins[442] have been synthesized in our laboratory and elsewhere. These polymers exhibit good mechanical properties, thermal stability, and fire resistance. Introduction of the phosphonyl group may increase the polarity of the polymers, and make them proton acceptors. Incorporating phosphonyl groups into the polymers is surmised to improve the surface adhesion between these polymers and other materials,

---

*Polym. Sci., Polym. Phys. Ed*. **1998**, *36*, 2291.
[428] Guo, Q.; Huang, J.; Chen, T. *Polym. Bull*. **1988**, *20*, 517.
[429] Dai, J.; Goh, S. H.; Lee, S. Y.; Siow, K. S. *Polymer* **1996**, *37*, 3259.
[430] Lau, C.; Zheng, S.; Zhong, Z.; Mi, Y. *Macromolecules* **1998**, *31*, 7291.
[431] (a) Singh, V. B.; Walsh, D. J. *J. Macromol. Sci. Phys*. 1986, B25, 65; (b) Reimers, M. J.; Barbari, T. A. *J. Polym. Sci., Polym. Phys*. **1994**, *32*, 131.
[432] Srinivasan, S.; Kagumba, L.; McGrath, J. E. *Macromol. Symp*. **1997**, *122*, 95.
[433] Wang, S.; Ji, Q.; Chatchoua, C. N.; Shultz, A. R. *J. Polym. Sci., Polym. Phys. Ed*. **1999**, *37*, 1849.
[434] Guo, Q. *Polymer* **1995**, *36*, 4753.
[435] Sun, J.; Cabasso, I. *J. Polym. Sci., Polym. Chem. Ed*. **1989**, *27*, 3985.
[436] Zhuang, H.; Pearce, E.; Kwei, T. K. *Macromolecules* **1994**, *27*, 6398.
[437] Wang, S.; Wang, J.; Ji, Q.; Shultz, A. R.; Ward, T. C.; McGrath, J. E. *Submitted to J. Polym. Sci., Polym. Phys. Ed.*
[438] Lesko, J. J.; Swain, R. E.; Cartwright, J. M.; Chin, J. W.; Reifsnider, K. L.; Dillard, D. A.; Wightman, J. P. *J. Adhesion* **1994**, *45*, 43.
[439] (a) Smith, C.D. *Ph.D. Dissertation* Virginia Polytechnic Institute and State University: Blacksburg, VA, **1991**; (b) Smith, C.D.; Grubbs, H.J.; Webster, H. F.; Gungör, A.; Wightman, J. P.; McGrath, J. E. *High Perform. Polym.* **1991**, *4*, 211; (c) Riley, D.J.; Gungör, A.; Srinivasan, S. A; Sankarapandian, M.; Tchatchoua, C. N.; Muggli, M.W.; Ward, T. C.; McGrath, J. E.; Kashiwagi, T. *Polym. Eng. Sci.* **1997**, 37, 150.
[440] (a) Liu, Y. *Ph.D. Dissertation* Virginia Polytechnic Institute and State University: Blacksburg, VA, **1998**; (b) Liu, Y.; McGrath, J. E. *Polymer* **2000** (in press).
[441] (a) Tan, B.; Tchatchoua, C.N.; Dong, L.; McGrath, J.E. *Polym. Adv. Technol.* **1998**, *9*, 84; (b) Zhuang, H. *Ph.D. Dissertation* Virginia Polytechnic Institute and State University: Blacksburg, VA, **1998**.
[442] Abed, J.C.; Mercier, R.; McGrath, J. E. *J. Polym. Sci., Polym. Chem. Ed.* **1997**, *35*, 977.

organic or inorganic, having hydroxyl groups. This promoted our research on the possibility of phosphorus-containing high performance polymers as interphase materials for composites having matrices such as epoxy resins or bisphenol A dimethacrylates. The major advantages of high performance polymers over common polymers include high $T_g$ and good mechanical properties. Another objective of our research was to develop some new polymer blends with improved mechanical and thermal properties based on high performance phosphorus-containing polymers. Recently, our research showed that bisphenol A or hydroquinone based poly(arylene ether phosphine oxide)s formed miscible blends with bisphenol A based poly(hydroxy ether) (phenoxy resin) (PHE).[432,433] Further work demonstrated that bisphenol A poly(arylene ether phenyl phosphine oxide) is miscible with both uncured and cured commercial bisphenol A dimethacylate composites (vinyl ester resin with styrene as the diluent).[437] The hydrogen bonding interaction between the hydroxyl group and the phosphonyl group was shown to be the driving force for the miscibility. However, miscibility depends on both the favorable specific interaction with the phosphonyl group and the less favorable, or unfavorable, interaction with other groups in the chain. Therefore, miscibility is a compromise of the favorable specific interaction with the phosphonyl groups and unfavorable interactions with other groups in the copolymer chains. Extension of our investigations to some other systems was important because the universality of compatibility by the phosphonyl/hydroxyl hydrogen bonding is still unknown. The present research was designed to systematically investigate the miscibility of PHE with phosphorus-containing poly(arylene ether)s, such as hexafluorobisphenol A or biphenol poly(arylene ether phosphine oxide)s, with poly(arylene thioether phosphine oxide) (abbreviated as SS-PTPO), and with polyimides (polymers prepared from 2,2'-bis[4-(3,4-dicarboxyphenoxy)phenyl]propane dianhydride (BPADA) and bis(*m*-aminophenyl) methyl phosphine oxide (DAMPO) (abbreviated as BPADA-DAMPO) or bis(*m*-aminophenyl) phenyl phosphine oxide (DAPPO) (abbreviated as BPADA-DAPPO). The structures of the above polymers and the related systems are shown in Scheme 3.1.1.

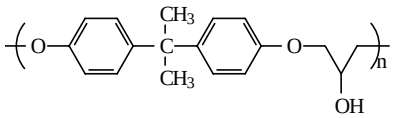


Bisphenol A Poly(hydroxy ether) “Phenoxy Resin” (PHE)

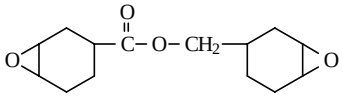

ERL-4221® (3,4-epoxycyclohexylmethyl-3,4-epoxycyclohexyl carboxylate) (ECHMECHC)

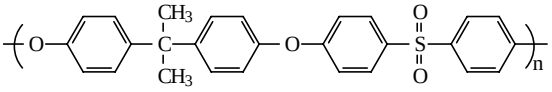

Udel® Bisphenol A Polysulfone

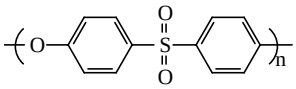

Victrex® Poly(ether sulfone)

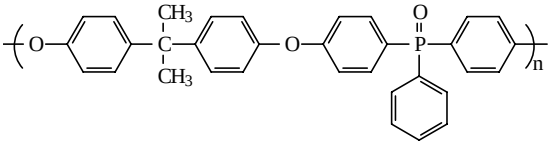

Bisphenol A Poly(arylene ether phenyl phosphine oxide) (BPA-PEPO)

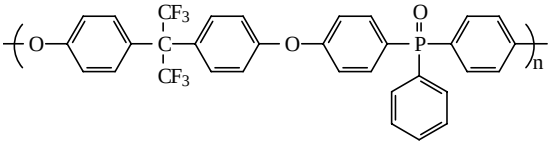

Hexafluorobisphenol A Poly(arylene ether phenyl phosphine oxide) (HFBPA-PEPO)

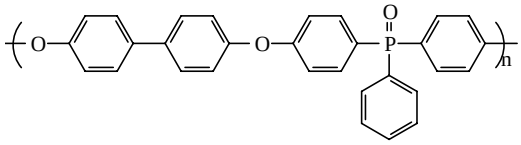

Biphenol Poly(arylene ether phenyl phosphine oxide) (BP-PEPO)

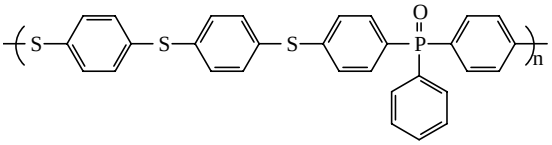

Thiodithiophenol Poly(arylene thioether phenyl phosphine oxide) (SS-PTPO)

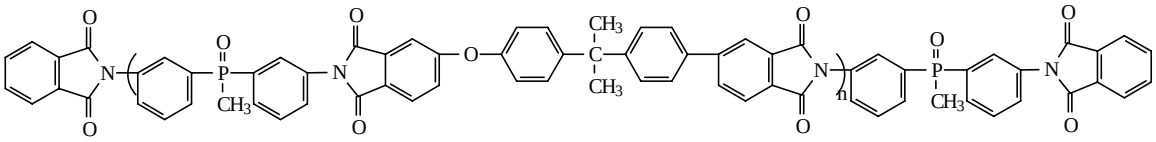

Polyimide from 2,2′-bis[4-(3,4-dicarboxyphenoxy)phenyl]propane dianhydride (BPADA) and bis(*m*-aminophenyl) methyl phosphine oxide (DAMPO) (BPADA-DAMPO)

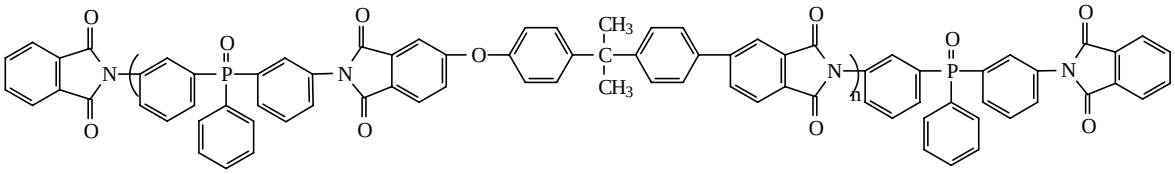

Polyimide from 2,2′-bis[4-(3,4-dicarboxyphenoxy)phenyl]propane dianhydride (BPADA) and bis(*m*-aminophenyl) phenyl phosphine oxide) (BPADA-DAPPO)

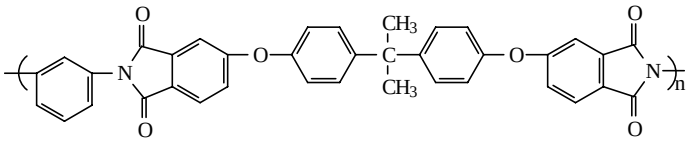

Ultem® (BPADA-*m*-PDA)

Scheme 3.1.1 Structures of bisphenol A poly(hydroxy ether), bisphenol A polysulfone, various phosphorus-containing poly(arylene ether)s, polyimides, and Ultem® resin.

## *3.2 Experimental*

### 3.2.1 Materials

Bisphenol A poly(hydroxy ether) (PHE) ($M_n$=20K) was supplied by Phenoxy Associates (Rock Hill, SC). A commercial polyimide, Ultem® resin (BPADA-*m*-PDA), was supplied by the General Electric Company (Schenectady, NY). A commercial cycloaliphatic epoxy resin, ERL-4221®, (3,4-epoxycyclohexylmethyl-3,4-epoxycyclohexyl carboxylate) (ECHMECHC) was obtained from the Union Carbide Chemicals and Plastics Company Inc. (Danbury, CT). Polymers BPA-PEPO, HFBPA-PEPO, BP-PEPO were prepared in our laboratory.[433,439] SS-PTPO was prepared in this laboratory and was reported elsewhere.[440] BPADA-DAMPO and BPADA-DAPPO polyimides were also synthesized in our laboratory.[441] The molecular weights and intrinsic viscosities of these polymers were tabulated in Table 3.2.1.

Table 3.2.1 GPC and Intrinsic Viscosity Characterization of Bisphenol A Poly(hydroxy ether), Bisphenol A Polysulfone, Poly(ether sulfone), Various Phosphorus-Containing Poly(arylene ether)s, Polyimides, and Ultem®

| | GPC | | | [η] (dl/g) |
|---|---|---|---|---|
| Sample | $M_n*10^{-3}$ | $M_w*10^{-3}$ | $M_w/M_n$ | $CHCl_3$, 25°C |
| BPA-PEPO-100 | 39 | 74 | 1.9 | 0.42 |
| BPA-PEPO-50 | 70 | 159 | 2.3 | 0.73 |
| HFBPA-PEPO | 58 | 237 | 4.0 | 0.67 |
| BP-PEPO | 53 | 278 | 5.2 | 1.09 |
| SS-PTPO | 42 | 92 | 2.2 | 0.48 |
| BPADA-DAMPO | 20 | 33 | 1.8 | 0.28* |
| BPADA-DAPPO | 19 | 38 | 2.0 | 0.28* |
| BPADA-*m*-PDA | 20 | 33 | 1.7 | 0.40 |
| Udel | 26 | 48 | 1.9 | 0.39 |
| Victrex | 21 | 34 | 1.6 | 0.34** |
| PHE | 20 | 46 | 2.3 | 0.28 |

* In NMP at 30 °C
** In NMP at 25 °C

### 3.2.2 Preparation of Polymer Blends

The BPA-PEPO, HFBPA-PEPO, SS-PTPO, BPADA-DAMPO, BPADA-DAPPO were separately dissolved in chloroform as 7.5 wt% solutions. These solutions were then mixed with portions of a 7.5 wt% PHE chloroform solution to achieve the desired blend compositions. The polymer mixtures were isolated by precipitating the solutions in methanol. The precipitates were dried in a vacuum oven for 24 h at 150 °C. Films for FTIR measurements were prepared by casting blend solutions onto glass slides or salt plates and drying in a vacuum oven in a similar manner. The films used for dynamic mechanical analysis (DMA) measurements were obtained by melt pressing the precipitates between metal plates for about 3 min at temperatures ranging from 160 °C for 100 wt% PHE to 280 °C for 100 wt of the phosphorus-containing polymers. The melt-pressed samples were allowed to cool to ambient temperature between the metal plates.

The polymer blends BPADA-MPDA/PHE and BP-PEPO/PHE were prepared in dimethylacetamide (DMAc) solutions instead of using chloroform. Other conditions were similar. Thermogravimetric analysis (TGA) and nuclear magnetic resonance spectroscopy (NMR) were used to determine that all the solvent was completely removed for the polymer blends.

### 3.2.3 Characterization

Intrinsic viscosities of the polymers were measured in chloroform or N,N-dimethylacetamide (DMAc) at 25 °C. GPC measurements were performed at 60 °C in a Waters 150C instrument to characterize the molecular weights and molecular weight distributions of the polymers. N-methyl pyrrolidone (NMP) containing 0.02M phosphorus pentoxide was the solvent. A differential refractive index detector and a Viscotek differential viscometer connected in parallel permitted calculation of absolute molecular weights and molecular weight distributions by applying the universal calibration principle.[443]

FTIR measurements were performed with a Nicolet Impact Mode 400 FTIR spectrometer. Each spectrum was an average of 256 scans at a resolution of 2 $cm^{-1}$.

Differential scanning calorimetry (DSC) thermograms were obtained on a Perkin-Elmer DSC-7 in a dry nitrogen atmosphere and were used to determine the glass transition temperatures of the polymer blends. The midpoint temperature of the specific heat increase in the glass transition region during a second heat at 10 °C/min was taken as the $T_g$.

Dynamic mechanical analyses (DMA) were performed at 1 Hz in a Perkin-Elmer DMA-7e with an extension probe at a heating rate of 2 °C/min.

NMR spectra of the polymer blends of BPADA-DAMPO polyimide and PHE were obtained employing a Bruker MSL 300 instrument according to the following procedures: The phosphorus NMR was measured under a standard $^{31}P$ CP-MAS condition, with 100-200 scans per FID using a spinning rate of 6.0-6.5 kHz. Measurements of proton spin-lattice relaxation times in the rotating frame ($T_{1\rho}$) under $^{13}C$ CP-MAS conditions by using a 90°

[443] (a) Konas, M.; Moy, T. M.; Rogers, M. E.; Shultz, A. R.; Ward, T. C.; McGrath, J. E. *J. Polym. Sci., Polym. Phys. Ed.* **1995**, *33*, 1429; (b) Konas, M.; Moy, T. M.; Rogers, M. E.; Shultz, A. R.; Ward, T. C.; McGrath, J. E. *J. Polym. Sci., Polym. Phys. Ed.* **1995**, *33*, 1441.

pulse, followed by a variable proton spin lock, followed by a fixed contact time. Twelve proton spin lock periods were used ranging from 0.25 to 20 ms. Measurements of the proton spin-lattice relaxation times in the rotating frame ($T_{1\rho}$) were obtained from a computer-generated best fit of the intensity of the $^{13}C$ NMR spectra to the single-exponential equation $M(t) = M(0)\exp(-\tau / T_{1\rho})$. All NMR measurements were performed at room temperature with 250-350 mg of sample in a Zirconia rotor with a Kel-F end cap. A 90° pulse of 5 μs was employed with 512 FID signal accumulations. Spinning rates were 6.0-6.2 kHz, and the Hartmann-Hahn match was adjusted before each accumulation using an adamantane reference sample.

## *3.3 Results and Discussion*

### 3.3.1 Hydrogen Bonding Between Phosphonyl and Hydroxyl Groups

#### *3.3.1.1 Poly(arylene ether phenyl phosphine oxide) or Poly(arylene thioether phenyl phosphine oxide)/PHE*

Hydrogen bonding interactions between the phosphonyl groups and the hydroxyl groups of alcohols, phenols, carboxylic acids, or chloroform.[444,445,446,447,448] The association constants for the triphenylphosphine oxide/phenol complex in carbon tetrachloride solvent are 1055 and 365 at 20 °C and 50 °C, respectively.[445] The driving force for the miscibility of phosphine oxide containing poly(arylene ether)s and PHE is the hydrogen bonding interaction.[432,433] FTIR spectra of bisphenol A poly(arylene ether phenyl phosphine oxide)/PHE showed a shift due to hydrogen bonding of the hydroxyl stretching vibration peak from 3445 $cm^{-1}$ to about 3300 $cm^{-1}$.[433] We previously reported similar hydrogen bonding interactions between bisphenol A poly(arylene ether phosphine oxide) and dimethacrylates.[437] This paper describes the hydrogen bonding interactions observed in the hexafluorobisphenol A and biphenol based poly(arylene ether phenyl phosphine oxide)s. Figures 3.3.1a and 3.3.1b show the stretching vibration of self-associated hydroxyl shifted to lower wave number.

---

[444] Hadzi, D. *J. Chem. Soc*. **1962**, 5128.
[445] Aksnes, G.; Gramstad, T. *Acta Chem. Scand*. **1960**, *14*, 1485.
[446] Gramstad, T. *Acta Chem. Scand*. **1961**, *15*, 1337.
[447] Maciel, G. E.; James, R. V. *Inorg. Chem*. **1964**, *3*, 1650.
[448] Hays, H. R.; Peterson, D. J. in *Organic Phosphorus Compounds, Vol. 3*. Kosolapoff, G. M.; Maier, L. Wiley-Interscience: New York, **1972**.

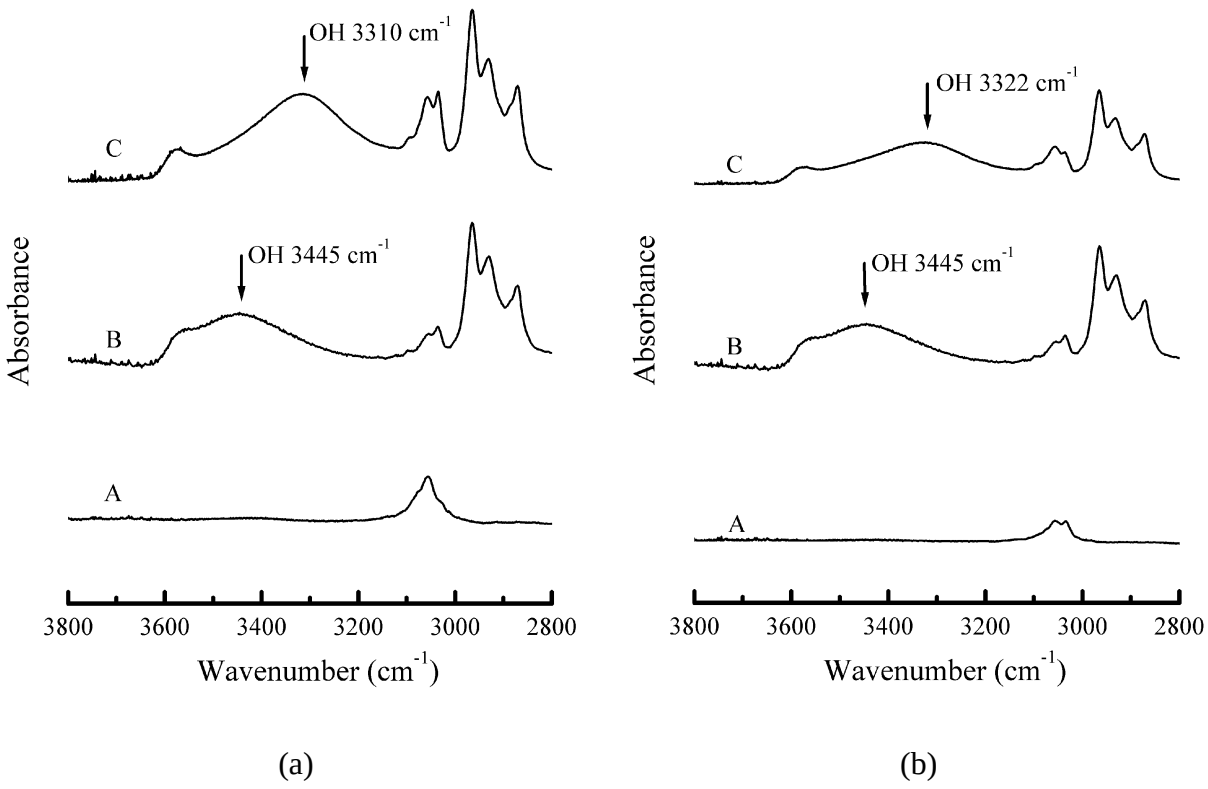


Figure 3.3.1 FTIR spectra of (a) HFBPA-PEPO/ PHE and (b) BP-PEPO/PHE blends recorded at room temperature in the hydroxyl stretching region (A) polymer; (B) PHE; (C) 50/50 wt% blend

It was not possible to eliminate the possibility of a significant contribution from the hydrogen bonding between the hydroxyl groups of PHE and the ether oxygen atoms of BPA-PEPO previously. Accordingly, a well-known miscible system poly(ether sulfone) (Victrex®)/PHE was employed as a model system to study the hydrogen bonding interaction between two components.[431] Figure 3.3.2 shows that the peak maximum at 3445 $cm^{-1}$ due to the stretching vibration of self-associated OH of PHE shifted to 3526 $cm^{-1}$ when PHE was blended with poly(ether sulfone). It was not certain whether the shift of hydrogen bonded OH was due to the interaction of the hydroxyl group with the ether oxygen or the interaction of the hydroxyl group with the sulfonyl group. In either case, the results suggested a quite weak specific interaction because the band attributed to self-associated OH stretching vibration shifted to higher wave numbers.[418] The hydrogen bonding interaction between the hydroxyl group of PHE and the ether group of the phosphorus-containing polymers is reasonably assumed to be similar to that observed in the poly(ether sulfone)/PHE blends. In these latter blends the interaction between the hydroxyl group of PHE and the ether oxygen of the

poly(arylene ether) should either be very weak or negligible. One should remember that any hydroxyl/ether oxygen interaction between PHE and another arylene ether polymer is in direct competition with the hydroxyl/ether oxygen interaction of PHE with itself. These results suggest that it is the strong hydrogen bonding interaction between phosphonyl groups and hydroxyl groups that is the driving force for miscibility in the blends examined in the present research.

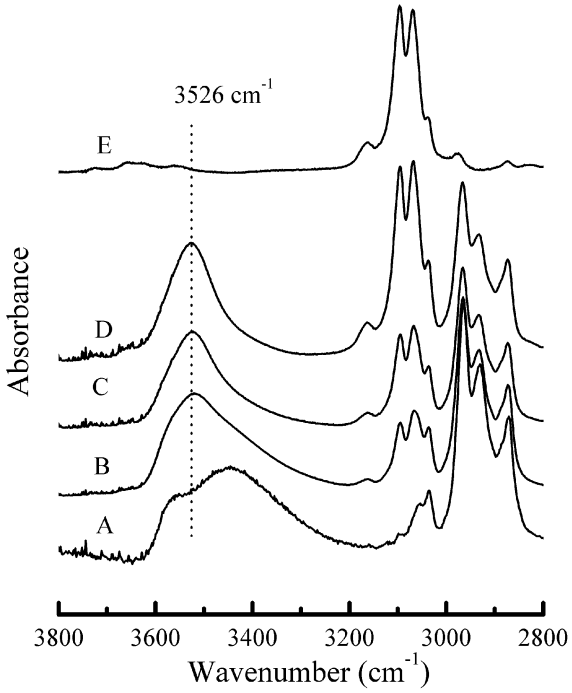


Figure 3.3.2 FTIR spectra of Poly(ether sulfone)/PHE blends at various compositions (repeat unit mole ratios) recorded at room temperature in the hydroxyl stretching region (A) 0:1; (B) 1:2; (C) 1:1; (D) 2:1; (E) 1:0

The self-associated hydroxyl group shifted down to low wave numbers with about the same $cm^{-1}$ shift as in the phosphorus-containing poly(arylene ether)/PHE blend systems in the thioether system, as shown in Figure 3.3.3. The thioether sulfur in SS-PTPO should act as a much weaker proton acceptor for hydrogen bonding compared with the ether oxygen, so the predominant contribution of hydrogen bonding should again come from the interaction between hydroxyl and phosphonyl group. These results suggested that the hydrogen bonding interaction between OH and phosphonyl group is relatively independent of the main chain structure.

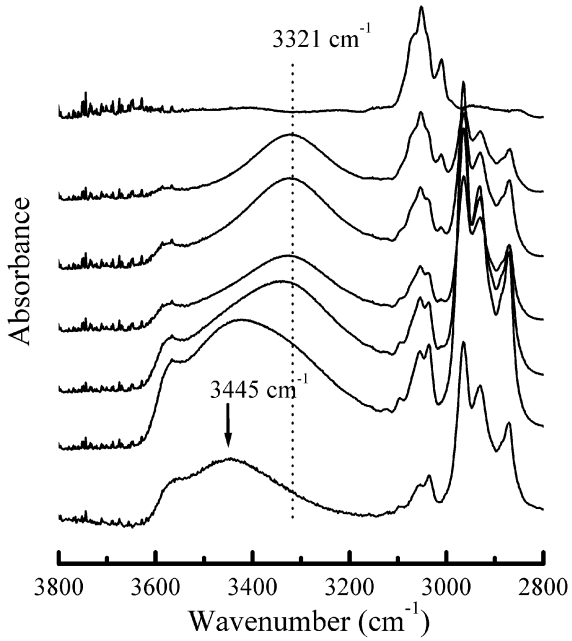


Figure 3.3.3 FTIR spectra of SS-PTPO/ PHE blends at various weight compositions recorded at room temperature in the hydroxyl stretching region at (A) 0/100; (B) 20/80; (C) 40/60; (D) 50/50; (E) 60/40; (F) 80/20; (G) 100/0 wt% compositions

Further characterization of the hydrogen bonding was also performed by means of solid-state $^{31}$P CP-MAS NMR. The $^{31}$P chemical shift was reported to shift downfield with phosphonyl group hydrogen bonds with other groups. In the BPA-PEPO/PHE, HFBPA-PEPO/PHE, BP-PEPO/PHE, and SS-PTPO/PHE blend systems, the phosphorus peak shifted from about 25 ppm down to about 29.5 ppm with increasing amounts of PHE in the polymer blends. Figures 3.4.4a, 3.4.4b show the $^{31}$P chemical shift in the BPA-PEPO-100/PHE and HFBPA-PEPO/PHE blend systems with various compositions, respectively. Table 3.3.1 shows the $^{31}$P chemical shifts in the various polymer blend systems. The chemical shifts are approximately the same as that of triphenylphosphine oxide in 2-propanol in 1:20 mole ratio solutions.[447] These spectra reveal changes in the chemical shifts that could be a result of specific molecular interactions between blend components. Changes in the chemical shift originate from relatively short range effects, so they necessarily indicate interaction between the blend constituents on a molecular level. Chemical shift changes may be induced directly by interchain shielding, that is by alteration of the phosphorus electron cloud by a change in chemical environment, or indirectly by changes in conformation through modification of

bond angles and variations in intrachain nearest-neighbor distances.[449] The spectral changes shown in Figure 3.3.4a and 3.3.4b provide strong evidence for intimate intermixing on a molecular scale.

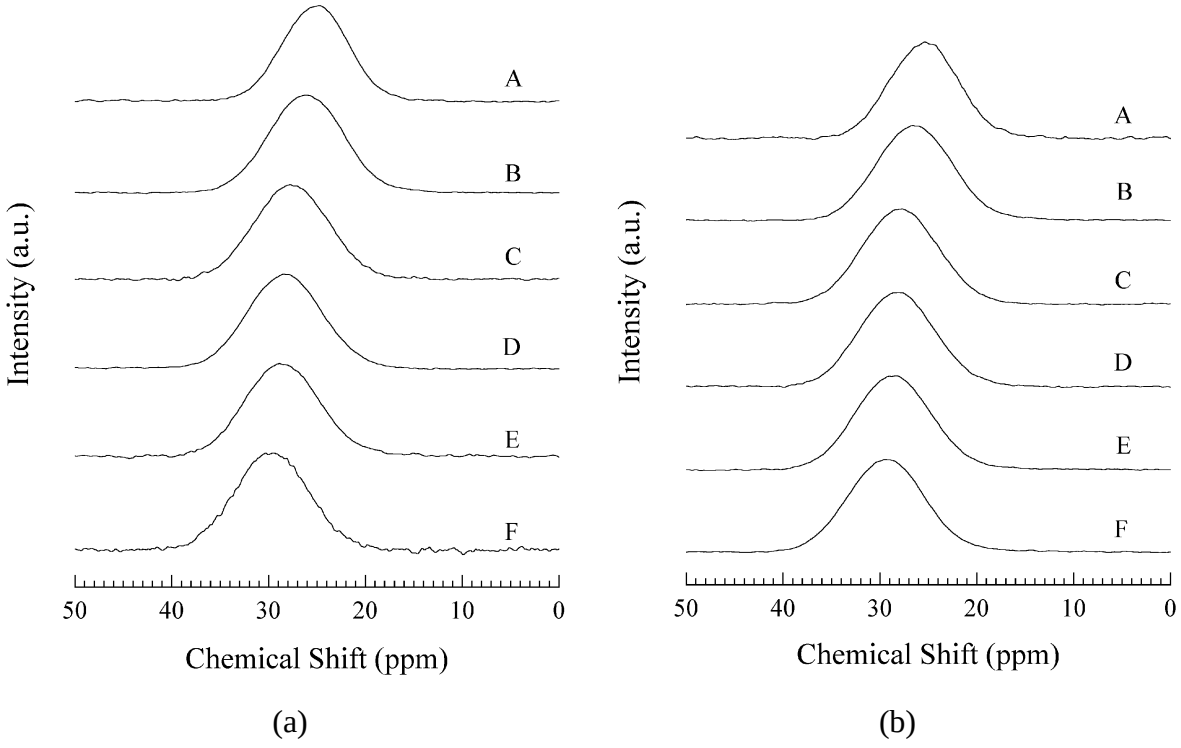


Figure 3.3.4 CP-MAS $^{31}$P NMR spectra of (a) BPA-PEPO/ PHE and (b) HFBPA recorded at room temperature at (A) 100/0; (B) 80/20; (C) 60/40; (D) 50/50; (E) 40/60; (F) 20/80 wt% compositions

Table 3.3.1 Chemical Shifts of Solid-State $^{31}$P CP-MAS NMR Resonances of Various Polymer Blends

| | Wt.% of X-PEPO, SS-PTPO, or X-DAMPO in the Blends | | | | | | |
|---|---|---|---|---|---|---|---|
| | 0 | 20 | 40 | 50 | 60 | 80 | 100 |
| Blend | Chemical Shift (ppm) | | | | | | |
| BPA-PEPO-100/PHE | - | 29.5 | 28.9 | 28.3 | 27.7 | 26.2 | 25.1 |
| BPA-PEPO-50/PHE | - | - | 29.0 | 28.3 | 27.6 | 26.3 | 25.0 |
| HFPBA-PEPO/PHE | - | 29.1 | 28.6 | 28.1 | 27.7 | 26.4 | 25.2 |
| BP-PEPO/PHE | - | 29.9 | 29.1 | 29.0 | 27.5 | 26.5 | 25.8 |
| SS-PTPO/PHE | - | 29.4 | 29.0 | 28.5 | 27.7 | 26.8 | 25.7 |

[449] Masson, J-F; Manley, R. St. J. *Macromolecules* **1992**, *25*, 589.

It should be noted that the chemical shift of phosphorus in a copolymer BPA-PEPO-50 (with 50:50 mole ratio of bis(4-fluorophenyl) phenyl phosphine oxide and 4,4′-dichlorodiphenyl sulfone as the comonomers) has the same chemical shift as the homopolymer BPA-PEPO. The BPA-PEPO-50/PHE blends showed the same tendency as homopolymer BPA-PEPO/PHE, suggesting that the chemical shift is not due to the dilution of phosphonyl groups in the blend systems.[450] For the blends with the same weight composition, the chemical shift is approximately the same. This may be explained by the accessibility of phosphonyl groups. Not all of the phosphonyl groups are accessible to hydrogen bonding due to the steric hindrance.

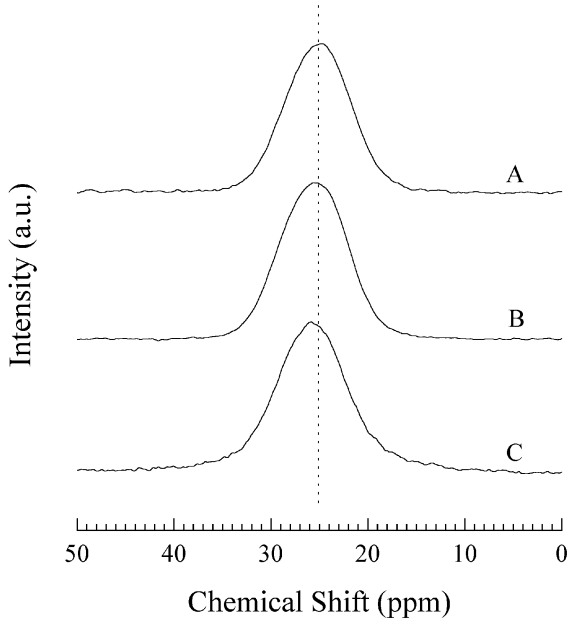


Figure 3.3.5 CP-MAS $^{31}$P NMR spectra of BPA-PEPO/ERL-4221® recorded at room temperature at (A) 100/0; (B) 60/40; (C) 40/60 wt% compositions

Further investigating the origin of the phosphorus chemical shifts of poly(arylene ether phenyl phosphine oxide)/PHE systems was attempted by selecting a model system BPA-PEPO/ERL-4221® (3,4-epoxycyclohexylmethyl-3,4-epoxycyclohexyl carboxylate) (ECHMECHC), a miscible blend system without hydrogen bonding.[451] Figure 3.3.5 shows the

[450] Assink, R.A. *Macromolecules* **1978**, *11*, 1233.
[451] It was found that BPA-PEPO/4221 is a miscible blend system. Further study of this system is on going and will be reported in later publications.

chemical shift of BPA-PEPO/ERL-4221® blends. Compared with that of BPA-PEPO/PHE, the phosphorus chemical shift only slightly moved downfield with the change of compositions in BPA-PEPO/ERL-4221® blend system. The results further suggest that the chemical shift of phosphorus is mainly due to the hydrogen bonding instead of other effects.

Figure 3.4.6 shows the $^{31}P$ chemical shift of SS-PTPO/PHE blends. As surmised before, the hydrogen bonding between hydroxyl and thioether sulfur should be relatively weaker in SS-PEPO/PHE blend system. So the chemical shift of phosphorus is a strong evidence of the hydrogen bonding between the phosphonyl groups and hydroxyl groups.

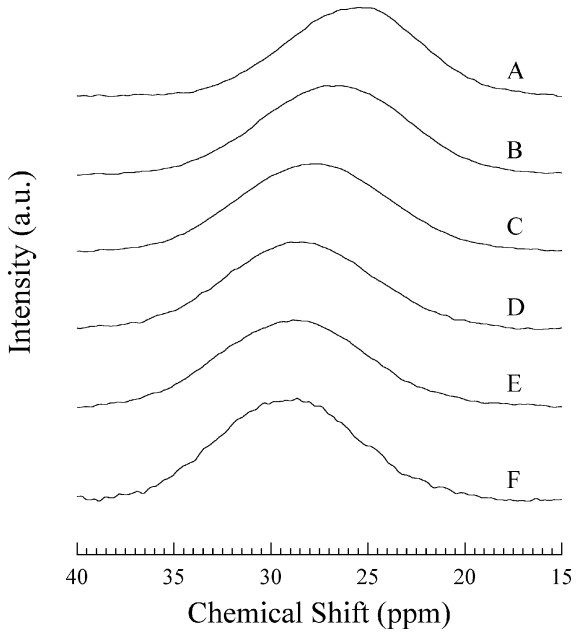


Figure 3.3.6 CP-MAS $^{31}P$ NMR spectra of SS-PTPO/ PHE recorded at room temperature at (A) 100/0; (B) 80/20; (C) 60/40; (D) 50/50; (E) 40/60; (F) 20/80 wt% compositions

#### *3.3.1.2 Phosphine oxide containing polyimide and bisphenol A poly(hydroxy ether) system (BPADA-DAMPO)/PHE*

FTIR spectra of BPADA-DAMPO polyimide, PHE, and their blends are displayed in Figure 3.3.7. It shows that the band of the hydroxyl stretching vibration shifted from 3445 $cm^{-1}$ to about 3320 $cm^{-1}$. The band due to the carbonyl stretching vibration did not shift, indicating little or no hydrogen bonding interaction between the carbonyl group of BPADA-DAMPO and the hydroxyl group of PHE. The immiscibility of the BPADA-*m*-PDA resin and PHE provides an indirect evidence of minimal interaction between the carbonyl group of polyimide and the hydroxyl group of PHE. The solid-state $^{31}P$ CP-MAS NMR spectra of the

blends (BPADA-DAMPO/PHE) show a progressive down field shifts in the chemical shift of phosphorus, as illustrated in Figure 3.3.8. Both FTIR and solid-state NMR results suggested hydrogen bonding interaction between the phosphonyl and hydroxyl groups of the two components.

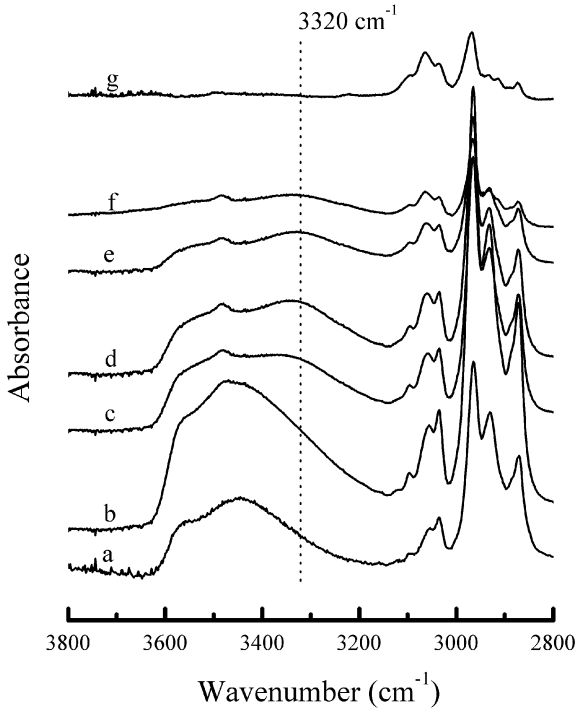


Figure 3.3.7 FTIR spectra of BPADA-DAMPO/ PHE blends at various weight compositions recorded at room temperature in the hydroxyl stretching region at (A) 0/100; (B) 20/80; (C) 40/60; (D) 50/50; (E) 60/40; (F) 80/20; (G) 100/0 wt% compositions

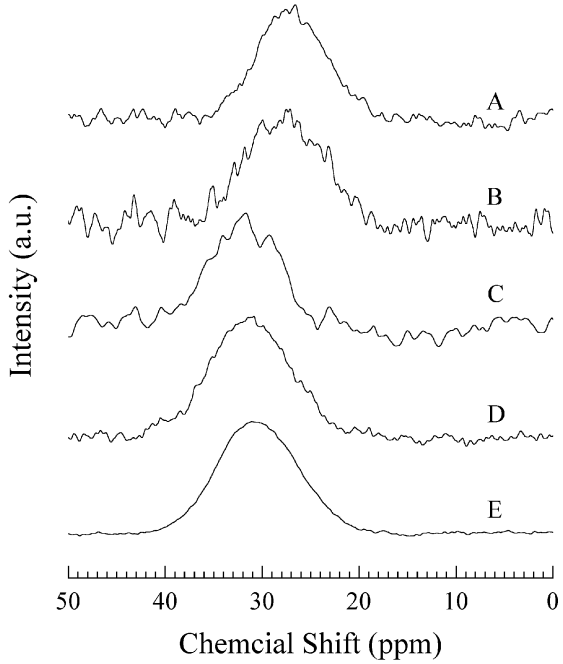


Figure 3.3.8 CP-MAS $^{31}$P NMR spectra of BPADA-DAMPO/ PHE recorded at room temperature at (A) 100/0; (B) 80/20; (C) 60/40; (D) 50/50; (E) 40/60 wt% compositions

### 3.3.2 Miscibility and Glass Transition Temperatures of Polymer Blends

The films of poly(arylene ether phenyl phosphine oxide)s, or poly(arylene thioether phenyl phosphine oxide), or phosphine oxide containing polyimides/PHE prepared by either solution casting or melt pressing are transparent, suggesting their miscibility. The determination of miscibility is dependent on the criteria of the physical method employed. Sometimes these criteria may give misleading results.[452] Thus, it is preferred to use more than one method to judge miscibility. Miscibilities of the above polymer blends were further characterized by DSC and DMA. A single $T_g$ at a temperature intermediate between those of the pure components indicates miscibility. In the present study, all the samples were completely freed of solvent as checked by TGA and NMR. The data were collected from second-run DSC scans. Thermal history and solvent effects were thus avoided. Figures 3.3.9a and 3.3.9b display the DSC thermograms of polymer blends at various compositions of HFBPA-PEPO/PHE and BP-PEPO/PHE, respectively. The DSC thermograms show single $T_g$ values for the polymer blends over the entire composition range, and the glass transition

[452] MacKnight, W.J.; Karasz, F. E. in *Polymer Blends Vol. I* Paul, D. R.; Newman, S., Ed., Acdemic Press: New York, **1978**.

temperature increases monotonically with increasing amounts of HFBPA-PEPO or BP-PEPO. DMA also showed a monotonous increase of the peak temperature of well-defined single tan δ loss peaks with increasing amounts of HFBPA-PEPO or BP-PEPO, as shown in Figure 3.3.10a and 3.3.10b. These results again strongly support our hydrogen bonding hypothesis in the previous papers.[432,433,437]

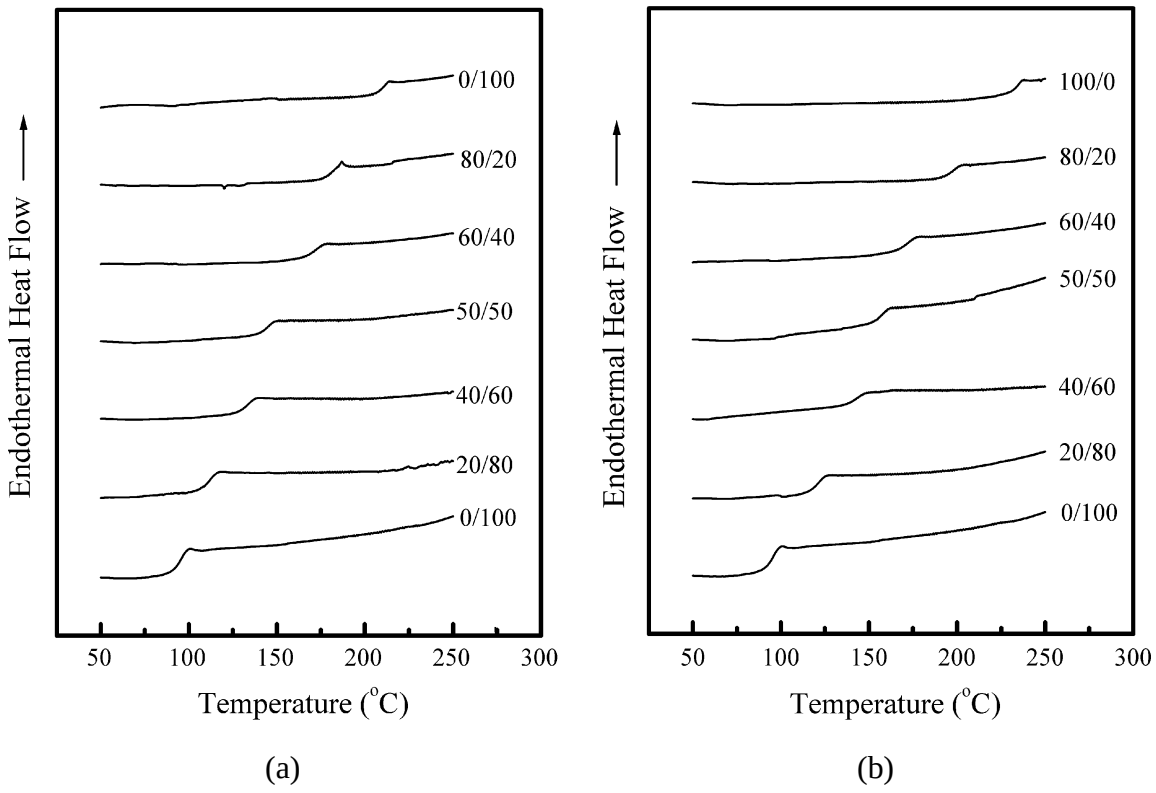


Figure 3.3.9 DSC thermograms of (a) HFPBA-PEPO/PHE and (b) BP-PEPO/PHE blends at various weight compositions.

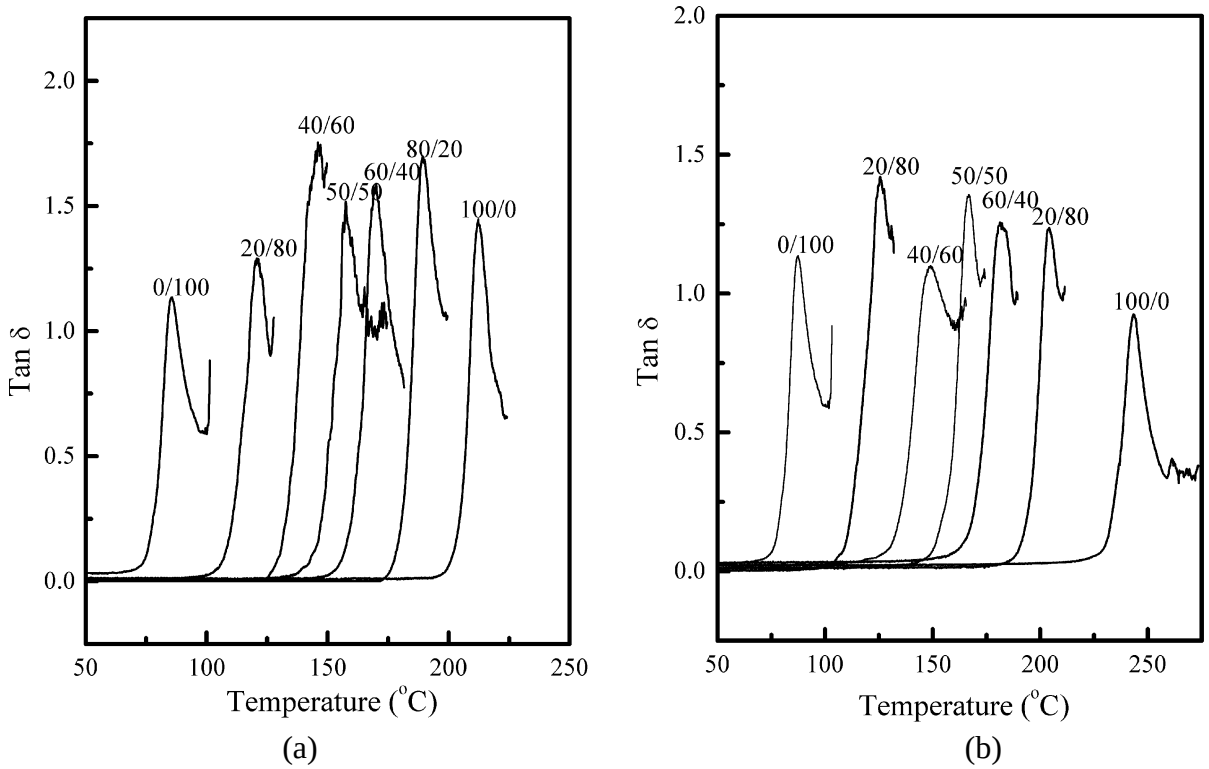


Figure 3.3.10 Mechanical loss tangents of (a) HFPBA-PEPO/PHE and (b) BP-PEPO/PHE blends at various weight compositions

The single glass transition behavior was also observed in the SS-PTPO/PHE system. Figure 3.3.11 illustrates the monotonous increase in $T_g$ with increase in the weight percent of SS-PTPO.

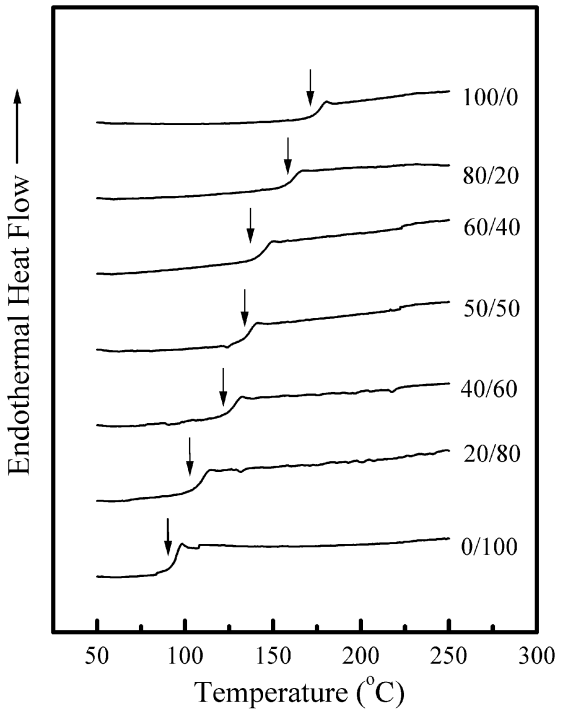


Figure 3.3.11 DSC thermograms of SS-PTPO/PHE blends at various weight compositions

A totally different system from the ones discussed above, phosphorus-containing polyimide/PHE blends, was also investigated. As an evidence of the miscibility of this system, the films of BPADA-DAMPO/PHE prepared by either solution casting or melt pressing were transparent. Further qualitative criteria indicating the miscibility of this blend system were provided by DSC and DMA data. Both DSC and DMA thermograms show single $T_g$ values for the polymer blends over the entire composition range. The glass transition temperatures increase monotonically with the increase of the amount of polyimide. To illustrate this finding, Figures 3.3.12a and 3.3.12b show the DSC and DMA results for BPADA-DAMPO/PHE blends. The DSC and DMA results are consistent. They indicate that the two polymer components are miscible, at least on the scale detectable by DSC and DMA. Further study of the effect of polyimide structure on the miscibility was done by blending a similar polyimide (BPADA-DAPPO) with PHE. The resulting polymer blends also showed a single $T_g$. Again, it suggests the determining factor for the miscibility is hydrogen bonding.

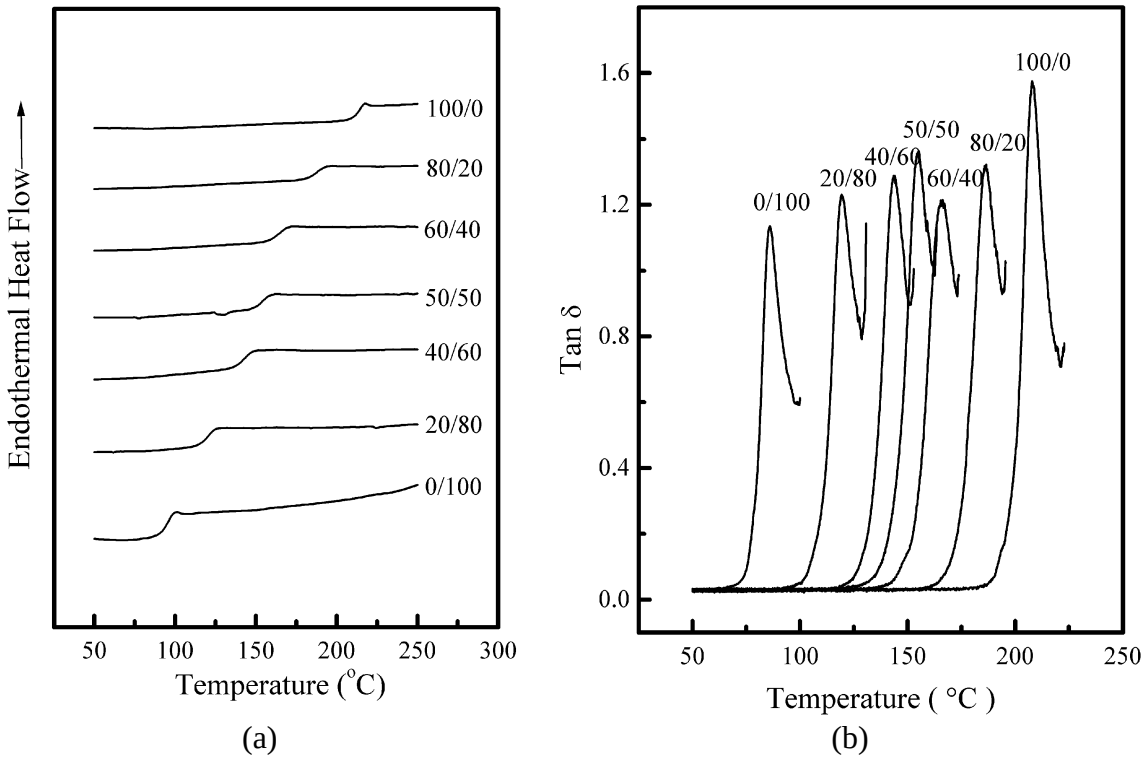


Figure 3.3.12 DSC thermograms (a) and mechanical loss tangents (b) of BPADA-DAMPO/PHE at various weight compositions

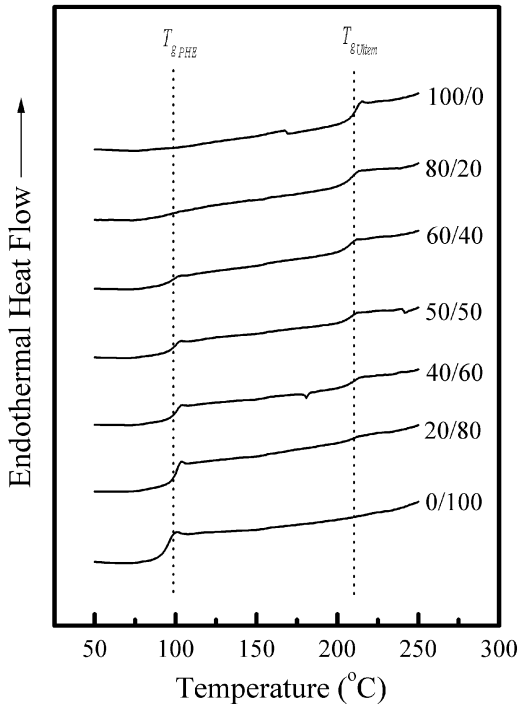


Figure 3.3.13 DSC thermograms of BPADA-*m*-PDA/PHE at various weight compositions

In contrast, the blends of commercial BPADA-MPDA (Ultem® resin) and PHE did not

yield transparent films either by solution casting or melt pressing, although the BPADA-*m*-PDA has a structure very similar to those of the above phosphorus-containing polyimides. In Figure 3.3.13, DSC thermograms show two $T_g$ values for the polymer blends corresponding to the $T_g$ values of the homopolymer components. It should be noted that neither the ether oxygen group nor the carbonyl group afforded significant hydrogen bonding with PHE. Thus, BPADA-*m*-PDA is not miscible with PHE. This result indirectly shows the importance of the phosphonyl group for the miscibility of phosphorus-containing polymers with PHE.

One of the most important ways of characterizing miscible polymer blends is the determination of the composition dependencies of their $T_g$ values. The study of the relationship of glass transition temperatures to the composition of mixtures is of both technological and scientific interest. The glass transition temperatures of some polymer blends measured by DSC and DMA are tabulated in Table 3.3.2 and Table 3.3.3, respectively. For simplicity, only $T_g$ values obtained by DSC will be discussed.

Table 3.3.2 Glass Transition Temperatures (DSC) of Polymer Blends of PHE with Various Phosphine Oxide Containing Polymers

| | Wt.% of X-PEPO or SS-PTPO in the Blends | | | | | | |
|---|---|---|---|---|---|---|---|
| | 0 | 20 | 40 | 50 | 60 | 80 | 100 |
| Blend | $T_g$ ($^oC$) | | | | | | |
| HFPBA-PEPO/PHE | 93 | 111 | 132 | 144 | 170 | 180 | 209 |
| BP-PEPO/PHE | 93 | 121 | 143 | 157 | 171 | 196 | 234 |
| SS-PTPO/PHE | 93 | 108 | 126 | 135 | 143 | 160 | 175 |
| BPADA-DAMPO/PHE | 93 | 120 | 143 | 154 | 164 | 187 | 213 |
| BPADA-DAPPO/PHE | 93 | 116 | 138 | 150 | 161 | 184 | 213 |

Since the purpose of the present effort was to study the effect of the polymer main chain structures of phosphorus containing polymers on the blend miscibilities, $T_g$ data, as tabulated in Table 3.3.3, were examined for five different polymer/PHE blends using four different $T_g$-weight fraction composition equations.

Table 3.3.3 Tan δ Peak Values of Polymer Blends HFBPA-PEPO/PHE, BP-PEPO/PHE, and BPADA-DAMPO/PHE

| | Wt.% of X-PEPO In the Blends | | | | | | |
|---|---|---|---|---|---|---|---|
| | 0 | 20 | 40 | 50 | 60 | 80 | 100 |
| Blend | $T_g$ (°C) | | | | | | |
| HFPBA-PEPO/PHE | 86 | 122 | 145 | 158 | 170 | 189 | 212 |
| BP-PEPO/PHE | 86 | 126 | 149 | 167 | 182 | 204 | 243 |
| BPADA-DAMPO/PHE | 86 | 119 | 144 | 155 | 166 | 186 | 208 |

The first three equations were derived on the bases of free volume additivity [Fox: Eq. 3.3.1],[453] free volume additivity corrected for thermal expansion coefficient differences [Gordon-Taylor: Eq. 3.3.2],[454] or a pseudo-second-order thermodynamic transition combination of entropic changes in the constituent polymers at their respective glass transitions [Couchman: Eq. 3.3.3].[455] The fourth equation [Kwei: Eq. 3.3.4][456] is an empirical equation of the Gordon-Taylor form to which a term representing specific interaction contributions has been added. A recent derivation similar in protocol to that of Couchman, but from an enthalpic approach and incorporating an enthalpy of mixing, has yielded an equation of the Kwei form expressed, however, in polymer unit mole fractions.[457]

Fox: $$\frac{1}{T_{g_m}} = \frac{w_A}{T_{g_A}} + \frac{w_B}{T_{g_B}}$$ Equation 3.3.1

Gordon-Taylor: $$T_{g_m} = \frac{w_A T_{g_A} + k_{GT} w_B T_{g_B}}{w_A + k_{GT} w_B}$$ Equation 3.3.2

Couchman: $$\ln T_{g_m} = \frac{w_A \ln T_{g_A} + k_C w_B \ln T_{g_B}}{w_A + k_C w_B}$$ Equation 3.3.3

Kwei: $$T_{g_m} = \frac{w_A T_{g_A} + k_K w_B T_{g_B}}{w_A + k_K w_B} + q w_A w_B$$ Equation 3.3.4

[453] Fox, T. G. *Bull. Am. Phys. Soc*. **1956**, *1*, 123.
[454] Gordon, M.; Taylor, J. S. *J. Appl. Chem.* **1952**, *2*, 493.
[455] Couchman, P. R. *Phys. Lett.* **1979**, *70A*, 155.
[456] Kwei, T. K. *J. Polymer Sci., Polym. Lett. Ed.* **1984**, *22*, 307.
[457] Painter, P. C.; Graf, J. F.; Coleman, M. M. *Macromolecules* **1991**, 24, 5630.

In the Fox equation, the predicted glass transition temperature is dependent only on the weight fraction compositions of the prepared blends and the experimentally determined glass transition temperatures of the constituent polymers. From the derivation of the Gordon-Taylor equation $k_{GT} = \frac{\alpha_{l_B} - \alpha_{g_B}}{\alpha_{l_A} - \alpha_{g_A}}$ is a compression constant involving the ratio of the thermal expansion coefficient changes of the constituent polymers at their respective glass transitions. The Couchman equation derivation gives $k_C = \frac{C_{l_B} - C_{g_B}}{C_{l_A} - C_{g_A}}$, the ratio of the specific heat increases of the constituent polymers at their respective glass transitions. The empirical Kwei equation, which has the form of the Gordon-Taylor equation plus an arbitrary "interaction contribution" term, could logically be applied by setting $k_K$ equal to the theoretical $k_{GT}$ and employing $q$ as an adjustable parameter. In $T_g$ data analyses of the composition dependencies of miscible polymer blends $k_{GT}$ and $k_C$ are often treated as adjustable, curve-fitting parameters which contain a combination of the individual constituent contributions and specific interaction contributions. Adopting such an empirical curve fitting approach to the present $T_g$-$w$ data we obtained the parameter values shown in Table 3.3.4. Rather than setting $k_K$ equal to the theoretical $k_{GT}$ as suggested above, $k_K$ is set equal to the theoretical $k_C$ of Couchman in calculating the q values listed in Table 3.3.4. The heat capacity increases at $T_g$ are 0.20, 0.20, 0.22, 0.25, 0.24 J/g$\bullet$$^oC$ for BFPA-PEPO, BP-PEPO, SS-PTPO, BPADA-DAMPO, BPADA-DAPPO respectively. The heat capacity increase at $T_g$ of PHE is 0.41 J/g$\bullet$ $^oC$.

Table 3.3.4 Empirical Constants Determined for the $T_g$/Composition Equations of PHE Blends

| Blend | $k_{GT}$ | $k_C$ | $q$ ($^oC$) |
|---|---|---|---|
| HFBPA-PEPO/PHE | 0.74 | 1.1 | 53 |
| BP-PEPO/PHE | 0.82 | 1.2 | 70 |
| SS-PTPO/PHE | 1.20 | 1.1 | 53 |
| BPADA-DAPPO/PHE | 0.89 | 1.0 | 60 |
| BPADA-DAMPO/PHE | 0.78 | 0.89 | 48 |

Figure 3.3.14 presents the observed $T_g$ values of HFPBA-PEPO/PHE, SS-PTPO/PHE, and BPADA-PEPO/PHE blends plotted against the weight fractions of the corresponding phosphine oxide containing polymers, representing three totally different kinds of polymer. The positive deviation of the blend $T_g$ relative to the Fox equation prediction (broken line) is observed for all the studied polymer blends. These observations are consistent with a free volume decrease with resultant increased $T_g$ in the blends due to favorable (exothermal, densifying) phosphonyl/hydroxyl group interactions. The deviation of the observed $T_g$ from the theoretical $T_g$ for the HFPBA-PEPO/PHE blend system is relatively smaller, although strong hydrogen bonding interaction was observed by FTIR and $^{31}P$ NMR. A possible explanation can be made as follows. Incorporating the relatively bulky $CF_3$ groups in the chain unit may make the polymer chain more open. Therefore, the hydrogen bonded polymer blends containing the hexafluoroisopropylidene may possess larger free volume than those of the other polymer blend systems. The result of this effect is that the polymer blends are closer to the free-volume additivity condition. Quantitative comparison among the different polymer blend systems is not possible, since both the specific interaction and the chain structure may affect miscibility. Fitting of the data to the Gordon-Taylor equation (solid curves in Figure 3.3.14) by an adjustable $k_{GT}$ is fairly successful.

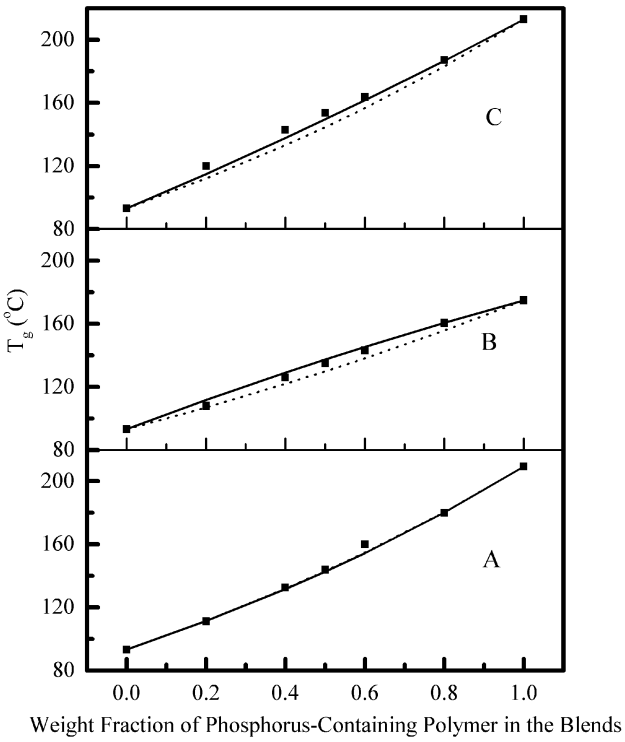


Figure 3.3.14 Fit of experimental $T_g$ versus composition data to the curves predicted by the Fox equation (broken line) and the Gordon-Taylor equation with empirically adjusted $k_{GT}$ (solid line). (A) HFBPA-PEPO/PHE; (B) SS-PTPO/PHE; (C) BPADA-PEPO/PHE

Figure 3.3.15 presents the same blend glass transition temperature data that were presented in Figure 3.3.14. The broken line curves correspond to the Couchman equation in which $k_C$ values were calculated from the individual constituent polymer specific heat changes at their glass transitions. The solid curves represent the fit using adjustable $k_C$ values. The increased $T_g$ elevation, relative to the theoretical Couchman equation prediction, with the incorporation of phosphine oxide content is consistent with favorable (exothermal, densifying) phosphonyl/hydroxyl group interactions.

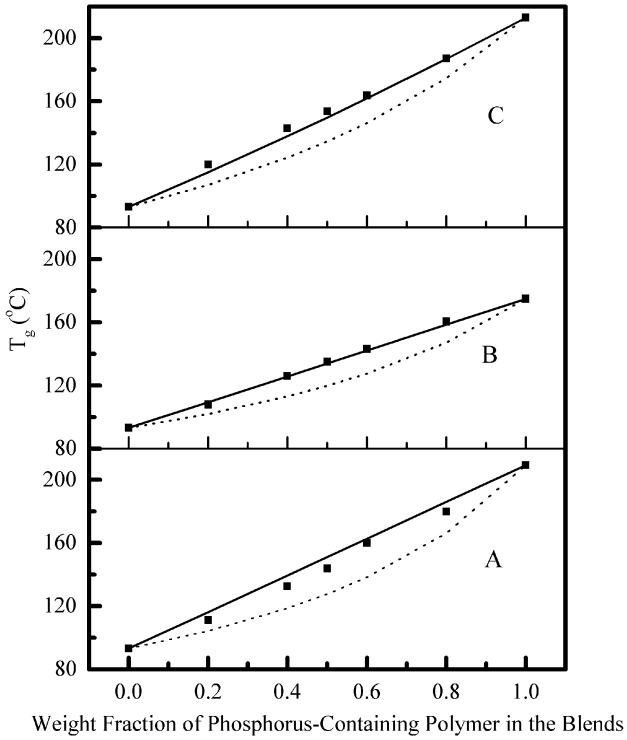


Figure 3.3.15 Fit of experimental $T_g$ values to those predicted by Couchman with $k_C$ as the ratio of the heat capacity increases of the components at their $T_g$ (broken line) and with empirical $k_C$ (solid line). (A) HFBPA-PEPO/PHE; (B) SS-PTPO/PHE; (C) BPADA-PEPO/PHE

Figure 3.3.16 presents the blend $T_g$ data, the $T_g$ values predicted by the theoretical Gordon-Taylor equation (with $k_{GT}=k_C$) represented by broken line curves, and the empirical Kwei equation fit (solid curves) of the data. Fitting the blend $T_g$ data by the Kwei equation with $q$ as an adjustable interaction parameter gives very good fits (solid line curves) with changes of q values in different systems, as tabulated in Table 3.3.4. This trend in enhancement of $T_g$ by the $qw_Aw_B$ term is definitely consistent with a favorable, hydrogen bonding interaction between the phosphonyl group of the polymer and the hydroxyl group of PHE.

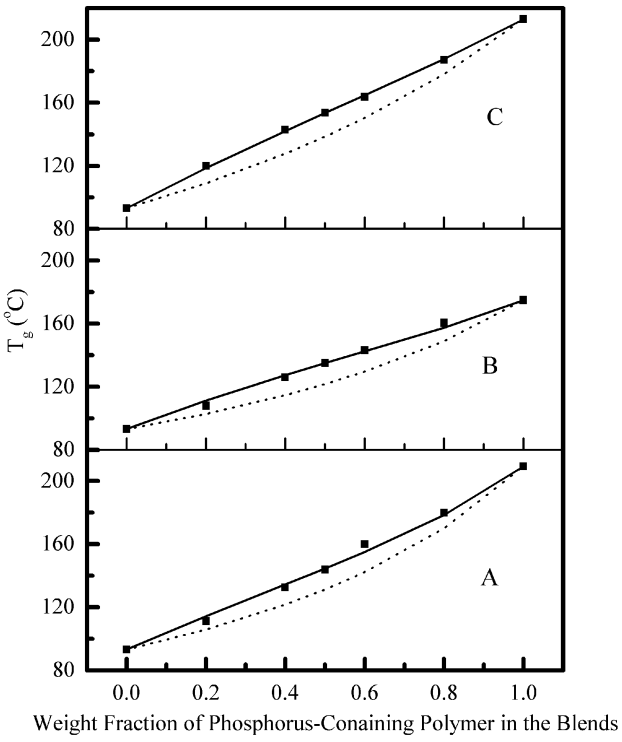


Figure 3.3.16 Fit of experimental $T_g$ values to those predicted by the Gordon-Taylor part term of the Kwei equation with $k_K=k_C$ (broken line) and the full form of Kwei equation (solid line). (A) HFBPA-PEPO/PHE; (B) SS-PTPO/PHE; (C) BPADA-PEPO/PHE

### 3.3.3 Scale of the miscibility of BPADA-MPDA/PHE

The properties of the polymer blends are dependent on their microstructures. Although DSC and DMA can afford some information of the homogeneity of the polymer blends, they usually provide information on a relatively larger phase scale. It is of interest to study the polymer blends in a small scale. $^{13}C$ CP-MAS NMR provides the possibility of evaluating the scale of miscibility of polymer blends according to the dynamic NMR relaxation measurement.[449,458,459,460,461,462,463,464,465] The interaction of the blend components by hydrogen bonding has been shown to cause changes in line shape and/or shifts in the $^{13}C$ resonance frequencies in the NMR spectra of the blend components, in comparison with the spectra of

[458] Stejskal, E. O.; Schaefer, J.; Sefcik, M. D.; McKay, R. A. *Macromolecules* **1981**, *14*, 275.
[459] Dickson, L. C.; Yang, H.; Chu, C.-W.; Stein, R. S.; Chien, J. C. W. *Macromolecules* **1987**, *20*, 1757.
[460] Schaefer, J.; Sefcik, M. D.; Stejskal, E. O.; McKay, R. A. *Macromolecules* **1981**, *14*, 188.
[461] Tekely, P.; Laupretre, F.; Monnerie, L. *Polymer* **1985**, *26*, 1081.
[462] Gobbi, G. C.; Silvestri, R.; Russell, T. P.; Lyerla, J. R.; Fleming, W. W.; Nishi, T. *J. Polym. Sci., Polym. Lett.* **1987**, *25*, *61*.
[463] Grobelny, J.; Rice, D. M.; Karasz, F. E.; MacKnight, W. J. *Macromolecules* **1990**, *23*, 22139.
[464] Sankarapandian, M.; Kishore, K. *Polymer* **1996**, *37*, 2957.

the pure polymer components.[425c,466] As discussed above, the hydrogen bonding interactions between phosphorus-containing polymers and PHE cause significant shifts in the $^{31}$P NMR resonance frequency. This suggests an intimate interaction between the two components with small domain size. In polymer blends the values of the proton rotating frame spin-lattice relaxation time $T_{1\rho}(H)$, are enhanced by the efficiency of spin diffusion among protons of the polymer components. This efficiency depends on short-range spatial proximity of neighboring chains with different chemical units. In a miscible binary polymer blend, the protons of the two components are closely coupled and expected to relax at an identical rate.[459,463,467] The relaxation measurements provide miscibility information on a very fine scale. Unfortunately, this method can only be applied to the BPADA-DAMPO/PHE blends in our study due to the overlapping of the spectra of the two components in other systems mentioned above. Even in this system, only $T_{1\rho}(H)$ measurement is available because the two components have similar $T_1$ values. The peak at 70 ppm has been ascribed to aliphatic $CH_2$ and CH carbons.[425c] The 165 ppm resonance peak has been ascribed to carbonyl carbon.[463] Initial measured spin-lattice relaxation times in the rotating frame ($T_{1\rho}(H)$) for the homopolymers and blends are shown in Table 3.3.5. In all the blends with various compositions, the $T_{1\rho}(H)$ values of both components are approximately the same.

Table 3.3.5 $T_{1\rho}(H)$ Values (ms) for PHE, BPADA-DAMPO, and Their Blends*

| BPADA-DAMPO/PHE wt % | BPADA-DAMPO 165 ppm (ms) | PHE 70 ppm (ms) | Calculated Value (ms) |
|---|---|---|---|
| 0/100 | - | 2.04 | 2.04 |
| 20/80 | 2.24 | 2.59 | 2.25 |
| 40/60 | 3.03 | 3.12 | 2.56 |
| 50/50 | 3.45 | 2.84 | 2.78 |
| 60/40 | 2.73 | 3.51 | 3.07 |
| 80/20 | 5.31 | 4.46 | 4.07 |
| 100/0 | 6.92 | - | 6.92 |

*Accuracy of the measurements is about ±10%.

[465] Zheng, S.; Guo, Q.; Mi, Y. *J. Polym. Sci., Polym. Phys. Ed.* **1998**, *36*, 2291.
[466] Qin, C.; Pires, A. T. N.; Belfiore, L. A. *Macromolecules* **1991**, *24*, 666.
[467] McBriety, V.J.; Douglass, D.C. *J. Polym. Sci., Macromol. Rev.* **1981**, *16*, 295.

If the motion of the polymer components in the blends is not greatly changed by blending, the average proton relaxation rate (the inverse of the relaxation time) of a homogeneous blend can be predicted by the model for linear additivity of relaxation times of pure components:[450,468]

$$\frac{1}{T_{1\rho}(H)_{AB}} = \frac{N_A}{N} \bullet \frac{1}{T_{1\rho}(H)_A} + \frac{N_B}{N} \bullet \frac{1}{T_{1\rho}(H)_B} \qquad \text{Equation 3.3.5}$$

where $\frac{1}{T_{1\rho}(H)_A}$, $\frac{1}{T_{1\rho}(H)_B}$, and $\frac{1}{T_{1\rho}(H)_{AB}}$ are the relaxation rates of polymer A, polymer B, and their blends, respectively; $N_A$, $N_B$, and $N_{AB}$ are the numbers of protons of the respective components, and for the polymer blends $N_{AB} = N_A + N_B$. The calculated values of the polymer blends are tabulated in Table 3.3.5. It is noted that there is a positive deviation of the experimental results from the calculated values. This has been ascribed to the hydrogen bonding interactions. Hydrogen bonding apparently makes the chains stiffer and hinders the segmental motion of the components. Thus, a slower spin-lattice relaxation rate was observed.

The approximate scale of mixing can be readily calculated with the equation $L^2 \approx L_0{}^2 t / T_2$, where $L_0$ is the distance between protons, typically 0.1 nm, t the measured relaxation time, and $T_2$ the spin-spin relaxation time which, below $T_g$, is ca. 10 μs.[432] Therefore, from the $T_{1\rho}(H)$ values, it is estimated that BPADA-DAMPO polyimide and PHE mix on a scale of about 3-4 nm.

A one-dimensional diffusion equation for the average diffusive path length can also be used to estimate the mixing scale: [461,462,469]

$$L = \sqrt{6DT_i} \qquad \text{Equation 3.3.6}$$

where $D$ is the spin-diffusion coefficient that depends on the average proton to proton distance as well as on dipolar interactions with a typical value of the order of $6 \times 10^{-16} m^2 s^{-1}$.

[468] Schaefer, J.; Slejskal, E. O. *J. Chem. Soc.* **1976**, *98*, 1031.
[469] (a) McBriety, V. J.; Douglass, D. C. *Phys. Rep*. **1980**, *63*, 61; (b) McBriety, V. J.; Packer, K. J. *Nuclear Magnetic Resonance in Solid Polymers* Cambridge University Press: Cambridge, UK, **1993**.

$T_i$ is the relaxation time according to the relaxation experiment. The estimated mixing scale is about 4 nm, which is consistent with the previous equation.

## 3.4 Conclusions

It has been demonstrated that a new series of phosphine oxide containing poly(arylene ether)s (BPA-PEPO, HFBPA-PEPO, BP-PEPO), poly(arylene thioether) (SS-PTPO), polyimides (BPADA-DAMPO, BPADA-DAPPO) are miscible with PHE on the basis of optical clarity, and on DSC and DMA data. Both DSC and DMA results show single $T_g$s for the polymer blends. The glass transition temperatures of the polymer blends were intermediate between those of the pure components and varied monotonically with the blend compositions. It is suggested that the intermolecular hydrogen bonding of phosphonyl groups with hydroxyl groups is the driving force for the miscibility. Several pieces of evidence support the hydrogen bonding hypothesis. It was observed that the band due to the hydrogen bonded hydroxyl stretching vibration shifts from about 3445 $cm^{-1}$ to about 3300 $cm^{-1}$ in phosphorus-containing polymers/PHE blends systems while that of poly(ether sulfone)/PHE blends shifts to a higher wave number. This is because these miscible polymer blends are induced by different hydrogen-bonding interactions. Furthermore, this shift is observed in SS-PTPO (without an ether group)/PHE and BPADA-DAMPO/PHE in which no carbonyl stretching vibration band shift is observed. In addition, solid-state $^{31}P$ CP-MAS NMR spectra show a significant down field of the phosphorus resonance band in phosphorus-containing polymer/PHE blends while it does not display a significant phosphorus chemical shift in a miscible blend BPA-PEPO/ERL 4421®.

Evidence for miscibility in BPADA-DAMPO/PHE blends is also obtained from spin-lattice relaxation ($T_{1\rho(H)}$) measurements. From solid state NMR relaxation measurements the homogeneity scale of the different blends was evaluated and the proximity of different chains is approximately within 4 nm. These results further suggest that varying the main chain structural units of the phosphorus-containing polymer does not significantly affect its miscibility with phenoxy resin.

# 4 MISCIBILITY AND MORPHOLOGIES OF POLY(ARYLENE ETHER PHENYL PHOSPHINE OXIDE/SULFONE) COPOLYMER/VINYL ESTER RESIN MIXTURES AND THEIR CURED NETWORKS

## *4.1 Introduction*

Thermosetting structural adhesive and composites matrix networks based on epoxy and dimethacrylate "vinyl ester" resin oligomers are important materials which display a number of excellent mechanical and adhesive properties (Scheme 4.1.1).[470] These oligomers are widely used as adhesives and thermosetting matrix materials for composites reinforced with glass, carbon, and aramide fibers. However, unmodified networks exhibit low-impact resistance when compared to most engineering thermoplastics. Many approaches have been investigated to address these problems. The incorporation of reactive liquid rubbers, e.g. butadiene-acrylonitrile copolymers is a widely used method to improve the fracture toughness, especially of the cured epoxy resins.[471,472,473,474,475,476,477,478] One disadvantage of this approach is that the polydiene rubbers deteriorate properties such as stiffness, strength, heat distortion temperature and also oxidative and chemical resistance. An alternative approach to improve the fracture toughness is to incorporate high performance thermoplastics which are either reactive or nonreactive, into the epoxy resins.[479,480,481,482,483,484] Relatively few attempts

[470] *International Encyclopedia of Composites*, Vol. 1-5, Lee, S. M. VCH Publisher:New York, **1990**.
[471] Sultan, J. N.; McGarry, F. J. *Polym. Eng. Sci.* **1973**, *13*, 29.
[472] Bucknall, C. B.; Yoshii, T. *Br. Polym. J.* **1978**, *10*, 53.
[473] Riew C. K., Gillham, J. K.Ed. *Rubber Modified Thermoset Resins*, Advances in Chemistry Series #208, American Chemical Society: Washington, D. C., **1984**.
[474] Butta, E.; Levita, G.; Marchetti, A.; Lazzeri A. *Polym. Eng. Sci.* **1986**, *26*, 63.
[475] Jakusik, R.; Jamaani, F.; Kinloch, A. J. *J. Adhesion* **1990**, *32*, 245.
[476] Kasemura, T.; Kawamoto, K.; Kashima, Y. J. Adhesion *J. Adhesion* **1990**, *33*, 19.
[477] Guild, F. J.; Kinloch, A. J. *J. Mater. Sci.* **1995**, *30*, 1689.
[478] Verchere, D.; Pascault, J. P.; Sautereau, H.; Moschiar, S. M.; Riccardi, C. C.; Williams, R. J. *J. Appl. Polym. Sci.* **1991**, *42*, 701.
[479] Bucknall, C. B.; Partridge, I. K. *Polymer* **1983**, *24*, 639.
[480] Bucknall, C. B.; Gilbert, A. H. *Polymer* **1989**, *30*, 213.
[481] Hedrick, J. L.; Yilgör, I.; Wilkes, G. L.; McGrath, J. E. *Polym. Bull.* **1985**, *13*, 201.
[482] Hedrick, J. L.; Yilgör, I.; Jurek, M.; Hedrick, J. C.; Wilkes, G. L.; McGrath, J. E. *Polymer* **1991**, *21*, 2020.
[483] Wilkinson, S. P.; Ward, T. C.; McGrath, J. E. *Polymer* **1993**, *34*, 870.
[484] Yoon, T. H.; Priddy, D. B., Jr.; Lyle, G. D.; McGrath, J. E. *Macromol. Symp.* **1995**, *98*, 673.

were made to improve the impact resistance of cured vinyl ester, since rubber additives such as vinyl-terminated butadiene-acrylonitrile copolymers are not miscible with bisphenol A based hydroxy ether dimethacrylates styrene solutions.[485,486,487] Very little has been published using high performance thermoplastic materials to toughen commercial vinyl ester resins.

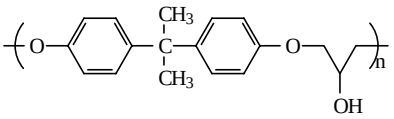

Phenoxy Resin

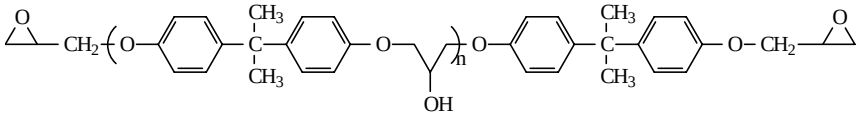

Epoxy Resin

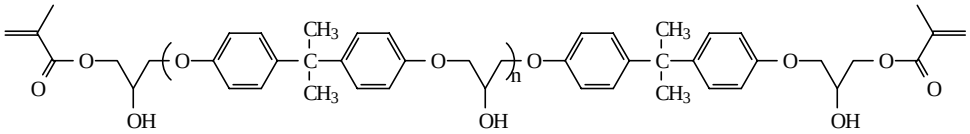

Vinyl Ester Resin

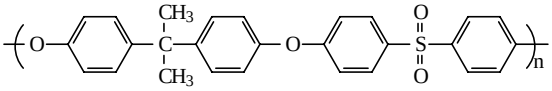

Bisphenol A Poly(arylene ether diphenyl sulfone)

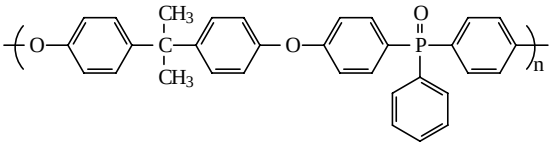

Bisphenol A Poly(arylene ether triphenyl phosphine oxide)

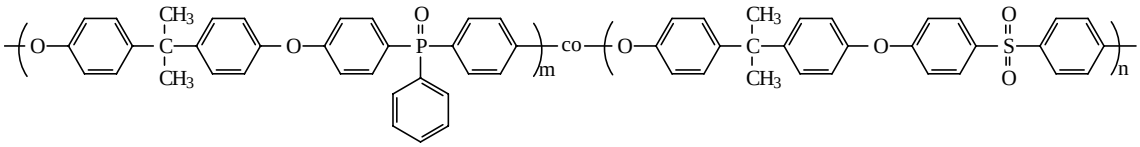

Bisphenol A Poly(arylene ether phenyl phophine oxide/sulfone) Statistical Copolymers

Scheme 4.1.1 Structures of Bis-A poly(arylene ether triphenyl phosphine oxide) homo- and diphenyl sulfone copolymers, phenoxy resin, and related systems.

It is hypothesized that adhesion improvements between a network matrix and fibers might be achieved with polymeric sizings on the fiber which are miscible with the network matrix

[485] Ullett, J. S.; Chartoff, R. P. *Polym. Eng. Sci.* **1995**, *35*, 1086.
[486] Dreerman, E.; Narkis, M.; Siegamann, J. R.; Dodiuk, H.; Dibenedetto, A. T. *J. Appl. Polym. Sci.* **1999**, *72*, 647.
[487] Burchill, P. J.; Pearce, P. J. in *CRC Encyclopedia of Polymer Materials* Salamone, J. C., Ed.; CRC Press: Boca Raton, FL **1994**.

and are more adherent to the fiber surface. This might possibly be achieved via specific interactions.[488] In our laboratory, various phosphine oxide containing polymers, such as poly(arylene ether)s,[489] polyimides,[490] and cyanate oligomers[491] were prepared and investigations on a model blend system poly(arylene ether phenyl phosphine oxide/sulfone) copolymer/phenoxy resin showed that the miscibility of the two components could be achieved, which depended on the mole content of phosphine oxide in the copolymer.[492,493] The specific interaction (hydrogen bonding) between the phosphonyl groups of the copolymer and hydroxyl groups of the phenoxy resin was demonstrated to be the driving force for miscibility.[493] However, studies on the miscibility between the phosphine oxide containing polymers and thermosetting oligomers such as epoxy and vinyl ester resin have not been reported. Relatively few thermoplastic polymers have been used to improve the interfacial adhesion of a vinyl ester matrix to the major reinforcing fibers.[494] The present research has systematically studied the effect of phosphonyl content in the copolymer on its miscibility with a vinyl ester resin, and on the morphologies and toughness of the cured vinyl ester system.

## *4.2 Experimental*

### 4.2.1 Materials

Bisphenol A was kindly supplied by Dow Chemical Company. The activated halide monomer 4,4′-dichloro diphenyl sulfone (DCDPS) was provided by BP-AMOCO. The monomer 4,4′-bis(fluorophenyl) phenyl phosphine oxide (BFPPO) was either synthesized in our laboratory or provided by Zeneca.[489] Commercial vinyl ester resin (Derakane 411-400 (28 wt % styrene)) was supplied by Dow Chemical Company. An experimental sample of methacrylate endcapped vinyl ester (~690 g/mol) without styrene was also donated by Dow

[488] Lesko, J. J.; Swain, R. E.; Cartwright, J. M.; Chin, J. W; Reifsnider, K. L.; Dillard, D. A.; Wightman, J. P *J. Adhesion* **1994**, *45*, 43.
[489] (a) Smith, C. D.; Grubbs, H. J.; Webster, H. F.; Gungor, A; Wightman, J. P.; McGrath, J. E. *High Perform. Polym.* **1991**, *4*, 211; (b) Riley, D. J.; Gungor, S. A.; Srinivasan, S. A.; Sankarapandian, M.; Tchatchoua, C.; Muggli, M. W.; Ward, T. C.; McGrath, J. E., Kashiwagi, T. *Polym. Eng. Sci.* **1997**, *37*, 1501.
[490] Tan, B.; Tchatchoua, C. N.; Dong, L.; McGrath, J. E. *Polym. Adv. Technol.* **1998**, *9*, 84.
[491] Abed, J. C.; Mercier, R.; McGrath, J. E. *J. Polym. Sci., Polym. Chem. Ed.* **1997**, *35*, 977.
[492] Srinivasan, S.; Kagumba, L.; Riley, D. J.; McGrath, J. E. *Macromol. Symp.* **1997**, *122*, 95.
[493] Wang, S.; Ji, Q.; Tchatchoua, C. N.; Shultz, A. R.; McGrath, J. E. *J. Polym. Sci., Polym. Phys. Ed.* **1999**, 37, 1849.
[494] Broyles, N. S.; Verghese, K. N. E.; Davis, S. V.; Li, H.; Davis, R. M.; Lesko, J. J.; Riffle, J. S. *Polymer* **1998**, *39*, 3419.

Chemical Company and was used as received. A liquid initiator t-butylperoxybenzoate (Atochem) was used as received.

### 4.2.2 Synthesis of Bisphenol A Poly(arylene ether phenyl phosphine oxide/sulfone) Statistical Copolymers

Phenolic hydroxyl-terminated bisphenol A poly(arylene ether phenyl phosphine oxide/sulfone)s of $M_n$=20 kg/mol were synthesized via aromatic nucleophilic substitution reactions, using a controlled excess amount of bisphenol A. The molar ratio of the reactant monomers required for obtaining the final product with the desired molecular weight was calculated according to the modified Carothers equation.[495] A 1-L, 4 neck round bottom flask equipped with an overhead stirrer, a nitrogen inlet, and a Dean Stark trap with a reflux condenser was employed for all of the polymerizations. As an example, a copolymer with 20 mole% of phosphine oxide was synthesized according to the following schedule: 38.0944 g (0.1669 mol) of bisphenol A were added along with 10.2528 g (0.03263 mol) of BFPPO and 37.4743 g (0.1305mol) of DCDPS. The amount of BFPPO and DCDPS can be varied with various mole ratios depending on the target composition of the copolymer. A 15 mol % excess of potassium carbonate (26.5 g, 0.192 mol) was also charged as the weak base for the nucleophilic reaction. A 70/30 volume ratio of dimethylacetamide/toluene mixture (560/240 mL) was used as the initial reaction medium. The reaction was heated to 135 °C reflux for 4 hours under a nitrogen atmosphere to dehydrate the system. Then, most of the toluene was removed and the reaction temperature was kept at 160 °C for 16 h to achieve high molecular weight. The viscous liquid was allowed to cool to room temperature, diluted with dimethylacetamide, filtered, and acetic acid was added to protonate the phenolate end groups. The polymer was precipitated into methanol, redissolved in chloroform, again precipitated into methanol, filtered and dried in a vacuum oven at 150 °C for 24 h.

### 4.2.3 Resin Preparation and Curing

The vinyl ester control sample was prepared by adding 1 wt % liquid initiator t-butylperoxybenzoate (mole ratio of t-butylperoxybenzoate:dimethacrylate:styrene ≈ 1:20:52) to the vinyl ester resin at approximately 80 °C. The mixture was stirred until homogeneous

[495] Odian, G. *Principles of Polymerization*, 2nd ed., Wiley-Interscience, New York, 1981, p113.

and then was degassed in a vacuum oven for about 1 minute. Care was taken to avoid significant loss of the styrene reactive diluent. Thermoplastic copolymer containing 20 mol % or more phosphonyl groups were successfully dissolved at 5-20 wt % into the commercial vinyl ester resin. When homogeneous, 1 wt % initiator was added and the mixture was degassed. Both the control and modified mixtures were added to preheated silicone rubber molds at 100 °C and covered with a steel plate in an air convection oven. The resin was cured at 100 °C for 1 h, followed by a post-cure at 140 °C for another hour and then cooled slowly in the oven.[496]

### 4.2.4 Characterization

Intrinsic viscosities were measured in chloroform at 25 °C. Gel Permeation Chromatography (GPC) measurements were performed to characterize the molecular weights and molecular weight distributions of the thermoplastic copolymers. N-methyl pyrrolidone (NMP) containing 0.02M phosphorus pentoxide was employed as the solvent at 60 °C.[497] A Waters 150C instrument, having a differential refractive index detector and a Viscotek differential viscometer in parallel, allowed calculation of absolute molecular weights by means of the universal calibration technique.

FTIR measurements utilized a Nicolet Impact 400 instrument with a resolution of 2 $cm^{-1}$ for an average of 256 scans. The copolymer, the styrene free vinyl ester resin, and their blends with various thermoplastic modifier compositions were dissolved in chloroform. The solutions were cast onto NaCl plates and dried overnight in a vacuum oven at 120 °C to remove the solvent.

Glass transition temperatures ($T_g$) of the thermoplastic copolymer/vinyl ester resin cured blends were measured with a Perkin-Elmer DSC-7 differential scanning calorimeter at a heating rate of 10 °C/min. All the results reported were obtained during a second heat after cooling from 250 °C. The midpoint temperature of the specific heat transition during the

[496] Li, H.; Rosario, A. C.; Davis, S. V.; Glass, T.; Holland, T. V.; Davis, R. M.; Lesko, J.J.; Riffle, J. S. *J. Adv. Mater.* **1997**, *28*, 55.
[497] (a) Konas, M.; Moy, T. M.; Rogers, M. E.; Shultz, A. R.; Ward, T. C.; McGrath, J. E. *J. Polym. Sci., Polym. Phys. Ed.* **1995**, *33*, 1429; (b) Konas, M.; Moy, T. M.; Rogers, M. E.; Shultz, A. R.; Ward, T. C.; McGrath, J. E. *J. Polym. Sci., Polym. Phys. Ed.* **1995**, *33*, 1441.

second heat was taken as the value of $T_g$.

A Perkin-Elmer DMA-7e instrument was employed for dynamic mechanical analysis (DMA) measurements. The samples were analyzed using the three-point bend mode at a frequency of 1Hz and a heating rate of 5 °C/min.

Thermogravimetric analyses (TGA) utilized a Perkin-Elmer TGA-7 instrument. Samples of 4-6 mg were heated at 10 °C/min from 25 to 800 °C in an air atmosphere.

The fracture surfaces of the modified resins were examined by scanning electron microscopy (SEM), using a Model ISI-SX-40 at an accelerating voltage of 20kV or 30kV. Fracture surfaces were produced at ambient temperature. All of the fracture surfaces were coated with Au to avoid charging problems during the electron beam scans.

Transmission electron microscopy (TEM) was conducted to determine the morphologies of the cured polymer modified vinyl ester networks. The bar samples were trimmed and ultramicrotomed with a Reichert-Jung Ultracut E equipped with a diamond knife. The sample thicknesses were about 700 Å. The electron micrographs were taken with a Philips 400T TEM instrument using an acceleration voltage of 100 kV.

The critical-stress-intensity factor, $K_{IC}$, a measure of plane-strain fracture toughness, was measured by the Single-Edge-Notched Bending (SENB) method, following ASTM Standard D-5045-91. The molded samples were ground with an emery paper to obtain a rectangular shape (3×6×40mm). Each specimen was sawed to generate a notch and then a crack was initiated by tapping with a liquid nitrogen chilled fresh razor blade. The samples were tested in a 3-point bending mode at a test rate of 1mm/min on an Instron Model 1123 apparatus. Approximately 10 samples of each blend were tested and the fracture toughness values were calculated by the formula provided in ASTM D-5045-91.

## *4.3 Results and Discussion*

The intrinsic viscosity and GPC results of for the hydroxyl-terminated bisphenol A poly(arylene ether phenyl phosphine oxide/sulfone) homo- and copolymers are shown in Table 4.3.1. The data show that the target molecular weights $M_n$=20 kg/mole were achieved. The objective of this investigation was to focus on the effect of the chemical structure of

these copolymers on the properties of the thermoplastic-modified networks. It was a goal to achieve good mechanical properties while preserving a relatively low viscosity in the thermoplastic/vinyl ester blends.

Table 4.3.1 GPC and Intrinsic Viscosity Characterization of Hydroxyl Terminated Bisphenol A Based Poly(Arylene Ether Triphenyl Phosphine Oxide/Diphenyl Sulfone) Homo- and Copolymers

| | BFPPO:DCDPS | GPC | | | [η] (dl/g) | [η] (dl/g) |
|---|---|---|---|---|---|---|
| Sample | (mol %) | $M_n$ | $M_w$ | $M_w/M_n$ | NMP 60 °C | $CHCl_3$ 25 °C |
| BPA-P20 | 20/80 | 21.9 | 42.1 | 1.9 | 0.31 | 0.40 |
| BPA-P30 | 30/70 | 21.3 | 40.8 | 1.9 | 0.32 | 0.37 |
| BPA-P50 | 50/50 | 22.7 | 42.0 | 1.8 | 0.30 | 0.35 |
| BPA-P100 | 100/0 | 24.2 | 57.9 | 2.4 | 0.24 | 0.45 |

### 4.3.1 Hydrogen Bonding

Further understanding of the specific interaction between the hydroxyl group of vinyl ester and the phosphonyl group of bisphenol A poly(arylene ether phenyl phosphine oxide) was achieved by FTIR measurements.[493] Figure 4.3.1 displays infrared spectra of the vinyl ester, the thermoplastic modifier, and their blends. For simplicity, only a commercial vinyl ester without styrene was employed. The hydrogen bonded hydroxyl stretching vibration of the vinyl ester was originally at about 3445 $cm^{-1}$. When it was blended with bisphenol A based poly(arylene ether phenyl phosphine oxide), it shifted to a lower frequency, as reported earlier for the "phenoxy system".[493] At 50 wt % BPA-P100 the VE hydrogen bonded hydroxyl stretching band peak showed a significant shift down to 3300 $cm^{-1}$. The results indicate a strong hydrogen bonding specific interaction between the hydroxyl group of the oligomeric dimethacrylate vinyl ester resin and the phosphonyl group. Although the samples were dried in a vacuum oven at 120 °C, a partial polymerization of vinyl ester should not affect our conclusions, since only the band shift of the hydrogen bonded hydroxyl group needed to be considered.

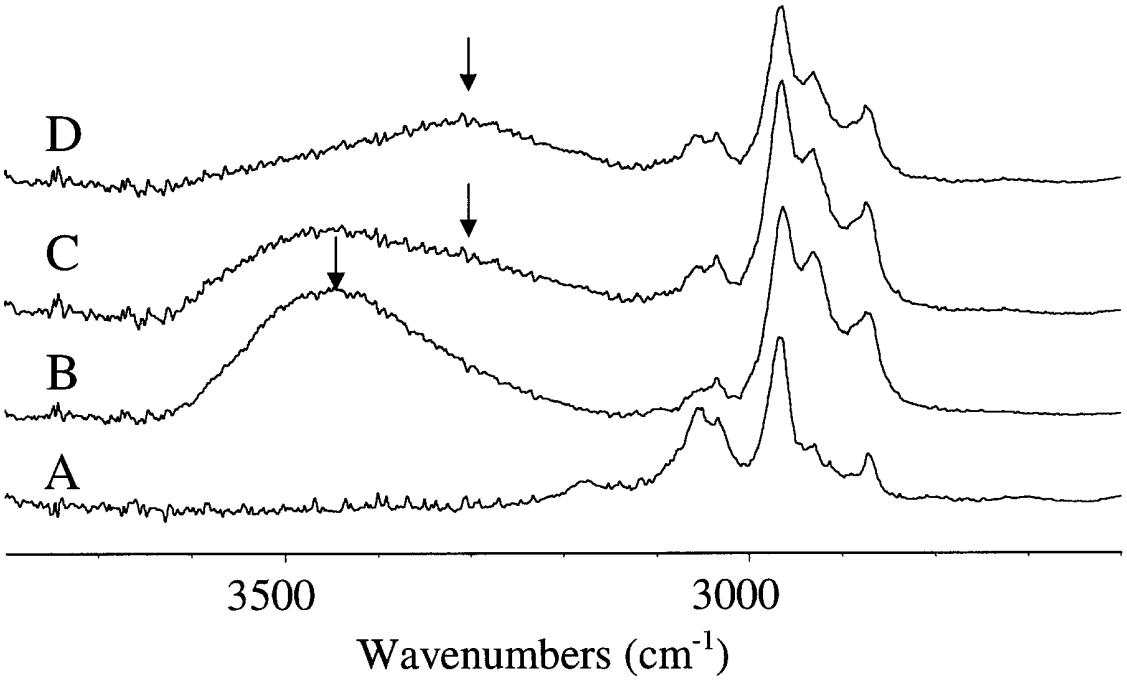


Figure 4.3.1 FTIR spectra of BPA-P100/Vinyl Ester (without styrene) blends at various weight ratios recorded at room temperature in the hydroxyl stretching region: (A) BPA-P100; (B) VE; (C) VE/BPA-P100 with 80/20 w/w; VE/BPA-P100 with 50/50 w/w

### 4.3.2 Miscibility

The phosphine oxide containing copolymers' miscibilities with a commercial vinyl ester resin were examined. Table 4.3.2 qualitatively shows that the miscibility of the vinyl ester/copolymer systems decreased with increasing copolymer concentration and increased with the amount of phosphine oxide (i.e., the hydrogen bonded site) in the copolymer. The commercial vinyl ester (Derakane 411-400) contains 28 wt % styrene, which is a nonsolvent for the bisphenol A based poly(arylene ether sulfone) control. The 10 mol % BFPPO copolymer was only slightly soluble in this commercial resin. Increasing the amount of phosphine oxide in the copolymer significantly increased solubility in the vinyl ester oligomer/styrene solution due to the hydrogen bonding between hydroxyl groups of vinyl ester resin and the phosphonyl groups. When the resin blends were cured, phase separation could be observed to occur with copolymers that had low phosphine oxide content. In contrast, the resin modified by homopolymer poly(arylene ether phenyl phosphine oxide) (BPA-P100) was transparent before and after curing. These results showed that the incorporation of phosphine oxide significantly improves the miscibility between the copolymer and vinyl ester network matrix. The copolymer modifier was restricted to ≤ 20

wt.% due to the high viscosity considerationins.

Table 4.3.2 Influence of Composition on Miscibility of Bisphenol A Based Poly(Arylene Ether Triphenyl Phosphine Oxide/Diphenyl Sulfone) Copolymer and Vinyl Ester (VE) Resin before Curing (Sol′n) and after Curing (Poly)

| | Wt % of BPA-Px in the Blends | | | | | | | |
|---|---|---|---|---|---|---|---|---|
| | 5 | | 10 | | 15 | | 20 | |
| Blend | Sol′n | Poly | Sol′n | Poly | Sol′n | Poly | Sol′n | Poly |
| VE/BPA-P20 | o | - | o | - | o | - | o | - |
| VE/BPA-P30 | + | - | + | - | o | - | o | - |
| VE/BPA-P50 | + | + | + | + | + | o | + | o |
| VE/BPA-P100 | + | + | + | + | + | + | + | + |

* Sol′n ≡ Solution, Polymer dissolved in commercial Vinyl Ester; Poly ≡ Polymer network after curing.

** Transparent (+); Translucent (o); Opaque (-)

*** BPA-P10 is only partially soluble in commercial vinyl ester

These results can be qualitatively explained according to the thermodynamic equation. $\Delta G = \Delta H - T\Delta S$, where $\Delta G$, $\Delta H$, $\Delta S$ and $T$ are the change of the Gibb's free energy, change of enthalpy, change of entropy, and temperature, respectively. $\Delta G$ is largely dependent on $\Delta H$ in the specific interaction system. A strong attractive interaction (hydrogen bonding) between bisphenol A based poly(arylene ether sulfone/phosphine oxide) yields $\Delta H << 0$ and thus $\Delta G$ can become negative. With $\Delta G < 0$ a homogeneous mixture of the copolymer and the vinyl ester resin can be generated. During network formation of the vinyl ester resin $\Delta S$ becomes smaller and phase separation can occur, if the attractive interaction between the copolymer and the cured vinyl ester resin is not strong.

### 4.3.3 Morphology

One goal was to study the effect of triaryl phosphine oxide concentration in the copolymers on the miscibility of, and/or adhesion to, the cured vinyl ester resin network. The fracture surface morphologies of the free radical cured composites were characterized by SEM. Figure 4.3.2 shows the effect of phosphine oxide content on the morphologies at a 20 wt.% copolymer loadings. Lower amounts of phosphine oxide in the copolymers (BPA-P20,

BPA-P30) produced mixtures which phase separated with the cured vinyl ester network to produce the dispersed phase and the thermoplastic copolymer as the continuous phase. Increasing phosphonyl concentration (BPA-P30) produced a less sharp phase boundary between the copolymer and the vinyl ester. Further increase to 50 mol % resulted in a “fuzzy” boundary, no doubt because of high miscibility with even the cured vinyl ester. The homopolymer (BPA-P100) generated a homogeneous network due to the high miscibility of the two components. The morphology also depends on the concentration of the thermoplastic copolymer. As an example, Figure 4.3.3 shows the morphology change with increase of the weight percentage of BPA-P30 in the BPA-P30/VE mixtures. The copolymer formed a dispersed phase in the vinyl ester network at 5 and 10 wt % copolymer loadings, but copolymer BPA-P30 showed continuous morphology with deformed vinyl ester spheres at the two higher loadings. This latter condition has also been termed “phase inverted morphology”.[484] In these systems, phase inversion occurred at 15 wt% BPA-P30.

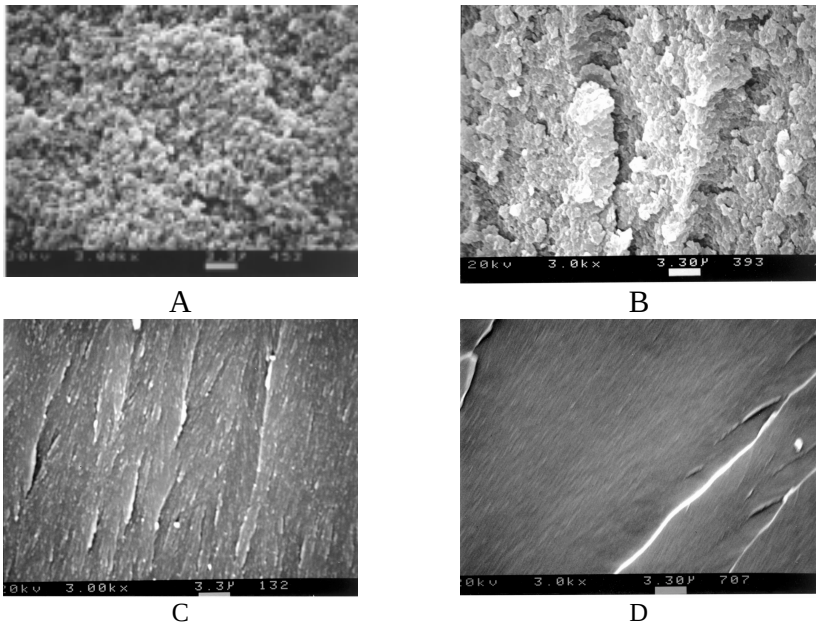


Figure 4.3.2 SEM micrographs of fracture surfaces of cured vinyl ester resin modified with BPA-Px with 20 wt% BPA-Px: (A) VE/BAP-P20; (B) VE/BAP-P30; (C) VE/BAP-P50; (D) VE/BAP-P100.

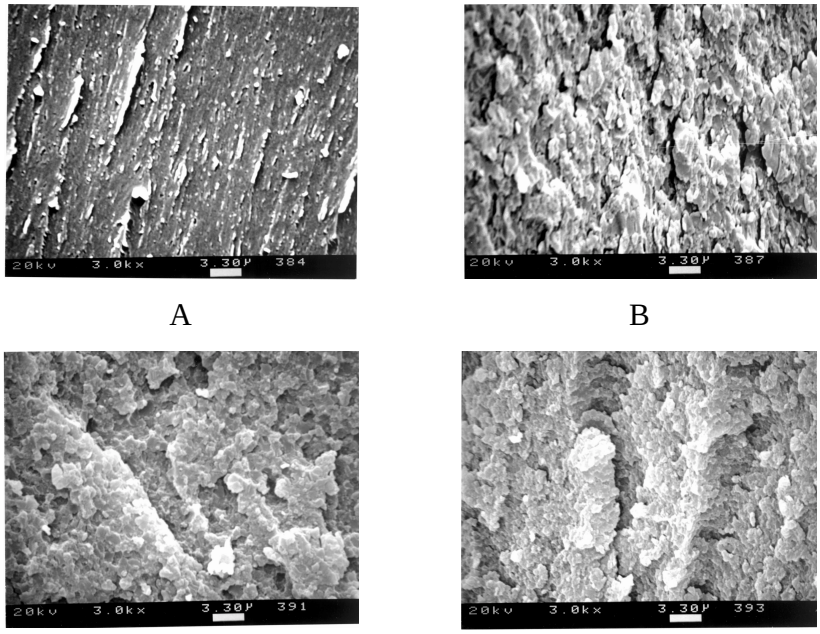


Figure 4.3.3 SEM micrographs of fracture surfaces of cured vinyl ester resin modified with BPA-P30 at various wt% loadings: (A) 5 % BPA-P30; (B) 10 % BPA-P30; (C) 15 % BPA-P30; (D) 20 % BPA-P30.

TEM was also used to investigate the morphologies of the cured networks. Figure 4.3.4 shows a gradual change of morphology with increasing amounts of phosphine oxide in the copolymer at 20 wt% copolymer loadings. The darker phase represents the BPA-Px phase, because of its higher electron density relative to the vinyl ester phase. Both BPA-P20 and BPA-P30 modified vinyl ester networks exhibited phase separation; the copolymers formed the continuous phase and the vinyl ester networks formed the dispersed phase. The BPA-P30 modified vinyl ester had a relatively narrow size distribution of vinyl ester network particles compared to the BPA-P20 system. Phase separation was barely discernable in the cured BPA-50/VE mixture and the cured PBA-P100/VE mixture was clearly homogeneous. These TEM results were consistent with the SEM results on fracture surfaces. Apparently, weak hydrogen bonding between phosphonyl groups of the BPA-Px copolymers and the hydroxyl groups of the vinyl ester is sufficient to solubilize the “precursor”. But, high concentration afforded strong hydrogen bonding, leading to homogeneity even in the cured network. Figure 4.3.5 shows the morphologies of various weight percentages of BPA-P30 in cured BPA-P30/VE mixtures. At 5 wt % BPA-P30 the copolymer appears to be the dispersed phase in a continuous VE matrix. At 10 wt % BPA-P30 cocontinuous phases of the copolymer and VE

network appear to exist. At 15 wt % and 20 wt % loadings of the BPA-P30 the thermoplastic copolymer forms the continuous phase and the VE network forms the dispersed phase in the cured mixtures. This phase inversion behavior is consistent with the SEM results.

The chemical resistances of the cured vinyl ester resin control and of the cured vinyl ester/copolymer mixtures were examined by immersing sample bars in chloroform. It was observed that the cured vinyl ester resin control bar remained clear and transparent even after a month of immersion. However, the cured bars containing 20 wt % of BPA-P20 or BPA-P30 copolymer became white and began to disintegrate. After about a month these samples had disintegrated into small pieces. It was noted that the cured bars with higher weight percentages of copolymer disintegrated faster. Cured bars containing 5 or 10 wt % of BPA-P30 were highly resistant to chloroform and did not disintegrate even after a month of immersion. A cured bar containing 15 wt% BPA-P30 disintegrated in chloroform. SEM and TEM measurements both showed that the cured mixtures which disintegrated in chloroform had vinyl ester microgel particles dispersed in a continuous thermoplastic copolymer phase. Their lack of solvent resistance is readily understood. Non-disintegrating cured mixtures were observed when the copolymer existed as the discontinuous (or cocontinuous?) phase within the VE network. Cured mixtures of VE/BPA-P100 were homogeneous and resistant to BPA-P100 leaching from the VE network.

The above observations indicate that it will be necessary to have reactive end groups[481,482,483,484] or reactive groups pendent on the copolymer chains[498] to assure that the thermoplastic copolymer will exist as dispersed, phase separated toughener domains. This need for the toughener to partially react with the matrix material to prevent inversion during the network formation has been noted in step-growth reaction matrix systems. In the vinyl ester resin free radical reaction, gelation occurs at very low conversions. Rapid autoacceleration of the polymerization in regions where gel has formed tends to yield discrete microgel particles with the thermoplastic toughener expelled as a continuous surrounding phase. This phase inversion occurs at lower toughener concentrations and at less unfavorable network/toughener interactions in free radical chain growth reactions than in step growth reactions. The need for a reactive toughener in the former instance is therefore more

stringent.

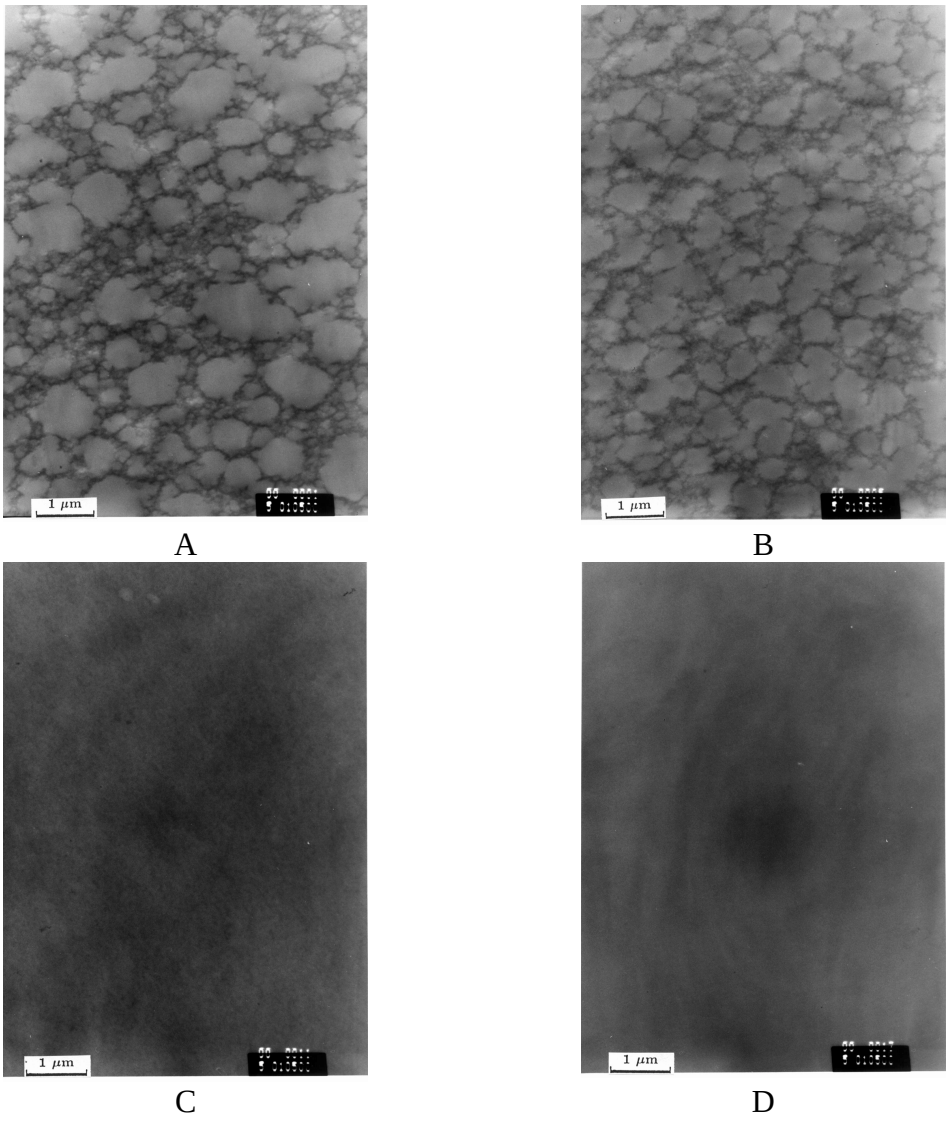


Figure 4.3.4 TEM micrographs of cured vinyl ester resin modified with BPA-Px at 20 wt% loadings: (A) VE/BAP-P20; (B) VE/BAP-P30; (C) VE/BAP-P50; (D) VE/BAP-P100.

[498] Pak, S. J.; Lyle, G. D.; Mercier, R.; McGrath, J. E. *Polymer* **1993**, *34*, 885.

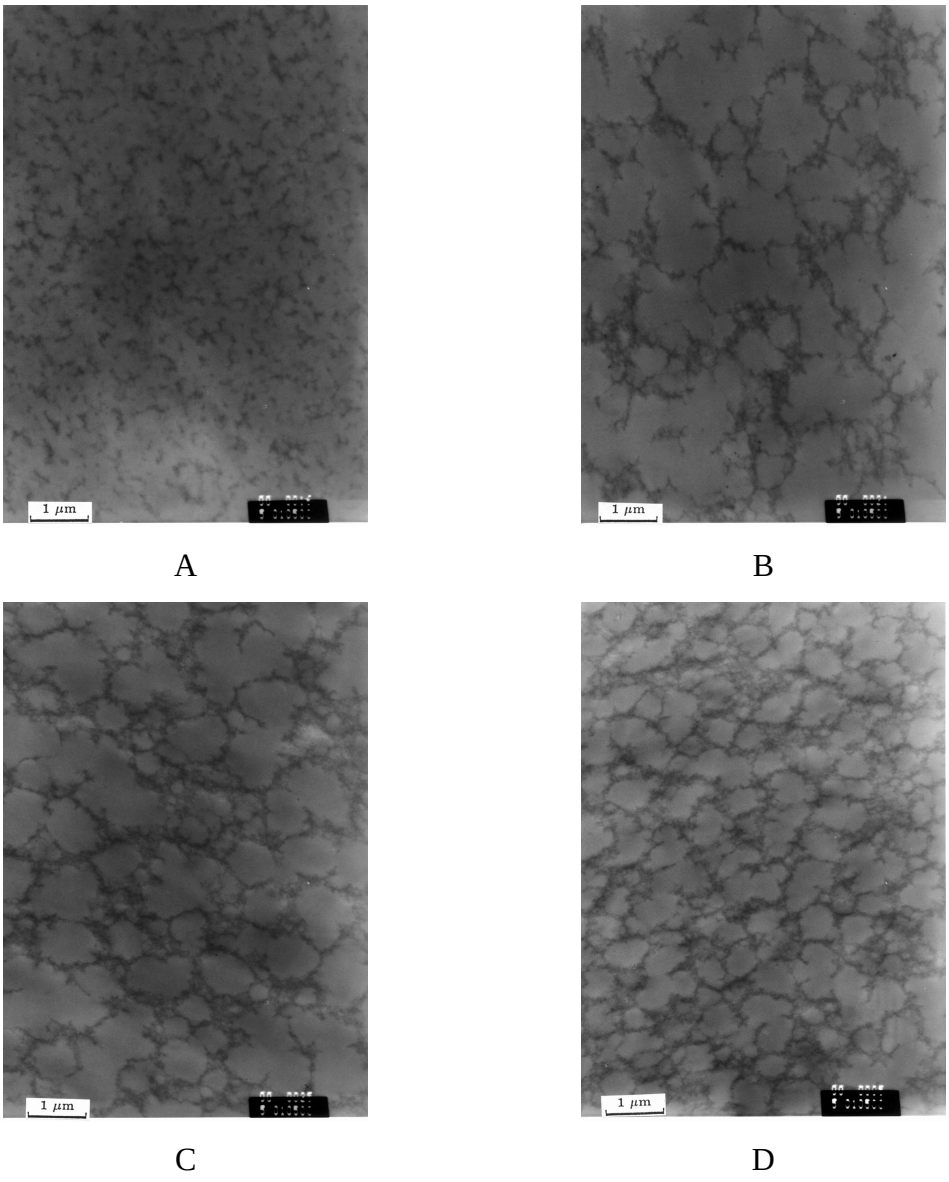


Figure 4.3.5 TEM micrographs of cured vinyl ester resin modified with BPA-P30 at various wt% loadings: (A) 5 % BPA-P30; (B) 10 % BPA-P30; (C) 15 % BPA-P30; (D) 20 % BPA-P30.

### 4.3.4 Effect of Modifier on Thermal Stability and Mechanical Properties

#### *4.3.4.1 Thermal Stability*

TGA results showed that the incorporation of 20 wt % of the copolymers or of the BPA-P100 homopolymer did not significantly affect the 5 % weight loss temperature, probably because the initial degradative process begins with the thermoset fraction (Figure 4.3.6). In the high temperature regime, the char yield increased with the phosphine oxide content of the copolymer. As is known, poly(arylene ether phenyl phosphine oxide/sulfone)s are fire

resistant copolymers.[471b] Therefore, the incorporation of the copolymers as tougheners in vinyl ester resin should, and did, increase the char yield.

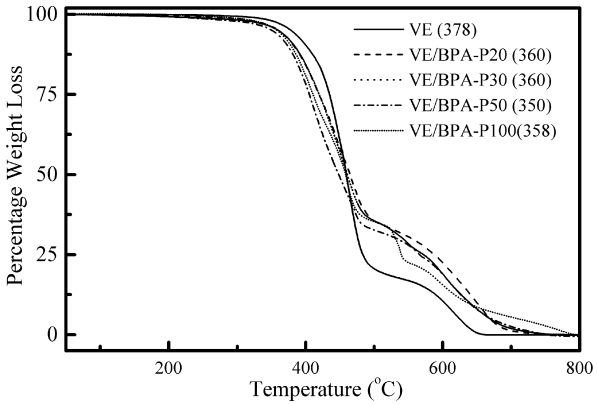


Figure 4.3.6 Thermogravimetric analysis of cured BPA-Px/Vinyl Ester with 20 wt% of BPA-Px at a heating rate of 10 °C/min in air. Numbers in parentheses are the temperatures at 5 % weight loss.

### *4.3.4.2 Thermal Transition Behavior*

Figure 4.3.7 presents the tan δ (mechanical loss tangent) *vs*. temperature curves of cured vinyl ester resin modified with BPA-P30 at various compositions. Similarly, Figure 4.3.8 lists the tan δ *vs*. temperature curves of vinyl ester resin modified with BPA-Px at 20 wt% loadings. The DMA results showed a slight increase of $T_g$ of the modified resins since the modifiers have higher glass transition temperatures (Figure 4.3.9). In all the resins the tan δ *vs*. temperature curves showed only a single damping peak no matter what the loading and the composition in the copolymers. Though the copolymer and the vinyl ester networks were phase separated, the tan δ peak of the higher $T_g$ could not be reached before sample failure. Phase separation was expected in the networks modified with copolymers containing low amounts of phosphine oxide. Although cocontinuous phases seemed to be observed on the fracture surfaces at high loadings of copolymers by SEM, TEM showed only crosslinked vinyl ester particles surrounded by a continuous thermoplastic phase. The $T_g$s of the thermoplastic polymers[493] are much higher than that of the vinyl ester network[494] and the amount of the thermoplastics polymer is relatively low. Therefore, due to experimental limitations, DSC could not detect the $T_g$ of the thermoplastic polymers in the presence of the rubbery vinyl ester network. Only a single $T_g$ that was nearly the same as that of the cured vinyl ester control was observed (Figure 4.3.10).

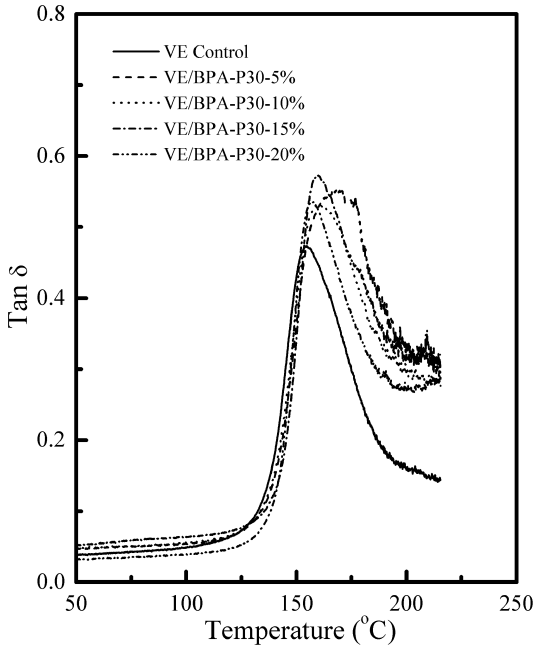


Figure 4.3.7 Mechanical loss tan δ of cured BPA-P30/Vinyl Ester at various BPA-P30 wt% at 1Hz and a heating rate of 2 °C/min.

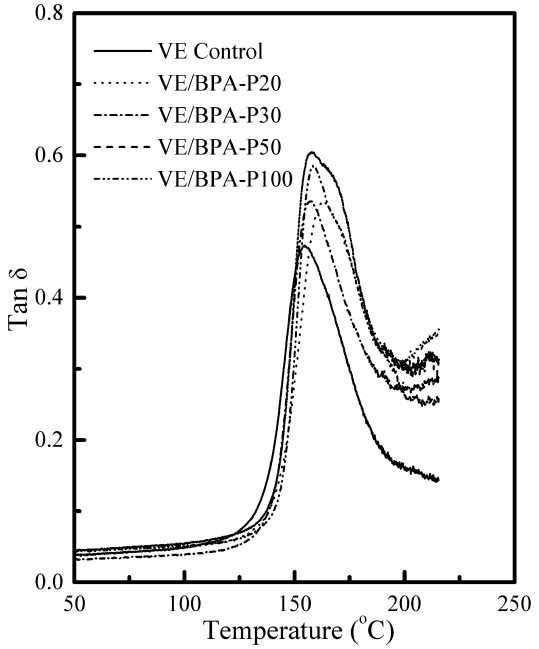


Figure 4.3.8 Loss tan δ of cured BPA-Px/Vinyl Ester mixtures with 20 wt% of BPA-Px with 1Hz at a heating rate of 2 °C/min.

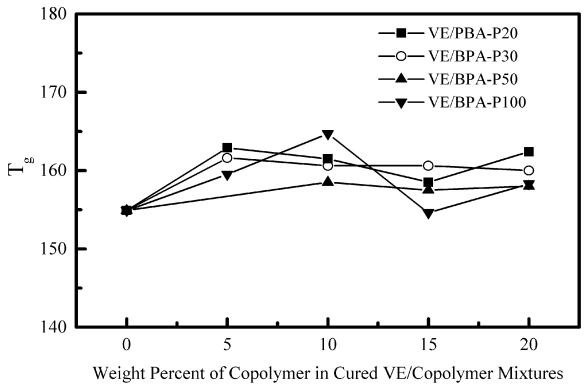


Figure 4.3.9 $T_g$ (tan δ peak temperature) of cured BPA-Px/Vinyl Ester mixtures at various loadings.

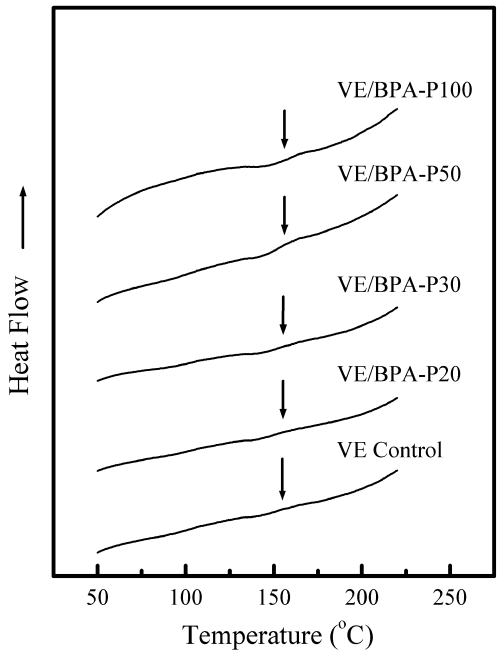


Figure 4.3.10 DSC thermograms of cured VE/BPA-Px mixtures at 80/20 w/w composition. Arrows indicate the location of $T_g$.

### *4.3.4.3 Fracture Toughness*

Table 4.3.3 shows the stress concentration factors, $K_{IC}$, of various cured VE/copolymer mixtures at four copolymer contents. The cured control vinyl ester is very brittle. For all the compositions examined, the fracture toughness was significantly improved with the incorporation of only 5 wt % of thermoplastic polymer. High amounts of thermoplastic copolymers led to significantly improved fracture toughness. However, these materials consisted of thermoplastic copolymer reinforced by VE microgel filler particles. The fracture toughness increased to more than two times that of the control with 20 wt % loading of the

copolymer BPA-P30. These results showed that both phase separation and interaction between the vinyl ester and the thermoplastic polymer were important for the improvement of the fracture toughness. As is well known, phase separation between the two components is often a requirement to increase impact strength. Also, good adhesion helps transfer stress from the continuous phase to the reinforcing filler particles. Small amounts of phosphine oxide in the copolymer may not enable maintenance of good adhesion while large amounts can lead to insufficient phase separation or even homogeneous systems. Therefore, a proper choice of the phosphine oxide content allows for both phase separation and good adhesion. Good phase separation with still strong adhesion between a thermoset network and modifier can significantly increase the fracture toughness in reactive modifier systems.[484] In a previous investigation, bis(4-fluorophenyl)-3-aminophenylphosphine oxide (amino DFTPPO) was incorporated as a comonomer into a bisphenol A based poly(sulfone). The resultant copolymers were used to toughen an epoxy resin. Only 2.5 mol% of the reactive phosphine oxide comonomer in the copolymer was needed to optimize the toughness,[498] even though no detailed study of the morphology was attempted. In a separate study the BPA-Px copolymers were used to toughen an epoxy resin. It was found that only low concentrations of phosphonyl groups in the copolymers were needed to significantly increase the fracture toughness.[499]

Table 4.3.3 Critical-Stress-Intensity Factor $K_{IC}$ ($MPa \cdot m^{0.5}$) of Polymer-Modified Vinyl Ester

| Sample | Wt% Loading Polymer in the Network | | | |
|---|---|---|---|---|
| | 5 | 10 | 15 | 20 |
| VE/BPA-P20 | 0.55±0.05 | 0.54±0.08 | 0.50±0.08 | 0.64±0.08 |
| VE/BPA-P30 | 0.64±0.10 | 0.66±0.08 | 0.68±0.22 | 0.80±0.11 |
| VE/BPA-P50 | 0.56±0.10 | 0.66±0.09 | 0.66±0.13 | 0.63±0.09 |
| VE/BPA-P100 | 0.52±0.15 | 0.47±0.07 | 0.47±0.09 | 0.63±0.13 |

* $K_{IC}$ of Control Vinyl Ester was 0.36±0.09 $MPa \cdot m^{0.5}$

## *4.4 Conclusions*

Mixtures of non-reactive bisphenol A based poly(arylene ether triphenyl phosphine

[499] Wang, J.; Wang, S.; Ji. Q.; McGrath, J. E.; Ward, T. C. *to be published.*

oxide/diphenyl sulfone) copolymers of 20k $M_n$ with a commercial vinyl ester resin exhibited increasing miscibility as a function of phosphine oxide content. FTIR spectra of bisphenol A based poly(arylene ether triphenyl phosphine oxide) homopolymer/vinyl ester (no styrene) mixtures showed that strong hydrogen bonding between the hydroxyl groups of the vinyl ester and the phosphonyl groups of the copolymer was the driving force for the miscibility of the two components. Whereas the polysulfone control was insoluble, the copolymer mixed homogeneously in all proportions, provided the phosphonyl groups exceeded 50 mol %. The homopolymer also formed homogeneous mixtures with a commercial VE resin and the networks appeared to be transparent after curing. This suggests the possible use of the homopolymer or of phosphine oxide containing copolymers as interphase materials between a VE resin matrix and glass, or carbon, or aramide fibers.

The morphologies of cured poly(arylene ether triphenyl phosphine oxide/diphenyl sulfone) copolymer/VE resin mixtures depended both on the phosphine oxide content of the thermoplastic copolymer and on the weight fraction composition of the mixtures. Only at ≤10 wt % of copolymer having a sufficient mole fraction of phenyl phosphine oxide units did the thermoplastic form a discrete internal phase in a crosslinked VE resin matrix. In general, phase inversion occurred producing a continuous thermoplastic phase reinforced by discrete microgel VE resin particles. Although a similar phase inversion occurs during cures in systems having non-reactive thermoplastics mixed with step-growth network forming resins (e.g. epoxies), the phase inversion is greatly encouraged by the rapid, low conversion attainment of gel in the free radical cure system. This further points out the necessity to have reactive groups on the thermoplastic component of the latter systems, to assure that it is forced to form the internal toughening phase.

The fracture toughness of all the cured thermoplastic-modified VE resin materials exceeded that of the cured VE resin control. However, in most instances the materials were composed of the thermoplastic reinforced by high loadings of particulate VE resin. The improved fracture toughness does indicate good adhesion of the thermoplastic to the cured VE resin.

The incorporation of copolymer in the VE resin system did not significantly influence the

5% wt loss temperature. Also the observed $T_g$ of the cured VE resin remained about the same as that of the unmodified cured resin. Both DMA and DSC could detect the $T_g$ of the thermoplastic polymer, but only the $T_g$ of the cured VE resin was detected. However, due to the phase-inverted morphologies of most of the networks their solvent ("chemical") resistances were poor. The amorphous continuous thermoplastic phase was extracted from the samples and the materials disintegrated to yield the discrete microgel particles of the cured VE resin. As discussed above, reactive thermoplastic modifiers will be expected to provide the desired toughening and increasing chemical resistance of the cured VE resin matrices, as was observed in analogous epoxy systems.[484]

# 5 Literature Review of Polymer-Inorganic Material Based Nanocomposites

## *5.1 Introduction*

The development of technology has illustrated the importance of new materials. In particular, nanoparticle-based materials have been developed due to their unique properties. Typically, the size of nanoparticles can range from less than 10 to a few hundred nanometers, as desired by the final applications.[500] The small nanoparticles have characteristic high surface-to-volume ratios. Consequently, a large fraction of the atoms are exposed on the surface, which affords different properties compared to the bulk due to a number of quantum-size effects.[501] Therefore, very unusual electrical, magnetic, mechanical, and thermal properties are observed. Some widely studied nanoparticles include metals, metal oxides, silica, and metal salts. Nanoscale metal particles, for example, example, exhibit an enhancement of some properties including magnetic and optical polarizability,[502] Raman scattering,[503] and chemical reactivity.[504] However, the prepared nanoclusters are not very stable and may be subjected to oxidation and coalescence. Other problems include poor processibility and mechanical properties.

Nanoclustered polymer-inorganic nanocomposites have generated great interest. The basic mechanical properties depend on the polymer matrix, which can be homopolymers, statistical copolymers, block copolymers, polymer blends, and dendrimers. Generally, most polymers are processible and some can self-assemble into specific structures. The combination of polymers and inorganic materials may allow that new materials to display some novel properties in addition to the advantages of both components, since the mechanical properties of the composites are mainly determined by the matrix, while other physical properties, e.g. transparency, are dependent on the nature of nanoparticles.[505,506,507]

---

[500] See, for example, the special issue "Nanostructured materials": *Chem. Mater*. **1996**, *8*.
[501] Henglein, A. *Chem. Rev.* **1989**, *89*, 1861.
[502] Blömer, M. J.; Haus, J. W. Ashley, P. R. *J. Opt. Soc. Am. B*, **1990**, *7*, 790.
[503] Otto, A.; Bornemann, T.; Erturk, U.; Mrozek, I.; Pettenkofer, C. *Surface Sci.*, **1989**, *210*, 363.
[504] Siegel, R. W. *Mater. Sci. Eng*. **1993**, *B19*, 37
[505] Roescher, A.; Moller, M. *Polym. Mater. Sci. Eng.* **1995**, *72*, 283.
[506] Longenbergers, L.; Thornton, S.; Mills, M. *Polym. Mater. Sci. Eng.*, **1995**, *73*, 164.

Nanoparticles may allow long-time stability in the composites by preventing both oxidation and coalescence. It is known that the novelty of polymer based nanocomposites in comparison with other nano-size objects lies in the influence of the matrix resin on composites performance and matrix/nanoparticles interaction.

Another distinctive feature of these systems is the cooperative behavior of interacting particles, particularly in the case of highly filled composites. This becomes observable at the percolation threshold where certain continuous structures of fillers are formed.[508] The classic percolation theory or the nearest-neighbor model assumes a statistical distribution of the discontinuous phase in a continuous matrix. The polymer-inorganic nanocomposites have been generated with electrical properties, nonlinear optical properties, improved mechanical properties, gas barrier, catalysts, fire retardant, among others, as described in review papers.[509,510,511]

This part of literature review will summarize general methods for the preparation of polymer-inorganic nanocomposites and some recent progress in this area.

## *5.2 Polymer-Metal Nanocomposites*

Zerovalent metal clusters with a high level of size/structure control would be of significant interest for use in catalysis,[512,513] or other nano-devices.[514] A number of different ways have been developed to prepare polymer-metal nanocomposites. These include, but are not necessarily limited to, photoreduction,[515] and reduction using various reducing agents in association with protective polymers.[516] The nanoparticles are mainly desired for noble metals, such as Cu, Ag, Cu, Pd, Ru, because of their good chemical stability, catalytic behavior, and excellent conductivity.

---

[507] Watkins, J. J.; MacCarthy, T. J. *Polym. Mat. Sci. Eng.* **1995**, *73*, 158.
[508] Godovski, D. Yu. *Adv. Polym. Sci.* **1995**, *119*, 79.
[509] Beecroft, L. L.; Ober, C. K. *Chem. Mater.* **1997**, *9*, 1302.
[510] Wang, Y.; Herron, N. *J. Phys. Chem.* **1991**, *95*, 525.
[511] Giannelis, E. P. *Adv. Mater.* **1996**, *8*, 29.
[512] Knapen, J. W. J.; van der Made, A. W.; de Wilde, J. C.; van Leeuwen, P. W. N. M.; Wijkens, P.; Grove, D. M.; van Koten, G. *Nature* **1994**, *372*, 659.
[513] Tomalia, D. A.; Dvornic, P.R. *Nature* **1994**, *372*, 617.
[514] Dagani, R. *Chem. Eng. News* **1998**, *27*.
[515] Huang, H. H.; Ni, X. P.; Loy, G. L.; Chew, C. H.; Tan, K. L.; Loh, F. C.; Deng, J. F.; Xu, G. Q. *Langmuir* **1996**, *12*, 909.
[516] Hirai, H.; Wakabayashi, H.; Komiyama, M. *Bull. Chem. Soc. Jpn.* **1986**, *59*, 367.

These polymer-metal composites generally are based on systems containing oxygen or nitrogen atoms, although some olefin polymers were also used. Oxygen and nitrogen atoms can form salts or complexes with metal ions. As an example, copper (II) acetate and poly(N-vinylpyrrolidone) (PVP) were dissolved into water or 2-ethoxy ethanol and the salt was reduced to copper metal by an excess of hydrazine monohydrate under refluxing in an nitrogen atmosphere.[517] The nanoparticles exhibited a distinct absorption peak in the region 572-582 nm. The average size variation from 6.6 to 22.7 nm in 2-ethoxy ethanol and from 15.5 to 30.2 nm in water was achieved by varying the amount of PVP.

The use of different polymers to control the particle size, morphology, and stability of the particles was reported by Mayer *et al.*[518] Some polymer complexes are thermal and/or photodegradable. Sohn et al obtained silver nanopartcles in norbornene based block copolymers by heating the silver (I) phosphine polymer complexes.[519,520] Huang, *et al.* reported that a poly(N-vinylpyrrolidone)-silver chloride aqueous solution exposed to 254 nm UV light afforded the silver particles with size ranging from 15.2 to 22.4 nm.[521]

Crosslinked epoxy-silver nanocomposites were reported by Rong *et al.*[522] In their work, silver nitrate was reduced with sodium borohydride and the generated nanoparticles were isolated by centrifugation. They were then dispersed into chloroform or acetone, via sonication. After the silver suspension was mixed with an epoxy resin and the solvent was removed, the dried mixture was cured into a network by triethoxyamine.

Dendrimers have large free volumes and can be used for the storage of nanoparticles. Pioneering research has been done by Zhao *et al.*[523] and Balogh, *et al.*[524] Both groups separately reported the reduction of the poly(aminoamine) (PAMAM)-copper(II) complex using the reducing agent $NaBH_4$ or hydrazine to achieve very stable copper particles. Scheme 5.2.1 shows the construction of dendrimer nanocomposites.[524] The particle size can be

[517] Huang, H. H.; Yan, F. Q.; Kek, Y. M.; Chew, C. H.; Xu, G. Q.; Ji, W.; Oh, P. S.; Tang, S. H. *Langmuir* **1997**, *13*, 172.
[518] Mayer, A. B. R.; Mark, J. E.; Hausner, S. H. *J. Appl. Polym. Sci.* **1998**, *70*, 1209.
[519] Sohn, B. H.; Cohen, R. E. *Acta Polym.* **1996**, *47*, 340.
[520] Sohn, B. H.; Cohen, R. E. *J. Appl. Polym. Sci.* **1997**, *65*, 723.
[521] Huang, *Langmuir* **1996**, *12*, 909.
[522] Rong, M.; Zhang, M.; Liu, H.; Zeng, H. *Polymer* **1999**, *40*, 6169.
[523] Zhao, M.; Sun, L.; Crooks, R. M. *J. Am. Chem. Soc.* **1998**, *120*, 4877.
[524] Balogh, L.; Tomalia, D. A. *J. Am. Chem. Soc.* **1998**, *120*, 7355.

controlled by varying the size of the host-dendrimer nanoreactor. Figure 5.2.1 shows the feature UV-visible spectra, indicating the produced particles were quite small, with a narrow size distribution.

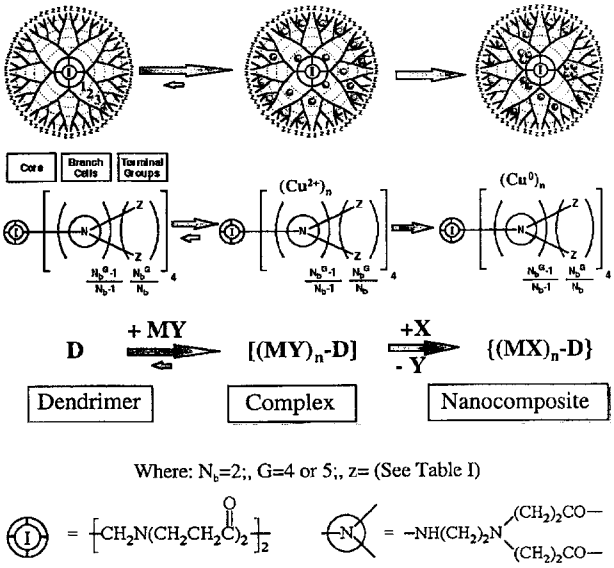


Scheme 5.2.1 Construction of dendrimer nanocomposites.[a] [524]

[a]Y are the ligands before complex formation and X are the ligands in the nanocomposite, provided by a second reactant. Note, that X may be missing in the case of zero valent metals.

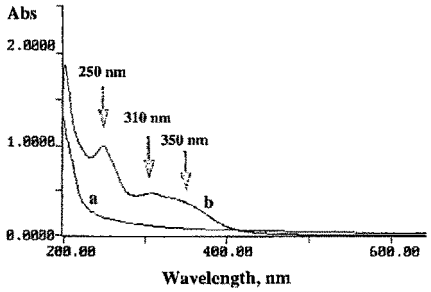


Figure 5.2.1 Comparison of UV-visible spectra of the {Cu(0)27-PAMAM_G5.P} nanocomposite (0.25mM) and PAMAM_G5.P (0.25mM) in methanol.[524]

## *5.3 Polymer-Metal Oxide Nanocomposites*

This part of review will discuss polymer-metal oxide nanocomposites. It will be divided into three parts: polymer-silica nanocomposites; polymer-titanium oxide/aluminium oxide/zirconium oxide nanocomposite; polymer-magnetic metal oxide nanocomposites.

### 5.3.1 Polymer-Silica Nanocomposites

The interest in polymer-silica nanocomposites is primary on their unique mechanical properties and physical properties, such as high modulus, high stiffness, high hardness, low coefficient of thermal expansion, low gas permeability, fire retardance, etc. In addition, they are relatively inexpensive. Common approaches for the preparation of these nanocomposites include sol-gel, solution and melt blending techniques.

#### *5.3.1.1 Polymer-Silica Nanocomposites Made by Sol-Gel Approach*

The invention of the sol-gel system is more than 150 years old. In 1846, the French scientist Elbelmen reported the synthesis of silicate monoliths from tetraethoxysilane precursor (made from tetrachlorosilane and ethanol).[525] In 1885, another French scientist, Ditte, studied a sol-gel process for the formation of vanadium pentoxide.[526] However, modern concepts of sol-gel science have been developed only in the past few decades. At first, scientists focused their interest on the favorable optical characteristics of silica, zirconia, and other transparent oxides. The major advantage of the process is that relatively low temperatures are used in this type of ceramics processing. Many ceramic precursors have been developed. Among them, tetraethoxysilane (TEOS) is the most common one. The structure is shown in Scheme 5.3.1 Organic modification may take place at any of the reactive alkoxide arms to change the monomer functionality and new precursor can be generated.

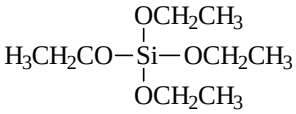

Scheme 5.3.1 Structure of tetraethoxysilane (TEOS)

Within the past 10-15 years, the sol-gel process has been used to create novel polymer-inorganic composite (hybrid) materials often called “ceramers” by Wilkes *et al.*[527] and “ormosils” or “ormocers” by Schmidt *et al.*[528] The hybrid materials prepared via sol-gel process can be divided into association system and chemical bonded system.

In the inorganic-organic association system there is no covalent bonding between the

[525] Elbelmen, J. *J. Ann. Chim. Phys.* **1846**, *16*, 129.
[526] Ditte, A. *C. R. Acad. Sci. Paris* **1885**, *101*, 698.
[527] Wilkes, G. L.; Orler, B.; Huang, H. *Polym. Prepr.* **1985**, *26*, 300.

organic polymer and inorganic network. Introducing hydrogen bonding or association/coupling equilibrium can generate this kind of system. Typically, like many organic polymer-polymer blends, most polymer-silica hybrids are phase separated when prepared by mixing noncovalently the polymer with inorganic sol-gel system. Specific interaction between the polymer and the sol-gel may delay the phase separation. Consequently, microphase separation may take place other than macrophase separation. Some polymers contain hydroxyl, carbonyl, amide, or other groups and these groups can be hydrogen-bonded with silanol groups. Polymers such as poly(methyl methacrylate) (PMMA),[529,530,531] poly(vinyl acetate) (PVAc),[532,533] poly(vinylpyrrolidone) (PVP),[534] poly(N, N-dimethylacrylamide) (PDMAc),[535] and poly(ethyloxazoline) (PeOx),[536,537] were shown to have hydrogen bonding with silanols on silicate network. Scheme 5.3.2 shows the structures of the above polymers.

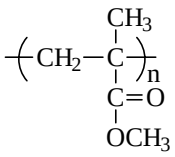

PMMA

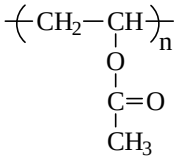

PVAc

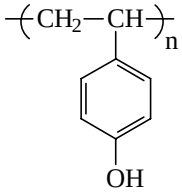

PVPh

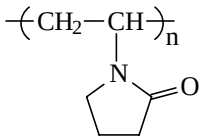

PVP

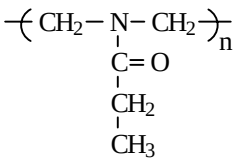

PeOx

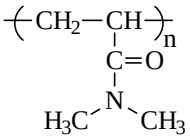

PDMAc

Scheme 5.3.2 Structures of polymers that can form hydrogen bonding with silanol groups.

Hydrogen bonding of the sol-gel with these polymers retards severe phase separation

---

[528] Schmidt, H. J. *Non-Cryst. Solids* **1985**, *73*, 681.
[529] Landry, C. J. T.; Coltrain, B. K. *U.S. Patent* 5,051, 298, **1991**.
[530] Landry, C. J. T.; Coltrain, B. K.; Brady, B. K. *Polymer* **1992**, *33*, 1486.
[531] Landry, C. J. T.; Coltrin, B. K.; Wesson, J. A.; Zumbulyadis, N.; Lippert, J. L. *Polymer* **1992**, *33*, 1496.
[532] Bechtold, M. F. *U.S. Patent* 2,404,357, **1946**.
[533] LeBoeuf, A. R. *U.S. Patent* 3,971,872, **1976**.
[534] Tokl, M.; Chow, T. Y.; Ohnaka, T.; Hideo, S.; Saegusa, T. *Polym. Bull.* **1992**, 29, 653.
[535] Saegusa, T.; Chujo, Y. Proceedings for the 33rd IUPAC Meeting on Macromolecules, Montreal, **1990**
[536] David, I. A.; Scherer, G. W. *Proceedings for the 33rd IUPAC Meeting on Macromolecules*, Monreal, **1990**.
[537] David, I. A.; Scherer, G. W. *Polym. Prepr. ACS* **1991**, *32(2)*, 514.

during network densification. Transparent films were obtained by this approach and very small sizes of silica particles were observed. A direct evidence for the hydrogen bonding between silanol of silica and carbonyl of poly(vinylpyrrolidone) was shown by the observation of $^{13}C$ NMR chemical shift of carbonyl groups.

Under some circumstances, only a small amount of monomers capable of hydrogen bonding is needed to copolymerize with some other monomers that do not contain hydrogen bonding moieties. The resulting copolymers can be used as a compatibilizer with other polymer systems thta are used for inorganic modification. Ideally, the compatibilizing polymer, which is only a small quantity of the copolymer, will diffuse to the interface of the two immiscible polymer systems and reduce the interfacial tension. This reduction of the interfacial tension creates a better organic-inorganic composite interface by reducing the dispersed-phase particle size and increasing the adhesion between the two phases.[538]

Hydrogen bonding interactions have also been used to generate nanofoam materials. In these materials, the size of the pores can be tailored by varying the structure of polymers. A commonly used approach is by sol-gel process in the presence of di- or triblock copolymers. The block copolymers generally contain blocks capable of hydrogen bonding with silanol groups and both blocks should have relatively low glass transition temperatures to allow high mobility and therefore rapid formation of structures with long range order even in the bulk. Poly(ethylene oxide) based nonionic surfactants were used to prepare such kinds of nanomaterials.[539,540,541] A triblock copolymer poly(ethylene oxide)-b-poly(propylene oxide)-b-poly((ethylene oxide) (PEO-b-PPO-b-PEO) was also used to prepare block copolymer-silica nanocomposites.[542] It was found that the degree of microphase separation and the resulting mesostructure of bulk samples were strongly dependent upon the concentration of block copolymer, with higher concentrations producing higher degrees of order. Polyisoprene-b-poly(ethylene oxide)s (PI-b-PEO) with spherical morphologies were also incorporated into the systems and both the cylinder and lamellar structures were observed, depending on the

[538] Landry, C. J. T.; Coltrain, B. K.; Teegraden, D. M.; Long, T. E.; Long, V. K. *Macromolecules* **1996**, *29*, 4712.
[539] Bagshaw, S. A.; Prouzet, E.; Pinnavaia, T. J. *Science* **1995**, *269*, 1242.
[540] Firouzi, A.; Atef, F.; Oertli, A. G.; Stucky, G. D.; Chmelka, B. F.*J. Am. Chem. Soc.* **1995**, *119*, 3596.
[541] Attard, G. S.; Glyde, J. C.; Goltner, C. G. *Nature* **1995**, 378, 366.
[542] Melosh, N. A.; Lipic, P.; Bates, F. S.; Wudl, F.; Stucky, G. D.; Fredrickson, G. H.; Chmelka, B. F. *Macromolecules* **1999**, *32*, 4332.

amount of copolymers used.[543] (Figure 5.3.1)

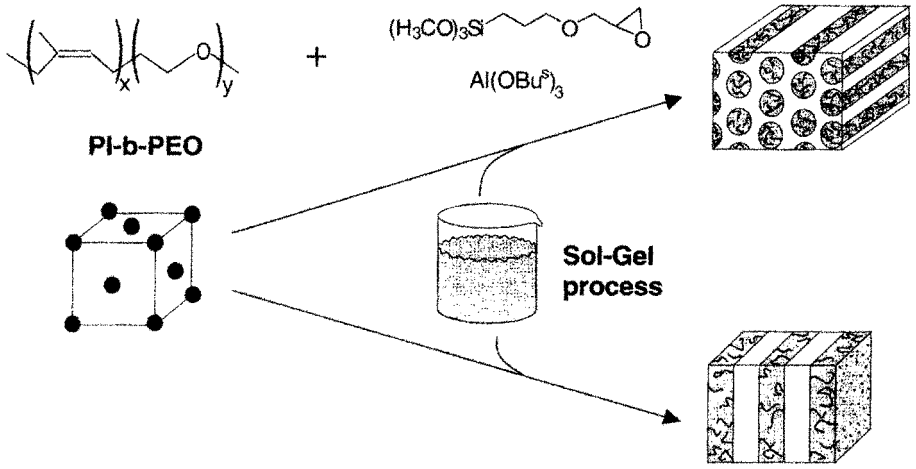


Figure 5.3.1 Schematic drawing of an approach for synthesizing organically modified silica mesostructures in reference.[543] Left: the morphology of the precursor block copolymer. Right: the resulting morphologies after addition of various amounts of the metal alkoxides.

Calcinating these block copolymer-silica composites leads to hydrothermally stable, mesoporous silica structures.[539,540,541] The size and shape of the pores can be tuned by varying the amount of polymers, polymer structures.

This approach offers a various advantages for the preparation of nanocomposites and porous glasses by solely changing the structure and the amount of copolymers.

Association/coupling equilibrium occurs in polymer systems containing hydroxyl moieties, which can be used for hydrogen bonding. A dynamic equilibrium between hydrogen bonded groups and a covalently bond exist, since the covalent –C-O-Si- bonds are hydrolytically unstable. Generally, the equilibrium is shifted towards the hydrogen bonded moieties. Also, polymers containing carboxylic acid endgroups undergo similar association/coupling equilibrium, because carboxylic acid endgroups are capable of catalyzing the equilibrium reaction.[538] The endgroups are then involved in the dynamic equilibrium between hydrogen bonded chain ends and covalently bound chain ends due to the instability of –C-O-Si- bonds, as shown in Scheme 5.3.3.[538] This in situ behavior also occurs in template systems, where an ionomeric membrane is utilized as a morphological template for in situ sol-gel reactions.

[543] Templin, M.; Franck, A.; Du Chesne, A.; Leist, H.; Zhang, Y.; Ulrich, R. Schädler, V.; Wiesner, U. *Science* **1997**,

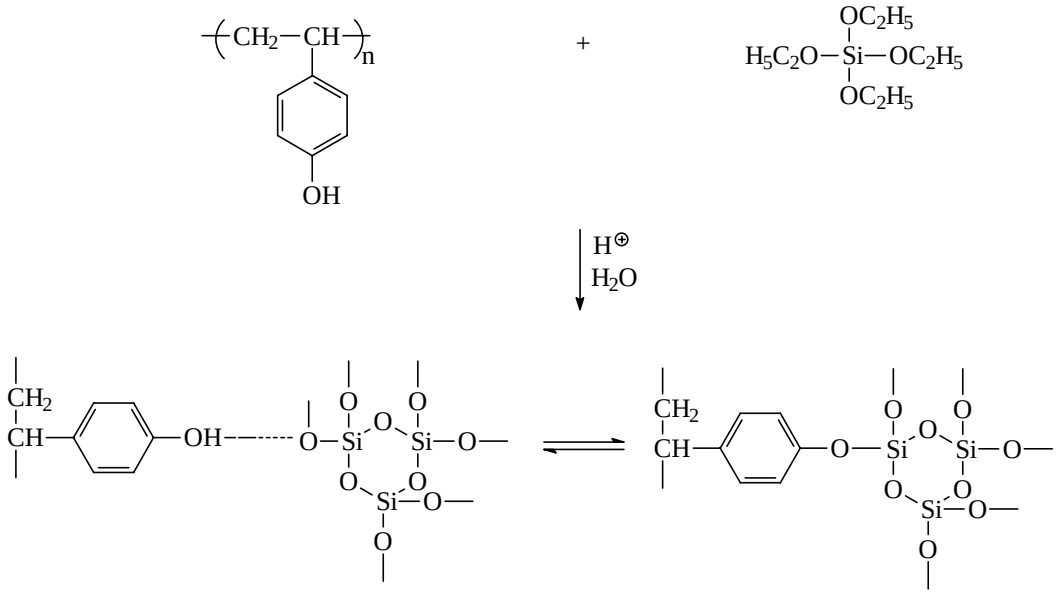

Scheme 5.3.3 Inorganic association/coupling equilibrium with polymers.[538]

Acid-base interaction was also used to synthesize polymer-silica nanocomposite. Yun *et al.* used a one-step sol-gel synthesis to hydrolyze various ratios of carboxylic endcapped poly(ethylene glycol) (PEGDA) and (3-aminopropyl)triethoxysilane (APTEOS).[544] The prepared hybrids were electrically conductive.

Obviously, the hydrogen bonding or association/coupling systems is only limited to polymers containing hydrogen bonding moieties. Moreover, instability may occur at high temperatures due to the hydrogen bonding dissociation.

Other than association-dissociation systems, organic polymers can be covalently bonded to silicate network. A widely used method to stabilize the hybrid system is to introduce some alkoxysilane moieties onto monomers or prepolymers. These reactive moieties can be readily hydrolyzed and chemically bonded to inorganic network through condensation. Compared to the approaches based on the specific interaction, this method is quite general and can be used in many different systems as long as the reactive alkoxysilane moieties can be introduced into monomers or prepolymers. Furthermore, the resulting system is more stable since organic polymer and inorganic network are covalently bonded. Many polymer-silica hybrids have been prepared by this approach. Incorporation of triethoxysilane endcapped monomer via

278, 5.

different approaches leads to different polymer-inorganic nanocomposites. Scheme 5.3.4 shows some widely used monomers for the preparation of polymer-silica nanocomposites.

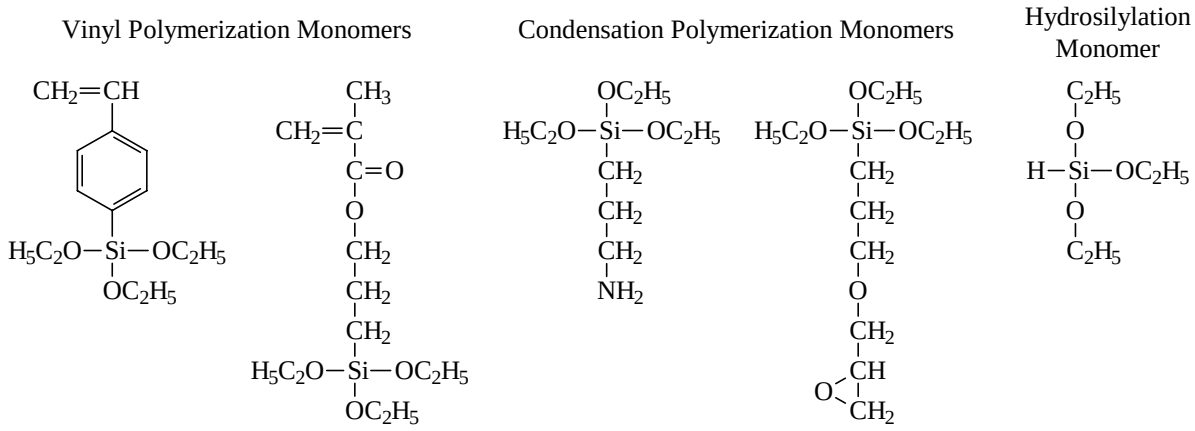


Scheme 5.3.4 Commonly used monomers for the preparation of polymer-silica nanocomposites.

These monomers can be copolymerized with other common monomers through free radical polymerization, condensation polymerization or via a post-reaction (such as hydrosilylation reaction).

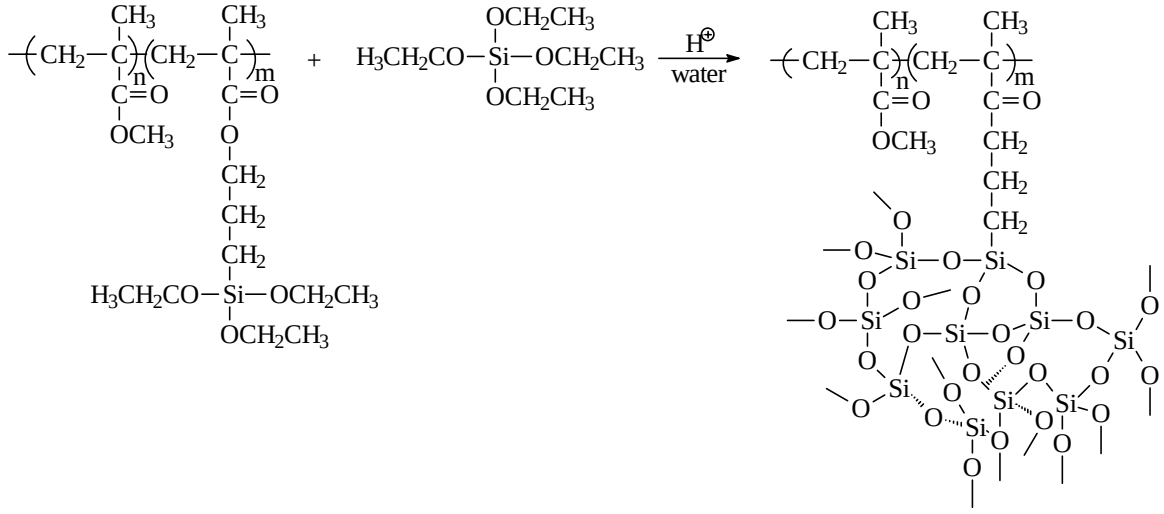


Scheme 5.3.5 Covalent IPN PMMA-silica hybrids.[545]

A polymer-inorganic hybrid material is afforded during the sol-gel process in the presence of polymer. As an example, triethoxysilane endcapped methacrylate monomer can be copolymerized with methyl methacrylate (MMA) and the resulting copolymer can be readily

[544] Yun, S. K.; Maier, J. *Chem. Mater.* **1999**, *11*, 1644.

hydrolyzed with TEOS to afford interpenetrating polymer network. Scheme 5.3.5 illustrates the formation of the IPN.[545]

Telechelic polymers are widely used to prepare polymer-silica nanocomposites. A telechelic polymer molecule contains one or more functional groups capable of reacting with some other functional groups. Once the telechelic polymer is triethoxysilane endcapped, it can simultaneously hydrolyze with the sol-gel monomers and consequently condense to afford covalent bonds between the polymer and the inorganic network during sol-gel process. Practically, polymers are made with reactive functional groups, either by copolymerizing with monomers containing triethoxysilane moietiesas endcapper via condensation polymerization or by chemically modifying the functionalized polymers with triethoxysilane funtionalized compounds. Scheme 5.5.6 shows a general structure of the telechelic polymers with triethoxysilane endgroups able to covalently bond to silica.

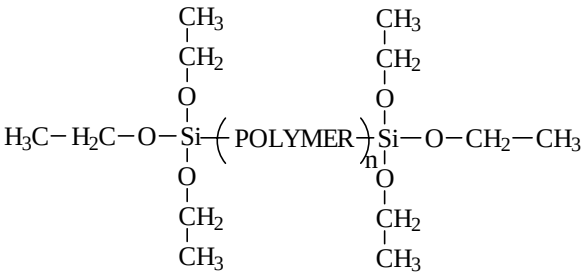


Scheme 5.3.6 A general structure of telechelic polymers with triethoxysilane endgroups.

For example, an amine-endcapped poly(ether ether ketone) was used to react with isocyanatopropyltriethoxysilane, a compound with the similar structure as 3-aminopropyltriethoxysilane, in THF. The triethoxysilane endcapped poly(ether ether ketone) was mixed with TEOS in THF. Then a definite amount of water was introduced into the system and the mixture was refluxed at 80 ºC for a half hour. The entire reaction mixture was allowed to further react in Teflon molds.[546] Tough transparent materials were obtained by this approach (Scheme 5.3.7). The sol-gel process was also used to prepare silica/poly(dimethyl siloxane) hybrid materials.[547]

[545] Sperling, L. H. *Interpenetrating Polymer Networks and Related Materilas* Plenum Press, **1981**. Chapter 1.
[546] Noell, J. L. W.; Wilkes, G. L.; Mohanty, D. K.; McGrath, J. E. *J. Appl. Polym. Sci.* **1990**, *40*, 1177.
[547] (a) Spinu, M. *Ph.D. Thesis* Virgnia Polytechnic Institute and State University: Blacksburg, VA, 1990; (b) Spinu, M.; McGrath, J. E. *J. Inorg. Organmet. Polym*. **1992**, *2*, 103.

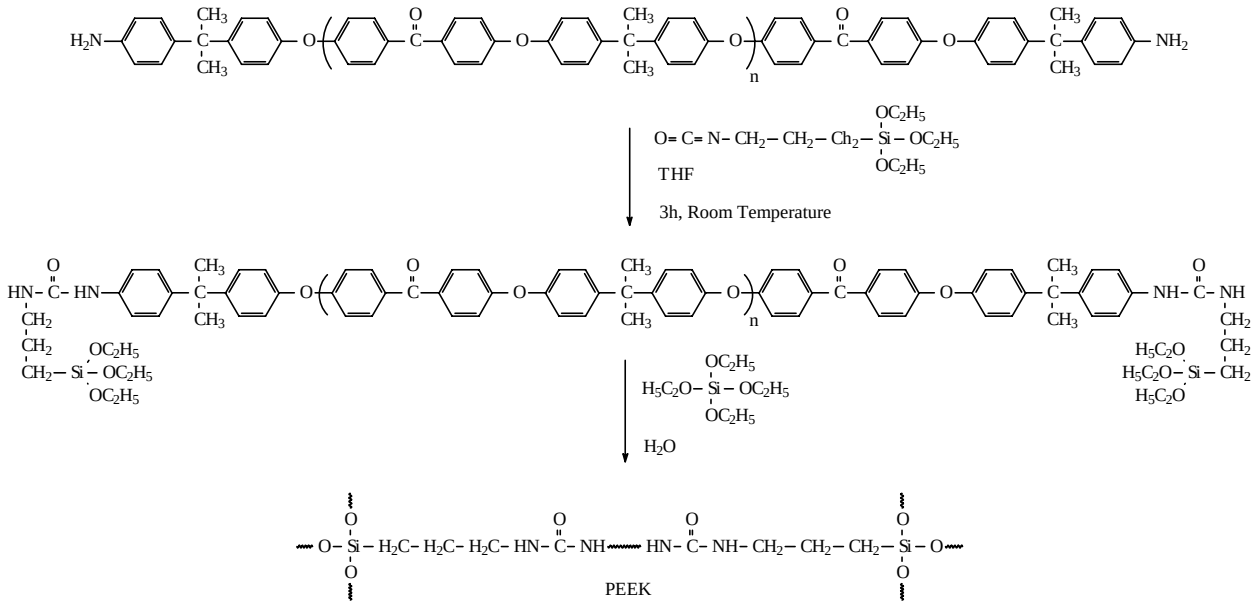


Scheme 5.3.7.The scheme for PEEK/silica hybrid films.[545]

A diamine monomer, 4-4′-oxydianiline (ODA), was used to react with pyromellitic dianhydride (PMDA) in N, N-dimethylacetamide (DMAc) in the presence of small amount of 3-aminopropyltriethoxysilane (APTES). Therefore, a triethoxysiloxane-endcapped polyamic acid was generated. Then, the polyamic acid solution was mixed with TEOS and small amount of water to afford a homogeneous solution. Finally, the solution was cast onto glass plates and dried at various temperatures. The prepared films were transparent up to 20 wt.% of silica.[548] The structure of triethoxysilane-endcapped poly(amic acid) is shown in Scheme 5.3.8.

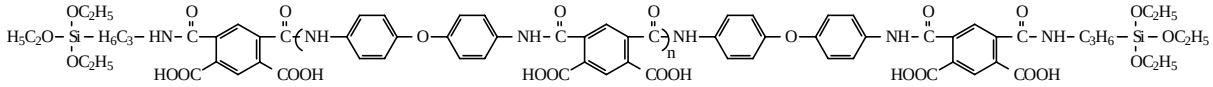

Scheme 5.3.8 Structure of triethoxysilane end-capped poly(amic acid).[548]

Although the above method provides a general approach for the preparation of polymer-silica nanocomposites with covalent bonds between organic phase and inorganic phase, macrophase separation may occur during the reaction. Also, this method is relatively complicated thus is not quite economical. In addition, processing these materials after reaction becomes unlikely due to crosslinking.

[548] Chen, Y.; Iroh, J. O. *Chem. Mater.* **1999**, *11*, 1218.

Some other special polymers were also used to prepare the polymer-silica nancomposites. Dendrimer-based xerogels have potential applications as catalyst,[549] catalyst and chromatographic supports,[550,551] and porous membranes.[552] As one example, a triethoxysilane-endcapped dendrimer was employed to prepare nanocomposites by Kriesel *et al.*[553] Scheme 5.3.9 showed their route to the dendritic xerogel.

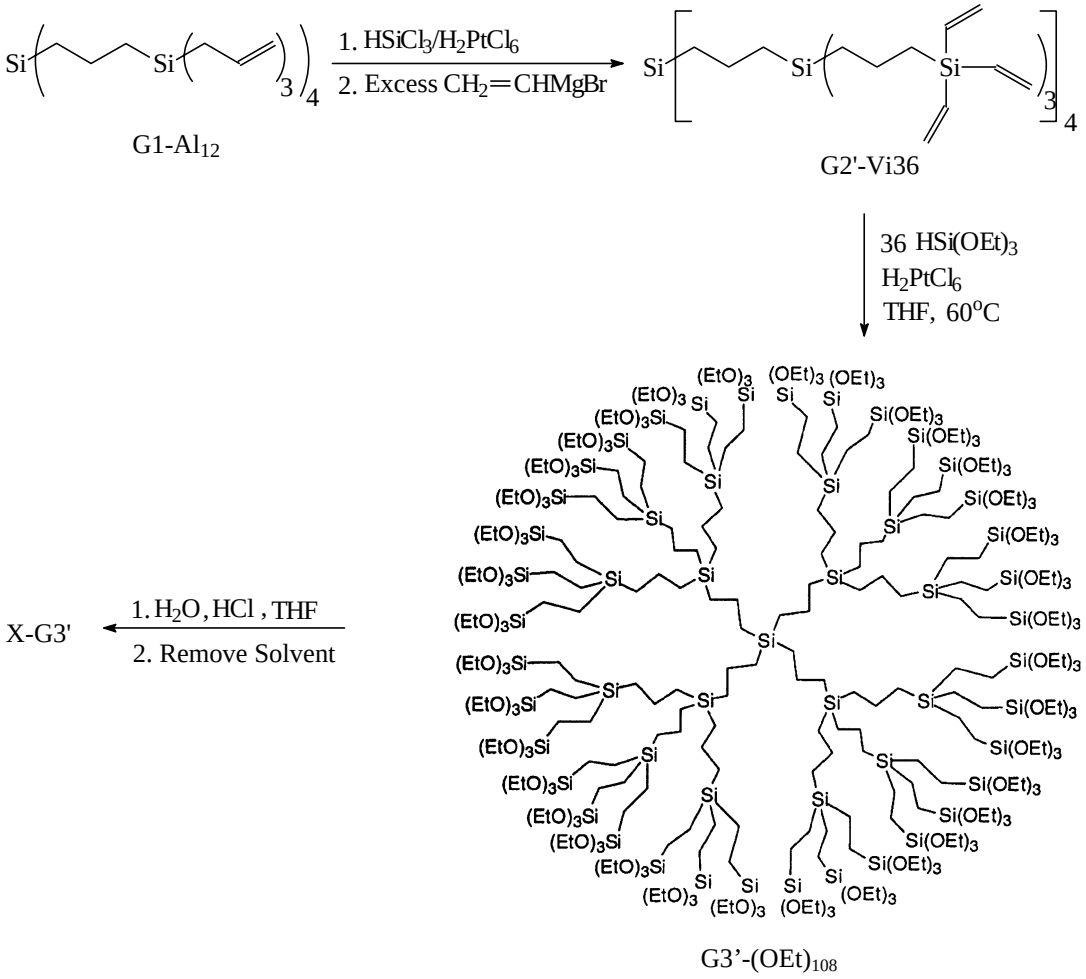


Scheme 5.3.9. Schematic approach for the preparation of xerogel.[553]

TEM images of X-G2′ and X-G3′ indicated that the dendrimers did not condense into well-ordered arrays, but are densely packed in a random network exhibiting some microporosity. In addition, the pore sizes of both gels are in the range of 7-60 Å, consistent

[549] Ko, E. I. *Chemtech.* **1993**, *23*, 31.
[550] Linder, E.; Kemmler, M.; Mayer, H. A.; Wegner, P. *J. Am. Chem. Soc.* **1994**, *116*, 348.
[551] Ramsay, J. D. F. *Pure Appl. Chem.* **1989**, *61*, 1963.
[552] Schubert, U.; Huesing, N.; Lorenz, A. *Chem. Mater*. **1995**, *7*, 2010.
[553] Kriesle, J. W.; Tilley, T. D. *Chem. Mater*. **1999**, *11*, 1190.

with the results from the nitrogen adsorption porosimetry. The produced dendrimer-based xerogels exhibit high surface areas, and an interesting relationship between generation number and surface area was observed.

#### *5.3.1.2 Polymer-Silica Nanocomposites via Solution Approach*

Polymer layered silicate (PLS) nanocomposites are hybrid organic polymer-inorganic materials with unique properties when compared with conventional filled polymers. In general these methods achieve molecular level incorporation of layered silicates into the polymer by addition of a modified silicate; during polymerization, or to a solvent swollen polymer, or to the polymer melt. Solution methods have been widely used to generate polymer-silica nanocomposites. The method was to modify the silica colloid or pellet. The basic idea for producing these nanocomposites was to render the silicate layers organophilicity by exchanging the interlayer cations with organic cation molecules and swelling the inorganic lattice of clay in the presence of a polar solvent. Then, the enlarged interlayer spacing allowed polymer molecules to enter and to intercalate silicate layers. Due to the size of the polymer molecules, the interlayer distance of the silicate can be increased to such an extent that exfoliated silicate layers in nanometer dimension might appear and be dispersed in the polymer matrix. Once the silica material was modified it can be added to polymer solution. For example, the modified silica material can be added into poly(amic acid) solution and the hybrid solution was cast onto a substrate and followed by drying at high temperatures. At high temperature the imidization reaction can be realized and a transparent polyimide-silica composite film can be obtained.

Yano *et al.* reported a method to prepare polyimide-montmorillonite composites.[554] Montmorillonite is composed of stacked silicate sheets with lower coefficient of thermal expansion (CTE) and high gas barrier property. A $Na^+$ type montmorillonite was dispersed into a solution of ammonium salt of dodecylamine in DMAc. The colloid solution was added to the solution of ammonium salt of dodecylamine to afford white precipitate. The white precipitate was then redispersed into dimethylacetamide (DMAc). Subsequently, this redispersed solution was used to mix with poly(amic acid) and the mixed solution were cast

[554] Yano, K.; Arimitsu, U.; Okada, A.; Kurauchi, T.; Kamigaito, O. *J. Polym. Sci., Part A. Polym. Chem.* **1993**, *31*, 2493.

onto glass plates. The final imidized film was transparent. In this process, the introduction of ammonium salt reduced the hydrophilicity so that the resulting montmorillonite could be dispersed into DMAc. Only 2 wt % of montmorillonite decreased the permeability coefficients of various gases to less than half of that of control ones. The incorporation of montmorillonite also significantly decreased CTE.

The ionic interaction between the poly(amic acid) and ammonium salt of dodecylamine may help to retard the phase separation between the montmorillonite and polyimide.

Since the swelling agent dodecylamine is basically nonreactive with the poly(amic acid) and remained in the polyimide-clay nanocomposites, the swelling agent would be detrimental to the thermal and mechanical properties of final products. To get around this problem, Tyan *et al.* adopted a diamine (*p*-phenylenediamine) as a swelling agent to treat montmorillonite in replacement of monoamine.[555] After one amino functional group of the swelling agent was converted into cation, the cation renders an ionic interaction with the negatively charged silicate layers, and the clay was intercalated by swelling agent. Meanwhile, the unionized amine functional group of the swelling agent can react with poly(amic acid) molecules diffused into the space between the silicate layers of the montmorillonite. Since the swelling agent becomes more permanent due to the reaction between poly(amic acid) and the swelling agent, the resulting nanocomposites were expected to have better thermal stability and mechanical properties.

#### *5.3.1.3 Polymer-Silica Nanocomposites via Melt Process*

Recent advances in this area include the melt process of the polymer-silica composites, so called direct polymer melt intercalation, which was invented by Giannelis and coworkers.[511] In this process, chemically modified layered silica was mixed with polymer. Then, the hybrid was heated above the soft temperature of polymer. Two terms are used to describe the two general classes of nano-morphology that can be prepared. The intercalated structures are where the extended polymer chains are inserted into the gallery space between the individual silicate layers. These are well ordered multilayered structures. The delaminated (or exfoliated) structures result when the individual silicate layers are well dispersed in the

[555] Tyan, H-L; Liu, Y-C; Wei, K-H. *Chem. Mater.* **1999**, *11*, 1942.

organic polymer. The interlayer spacing (20 nm-200 nm) is on the order of the radius of gyration of the polymer. The silicate layers in a delaminated structure are not as well ordered as in an intercalated structure. Figure 5.3.2 shows the structure difference of intercalated composite and delaminated composite.

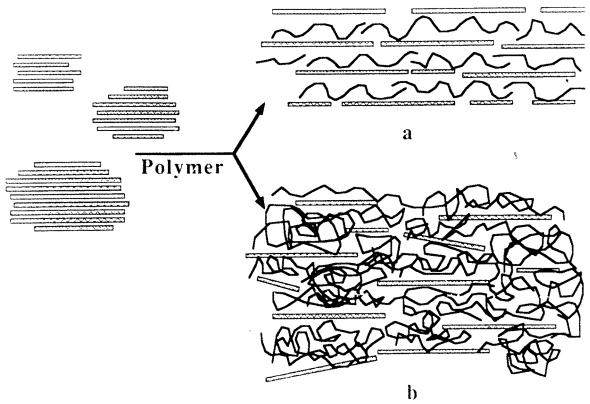


Figure 5.3.2 Schematic of composite structures obtained using layered silicates. The rectangular bars represent the silicate layers. (a) Single polymer layers intercalated in the silicate galleries (intercalated hybrids). (b) Composites obtained by delamination of the silicate particles and dispersion in a continuous polymer matrix (delaminated hybrids).[511]

This process has been used to prepare quite a few polymer-silica composites, such as PEO,[556] polystyrene,[557] polyamide, polyesters, polycarbonate, polyphosphazene,[558] polysiloxane.[559]

Intercalation of poly(ethylene oxide), PEO was accomplished by heating the mixture of polymer and montmorillonite at 80 ºC. X-ray diffraction patterns of PEO/$Na^{\oplus}$-montmorillonite hybrids before and after heating were quite different (Figure 5.3.3).[556]

After 6 h, only reflections corresponding to the PEO-intercalated silicate were observed signifying the completion of intercalation. The method afforded a d-spacing of 1.77 nm that is identical to that previously obtained for PEO intercalation from solution.[560,561,562,563] DSC showed that the PEO melting peak disappeared after 6 h and a new $T_g$ appeared, indicating

[556] Vaia, R. A.; Vasudevan, S.; Krawiec, W.; Scanlon, L. G.; Giannelis, E. P. *Adv. Mater*. **1995**, *7*, 154.
[557] Vaia, R. A.; Ishii, H.; GiannelisE. P. *Chem. Mater*. **1993**, *5*, 1694.
[558] Vaia, R. A.; Ph.D. Thesis, Cornell University, **1995**.
[559] Burnside, S.; Giannelis, E. P. *Chem. Mater*. **1995**, *7*, 1597
[560] Mehrotra, V.; Giannelis, E. P. *Solid State Commun*. **1991**, *77*, 155.
[561] Aranda, P.; Ruiz-Hitzky, *Adv. Mater*. **1990**, *2*, 545.
[562] Aranda, P.; Ruiz-Hitzky, *Chem. Mater*. **1992**, *4*, 1395.
[563] Wu, J.; Lerner, M. M. *Chem. Mater*. **1993**, *5*, 835.

intercalation (Figure 5.3.4.).

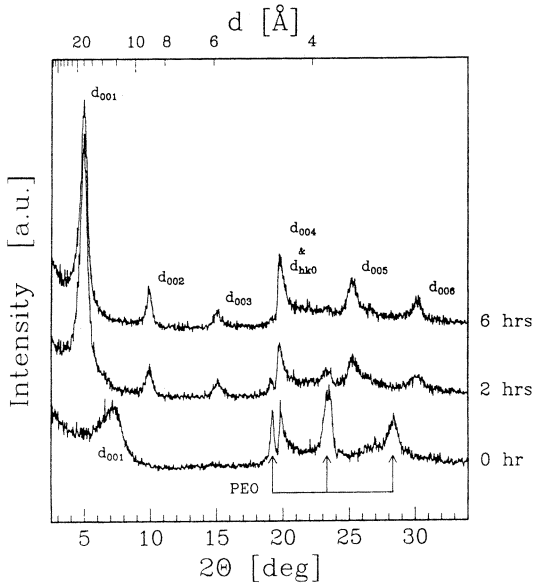


Figure 5.3.3 X-ray diffraction pattern of PEO/$Na^{\oplus}$-montmorillonite hybrid heated to 80 ºC for 0, 2, and 6 hours.[556]

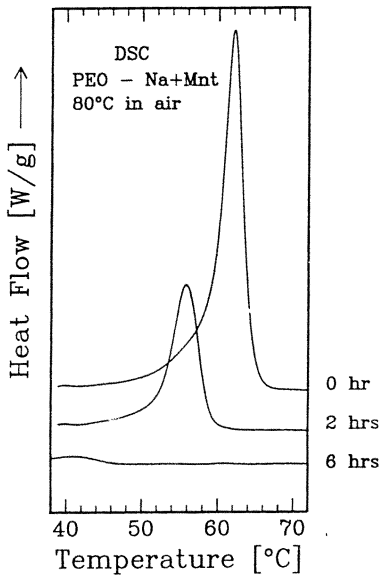


Figure 5.3.4 DSC traces for PEO/$Na^{\oplus}$-montmorillonite hybrids heated to 80 ºC for 0, 2, and 6 hours.[556]

In contrast, polystyrene (PS) cannot intercalate in pristine silicates. However, polystyrene can intercalate with an organosilicate such as dimethylditallow-exchanged montmorillonite.[557] The resulting gallery height increase of 0.7 nm corresponds to a monolayer of nearly collapsed polymer chains. DSC does not show the glass transition temperature of the PS/Montmorillonite, further suggesting the formation of intercalation.

Generally, the polymer-silica nanocomposites significantly improved the mechanical properties and fire retardance compared with the pristine polymer or immiscible polymer-silica composites.[564] Figure 5.3.6 showed the heat release rate versus time of polystyrene-clay composites. The intercalated form of the nanocomposite, at a low clay mass fraction, is homogeneous, with intercalated-PS-clay domains dispersed in pure PS. The heat releasing rate (HRR) data revealed that the intercalated nanocomposite, with a mass fraction of only 3 %, has a 45 % lower peak HRR than the immiscible PS-clay mixture. The results suggested that the intercalated nanomorphology is necessary for improved flammability.

[564] Gilman, J. W.; Kashiwagi, T.; Giannelis, E. P.; Manias, E.; Lomkin, S.; Lichtenhan, J. D.; Jones, P. *The 6th European Meeting on Fire Retardancy of Polymeric Materials* September 24-26, **1997**. Proceedings. Special Publication No. 224.

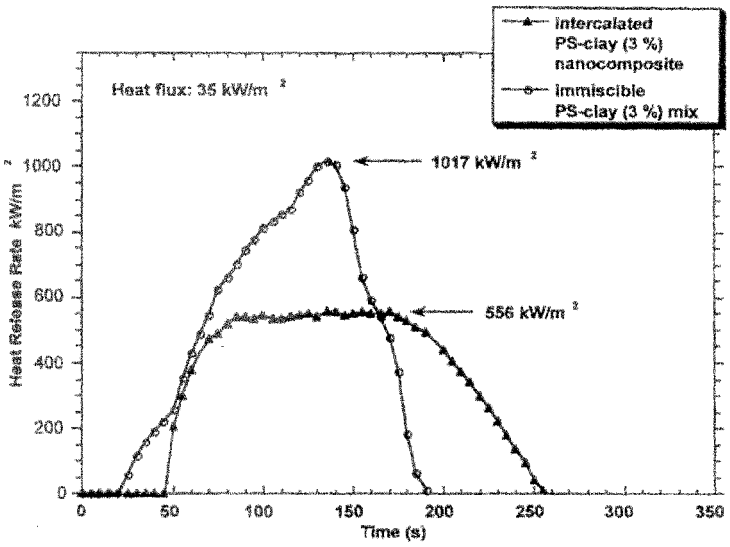


Figure 5.3.5**.** Heat release rate versus time plot for the intercalated PS-clay nanocomposite and that for the immiscible PS-clay mixture.[564]

This approach is environmentally friendly since no solvent is involved during the process. In addition, it is usually economical since very high weight percentages of montmorillonite can be used. The limitation is the complex modification of silica starting material. For different polymers, different modification methods have to be used. Processibility needs further definition.

### 5.3.2 Polymer-Titanium Oxide/Aluminium Oxide/Zirconium Oxide Nanocomposite

The polymer-metal oxide nanocomposites have some similar properties to that of polymer-silica composites. The widely used metal oxides for the preparation of polymer-metal oxide nanocomposites are titanium oxide, zirconium oxide, aluminum oxide, and some metal oxides with magnetic properties. Some of these nanocrystalline metal oxides have some potential or demonstrated applications in many technologies, including solar energy conversion, batteries, catalysis, and ductile ceramics.[500] Basically, the sol-gel approach used for the preparation of polymer-silica nanocomposites can be used for the preparation of these composites, because the hydrolysis and the dehydration mechanisms are quite similar to silica sol-gel process.

The Wilkes group has been a leader in this area. This group reported using metal alkoxides, such as titanium (IV) isopropoxide, zirconium *n*-propoxide, aluminum sec-

butoxide to react with oligomers like poly(tetramethylene oxide), polyimide, poly(ether ketone), and polysulfone end-capped with silicon alkoxide functionalities to yield polymer-metal oxide nanocomposites.[565,566,567] Scheme 5.3.10 showed the trimethoxysilane end-capped polyimide, which was used to prepare polymer-titanate composites.

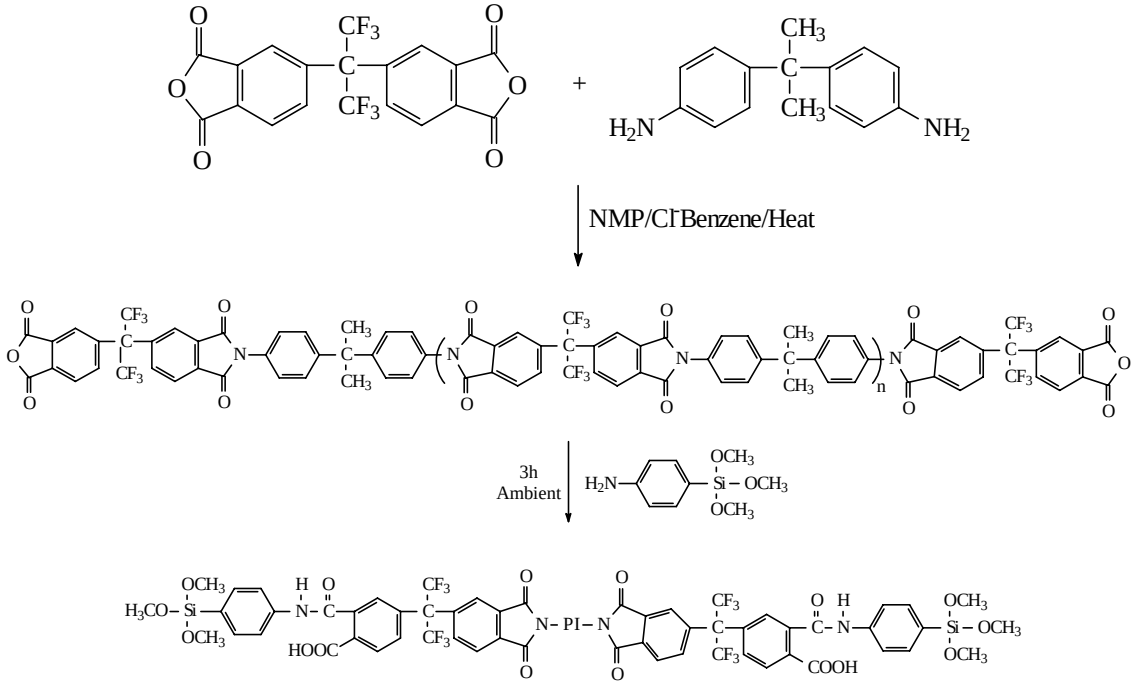


Scheme 5.3.10 Reaction scheme for end-functionalized 6-fluorobenzophenonetetracarboxylic acid dianhydride/bisaniline (6F-BTDA/bisphenol A) polyimides.[566]

PVPh was used to prepare PVPh/titanium oxide and PVPh/zirconium oxide composites.[568] However, only PVPh/titanium oxide composite films were transparent. Furthermore, PVPh was found to an effective compatibilizer in polystyrene-titania composites.

In some cases, cross reaction between different metal alkoxides can be used to yield hybrids.[543]

### 5.3.3 Polymer-Magnetic Metal Oxide Nanocomposites

Magnetic nanomaterials with a size range of 10 to 100 Å have potential applications in

[565] Huang, H.; Orler, B.; Wilkes, G. L. *Polym. Bull.* **1985**, *14*, 557.
[566] Huang, H.; Orler, B.; Wilkes, G. L. *Macromolecules* **1987**, *20*, 1322.
[567] Wang, B.; Brennan, A. B.; Huang, H.; Wilkes, G. L. *J. Macromol. Sci., Chem.* **1980**, *A27*, 1449.
[568] Landry, C. J.; Coltrain, B. K.; Teegraden, D. M.; Long, T. E.; Long, V. K. *Macromolecules* **1996**, *29*, 4712.

information storage,[569,570] color imaging,[571] bioprocessing,[572,573] magnetic refrigeration,[574] and ferrofluids.[575] Nanomaterials from molecular clusters are not very stable and difficult to process due to their tendency to aggregate to reduce the energy associated with the high surface area to volume ratios. Supporting the nanoparticles onto polymer matrix may improve the processibility and stabilize the particles.

The in situ synthesis of magnetic material, either $\gamma$-$Fe_2O_3$ or $Fe_3O_4$, while preparing the polymeric substrates, is very important for magnetic tapes. This can be realized by either thermally decomposing a metal complex contained in the polymer film or by infusing additional reactants from solution into the polymer to transform an encapsulated metal complex to its corresponding oxide.[576]

Bergmeister et al prepared polyimide-iron oxide nanocomposites. They first incorporated up to 4.2 wt % iron (III) acetate into a poly(amic acid) solution of 3,3′,4,4′-benzophenonetetracarboxylic dianhydride (BTDA) and 4,4′-oxydianiline (ODA).[576] Then, the solution was cast onto a glass plate via a doctor blade. The obtained film was gradually dried with increased temperatures. TEM showed that the small particles were evenly dispersed into the polymer film. X-ray diffraction results suggested the formation of $\gamma$-$Fe_2O_3$ in air. Thermal treatment of composites at 300 °C in dry air transformed the ion (III) salt into $\gamma$-$Fe_2O_3$. The above method may provide an alternative route to prepare magnetic tapes and disks in substitution of typical approach by coating slurry of magnetic oxide and binder onto the substrate.

Ziolo *et al.* reported the use of a commercial ion-exchange resin manufacture to prepare polymer $\gamma$-$Fe_2O_3$ nanocomposite.[577] Over 40 wt.% of $\gamma$-$Fe_2O_3$ can be obtained. Basically, Fe(II) or F(III) was exchanged onto the resin and the result resin was exposed to NaOH

[569] Gunther, L. *Phys. World* **1990**, 3, 28.
[570] Audran, R. G. L.; Huguenard, A. P. U.S. Patent **1981**, 4,302,523.
[571] Ziolo, R. F.; U.S. Patent **1984**, 4,,474,866.
[572] Nixon, L.; Koval, C. A.; Noble, R. D.; Slaff, G. S. *Chem. Mater*. **1992**, *4*, 117.
[573] Marchessault, R. H.; Ricard, S.; Rioux, P. *Carbohydrate Res*. **1992**, *224*, 133.
[574] McMichael, R. D.; Shull, R. D.; Swartzendruber, L. J.; Bennett, L. H.; Watson, R. E. *J. Magn. Magn. Mater.* **1992**, *111*, 29.
[575] Anton, I. *Et al.*, ibid. **1990**, *85*, 219.
[576] Bergmeister, J. J.; Rancourt, J. D.; Taylor, L. T. *Chem. Mater*. **1990**, *2*, 640.
[577] Ziolo, R. F.; Giannelis, E. P.; Weinstein, B. A.; O'Horo, M. P.; Ganguly, B. N.; Mehrotra, V.; Russell, M. W.; Ruffman, D. R. *Science* **1992**, *257*, 219.

aqueous solution to afford iron (II) or iron (III) hydroxide. The detailed procedure varies with different hydroxides. The procedure for Fe(II) was represented schematically as in Figure 5.3.6.

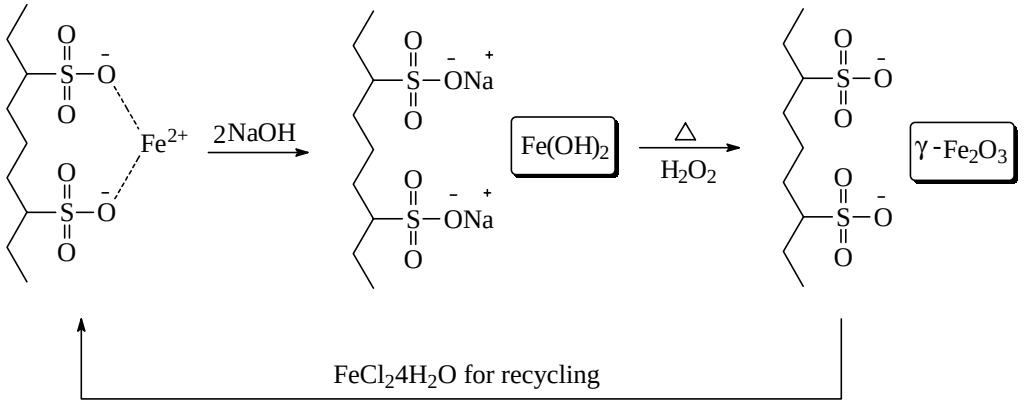


Figure 5.3.6 Schematic of the γ-$Fe_2O_3$ precipitation process using Fe(II) in an ion-exchange.[577]

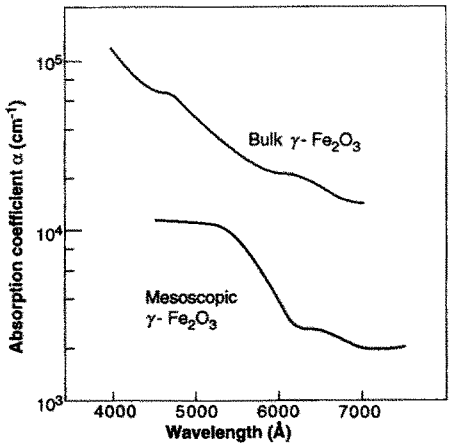


Figure 5.3.7. Room-temperature optical absorption spectra of mesoscopic and single-crystal γ-$Fe_2O_3$.[577]

The obtained materials showed a disproportionately large degree of optical transparency in the visible region than its magnetic strength would suggest when compared to other magnetic materials, especially bulk γ-$Fe_2O_3$. The mesoscopic form of γ-$Fe_2O_3$ was up to an order of magnitude more transparent to visible light than the single-crystal γ-$Fe_2O_3$ thin-film epitaxially grown on an MgO substrate, indicating a strongly reduced oscillator strength (Figure 5.3.7). Although many factors, such as high surface to volume ratio of the γ-$Fe_2O_3$ particles, cation impurities and vacancy distribution in the γ-$Fe_2O_3$, and chemical interactions with the matrix may result in this result, the authors suggested the importance of appreciable electron correlation interactions in the mesoscopic γ-$Fe_2O_3$. They argued that the reduction in

oscillator strength arises because confinement within dimensions of a few hundred angstroms can inhibit exchange coupling. Furthermore, these materials possess practical levels of magnetization at room temperature with enabled transparency in the visible region, while many magnetic materials do not possess both properties.

Verelst *et al.* described a new way to incorporate magnetic metal oxides, such as CoO, $Co_3O_4$ into the polymer.[578] An organic precursor ($Co(\eta^3\text{-}C_8H_{13})(\eta^4\text{-}C_8H_{12})$) reacts in a THF solution with dihydrogen in the presence of a polymer to yield cobalt particles. The particle size depends on the nature of matrix polymers. Use of poly(vinylpyrrolidone) (PVP) yields a small particle size of 1.6 nm while use of poly(dimethyl phenyleneoxide) (PPO) generates a relatively large size of 5 nm. The cobalt particles can be easily oxidized in air. Low temperature generates CoO while high temperature affords $Co_3O_4$.With cobalt particles of a few nanometers, air oxidation at room temperature results in a surface passivation. As a result, the particles show a composite structure with a metallic core surrounded by an oxide surface layer.

Incorporation of magnetic nanoclusters into electrically conductive polymers has arisen special interest. These materials can be used in electromagnetic interference shielding,[579]; electrochromic devices,[580] sensing and actuating technologies,[581] nonlinear optical systems,[582,583] Kryszewski, *et al.* reviewed the recent advances in this area.[584] Most of these nanocompositess are based on $\gamma\text{-}Fe_2O_3$. The incorporation of $\gamma\text{-}Fe_2O_3$ can be realized either by polymerization in the presence of iron salt followed by converting the salt into iron oxide or by dissolving the polymer and the iron salt in a common solvent followed by chemical conversion of the salt into iron oxide. As an example, sodium pyrrole-N-propylsulfonate (PyS) was polymerized in the presence of $FeCl_3$ and followed by oxidizing the polymer product.[585] Jarjayes *et al.* used an electropolymerization technique to embed “chelating

[578] Verelst, M.; Ely, T. O.; Amiens, C.; Snoeck, E.; Lecante, P.; Mosset, A.; Respaud, M.; Broto, J. M.; Chaudret, B. *Chem. Mater.* **1999**, *11*, 2702.
[579] Miyauchi, S.; Abiko, H.; Sorimashi, Y.; Tsubata, I. *J. Appl. Polym. Sci.* **1989**, *37*, 289.
[580] Shen, P. K.; Huang, H. T.; Tseung, A. C. C. *J. Electrochem. Soc.* **1992**, *139*, 1840.
[581] Gandhi, M. V.; Thomspon, B. S. In *Smart Materials and Structures*; Chapman&Hall: London, **1992**.
[582] Peng, X.; Zhang, Y.; Yang, J.; Zou, B.; Xiao, L.; Li, T. *J. Phys. Chem.* **1992**, 96, 3412.
[583] Zou, B. S.; Zhang, Y.; Xiao, L. Z.; Li, T. J. *Chin. J. Semicond.* **1991**, *12*, 145.
[584] Kryszewski, M.; Jeszka, J. K. *Synth. Met.* **1998**, *94*, 99.
[585] Nguyen, T.; Diaz, A. *Adv. Mater.* **1994**, *6*, 858.

ligand"-coated γ-$Fe_2O_3$ nanoparticles in polypyrrole (PPy).[586,587,588] Polyaniline/$Fe_3O_4$ nanocomposites were reported by Wan *et al.*[589,590] Polyaniline was dissolved in NMP and mixed with iron (II) sulfate aqueous solution at different pH value. Unfortunately, all of the composites prepared by the above methods have lower electrical conductivity values compared with corresponding anionic doped polymers.

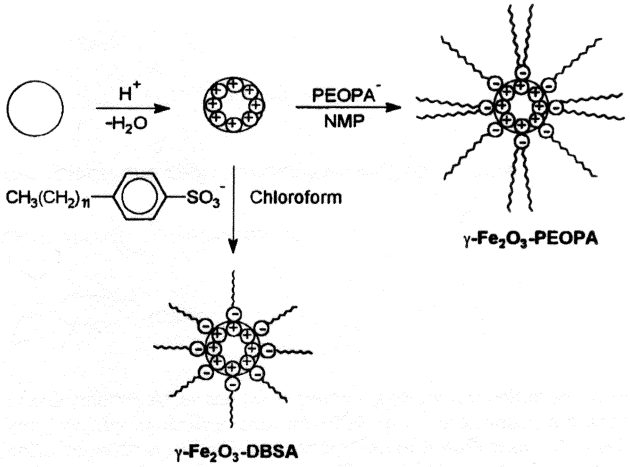


Scheme 5.3.11 Schematic of the formation of anionic surfactant coated γ-$Fe_2O_3$.[591]

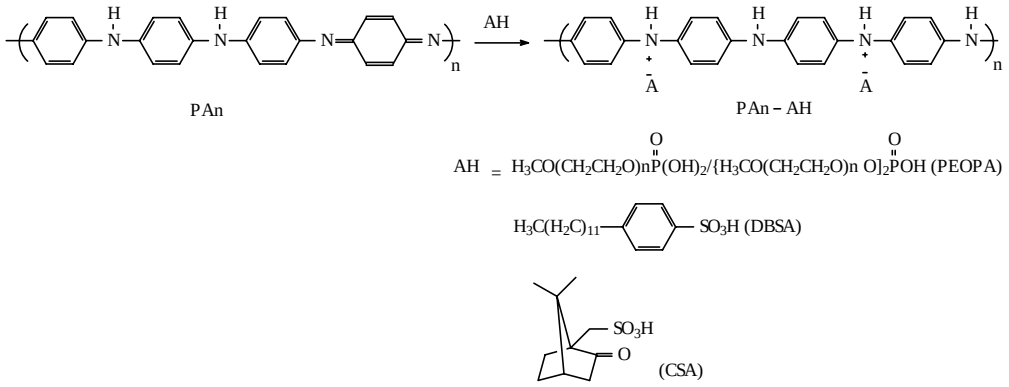


Scheme 5.3.12. Sketchs of the formation of anionic doped PAn chains.[591]

Recently, Tang, *et al.* reported polyaniline-γ-$Fe_2O_3$ composites with high electrical conductivity (σ = 82-237 S/cm) and superparamagnetic properties.[591] In this paper, γ-$Fe_2O_3$ nanopartiles were coated and PAn chains were adopted by anionic surfactants. The prepared

[586] Bidan, G.; Jarjayes, O.; Fruchart, J. M.; Hannecart, E. *Adv. Mater*. **1994**, *6*, 152.
[587] Jarjayes, O.; Auric, P. *J. Magn. Magn. Mater*. **1994**, *138*, 115.
[588] Jarjayes, O.; Fries, P. H.; Bidan, G. *Synth. Met.* **1995**, *69*, 343.
[589] Wan, M.; Li. *J. Polym. Sci. Polym. Chem.* **1997**, *35*, 2129.
[590] Wan, M.; Zhou, W.; Li, J. *Synth. Met.* **1996**, *78*, 27.

nanocomposites were processible. The formation of the anionic surfactant coated γ-$Fe_2O_3$ particles and the formation of the anionic doped PAn chains were shown in Scheme 5.3.11 and Scheme 5.3.12, respectively.

## *5.4 Polymer-Inorganic Salt Nanocomposites*

Polymer-Inorganic salt nanocomposites can be divided into two groups: polymer and salt with strong interactions; polymer and salt with weak interactions. Polymer-salt with strong interactions between the salt and polymer is the driving force for the stability, while in the polymer-salt nanocomposites with weak interactions the polymer behaves more like a matrix. In the following section, we will review the progress in this area.

### 5.4.1 Polymer-Inorganic Salt Nanocomposite Based on Strong Interactions

Some polymers contain atoms like oxygen, nitrogen, phosphorus, etc. Since they contain lone pair electrons, these atoms tend to have some strong interaction with metal ions, especially transitional metal ions. The ionic polymers can certainly have strong Coulomb interactions with metal salts and these interactions are beyond our discussion. In this part, we will focus on the systems with specific interaction between neutral polymer and inorganic salt.

The interactions between a metal ion and a neutral polymer may be covalent bonds (coordination) or polar interaction. The introduction of metal salts into polymers may significantly affect the polymer properties. A typical example is the salt-doped poly(ethylene oxide), which can be used as polyelectrolyte.[592] Eisenberg reviewed the effect of ions on the glass transition temperature.[593] Moacanin *et al.* reported that poly(propylene oxide) could form complexes with $ZnCl_2$ and $CoCl_2$.[594] Both $ZnCl_2$ and $CoCl_2$ increased in $T_g$ of the polymer with larger increase with the incorporation of $CoCl_2$ compared with $ZnCl_2$.[595] A complex model was proposed to explain the results and was shown in Scheme 5.4.1.

---

[591] Tang, B. Z.; Geng, Y.; Lam, J. W. Y.; Li, B.; Jing, X.; Wang, X.; Wang, F. *Chem. Mater.* **1999**, *11*, 1581.
[592] Gray, F. M. in "*Solid Polymer Electrolytes: Fundamentals and Technological Applications*" VCH Publishers, Inc. **1991**.
[593] Eisenberg, A. *Macromolecues* **1971**, *4*, 125.
[594] Moacanin, J.; Cuddihy, E. F., in *Transitions and Relaxations in Polymers* (*J. Polym. Sci. C*, 14), Boyer, R. F., Ed., Interscience, New York, 1966, p.313.
[595] Wetton, R. E.; James, D. B.; Whiting, W. *Polym. Lett. Ed.* **1976**, *14*, 577.

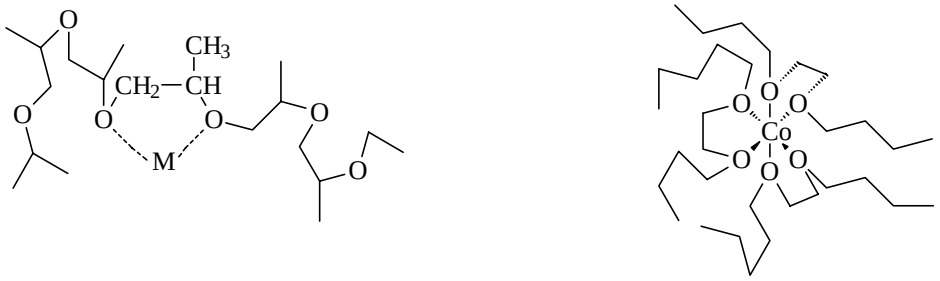


(a) (b)

Scheme 5.4.1 Structures of PPO-metal ion complexes: (a) Five-membered intramolecular chelate ring, and (b) Octahedral coordination around the cobalt center.

In $ZnCl_2$ case, five-membered chelate rings by coordination of two adjacent oxygen atoms in the polymer chain with a $ZnCl_2$. $Zn^{2+}$ favors a tetrahedral configuration involving $sp^3$ hybridization, whereas $Co^{2+}$ favors octahedral coordination with $sp^3d^2$ hybridization. Since $Co(II)Cl_2$ is more ionic than $ZnCl_2$, it is probable that free $Cl^-$ ions exist in Co(II) complexes. Hence, it is possible for Co(II) ion to coordinate up to six ether oxygen atoms. Strong intermolecular crosslinking could occur by the formation of three chelate rings from three polymer chains, involving two ether oxygens from each chain. Thus, in PPO(L)-$CoCl_2$ complexes, coordination occured intermolecular as well as intramolecular, whereas in PPO-$ZnCl_2$ complexes intramolecular coordination dominated.

Some other workers reported crystalline adducts from poly(ethylene oxide) treated with $Hg(II)Cl_2$.[596] Ciferri *et al.*[597] and Valenti *et al.*[598] investigated the effects of various metal salts on the glass transition and crystallinity of some polyamides. Later, Hannon and Wissbrun elevated the $T_g$ of the condensation polymer formed from an aromatic polyether by dissolving calcium thiocyanate in the polymer.[599] They suggested that the increase in $T_g$ was due to the salt reducing the free volume. Wissbrun and Hannon also observed increase in $T_g$ of several polymers with metal nitrates.[600] Poly(propylene oxide) and poly(ethylene oxide) have also been shown to complex with a number of metal compounds, eg., NaI,[601] $FeCl_3$.[602] A

[596] Andrews, R. D.; paper presented at the *2nd International Conference on Yield, Deformation and Fracture of Polymers*, Cambridge, March, 26-29, 1973.
[597] Ciferri, A.; Bianchi, E.; Marchese, F.; Tealdi, A. *Makromol. Chem.* **1971**, *150*, 265.
[598] Valenti, B.; Bianchi, E.; Greppi, G.; Tealdi, A.; Ciferri, A., *J. Phys. Chem.* **1973**, *77*, 389.
[599] Hannon, M. J.; Wissbrun, K. F. *J. Polym. Sci., Polym. Phys. Ed.* **1975**, *13*, 223.
[600] Wissbrun, K. F.; Hannon, M. J. *J. Poly. Sci., Polym. Phys.Ed.* **1975**, *13*,233.
[601] Forsyth, M.; Shriver, D. F.; Ratner, M. A.; DeGroot, D. C.; Kannewurf, C. R. *Macromolecules* **1993**, *5*, 1073.
[602] Rabek, J. F.; Lucki, J.; Qu, B. J.; Shi, W. F. *Macromolecules* **1991**, *24*, 836.

detrimental effect of the metal salts in polymer is that the incorporation of salts into poly(ethylene oxide) may also promote its degradation by UV-radiation.[603,604]

In recent years, some new systems were also investigated. The metal salts can both increase and decrease the $T_g$ of the polymer, depending on the kind of salt and the polymer.[605]

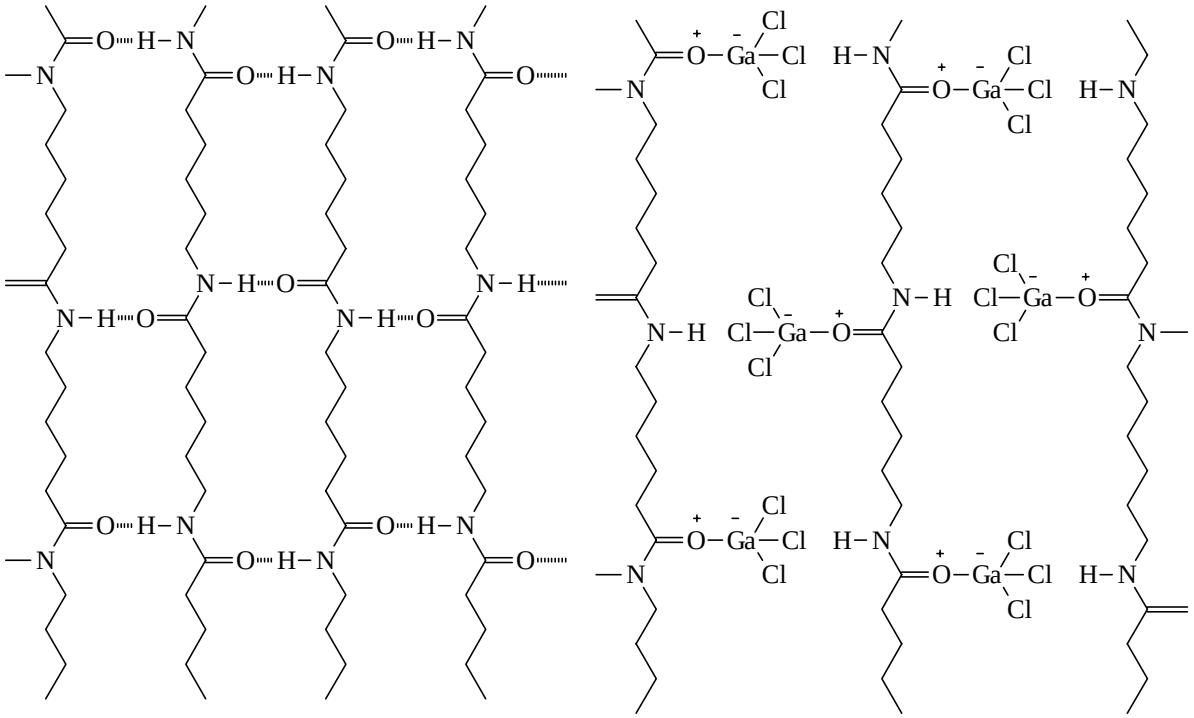

(a) (b)

Figure 5.4.1 (a) Hydrogen-bonded ("zippered") sheet structure in nylon 6 and (b) non-hydrogen-bonded ( "unzipped")structure of the nylon 6-$GaCl_3$ complex.[590]

Some strong hydrogen bonded polymers, like polyamides may undergo complex-forming reactions with strong Lewis acids such as $GaCl_3$, $BF_3$, $BCl_3$, and $AlCl_3$ on the two Lewis base sites (-NH-CO-) in the polymers. The Lewis acid-base complexation reactions of polymers can be utilized as an approach to modify polymer structure and properties, an approach to mediate solubility and solution or melt processing rigid-chain polymers, and a means to probe intermolecular and intramolecular interactions (hydrogen bonding, for example). The

[603] Kaczmarek, H.; Kaminska, A.; Linden, L. A.; Rabek, J. F. *Polymer* **1996**, *37*, 4061.
[604] Kaminska, A.; Kaczmarek, H.; Kowalonek, J. *Polymer* **1999**, *40*, 5781.
[605] (a) Bontaplat, E. *M.S. Thesis* Virginia Tech: Blacksburg, VA, **1994**; (b) Bonaplata, E.; Smith, C. D.; McGrath, J. E. in *High-Temperature Properties and Applications of Polymers* ACS Symposium Series, No 603 ; (c) Belfiore, L. A.; McCurdie, M. P.; Ueda, E. *Macromolecules* **1993**, *26*, 6908.

incorporation of $GaCl_3$ significantly decreased the glass transition temperatures of poly(p-phenylenebenzobisthiazole) (PBZT) and poly(benzimidazobenzophenanthroline)s (BBL, BBB).[606,607] The obtained complexes were rubber-like materials and readily soluble in organic solvent. $GaCl_3$ can also form complexes with polyamides.[608] The interaction of carbonyl group and $GaCl_3$ damaged hydrogen bonding. Therefore, the complexed polyimides more soluble and lower $T_g$ values compare with the pristine polymer. The N-H stretching vibration was observed to shift to high wave number, suggesting the decrement of hydrogen bonding. A proposed structure of nylon 6 before and after the formation of the complex was proposed as Figure 5.4.1.

Bonaplata et al reported that the incorporation of $CuCl_2$, $CoCl_2$, $FeCl_3$ into a phosphine oxide containing poly(arylene ether) may afford transparent films.[609] The films have higher moduli compared with polymer control. The salts may also affect the glass transition temperatures and thermal stability. NMR results suggested the strong interaction between phosphonyl group and the metal ions.

### 5.4.2 Polymer-Inorganic Salt Nanocomposites Based on Weak Interaction

Many inorganic salts can be incorporated into polymers with only weak interaction between polymer and inorganic salt. However, the main interest in this area is the incorporation of semiconductive nanoparticles due to the enhanced optical applications of these materrials.[509] The incorporation of semiconductive nanoparticles will be reviewed in this part. Early work with quantum-confined semiconductors was performed in colloid solutions,[610,611,612] which could often be stabilized with small amount of polymer.[613] The optical properties of polymer-semiconductive particle nanocomposites are directly related to the size and size distribution of the nanocrystals. If crystallite sizes are below the Bohr radius of both the holes and the electrons in the semiconductor, strong quantum confinement

[606] Jenekhe, S. A.; Johnson, P. O.; Agrawal, A. K. *Macromolecules* **1989**, *22*, 3216.
[607] Jenekhe, S. A.; Johnson, P. O. *Macromolecules* **1990**, *23*, 4419.
[608] Roberts, M. F.; Jenekhe, S. A. *Macromolecules* **1991**, *24*, 3142.
[609] Bonaplata, E.; Smith, C. D.; McGrath, J. E. in *High Temperature Properties and Applications of Polymeric Materials*, ACS Series 603: 227-237, **1995**.
[610] Berry, C. R. *Phys. Rev.* **1967**, *61*, 848.
[611] Heinglein, A. *Ber. Bunsen-Ges. Phys. Chem.* **1982**, *86*, 301.
[612] Ramsden, J. J.; Gratzel, M. *J. Chem. Soc., Faraday Trans.* **1984**, *80*, 919.
[613] Kalyanasundaram, K.; Borgarello, E.; Duonghong, D.; Gratzel, M. *Angew. Chem., Int. Ed. Engl.* **1981**, *20*, 987.

occurs.[614] Table 5.4.1 lists the maximum diameter for strong confinement for several common semiconductors.[615,616]

Table 5.4.1 Maximum Crystallite Size for Strong Confinement in Several Semiconductors[509]

| semiconductor | max diameter (nm) | semiconductor | max diameter (nm) |
|---|---|---|---|
| CdS | 0.9 | PbSe | 46 |
| PbS | 20 | GaAs | 2.8 |
| CdSe | 2 | CuCl | 0.3 |

The confinement effect appears as a shift to lower wavelengths in the absorption spectrum representing a changing bandgap. The absorption shift and spectral features can act as a measure of particle size and size distribution. Control of these parameters is extremely important in the enhancement of $\chi_3$ effects.

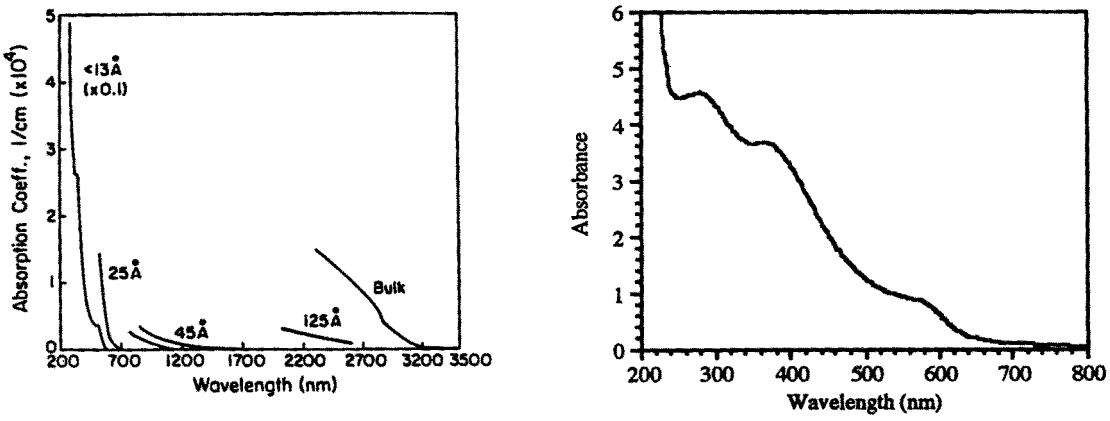


(a) (b)

Figure 5.4.2 (a) Absorbance spectra shifts as a function of particle size. (b) Absorbance spectrum with exciton features from PbS in PVA.[509]

As is well known, the optical properties are directly related to the size and size distribution of the nanocrystals that can be extracted form the optical absorption spectrum. The shift in absorption is illustrated in Figure 5.4.2a, which shows a blue-shift with decreasing PbS nanocrystals above 25 Å are featureless, but those below 13 Å show some

[614] Banyai, L.; Hu, Y. Z.; Lindberg, M.; Koch, S. W. *Phys. Rev. B.* **1988**, *38*, 8142.
[615] Ozin, G. A.; Kirkby, S.; Meszaros, M.; Ozkar, S.; Stein, A.; Stucky, G. D. *Materials for Nonlinear Optics*; Marder, S. R.; Sohn, J. E.; Stucky, G. D. Eds. American Chemical Society: Washington, D.C., **1991**; Vol. 455, p 554.
[616] PbS, PbSe, and CdSe values caculated by Inuk Kang.

structure indicating a narrow size distribution in the sample.[617] The bandgap of the smallest particles exhibits a remarkable shift from the bulk value of 0.41 eV to 2.3 eV. Figure 5.4.2b displayed an absorption spectrum with strong exciton feature of PbS in poly(vinyl alcohol) made by Ober *et al.*[509] following a modified procedure of Nenadovic *et al.*[618] A narrow particle size distribution could be inferred by the strong exciton features. The magnitude of the bandgap shift has been correlated with particle sizes of 4 nm, although the shift is at a slightly lower wavelength than that shown for 4.5 nm particles in Figure 5.4.2a.

At the very beginning, quantum-confined semiconductors were performed in colloid solutions.[619,620,621] Addition of small amount of polymer may help to stabilize the colloid solution.[622] The first group to formally recognize semiconductor polymer composites such as those in terms of engineered optical media was Akimov *et al.* in 1992.[623] In this work, CdS nanocrystals from 2 to 50 nm in size were prepared in poly(vinyl alcohol), poly(vinylpyridine), and photographic gelatin. Remarkably high CdS concentrations, up to 50 wt%, could be prepared without agglomeration. The composites exhibited good photosensitivity and photoconductivity. Particular applications of interest to the authors included dispersive optical elements, bandpass and cutoff filters, and electrophotographic and photothermoplastic materials.

Earlier the work in this area was focused on the catalytic properties rather than optical properties.[624] Krishnan *et al.* invented in situ synthesis methods for the preparation of these nanomaterials.[625] In their approach, $Cd^{2+}$ ion was exchanged onto a Nafion matrix (perfluoroethylenesulfonic acid ion-exchange polymer) and submicro-particles were generated by exposing the resulting material to $H_2S$. A similar method was employed to create 20 nm size particles which were used for photocatalytical hydrogen generation in the

[617] Wang, Y.; Suna, A.; Mahler, W.; Kasowski, R. *J. Chem. Phys.* **1987**, *87*, 7315.
[618] Nenadovic, M. T.; Comor, M. I.; Vasic, V.; Micic, O. I. *J. Phys. Chem.* **1990**, *94*, 6390.
[619] Berry, C. R. *Phys. Rev.* **1967**, *161*, 848.
[620] Heinglein, A. *Ber.Bunsen-Ges. Phys. Chem.* **1982**, *86*, 301.
[621] Ramsden, J. J.; Gratzel, M. *J. Chem. Soc., Faraday Trans.* **1984**, *80*, 919.
[622] Kalyanasundaram, K.; Borgarello, E.; Duonghong, D.; Gratzel, M. *Angew. Chem., Int. Ed. Engl.* **1981**, *20*, 987.
[623] Akimov, I. A.; Denisyuk, I. Yu.; Meshkov, A. M. *Opt. Spectros.* **1992**, *72*, 558.
[624] Meissner, D.; Memming, R.; Kastening, B. *Chem. Phys. Lett.* **1983**, *96*, 34.
[625] Krishnan, M.; White, J. R.; Fox, M. A.; Bard, A. J. *J. Am. Chem. Soc.* **1983**, *105*, 7002.

presence of platinum catalyst.[626]

The general approach employed to prepare polymer-semiconductor composites in situ is shown in Scheme 5.4.2.[509] In a typical experiment, the matrix material and metal ions are mixed in solution followed by exposing to the counterion ($S^{2-}$, $Se^{2-}$) in the form of gas or as ions dissolved in solution. The composite may be cast as a film before or after exposure to the counterion.

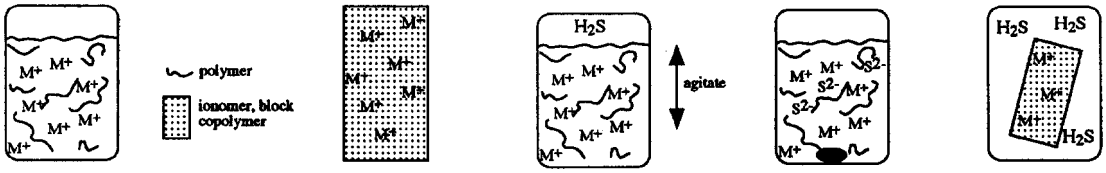


1. Mix matrix with metal ion ($M^+$) 2. Expose to counterion ($S^{2-}$)

Scheme 5.4.2 Schematic of in situ polymer synthesis methods

Apparently, control of particle size is critical for the application, since the properties are dependent on the size of the particles. The particle size affects the magnitude of the shift in absorption (change in bandgap), while the distribution affects the strength of the quantum effect at a given wavelength.

The methods for the control of particle size and its distribution can be roughly divided into chemical and physical approaches. Chemical approaches include control of chemical reaction, architecture, self-assembly, ex situ among others. Physical approaches include heat treatment. In some situations, the physical and chemical approach can be used in combination.

The architecture of the polymer matrix can be used to control of these parameters. Since block copolymers and polymer blends may undergo microphase separation, these structures may help disperse the semiconductor clusters as they form. Under some circumstances the controlled phase separation may result in superlattice structures. Most work in the area of superlattices have been with colloid solids,[627,628] however, similar structures may be possible with composites.

---

[626] Mau, A. W.; Huang, C.; Kakuta, N.; Bard, A. J.; Campion, A.; Fox, M. A.; White, J. M.; Webber, S. E. *J. Am. Chem. Soc.* **1984**, *106*, 6537.
[627] Weller, H. *Angew. Chem., Int. Ed. Engl.* **1996**, *35*, 1079.
[628] Murray, C. B.; Kagan, C. R.; Bawendi, M. G. *Science* **1995**, *270*, 1335.

A copolymer with a composition of 85% ethylene and 15% methacrylic acid units was employed to synthesize PbS-containing composites.[629] The particle sizes could be altered by changing the concentration of $Pb^{2+}$ in the films and by subsequent heat treatments. Bandgap and absorption measurements were made over a range of crystallite size, and theoretical models were used to explain the trends of the data. Use of poly(vinyl alcohol) as a stabilizer and matrix materials for PbS has consistently shown shifted and featured absorption spectra. These results were illustrated by the absorption and fluorescence properties. Similar results were also obtained by the study of the effects of surface properties on the bleaching of PbS.

Cohen et al have done extensive work with block copolymers synthesized via ring-opening metathesis polymerization (ROMP) technique. Good stabilization of the semiconductor was achieved due to the microphase separation. STEM studies showed that small particles of PbS,[630] CdS, and ZnS[631] could be achieved by using spherical phase separation of the metal-containing phase.

Similar block copolymers with lamellar and spherical morphologies were utilized to prepare ZnS and Zn-containing composites. Figure 5.4.3 showed that the lamellar and spherical morphologies effectively isolated the ZnS particles in a controlled manner.[632] X-ray and X-ray photoelectron spectroscopy were also used to characterize these materials.

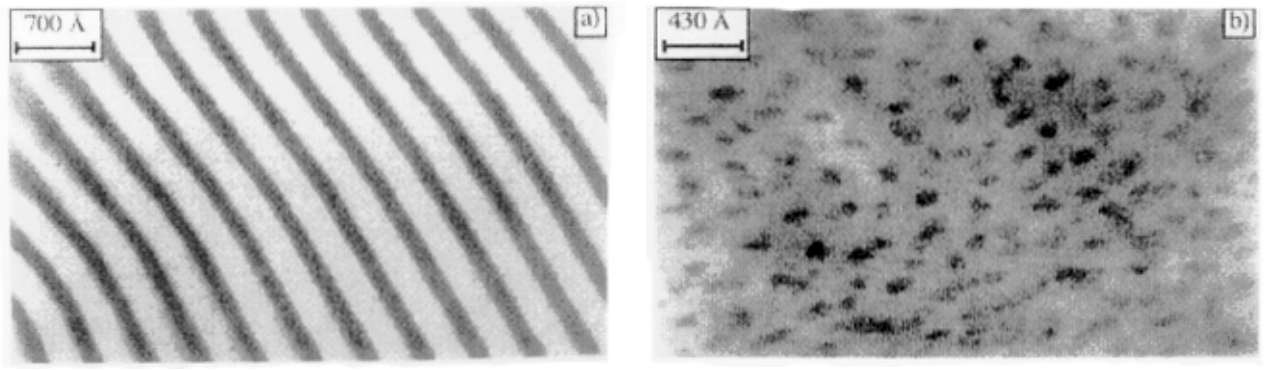


Figure 5.4.3 TEM micrographs of ZnS in a block copolymer. (a) Lamellar morphology, (b) spherical morphology.[632]

[629] Mahler, W. *Inorganic Chem.* **1988**, *27*, 435.
[630] Sankaran, V.; Cummins, C. C.; Schrock, R. R.; Cohen, R. E.; Silbey, R. J. *J. Am. Chem. Soc.* **1990**, *112*, 6858.
[631] Cummins, C. C.; Schrock, R. R.; Cohen, R. E. *Chem. Mater.* **1992**, *4*, 27.
[632] Sankaran, V.; Yue, J.; Cohen, R. E.; Schrock, R. R.; Silbey, R. J. *Chem. Mater.* **1993,**, *5*, 1133.

Polystyrene-block-poly(vinylpyridine) with spherical morphology was used by Möller to investigated the growth of nanocrystals of many semiconductors, including CuS, CdS, and PbS.[633] The shift of the absorption spectra suggested small particle size. However, the featureless absorbance spectra indicated polydispersed particles. Wang *et al.* employed a hydroxylated polystyrene-b-polybutadiene-b-polystyrene (HO-SBS) to prepare CdS with controlled size.[634]

Utilizing polymer blends as matrix materials is an alternative approach to prepare the polymer/semiconductor composites. Yuan *et al.* reported the preparation of quantum confined CdS in poly(styrene phosphonate diethyl ester) (PSP) and cellulose acetate (CA) polymer blends and structured absorption spectra were observed.[635,636] The phosphonate ester may act as ligand to chelate metal ions. Therefore, the ions are isolated before being converted into CdS. The particle sizes were measured by absorbance edge position of fluorescence spectra and composites with particle sizes of 44 Å, 58 Å, and 82 Å were made by varying the ratio of PSP:CA.

Self-assembly of polymer thin films may provide a new approach for the control of particles. Xiong *et al.* reported that CdS nanoparticles were successfully sandwiched into poly(sodium styrene sulfonate) and poly(vinyl pyridine) multiple layer film.[637] $Cd^{2+}$ was exchanged onto poly(sodium styrene sulfone) cast onto a clean $CaF_2$ slide or silicone wafer. Then the same substrate was immersed into poly(vinyl pyridine). An alternating $PSS(Cd)_{12}$/PVP multilayered film was obtained by repeating the above process. The authors claimed that this method was also used to prepare polymer/$Cu_2S$ and polymer/PbS nanocomposites. However, they did not report the size of the particles.

One method used to get better controlled nanocomposites is the ex situ capping. Typical capping agents are thios or mercaptans since they can compete with sulfur or other counterions for $Pb^{2+}$ or $Cd^{2+}$ surfaces. The particle size is dependent on the molar ratio of the capping agent to sulfur. In addition, the capping agents may help the dispersion of particles

[633] Möller, M. Synth. Met. 1991, 41, 1159.

into various matrix materials because they act as surface treatment for the particles. Scheme 5.4.3 displayed the formation of the capped particles schematically.[491] Typically, the sulfide (or other counterions) and capping agent ($RS^-$) ions are mixed in solution. Then, the metal ion solution is added to the that solution. The semiconductor particles are readily generated with controlled size by varying $S^{2-}/Rs^-$ ratio.

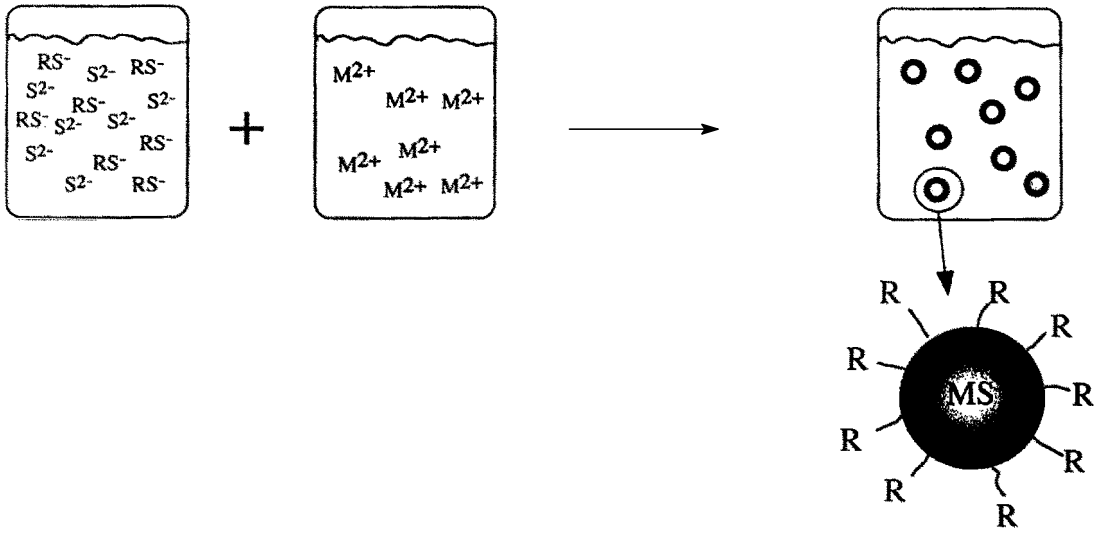


Scheme 5.4.3 Schematic of ex situ capped semiconductor (MS) synthesis. RS- is the capping agent, $S^{2-}$ is the sulfur, and $M^{2+}$ is the metal ion.[509]

The DuPont investigators synthesized CdS particles capped with thiophenol. X-ray diffraction and absorbance measurements showed the particle sizes could be tuned by varying the ratio of capping agent to sulfur ions.[638,639] The nonlinearity of these clusters was measured by third harmonic generation ($\chi_3$). The $\chi_3$ significantly increased with increasing particle size from 7 Å to 30 Å. The particles were further characterized by capped precursor synthesis[640] and inelastic neutron-scattering studies.[641] However, introducing surfacant may change the nanoparticle properties.

---

[634] Wang, D.; Cao, Y.; Zhang, X.; Liu, Z.; Qian, X.; Ai, X.; Liu, F.; Wang, D.; Bai, Y.; Li, T.; Tang, X. *Chem. Mater.* **1999**, *11*, 392.
[635] Yuan, Y.; Cabasso, I.; Fendler, J. *Macromolecules* **1990**, *23*, 3198.
[636] Yuan, Y.; Fendler, J.; Cabasso, I. *Chem. Mater.* **1992**, *4*, 312.
[637] Xiong, H.; Zhou, Z.; Wang, Z. Q.; Zhang, X.; Shen, J. *Supramol. Sci.* **1998**, *5*, 623.
[638] Wang, Y.; Herron, N.; Mahler, W.; Suna, A. *J. Opt. Soc. Am. B*. **1989**, *6*, 808.
[639] Herron, N.; Wang, Y.; Eckert, H. *J. Am. Chem. Soc*. **1990**, *112*, 1322.
[640] Herron, N.; Suna, A.; Wang, Y. *J. Chem. Soc., Dalton Trans*. **1992**, 2329.
[641] Markichev, I.; Sheka, E.; Natkaniec, I.; Muzychka, A.; Khavryutchenko, V.; Wang, Y.; Herron, N. *Physicas B* **1994**, *198*, 197.

Heat treatments and additives have been coupled with composites synthesis strategies to control particle size and distribution. Wang et al reported control of PbS particle size was reported by varying the concentration of the $Pb^{2+}$ and heat treatment of the samples.[642] Heat treatment was also applied to control the particle size of CdS in Nafion.[643] Sankaran *et al.* found that ZnS cluster size was increased when the block copolymer films were exposed to $H_2S$ at higher temperatures or in the presence of solvent vapor.[632] Nevertheless, annealing after ZnS formation did not increase the particle size probably because the matrix acted as diffusion barrier.

Kyprianidou-Leodidou *et al.* varied the size of PbS in poly(ethylene oxide) from 4 to 80 nm using acid and surfactant additives.[644] As a control, the system without additive gave a particle size of about 29 nm. Acetic acid increased the particle sizes, while sodium dodecyl sulfate, a surfactant, decreases the particle sizes. Although the control of average particle size was demonstrated, the size distributions were pretty large.

In addition to the particle size and its distribution, the surface and the inner structure of the particles play equally importance in determining the final properties of the nanocomposites. The quantum yield of emission is usually reduced by surface defects and the concommitant surface-related nonradiative recombination. By passivating the semiconductor nanoclusters the contribution from the surface defects can be avoided.[645]

Introducing an impurity to a quantum dot affords doped nanocrystalline materials, in which increasing the quantum yield of emission was observed by Bhargava *et al.*[646] Mn-doped and Tb-doped ZnS nanoclusters with controllable size and narrow size distribution within the microphase –separated films were also prepared by Kane *et al.*[647] The doped ZnS nanoclusters were formed by subsequently treating the ion-loaded films with $H_2S$. The doped nanocomposites are optically active and show emission characteristic of the impurity ions.

Although most work focuses on salts based on $S^{2-}$, $Se^{2-}$, $As^{-3}$, some other salts have also

[642] Wang, Y.; Suna, A.; Mahler, W.; Kasowski, R. *J. Chem. Phys.* **1987**, *87*, 7315.
[643] Wang, Y.; Suna, A.; McHugh, J.; Hillinski, E. F.; Lucas, P. A.; Johnson, R. D. *J. Chem. Phys.* **1990**, *92*, 6927.
[644] Kyprianidou-Leodidou, T.; Caseri, W.; Suter, U. *J. Phys. Chem.* **1994**, *98*, 8992.
[645] Murray, C. B.; Norris, D. J.; Bawendi, M. G. *J. Am. Chem. Soc.* **1993**, *115*, 8706.
[646] Bhargava, R. N.; Gallagher, D.; Hong, X.; Nurmikko, A. *Phys. Rev. Lett.* **1994**, *72*, 416.
[647] Kane, R. S.; Cohen, R. E.; Silbey, R. *Chem. Mater.* **1999**, *11*, 90.

been of interest. Among those is barium titanate ($BaTiO_3$). $BaTiO_3$ is useful for the manufacture of multiplayer ceramic capacitors and electrooptic components. The conventional methods to prepare $BaTiO_3$/polymer composites were used to entail mixing micrometer-scale $BaTiO_3$ powders with either a polymer-solvent solution[648] or a polymer melt.[649]. These methods are generally limited by powder coagulation and are not amenable to processing thin films. An alternative approach involves the use of chemical-solution methods in which crystalline $BaTiO_3$ is precipitated from the reaction of a titanium alkoxide and $Ba(OH)_2$. Precursors to $BaTiO_3$/polymer composites may be processed by mixing a titanium alkoxide and a polymer in a common solvent. The low viscosity of the precursor solution facilitates thin film deposition methods including spin casting, dipping, or spray casting. After solvent removal, the titanium alkoxide is converted to $BaTiO_3$ by reacting the films below 100ºC in aqueous alkaline solutions containing barium.[650] This approach does not guarantee a homogeneous dispersion of $BaTiO_3$ particles, and a segregated composite microstructure will develop if the titanium alkoxide and polymer, although soluble in a common solvent, are immiscible in one another.[651,652,653]

A new approach, by covalently bonding a metal alkoxide or exchanging $TiO^{2+}$ onto the polymer matrix has been used to form monolithic materials in order to minimize the immiscibility. Collins *et al.* prepared $BaTiO_3$/polymer thin films using the following methods.[654] Titanium diisopropoxide bis(ethylacetoacetate) (TIBE) was dissolved in toluene with poly(styrene-co-maleic anhydride), (S-MAH) copolymer. The spin cast films were dried and followed by immersing into aqueous solutions of 1.0 M $Ba(OH)_2$ at 80 ºC for 1 h. The dried $BaTiO_3$/S-MAH film consisted of a uniform dispersion of $BaTiO_3$ nanoparticles throughout the S-MAH matrix. Powder X-ray diffraction indicated that the particles were crystalline. Electron diffraction suggested the particles were nanocrystalline $BaTiO_3$. The improved dispersion of $BaTiO_3$ could be explained with bonding between the TIBE and

[648] Gregorio, R., Jr.; Cestari, M.; Bernardino, F. E. *J. Mater. Sci.* **1996**, *31*, 2925.
[649] Aulagner, E.; Guillet, J.; Setyre, G.; Hantouche, C.; Le Gonidec, P.; Terzulli, G. *IEEE 5th International Conference on Conduction and Breakdown in Solid Dielectrics* **1995**, *423*.
[650] Collins, D. E.; Slamovich, E. B. *Mater. Res. Symp. Proc.*; Komarneni, S.; Parker, J., Wollenberger, H., Eds. 1997, 457, 445.
[651] Embs, F. W.; Thomas, E. L.; Wung, C. J.; Prasad, P. N. *Polymer* **1993**, *34*, 4607.
[652] Burdon, J. W.; Calvert, P. *Mater. Res. Soc. Symp. Alper, M., Ed.* **1991**, *218*, 203.
[653] Collins, D. E.; Slamovich, E. B. Submitted to the *J. Mater. Res.*

maleic anhydride (MAH) groups in S-MAH. FTIR spectra of TIBES-MAH precursor showed the cyclic anhydride carbonyl peaks (1855 and 1780 $cm^{-1}$). After gel formation, a new peak at 1730 $cm^{-1}$ appears. The initial stages of the reaction involves a nucleophilic attack on TIBE from a carboxylate ion ($-COO^-$) of MAH. The subsequent decomposition of the anhydride structure forms Ti-OOC- and $–COO^-$, a possible origin of 1730 $cm^{-1}$ band.

Oledzka *et al.* reported that a styrene and divinyl benzene based chelating cation-exchange resin was used to prepare a Ti-loaded polymer by exchanging $TiOSO_4$ solution.[655] The Ti-loaded polymer beads were subjected to aqueous $Ba(OH)_2$ solutions at temperatures from 65 to 200 ºC under hydrothermal conditions. Nucleation of spindlelike $BaTiO_3$ particles was observed on the polymer surface after reactions lasting 5 h. Compared to the solution route, hydrothermal synthesis takes place in a more benign experimental environment with low cost.

## *5.5 Characterization of Nanocomposites*

Characterization of the nanocomposites is dependent on the types of nanomaterials and their final applications. Some basic aspects of the characterization will be discussed in this paragraph. The particle size and particle size distribution of the nanoparticles determine the properties of composites and the widely used method is to measure their absorbance spectra. Only very small particles with narrow particle distribution show feature spectra. Small angle X-ray scattering may also be used to determine the size of the particle in some systems, like polymer/silica or other metal oxide prepared by sol-gel process. X-ray diffraction places equally importance for the determination of crystal type, because only some type of crystals can be used for the applications, especially for optical, electrical, and magnetic applications. Morphology is also very important for the determination of the nanocomposites properties. X-ray diffraction and electron diffraction can be used to determine whether the particles are crystalline or amorphous. Some times SEM and TEM can be used to observe the particle size. However, if the particle size is too small, this information may not be available. Nevertheless, TEM can provide supramolecular information on complicated systems. This has been successfully used to observe the micrographs of ZnS in a block copolymer and the

[654] Collins, D. E.; Slamovich, E. B. *Chem. Mater*. **1999**, *11*, 2319.

micrographs of a polyisoprene-*b*-polyethylene oxide/silica-alumina nanocomposite system.[525]

Some other characterizations of the nanocomposites have also been performed. These include thermal transition behavior, fire retardance, gas permeability, abrasion, tensile modulus, electrical and thermal conductivity, photoconductivity, and nonlinear optical properties, among others. The measurements of these composites are dependent on the type of materials and their applications.

Although many researchers are very interested in the enhanced nonlinear optical properties of quantum confined semiconductors, very few have been reported. Wang et al did the pioneering work measuring the degenerate four-wave mixing (DFWM) of CdS/Nafion composites.[656] In their work, they reported that in DFWM experiments an absorption saturation phenomenon was observed, confirming the interesting nonlinear optical properties of these composites. Later on, crystals in a range of sizes up to 40 Å were synthesized and passivated with ammonia. A higher $\chi_3$ nonlinearity was observed in the surface passivated samples. Nonlinear optical measurements were also made on CdS grown in a swollen, crosslinked, copolymer matrix.

## *5.6 Applications*

The nanocomposites have tremendous present and potential applications, depending on the type of nanomaterials. In addition to their improved thermal and mechanical properties, electrical, magnetic, and optical applications are also important.

Although a lot of new materials have been developed, studies on devices based on these materials are still relatively few. Colvin *et al.* prepared light-emitting diodes using p-phenylenevinylene/CdSe composite.[657] The composites have threshold voltage of 4V, which is lower than that for PPV alone. The low voltage can lead to luminescence in the range of red to yellow, depending on particle size. Meanwhile, larger voltages resulted the PPV to luminescence in the green. Figure 5.6.1 shows electroluminescence from a CdSe/PPV composite. The voltage-tunable light source could be utilized to display technology in which the color of a pixel could be tuned by tuning the applied voltage.

---

[655] Oledzka, M.; Brese, N. E.; Riman, R. E. *Chem. Mater.* **1999**, *11*, 1931.
[656] Wang, Y.; Mahler, W. *Opt. Commun.* **1987**, *61*, 233.

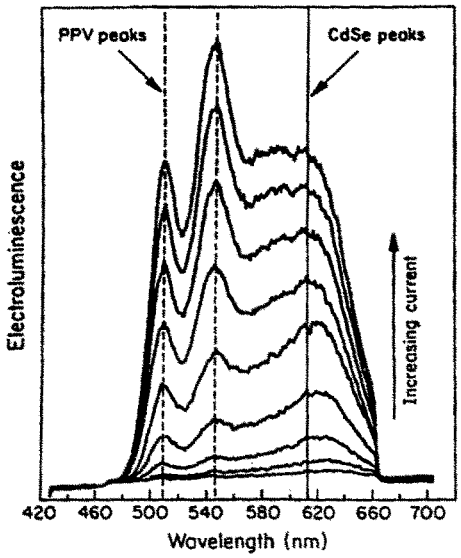


Figure 5.6.1 Electroluminescence from a CdSe/PPV composite.[657]

Dabbousi *et al.* observed electroluminescence from a homogeneous composite of 5-10% CdSe in poly(vinylcarbazole) and an oxadiazole derivative.[658] The tune-on voltage was at 13 V and the emission was observed from 530 to 650 nm with three particle sizes. Seemly, the light emission was dependent on the applied voltage and the light covers from red to whit with increased voltage.

Ziolo *et al.* reported the optically transparent magnetic composites.[577] The absorption coefficient was nearly an order of magnitude less than the bulk crystal.

Higher refractive index polymers have many present and potential applications ranging from antireflection coatings for solar cells to high refractive index lenses. Semiconductor polymer composites can exhibit high refractive indices due to the high RI of the semiconductor phase. Zimmerman *et al.* prepared gelatin/PbS composites with continuously increased refractive index from 1.5 to 2.5.[659] These materials represented some of the highest refractive index polymers available and were targeted for antireflection coatings for solar cell materials. PbS was also incorporated into poly(ethylene oxide) with particle size ranging from from 4 to 80nm by the same research group.[660] The refractive index of the composite can

[657] Colvin, V. L.; Schlamp, M. C.; Alivisatos, A. P. *Nature* **1994**, *370*, 354.
[658] Dabbousi, B. O.; Bawendi, M. G.; Onitsuka, O.; Rubner, M. F. *Appl. Phys. Lett.* **1995**, *66*, 1316.
[659] Zimmerman, L.; Weibel, M.; Caseri, W.; Suter, U. *J. Mater. Res.* **1993**, *8*, 1742.
[660] Kyprianidou-Leodidou, T.; Caseri, W.; Suter, U. *J. Phys. Chem.* **1994**, *98*, 8992.

be as high as 3.9. The extrapolated RI of particles greater than 25 nm in size was found to agree with the bulk RI of PbS (4.3). It was noted that the refractive index was highly dependent on particle size below 20 nm. These effects may be due to quantum confinement as strong confinement should become evident at particle sizes near and below 20 nm.

## *5.7 Conclusions*

Nanocomposites based on inorganic nanoparticles dispersed into the organic polymer matrix systems have many potential applications, since these new materials can afford new materials with novel properties which otherwise would not be obtained by conventional methods. Theoretically, any polymer can be used as long as the matrix can stabilize the nanoparticles. Processing of polymer-inorganic nanocomposites is quite flexible and the materials can be made into film or fiber or some other forms. Many new materials have been developed and are being developed. Control of the particle size, particle size distribution, and morphology remains crucial to the practical application of these new materials. Also, there is still a huge gap between the laboratory and the industrial applications. From laboratory to the industrial application is a large transition. Control of particle size and size distribution, preparation of stable materials are still tedious. Developing new materials is still under its infancy. More new materials require new methods and new techniques to develop. Utilizing laboratory techniques for the industrial products requires much research including making new devices.

# 6 METAL CHLORIDE/PHOSPHORUS-CONTAINING POLYMERIC COMPLEXES AND NANOCOMPOSITES

## *6.1 Introduction*

Incorporating inorganic salts into a polymer matrix may often have a profound impact on the properties of both the inorganic salts and the polymer matrix. Some inorganic salt additives have been found to change the polymer glass transition temperature, conductivity, and processibility.[661,662,663,664,665] Recent progress has rejuvenated interest in this area, since by controlling the particle size, particle size distribution and varying the types of inorganic salts, many novel fascinating nanocomposites have been prepared with potential in optical, electronic, and fire retardant applications, among others.[666,667]

The extensive hydrogen bonding between phosphonyl and hydroxyl groups has sparked new interest in preparing some new phosphorus-containing polymers, because this hydrogen bonding promotes polymer-polymer miscibility and improves the polymer surface properties.[668,669,670,671,672] Moreover, the phosphonyl oxygen bond can be used to coordinate with selected metal ions. Cabasso *et al.* reported poly(styrenephosphonate diethyl ester) interacted with $UO_2^+$ and transparent films were obtained.[668] Over the past 10 years many phosphorus-containing poly(arylene ether)s,[673] poly(arylene thioether),[674] polyimides,[675] and

---

[661] Wetton, R. E.; James, D. B.; Whiting, W. *J. Polym. Sci*., *Polym. Lett*. Ed. **1976**, *14*, 577.
[662] Agnew, N. H. *J. Polym. Sci*., *Polym. Chem. Ed*. **1976**, *14*, 2819.
[663] (a) Roberts, M. F.; Jenekhe, S. A. *Macromolecules* **1990**, *2*, 224; (b) Roberts, M. F.; Jenekhe, S. A. *Macromolecules* **1991**, *24*, 3142.
[664] Bonaplata, E.; Smith, C. D.; McGrath, J. E. in *High-Temperature Properties and Applications of Polymers,* ACS Series 603: 227, **1995**.
[665] Belfiore, L. A.; Indra, E.; Das, P. *Macromol. Symp*.**1997**, *114*, 35.
[666] See, for example, the special issue "Nanostructured Materials": *Chem. Mater*. **1996**, *8*.
[667] Beecroft, L. L.; Ober, C. K. *Chem. Mater*. **1997**, *9*, 1302.
[668] Sun, J.; Cabasso, I. *J. Polym. Sci., Polym. Chem. Ed*. **1989**, *27*, 3985.
[669] Zhuang, H.; Pearce, E.; Kwei, T. K. *Macromolecules* **1994**, *27*, 6398.
[670] Srinivasan, S.; Kagumba, L.; Riley, D. J.; McGrath, J. E. *Macromol. Symp*. **1997**, **1997**, 122, 95.
[671] Wang, S.; Ji, Q.; Chatchoua, C. N.; Shultz, A. R. *J. Polym. Sci., Polym. Phys. Ed*. **1999**, *37*, 1849.
[672] Wang, S.; Wang, J.; Ji, Q.; Shultz, A. R.; Ward, T. C.; McGrath, J. E. *Submitted to J. Polym. Sci., Polym. Phys. Ed.*
[673] (a) Smith, C.D. *Ph.D. Dissertation* Virginia Polytechnic Institute and State University, **1991**; (b) Smith, C.D.; Grubbs, H.J.; Webster, H. F.; Gungör, A.; Wightman, J.P.; McGrath, J. E. *High Perform. Polym.* **1991**, *4*, 211; (c) Riley, D.J.; Gungör, S. A.; Srinivasan, S.; Sankarapandian, M.; Tchatchoua, C. N.; Muggli, M.W.; Ward, T. C.; McGrath, J. E.; Kashiwagi, T. *Polymer Eng. Sci.* **1997**, 37, 150.
[674] Liu, Y. N.; McGrath, J. E. *Polymer* **2000** (in press); Liu, Y. N. *PHD Thesis*, Virginia Polytechnic Institute and State

cyanate resins[676] have been successfully synthesized. Polymers containing the phosphonyl group have good thermal stability and mechanical properties, and are miscible with bisphenol A poly(hydroxy ether), epoxy, and vinyl ester resins. Recently, optically clear films were obtainind by casting DMAc solutions containing biphenol poly(arylene ether phenyl phosphine oxide) (BP-PEPO) and inorganic salts, such as $CoCl_2$, $CuCl_2$, etc. The optical clarity was ascribed to the interaction between the phosphonyl group and the metal cation. This class of new materials may have potential applications in a number of areas. The present research was initiated to further develop new polymer-inorganic salt nanocomposites and to better understand the phosphonyl-metal ion interactions and their effects in selected applications.

## *6.2 Experimental*

### 6.2.1 Materials

The bisphenol A poly(arylene ether phenyl phosphine oxide/sulfone) homo- and copolymers were prepared by aromatic nucleophilic substitution step polymerization using bisphenol A and dihalides.[673] The copolymer compositions were controlled by varying the ratio of bis-(4-fluorophenyl phenyl phosphine oxide (BFPPO) to 4,4′-dichlorodiphenyl sulfone (DCDPS). The phosphorus-containing polyimide used for this study was prepared from bisphenol A dianhydride (BPADA) and 3,3'-diaminophenyl methyl phosphine oxide (DAMPO) via the ester-acid approach. Udel® resin and Ultem® resin are commercial products manufactured by BP-AMOCO and General Electrical Company, respectively. The structures and characterization of the polymers used for this study are shown in Scheme 6.2.1 and Table 6.2.1, respectively. The inorganic salts $CoCl_2$ and $CuCl_2$, having purities of 97 wt %, were purchased from Aldrich and used as received.

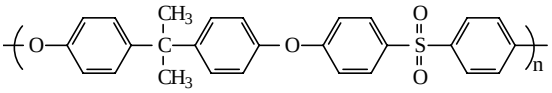

Udel® Resin (Bisphenol A Polysulfone)

University: Blacksburg, Virginia, 1998.

[675] Tan, B.; Tchatchoua, C.N.; Dong, L.; McGrath, J.E. *Polym. Adv. Technol.* **1998**, *9*, 84; (f) Zhuang, H. *Ph.D. Dissertation* Virginia Polytechnic Institute and State University: Blacksburg, Virginia, **1998**.

[676] Abed, J.C.; Mercier, R.; McGrath, J. E. *J. Polym. Sci., Polym. Chem. Ed.* **1997**, *35*, 977.

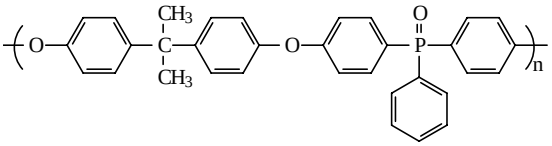

Bisphenol A Poly(arylene ether phenyl phosphine oxide) (BPA-PEPO)

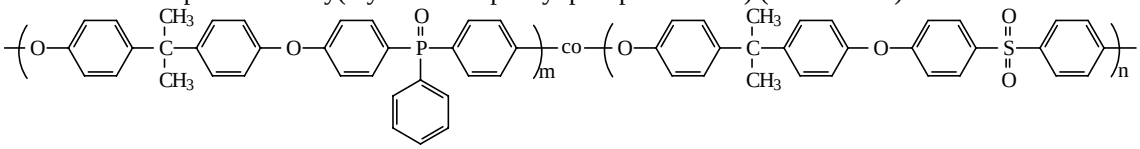

Bisphenol A Poly(arylene ether phenyl phosphine oxide/sulfone) Statistical Copolymers

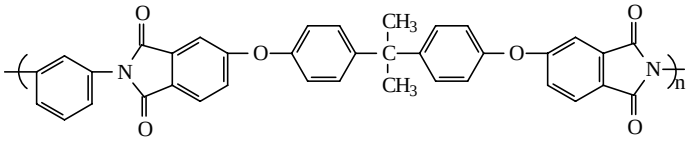

Ultem® polyimide resin (BPADA-*m*-PDA)

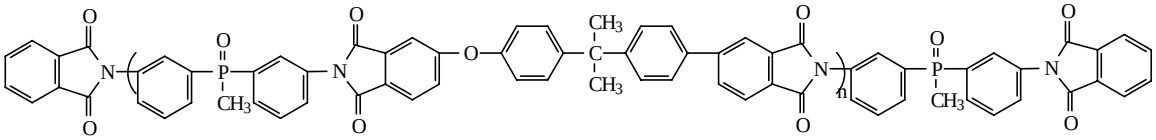

2,2'-bis[4-(3,4-dicarboxyphenoxy)phenyl]propane dianhydride (BPADA) and bis(*m*-aminophenyl) methyl phosphine oxide (DAMPO)) (BPADA-DAMPO)

Scheme 6.2.1 Structures of Udel® resin (bisphenol A polysulfone), bisphenol A poly(arylene ether phenyl phosphine oxide), bisphenol A poly(arylene ether phenyl phosphine oxide/sulfone)s, Ultem® resin (BPADA-*m*-PDA), and a phosphorus-containing polyimide (BPADA-DAMPO).

Table 6.2.1 GPC, Intrinsic Viscosity, and $T_g$ Characterization of Udel® resin, Various Phosphorus-Containing Poly(arylene ether)s, Polyimide, and Ultem® resin

| | GPC | | | [η] (dl/g) | $T_g$ |
|---|---|---|---|---|---|
| Sample | $M_n*10^{-3}$ | $M_w*10^{-3}$ | $M_w/M_n$ | $CHCl_3$, 25 °C | (°C) |
| BPA-PEPO-100 | 24 | 57 | 2.4 | 0.33 | 198 |
| BPA-PEPO-50 | 70 | 159 | 2.3 | 0.73 | 200 |
| BPA-PEPO-40 | 37 | 63 | 1.7 | 0.37 | 197 |
| BPA-PEPO-30 | 25 | 44 | 1.8 | 0.33 | 197 |
| BPA-PEPO-20 | 44 | 85 | 1.9 | 0.62 | 196 |
| BPA-PEPO-10 | 39 | 67 | 1.7 | 0.55 | 192 |
| Udel | 26 | 48 | 1.9 | 0.39 | 186 |
| BPADA-DMPDA | 20 | 33 | 1.7 | 0.28* | 219 |
| Ultem | 20 | 46 | 2.3 | 0.40 | 213 |

* In NMP at 30 °C

** In the designation, BPA-PEPO-X, X-represents the mol% of the phosphonyl groups in replacement of sulfonyl groups in the statistical copolymers.

### 6.2.2 Preparation of Polymeric Complex/Nanocomposite Materials

The polymers and the inorganic salts were dissolved in N,N-dimethylacetamide (DMAc)

at 25 °C in various molar proportions. The weight of salt required was calculated according to the following equation for the homopolymers.[664]

$$W_{SALT} = \frac{W_{POLYMER}}{MW_{UNIT}} \cdot \frac{Mol\%_{SALT}}{100} \cdot FW_{SALT} \qquad \text{Equation 6.2.1}$$

where $W_{POLYMER}$ is the weight of the polymer, $MW_{UNIT}$ is the molar weight of the repeat unit, $Mol\%_{SALT}$ is the metal salt:phosphonyl group mol ratio in percentage, and $FW_{SALT}$ is the gram formula weight of the salt. As an example, for 20 mole% $CoCl_2$ in BPA-PEPO-100, 1.0 g of BPA-PEPO (molecular weight of repeat unit = 502.55 g/mol), 0.0552 g $CoCl_2$ (FW=129.84 g/mol), and 7 ml of DMAc were used.

For a copolymer, a similar method was used to calculate the amount of salt required for a desired composition. The above equation was modified as the following

$$W_{SALT} = \frac{W_{POLYMER}}{\overline{MW}_{UNIT}} \cdot \frac{Mol\%_{SALT}}{100} \cdot \frac{Mol\%_{PEPO}}{100} \cdot FW_{SALT} \qquad \text{Equation 6.2.2}$$

where $\overline{MW}_{UNIT}$ is the number average molar weight of the repeat unit, considering the composition of the copolymers; $Mol\%_{PEPO}$ is the *mol%* of the phosphonyl containing groups in the main chain.

The solution was stirred for several hours or until visually homogeneous, and filtered to remove any dirt particles. The solutions were cast onto a glass plate contained in a closed glass box in a nitrogen atmosphere. The solvent was slowly evaporated at 65 °C using an infrared lamp or hot plate to remove most of the solvent (about 12 h) after which the film was peeled off the glass plate. It was further dried in a vacuum oven at ambient temperature for 4 h followed by slowly increasing the temperature to 120 °C for 4h. The film was heated to just below $T_g$ of the unmodified polymers, and maintained there for several hours in order to ensure the removal of any trapped solvent. TGA and NMR were used to determine the removal of trace amounts of the solvent DMAc.

The films made by solution casting were also melt pressed at about 280 °C. The exact pressing temperature depended on the amount of salt incorporated. The temperature was

maintained for 3 min under pressure, kept for 5 min and then quenched to room temperature in a press under continuous pressure.

### 6.2.3 Characterization

Intrinsic viscosities of the polymers were measured in chloroform or N-methyl pyrrolidone (NMP) at 25 °C unless otherwise noted. GPC measurements were conducted at 60 °C in a Waters 150C instrument to characterize the molecular weights and molecular weight distributions. N-methyl pyrrolidone (NMP) containing 0.02 M phosphorus pentoxide was the solvent. A differential refractometer and a Viscotek differential viscometer, connected in parallel, permitted calculation of absolute molecular weights and molecular weight distributions by applying the universal calibration principle.[677]

FTIR measurements were performed with a Nicolet Impact Mode 400 FTIR spectrometer. Each spectrum was an average of 256 scans at a resolution of 2 $cm^{-1}$.

Glass transition temperatures ($T_g$) of the thermoplastic copolymer/vinyl ester resin cured blends were measured with a Perkin-Elmer DSC-7 differential scanning calorimeter at a heating rate of 10 °C/min. All the results reported were obtained during a second heat after cooling from 300 °C. The midpoint temperature of the specific heat transition during the second heat was taken as the value of $T_g$.

A Perkin-Elmer DMA-7e instrument was employed for dynamic mechanical analysis (DMA) measurements. The samples were analyzed using the extension mode at a frequency of 1 Hz and a heating rate of 2 °C/min.

Thermogravimetric analyses (TGA) utilized a Perkin-Elmer TGA-7 instrument. Samples of 4-6 mg were heated at 10 °C/min from 25 to 800 °C in an air atmosphere.

Transmission electron microscopy (TEM) was conducted to determine the morphologies of the cured polymer modified vinyl ester networks. The samples were imbedded in an epoxy resin in order to facilitate the cutting of a small film section. The imbedded samples were trimmed and ultramicrotomed with a Reichert-Jung Ultracut E apparatus equipped with a

[677] (a) Konas, M.; Moy, T. M.; Rogers, M. E.; Shultz, A. R.; Ward, T. C.; McGrath, J. E. *J. Polym. Sci., Polym. Phys. Ed.* **1995**, *33*, 1429; (b) Konas, M.; Moy, T. M.; Rogers, M. E.; Shultz, A. R.; Ward, T. C.; McGrath, J. E. *J. Polym. Sci., Polym. Phys. Ed.* **1995**, *33*, 1441.

diamond knife. The sample thicknesses were about 700 Å. Electron micrographs were taken with a Philips 400T TEM instrument using an acceleration voltage of 100 kV.

X-ray photoelectron spectroscopy (XPS) analysis was performed using a Perkin-Elmer PHI 5400 x-ray photoelectron spectrometer with an achromatic Mg Kα X-ray source 91253.6 eV). All spectra were collected with the X-ray source operated at 15 kV and 400 W. The spot size used was 1 mm × 1 mm and the take-off angle was 45°. The spectrometer was typically run in the $10^{-8}$ torr pressure range.

For each sample, a wide survey scan (0-1100 eV, 44.75 eV pass energy) was first carried out for element identification. Narrow multiple scans (ranging from 20 to 30 eV) were then taken for all the significant peaks for atomic concentration analysis and peak position examination. Data acquisition and analysis were performed with an Apollo 3500 series computer, using PHI software version 4.0. Binding energies were normalized to that of Au 4f at 83.7 eV.

The melt molded films were used for stress-strain tests. The stress-strain behavior was analyzed at room temperature using an Instron 1123 instrument equipped with a strain gauge extensiometer (Instron 2630-013). The dog-bone shape samples (ASTM D685 type V) were cut from a compression molded plaque having thickness of 0.010-0.020 inches. The samples were tested at an average cross head speed of 0.05 in/min and a distance of 1.00 inch between grips (ASTM D-638). Approximately 8 samples were tested and the results were averaged.

## *6.3 Results and Discussion*

### 6.3.1 Effect of preparation condition on the clarity of the polymer-inorganic films

The films were prepared in a dry nitrogen atmosphere to prevent moisture induced effects. The solvent was evaporated very slowly to avoid bubble formation. The films were dried near the glass transition temperature of the polymer matrix to remove all of the solvent. Even a trace amount of DMAc may affect the formation of the polymer-metal interaction by forming solvent complexes with the phosphonyl group.[678,679] Agglomeration of the metal salt during the drying process can be prevented by making relatively thicker films (> 0.1 mm). In

[678] Drago, R. S.; Calson, R. L.; Purcell, K. F. *Inorg. Chem.* **1965**, *4*, 15.
[679] Waghorne, W. F.; Rubalcava, H. *J. Chem. Soc., Farady Trans. I.* **1982**, *78*, 1199.

general, the films prepared from solution were homogeneous, clear, and tough with colors varying from yellow for the copper salt to deep blue for the cobalt salt.

The solvent cast films with various salt contents up to a 20:100 mol ratio of salt to BPA-PEPO-100 units can be pressed into transparent, tough films. 50:100 and 100:100 mole ratio films can still be pressed at relatively high temperatures, and the pressed films are transparent. However, these high salt content films are quite brittle. Generally, pressing $CoCl_2$/BPA-PEPO-100 composites requires higher temperatures than that required for the BPA-PEPO-100 control. The $CoCl_2$/BPA-PEPO-100 composites with high concentrations of $CoCl_2$ need to be fabricated at high temperatures. To the contrary, fabricating $CuCl_2$/BPA-PEPO-100 composites requires press temperatures lower than that for the pristine polymer.

For comparison, a commercial polysulfone (Udel®) was codissolved with $CoCl_2$ and with $CuCl_2$ in DMAc to give clear solutions. However, these clear solutions did not yield any transparent films upon drying.

### 6.3.2 Stability of Composite Films

Both the solution cast and the melt fabricated films are found to be still soluble in DMAc. Those films containing from 0 to 20 mol % of the metal salts are very stable and can be stored in air or desiccators for a year without visually obvious color change. A 20:100 mol ratio of $CoCl_2$/BPA-PEPO-100 or $CuCl_2$/BPA-PEPO-100 nanocomposite film was soaked in deionized water for a year, no obvious color change was observed. These results suggested a strong specific interaction between the polymer and the salt. The composite films with a 50:100 mol ratio of salt:BPA-PEPO-100 were stable in air, but when they were soaked in water for 2 days, obvious color fading was observed. A composite film with a 100:100 mol ratio of salt:BPA-PEPO-100 was very stable when stored in desiccators. However, when it was exposed in air for a year, some tiny salt crystals were observed on the film surface. When the same film was soaked in water for a day, the color disappeared. Compared to salt-containing BPA-PEPO films, the salt-containing Udel® films bleached immediately when soaked in water. Some tiny crystals were observed when a $CoCl_2$-Udel film was exposed in air for a few months. In summary, low amounts of salt form stable complexes with BPA-PEPO-100 while high salt contents allow only partial interaction with the polymer. With

Udel® resin no stable complexes formed at any investigated mole ratio of salt:polymer unit.

### 6.3.3 Specific Interactions Between Metal Ions and Phosphonyl Groups

The specific interactions between metal ions, such as Co(II) and Cu(II) and the phosphonyl groups of the polymers were investigated by FTIR. Figure 6.3.1 shows the spectra of BPA-PEPO-100 (A), $CoCl_2$/BPA-PEPO-100 with 20:100 mol ratio (B), and $CuCl_2$/BPA-PEPO-100 with 20:100 mol ratio (C), respectively. The absorption band at 2967 $cm^{-1}$ has been assigned to the CH stretching vibration and is assumed not to be greatly affected by the complexation between the metal ions and the phosphonyl groups. To study the effect of the complexation between the metal salt and the phosphonyl groups on the intensity and the wave number of the band associated with the complexation group, the FTIR spectra were normalized to the 2967 $cm^{-1}$ band. The spectra show a significant decrease in the intensity of the band at 1197 $cm^{-1}$ assigned to the phosphonyl stretching vibration. A new absorption band at 1145 $cm^{-1}$ appears. Cotton *et al.* reported that the phosphonyl stretching frequency is decreased upon complexation of tertiary phosphine oxides with metal salts.[680] They attributed the absorption decrease to an approximate 20% decrease in the phosphonyl bond force constant and a 20 to 30% decrease in the phosphonyl bond order. The magnitude of this change in the phosphonyl stretching frequency of triphenylphosphine oxide was used as a measure of the strengths of a variety of Lewis acids by Frazer *et al.*[681] According to their results, the absorption band at 1145 $cm^{-1}$ is tentatively assigned as the stretching vibration of the complexed phosphonyl group. In fact, the decrease in intensity of the phosphonyl absorption band at 1197 $cm^{-1}$ has been observed in complexes of inorganic salts ($CoCl_2$, $CuCl_2$, $FeCl_3$) with biphenol poly(arylene ether phenyl phosphine oxide). A shift in the resonance absorption of $^{31}P$ solution NMR was also observed in salt/small molecule complexes and in the salt/polymer complexes.[664,682] All of these results indcate a complexation interaction between the metal ions and the phosphonyl group.

[680] Cotton, F. A.; Barnes, R. D.; Bannister, E. *J. Chem. Soc.* **1960**, 2199.
[681] Frazer, M. J.; Gerrard, W.; Twaits, R. *J. Inorg. Nucl. Chem.* **1963**, *25*, 637.
[682] Revilla, E. B. *M.S. Thesis*, Virginia Tech: Blacksburg, VA, **1994**.

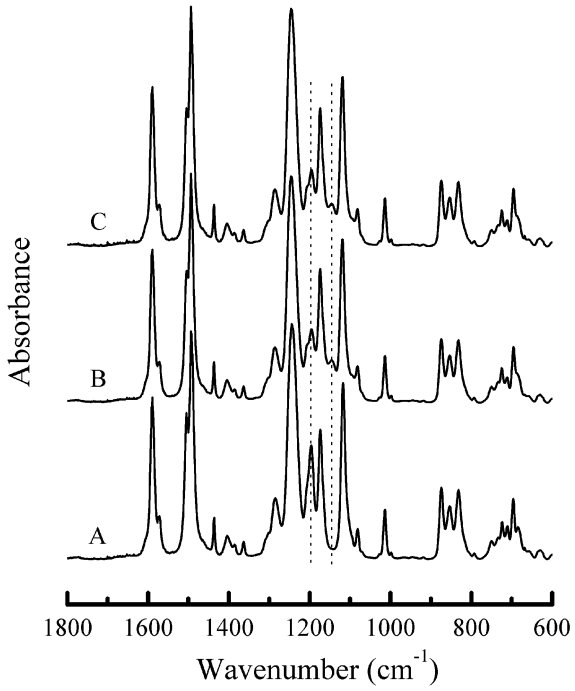


Figure 6.3.1 FTIR spectra of (A) BPA-P100; (B) $CoCl_2$/BPA-PEPO-100; and (C) $CuCl_2$/BPA-PEPO-100 in the phosphonyl stretching vibration region.

### 6.3.4 Morphology

The $CoCl_2$ or $CuCl_2$ salt-BPA-PEPO composite films prepared either by solution casting or melt pressing are transparent, indicating homogeneity or the presence of extremely small particles in the films. In contrast, the inorganic salt/Udel® resin films are opaque, suggesting very weak or no interactions between the inorganic salts and the polymer. Since the particle size may finally determine the mechanical and other properties of the polymer-inorganic materials, it is of interest to further investigate the morphology of these materials. A morphological study of the solution cast films was conducted to explore the bulk structures of the metal chloride/BPA-PEPO composites. It was expected that the polymer and the inorganic salt should have considerably different electron densities and the contrast should be satisfactory for transmission electron microscopy. To investigate the effect of the amount of the inorganic salt on the film morphology, $CoCl_2$/BPA-PEPO-100 composites with different amounts of $CoCl_2$ were investigated by transmission electron microscopy. Figure 6.3.2 shows the change of the morphology with increasing amounts of cobalt salt in the inorganic salt-polymer nanocomposites. No phase separation was observed even at high resolution for a $CoCl_2$:BPA-PEPO at 20:100, indicating homogeneous morphology at this composition. No

higher resolution was attempted due to experimental limitations. Further increasing the mol ratio of $CoCl_2$:BPA-PEPO-100 to 50:100 resulted in a two-phase morphology with inorganic salt crystals with an average particle size of about 300 nm evenly dispersed in the polymer matrix. The $CoCl_2$ concentration has exceeded its saturation limit in the matrix polymer. Triphenylphosphine oxide has been reported to form complexes with a number of metal ions.[683] Triphenylphosphine oxide was reported to form 2:1 complexes with certain salts of Co(II),[684] Ni(II) and Cu(II).[685] Tertiary phosphine oxides may also form $M(L)^{n+}$ complexes with the perchlorates of Co(II), Ni(II),[686] and Cu(II).[687] No attempts were made to determine the coordination number and the structure in these inorganic salt/polymer complex systems in this paper because of its complexity. However, it is reasonable to assume that the complexation ratio of the phosphonyl group of polymer and the metal ion of the inorganic salt is ≥ 2:1. That is to say, the maximum theoretical composite mole ratio of inorganic salt:polymer is 50:100 to form stable complexes without phase separation between polymer and the inorganic salt. In the real system, this ratio may be a little bit lower than 50:100, because steric hindrance may hamper the complexation of some phosphonyl groups with the metal ions. It should be noted that the salt-polymer composite films with transparency and visual homogeneity were obtained even at a ratio as high as 100:100. This is probably due to the interactions between metal ions on the salt particle surface and the phosphonyl groups of the polymer that help stabilize nanosize salt particles. One still needs to understand whether the particles are crystalline or amorphous for the composites with high amounts of salt (>20:100) and whether there are any extremely small particles in the 20:100 or 50:100 composites of $CoCl_2$:BPA-PEPO100 or $CuCl_2$:BPA-PEPO-100. The electron diffraction patterns clearly showed that the particles in the metal salt/polymer composites could be observed and are crystalline with salt ≥ 50 mol % based on the moles of phosphonyl groups. X-ray diffractometry was also employed to measure these samples. However, because of the relatively low salt concentration and the strong scattering background of the polymer, no

[683] Hays, H. R.; Peterson, D. J. in *Organic Phosphorus Compounds*, Vol. 3, Kosolapoff, G. M.; Maier, L. Eds., Wiley-Interscience: New York, **1972**, p341.
[684] Cotton, F. A.; Soderberg, R. H. *J. Am. Chem. Soc*. **1960**, *82*, 5771.
[685] Lindquist, I.; Zackrisson, M. *Acta Chem. Scand*. **1960**, *14*, 453.
[686] Karayannis, N. M.; Mikulski, C. M.; Pytlewski, L. L.; Labes, M. M. *Inorg. Chem*. **1970**, *9*, 582.
[687] Brodie, A. M.; Hunter, G. A.; Rodley, G. A.; Wilkins, C. *J. Inorg. Chim. Acta* **1968**, 195.

conclusive results could be inferred from the X-ray scattering data.

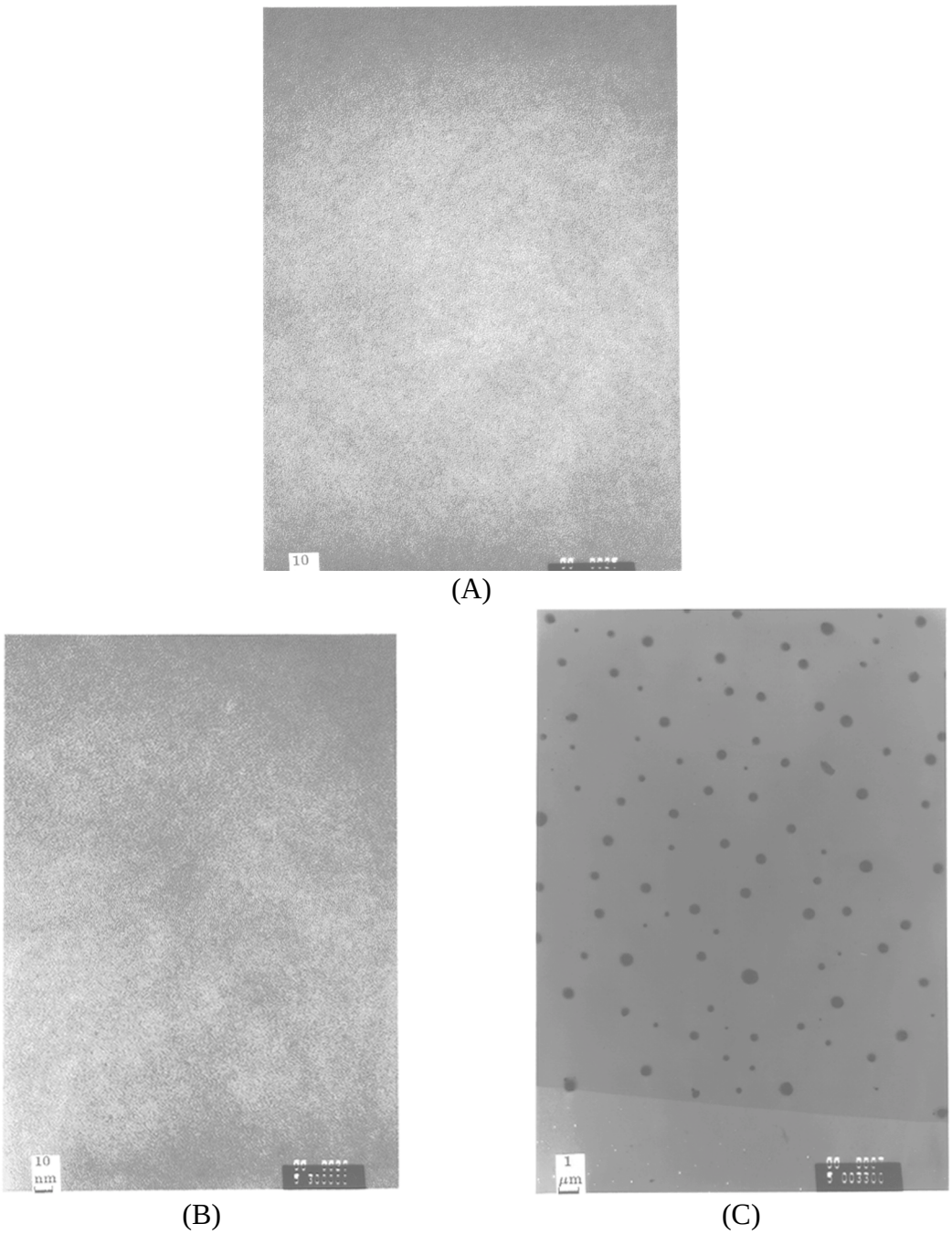


Figure 6.3.2 TEM micrographs of $CoCl_2$/BPA-PEPO-100 composites with salt to polymer repeat unit mol ratios and magnifications of (A) 0:100, 535,000; (B) 20:100, 535,000; (C) 50:100, 5,900.

### 6.3.5 Glass Transition Temperatures of the Polymer-Inorganic Salt Nanocomposites

The incorporation of the inorganic salts into the phosphorus containing polymer system also alters $T_g$. Figure 6.3.3 shows that $T_g$ gradually increases with increasing amounts of

$CoCl_2$. A similar result was also reported in the previous paper.[664] Varying the main chain structure of the copolymer shows a similar behavior. Figure 6.3.3 displays the effect of the CoCl salt concentration on $T_g$ of BPA-PEPO-100. Figure 6.3.4 displays the change in $T_g$ caused by a 20:100 mole ratio of metal ion to phosphonyl group in both $CoCl_2$/BPA-PEPO-X and $CuCl_2$/BPA-PEPO-X composites (X represents the mol % of phosphorus containing monomer used for the synthesis of the copolymers). The significant elevation in $T_g$ in the composites containing $CoCl_2$ is due to the immobilization of the phosphonyl group.[661] Introducing $CoCl_2$ into low molecular weight poly(ethylene oxide) (PEO) was also reported to increase the PEO $T_g$.[661] Belfiore et al also reported a similar phenomenon in a $CoCl_2$/poly(vinyl amine) complex system. As expected, reducing the amounts of phosphonyl groups in the main chain led to less effect of the salts on the $T_g$ of the polymer, because the number of specific interactions decreased. All of these results show that the greater the number of interactions the larger the effect on $T_g$.

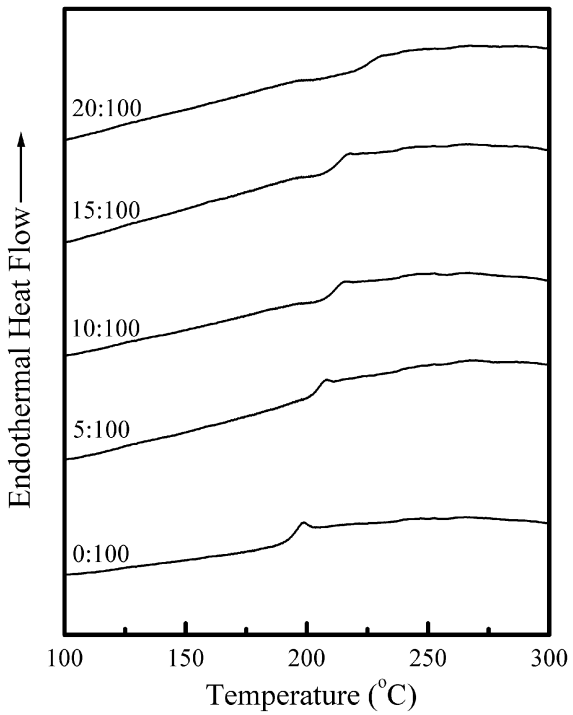


Figure 6.3.3 DSC thermograms of $CoCl_2$/BPA-PEPO-100 composites at various salt to polymer repeat unit mol ratios at a heating rate of 10 °C/min in nitrogen.

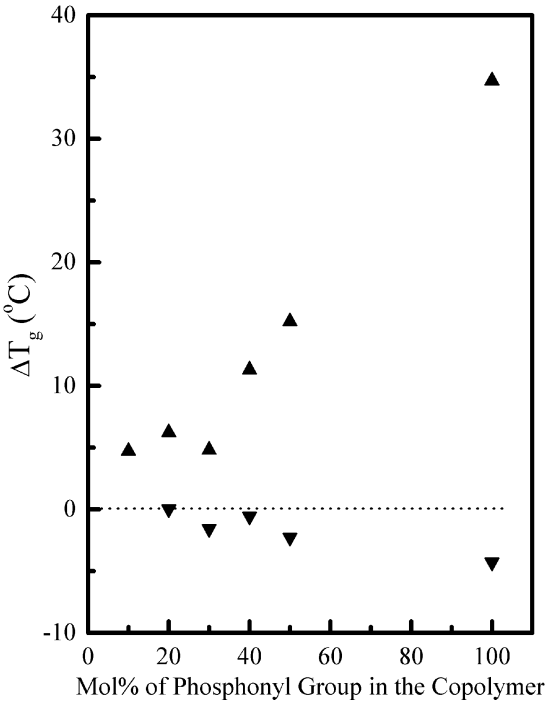


Figure 6.3.4 Effect of the mol% of phosphonyl groups in copolymers on $T_g$ of $CoCl_2$/BPA-PEPO-x (up triangles) and $CuCl_2$/BPA-PEPO-x (down triangles) composites at a mol ratio of 20:100 (metal ion:phosphonyl group). As a reference, there is no $T_g$ change on the broken line.

While $CoCl_2$ increases $T_g$, $CuCl_2$ slightly decreases $T_g$. That introducing an inorganic salt can decrease the $T_g$ of a polymer control was observed in some other systems, especially in Lewis aid-base interaction systems (e.g., $GaCl_3$/nylon 6).[645] As discussed before, the salt-polymer complexes/nanocomposites are thermally reversible, because they can be melt fabricated after formation. An increase in $T_g$ for BPA-PEPO-$CoCl_2$ composites suggests strong interaction between $CoCl_2$ and the polymer chain even at high temperature. The salts act as a kind of crosslinking reagent. Moreover, the crosslinked complexes/nanocomposites of the polymer and the salt are thermally reversible. The different thermal behavior between the $CoCl_2$/BPA-PEPO and $CuCl_2$/BPA-PEPO may be due to the nature of the complexes. A thermally reversible dissociation mechanism was proposed to explain this phenomenon, as is shown in Scheme 6.3.1. Both cobalt and copper ions can interact with phosphonyl groups through intrachain complexation (A) or interchain complexation (B). Although only two phosphonyl groups are illustrated in Scheme 6.3.1 to complex with metal ions, the actual complexation number of phosphonyl groups can be more than two. The incorporation of copper salt increases the polymer-inorganic salt complex rigidity at and slightly above

ambient temperature. However, the copper complexes appear not to be as stable as the cobalt complexes at high temperature. Furthermore, copper ions may complex with fewer phosphonyl groups than do cobalt ions. This also may increase the probability of complexes/nanocomposites of $CuCl_2$-polymer dissociating to a complex with a structure shown in Scheme 6.3.1. The result of the dissociation of copper-polymer complex is that a $CuCl_2$ acts as a pendant group on the polymer chain by interacting with only one phosphonyl group, similar to Lewis acid-base complexes. In addition, $CuCl_2$ is more acidic than $CoCl_2$, thus, it may behave more like a Lewis acid at high temperature. The Lewis acid-base complexes may have lower $T_g$ values than that of the pristine polymer, as was reported in the study of $GaCl_3$-nylon 6 Lewis acid-base complexes.[663]

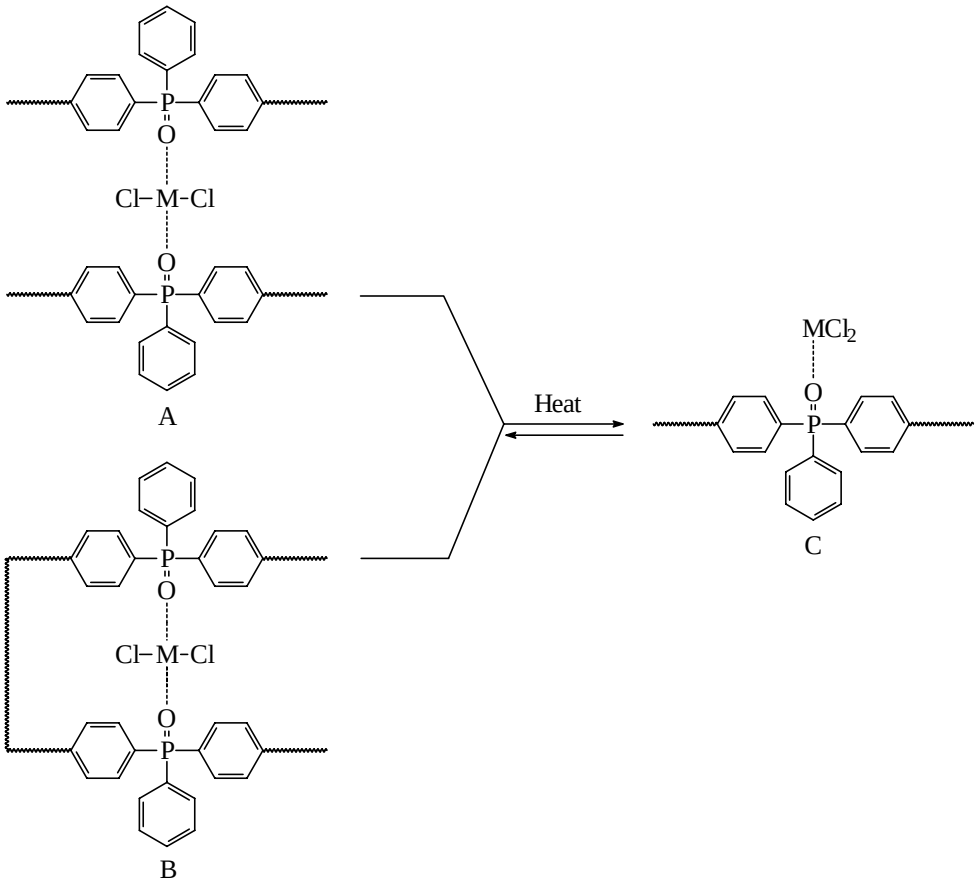


Scheme 6.3.1 Proposed structures of salt-polymer complexes and the thermal dissociation mechanism

The $CoCl_2$/BPA-PEPO-100 composites were also subjected to DMA measurements. Figure 6.3.5 shows the results of the $CoCl_2$/BPA-PEPO-100 composites. The temperatures corresponding to the tan δ peaks increase monotonously with increasing amounts of $CoCl_2$ in

the $CoCl_2$/BPA-PEPO-100 composites. The results are consistent with those of DSC $T_g$ measurements and indicate a strong specific interaction of Co(II) with the phosphonyl group.

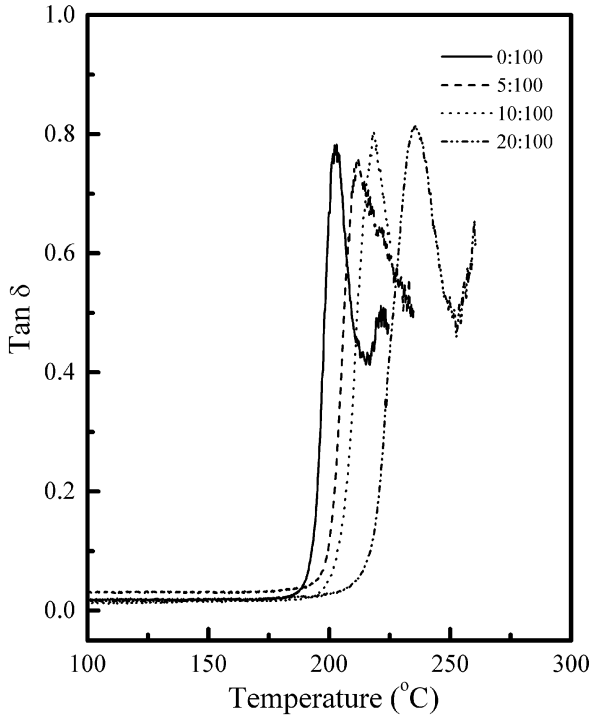


Figure 6.3.5 Mechanical loss tangents of $CoCl_2$/BPA-PEPO-100 composites at various salt to polymer repeat unit mol ratios in an extension mode at a frequency of 1 Hz and a heating rate of 2 °C/min

### 6.3.6 Mechanical Properties of the Composites

The incorporation of $CoCl_2$ and $CuCl_2$ may improve the mechanical properties of phopshonyl containing polymers. Figure 6.3.6 displays stress-strain curves of some $CoCl_2$/BPA-PEPO-100 composites. The stress-strain test results for Young's modulus, tensile strength, and elongation at break are summarized in Table 6.3.1. Compared with the BPA-PEPO-100 control, the incorporation of $CoCl_2$ increases both the Young's modulus and tensile strength. The Young's modulus and tensile strength of $CoCl_2$/BPA-PEPO-100 (20:100) composite are increased by about 30 %, and 20 %, respectively, while the elongation at break was significantly decreased. Incorporating $CuCl_2$ can further increase the Young's modulus and tensile strength. The Young's modulus and tensile strength of $CuCl_2$/BPA-PEPO-100 (20:100) are increased by about 45 %, and 30 %, respectively. In contrast, the incorporation of $CoCl_2$ does not obviously affect the Young's modulus and tensile strength of Udel® resin. These results again suggested the existence of strong interactions between the

metal ions and the phosphonyl groups. The specific interaction makes the polymer chain more rigid. Therefore, the composites exhibit higher Young's moduli and tensile strengths. Also, the rigidity of the composites affords lower elongation at break. The reason why $CuCl_2$ increases the Young's moduli and tensile strengths is still not quite understood. A possible explanation is that $CuCl_2$ yields composites with somewhat more ordered chain structure in the glassy state at room temperature.

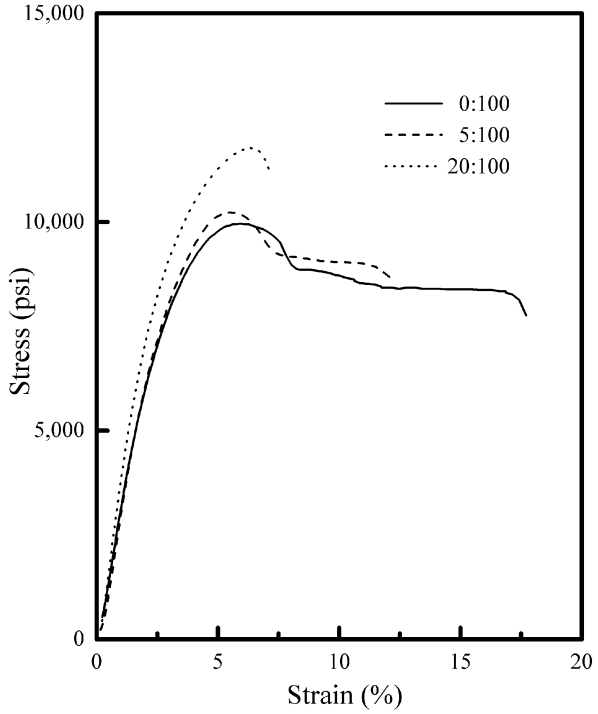


Figure 6.3.6 Stress-strain curves of $CoCl_2$/BPA-PEPO-100 composites at various salt to polymer unit mol ratios at a strain rate of 0.05 in/min and room temperature.

Table 6.3.1 Room Temperature Stress-Strain Behavior of Compression Molded Metal Salt/BPA-PEPO-100 Composites

| Sample | Young's Modulus (ksi) | Tensile Strength (ksi) | Strain at Break (%) |
|---|---|---|---|
| BPA-PEPO-100 | 333 ± 22 | 9.7 ± 0.4 | > 15 |
| $CoCl_2$/BPA-PEPO-100 (5:100) | 399 ± 47 | 9.8 ± 0.7 | 11.2 ± 1.9 |
| $CoCl_2$/BPA-PEPO-100 (10:100) | 410 ± 31 | 10.3 ± 0.4 | 8.4 ± 1.8 |
| $CoCl_2$/BPA-PEPO-100 (15:100) | 418 ± 37 | 11.8 ± 0.4 | 7.8 ± 1.6 |
| $CoCl_2$/BPA-PEPO-100 (20:100) | 434 ± 24 | 11.7 ± 0.3 | 7.5 ± 2.5 |
| $CuCl_2$/BPA-PEPO-100 (20:100) | 476 ± 36 | 12.9 ± 0.3 | 5.0 ± 1.0 |
| Udel | 328 ± 19 | 9.3 ± 0.8 | > 15 |

| | | | |
|---|---|---|---|
| $CoCl_2$/Udel (20:100) | 333 ± 20 | 9.3 ± 0.4 | 9.3 ± 1.6 |

### 6.3.7 Thermal Stability of the Metal Salt-Polymer Complex Nanocomposites

The effect of the metal salts on the thermal stability in air of the phosphonyl containing polymers was investigated using thermogravimetric analysis. Incorporating $CoCl_2$ and $CuCl_2$ salts into bisphenol A polysulfone does not significantly increase the char yield. However, when the inorganic salts were introduced into BPA-PEPO-100, the char yield was significantly increased. Figure 6.3.7 displays the effect of the amount of $CoCl_2$ in the composites on the char yield of BPA-PEPO-100. Incorporating a very small amount of $CoCl_2$ (1.3 Wt%) increased the char yield by about 10 wt % at 800 °C. When the amount of $CoCl_2$ was increased to 2.5 wt%, the char yield increased about 30 wt %, compared with that of the BPA-PEPO control. Further increasing the amount of $CoCl_2$ had no significant effect on the char yield.

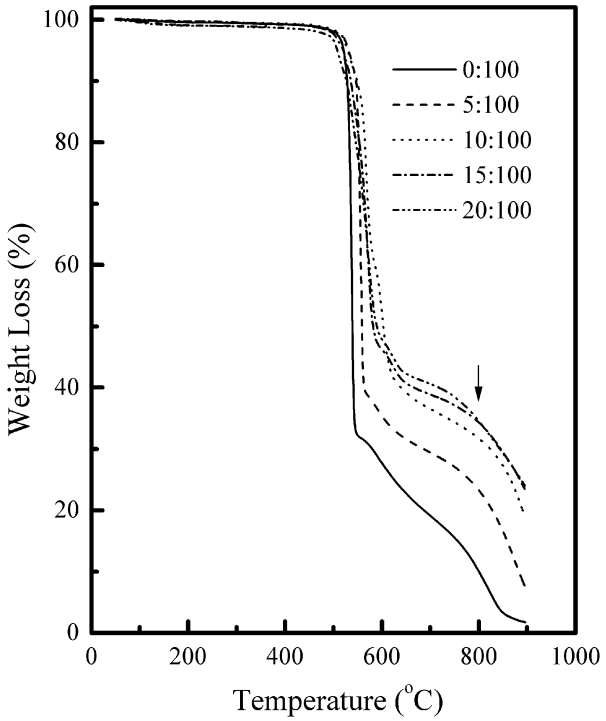


Figure 6.3.7 TGA results of $CoCl_2$/BPA-PEPO-100 composites at various salt to polymer repeat unit mol ratios at a heating rate of 10 °C/min in air

Compared with $CoCl_2$/BPA-PEPO composites, $CuCl_2$/BPA-PEPO composites afford a

lower char yield, although incorporating $CuCl_2$ may also increase the char yield of the BPA-PEPO. Figure 6.3.8 shows the TGA results of $CuCl_2$/BPA-PEPO composites in air. The high char yield of $CoCl_2$-BPA-PEPO-100 suggested that incorporating $CoCl_2$ might improve the fire retardancy of BPA-PEPO-100. The interaction between the polymer and the inorganic salt might change the polymer decomposition and oxidation mechanism. To further understand the mechanism, the char obtained after heating the composite in air to 800 °C was analyzed by X-ray photon-electron spectroscopy. Figure 6.3.9 illustrates the effect of $CoCl_2$ on the XPS spectrum of the char after heating a 20:100 (mole ratio) $CoCl_2$:BPA-PEPO-100 sample. Both cobalt and phosphorus were found in the char. No chlorine was found in the char. Compared with the char of the polymer control, more phosphorus was left in the char. The formation of a cobalt phosphate may be beneficial for the retardancy of further decomposition or oxidation of the polymer. Cobalt may also scavenge free radicals during the decomposition or prevent further burning the polymer by forming cobalt phosphate. In the copper salt composites the copper may not be able to similarly eliminate the free radicals or form a fire retardant phosphate salt. $CoCl_2$/polymer composites may afford higher char yields due to this difference in free radical eliminating ability.

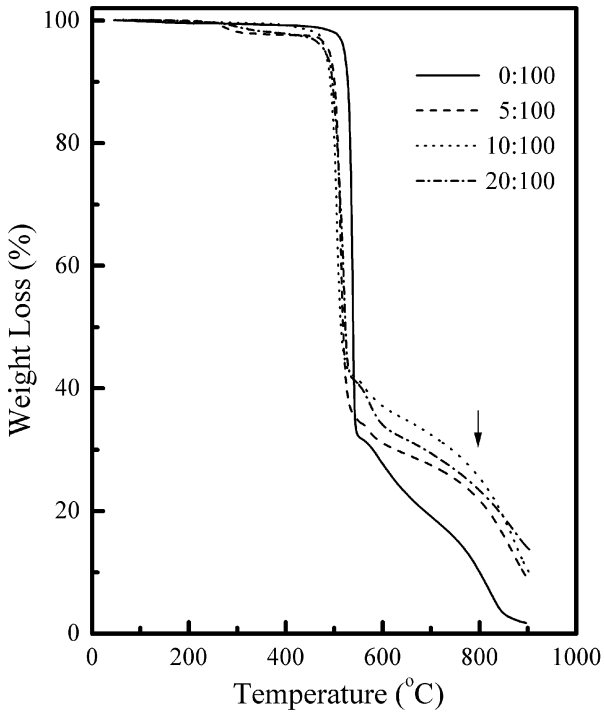

Figure 6.3.8 TGA results of $CuCl_2$/BPA-PEPO-40 composites at mol ratios 20:100 (metal ion:phosphonyl group) at a heating rate of 10 °C/min in air

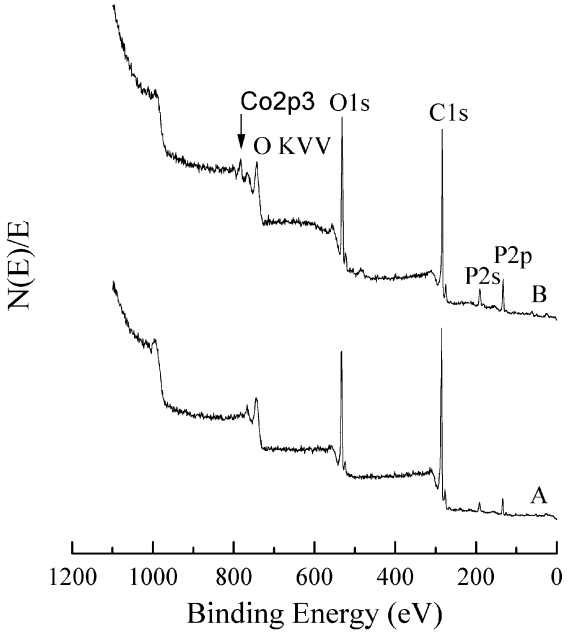


Figure 6.3.9 XPS analysis of char of $CoCl_2$/BPA-PEPO-100 nanocomposites at 0:100 and 20:100 mol ratios of salt to polymer repeat unit

### 6.3.8 Effect of the Main Chain Structure on the Inorganic Salt-Polymer Composite Thermal Properties

To study further the effect of the structure of the phosphorus-containing polymer on the inorganic salt-polymer composites, preliminary investigations were carried out on $CoCl_2$/BPADA-DAMPO composites. For comparison, $CoCl_2$/BPADA-*m*-PDA (Ultem® resin) composites were also prepared under the same conditions. Although both BPADA-DAMPO and Ultem® did yield transparent solutions with $CoCl_2$ in DMAc, only BPADA-DAMPO afforded transparent composite films after drying. These results further suggested the importance of the phosphonyl group for interaction between the inorganic salt and the polymer chains. Incorporating $CoCl_2$ into BPADA-DAMPO also increased the $T_g$ of the composites, as is shown in Figure 6.3.10. This can be explained in the same way as in the $CoCl_2$/BPA-PEPO composite system. It should be noted the effect of the inorganic salt is relatively small in this system. This is probably because BPADA-DAMPO has a relatively larger repeat unit than that of the poly(arylene ether). The number of phosphonyl groups per

unit volume is smaller. Therefore, the lower number of specific interactions in a unit volume results in a less significant increase in $T_g$.

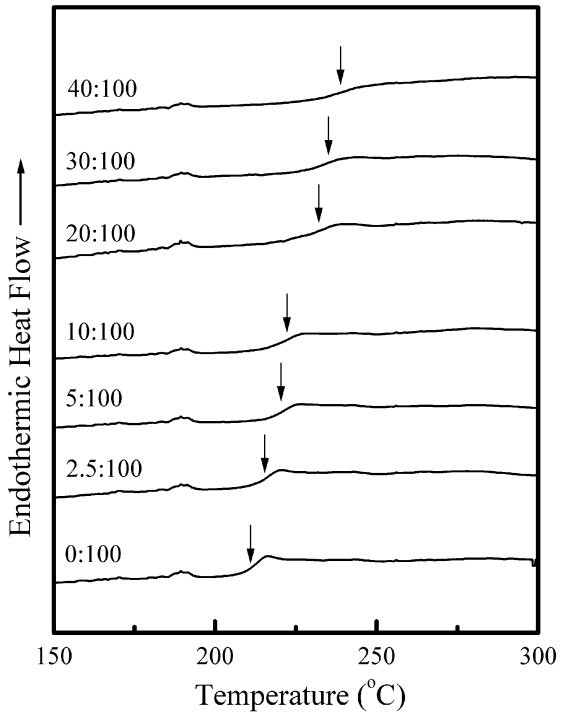


Figure 6.3.10 DSC thermograms of $CoCl_2$/BPADA-DAMPO composites at various salt to polymer repeat unit mol ratios at a heating rate of 10 °C/min in a nitrogen atmosphere

When cobalt salt was introduced into a phosphorus-containing polyimide, it significantly affects the thermal stability. Figure 6.3.11 shows TGA results for composites of $CoCl_2$/BPADA-DAMPO. A small amount of cobalt salt (5 moles $CoCl_2$ per 100 moles of chain units) significantly increased the char yield in air at 800 °C. When the amount of $CoCl_2$ was increased to 10 mol % of the BPADA-DAMPO units, the char yield showed no further increase. Further increasing the amount of cobalt salt had a detrimental effect on the char yield. This is quite different from the effect observed in the BPA-PEPO systems. Apparently, the differences in chemical structure of the polyimide and poly(arylene ether) lead to different decomposition mechanisms. Small amounts of cobalt salt may generate some cobalt atoms that can scavenge the free radicals and concurrently generate some phosphate salt that can cover the char surface to prevent further decomposition of the composite. Large amounts of the metal chloride salts may generate apprecial HCl during the decomposition. This acid could promote the decomposition of the polyimide, but have little effect on the poly(arylene

ether).

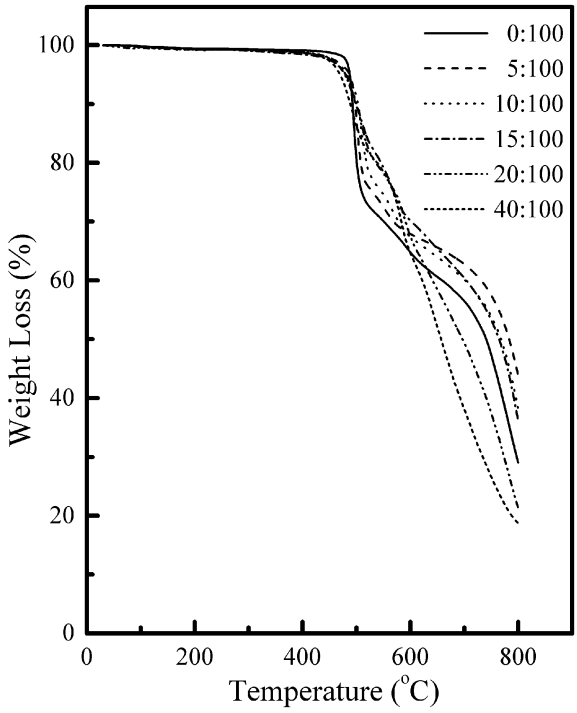


Figure 6.3.11 TGA results of $CoCl_2$/BPADA-DAMPO composites at various salt to polymer repeat unit mol ratios at a heating rate of 10 °C/min in air

## *6.4 Conclusions*

Homogeneous, clear tough metal chloride/BPA-PEPO-X composite films were successfully made by casting bisphenol A based poly(arylene ether phenyl phosphine oxide/sulfone) copolymers and inorganic salts such as $CoCl_2$ and $CuCl_2$ solutions in DMAc. The films prepared with a molar ratio of salt:BPA-PEPO-100 ≤ 20:100 are quite stable in air and in water. The solution cast films can be redissolved in DMAc and melt fabricated. FTIR results revealed a decrease in intensity of the phosphonyl stretching vibration at 1197 $cm^{-1}$ and the appearance of a new absorption band at 1145 $cm^{-1}$. These results suggest a thermally reversible complexation between the metal ions and the phosphonyl groups. TEM results illustrated that the inorganic salts were uniformly dispersed in the system. Moreover, composites with mol ratio of salt:BPA-PEPO-100 units ≤ 20:100 must have particle sizes smaller than 10 nm (if any particles exist). Composites with mole ratios of salt:BPA-PEPO-100 unit ≥ 50:100 had crystalline salt particles of about 300 nm. This inorganic salt saturation most likely occurs because the phosphonyl groups can complex only a small amount of the

metal salts. High amounts of the metal salts result in their separation into nanoscale particles. The incorporation of $CoCl_2$ significantly increases both the $T_g$ and the char yield of poly(arylene ether phenyl phosphine oxide/sulfone) while incorporating $CuCl_2$ slightly decreases the $T_g$ of the same polymer. The inorganic salt/BPA-PEPO mixtures show improved Young's moduli and tensile strengths; however, the percent elongations at break decrease. All of these results can be explained by specific interactions of the metal ions with the phosphonyl groups by various complexation modes.

In addition, $CoCl_2$/BPADA-DAMPO composites are also homogeneous and exhibit increased $T_g$. TGA results, however, show that small amounts of $CoCl_2$ provide beneficial increases in the char yield for polyimide, but larger amounts are detrimental. This may be due to the different thermal decomposition mechanisms for the salt/polyimide system and the salt/poly(arylene ether) system. The commercial bisphenol A based polysulfone Udel® and polyimide Ultem® containing salts do not yield transparent films.

# 7 SYNTHESIS AND CHARACTERIZATION OF NEW SILICA/PHOSPHORUS-CONTAINING POLYMER HYBRID NANOCOMPOSITES

## *7.1 Introduction*

Nanomaterials are materials having components of nanoscale dimensions. Due to the extremely small dimensions (1-100 nm) of the dispersed fillers, nanocomposites may exhibit improved or even novel properties, when compared with their micro- or macrocomposite counterparts. The nanocomposites based on silica/polymer, alumina/polymer, and titania/polymer are of special interest, because these inorganic materials are relatively inexpensive and can significantly improve the polymer properties.[688, 689,690,691,692,693,694,695,696,697,698] In addition, based on these nanoscale composites, some novel porous inorganic materials can be derived by removing the organic polymers.[699,700,701,702,703] Several approaches have been reported to prepare silica/polymer nanocomposites.

One approach is the sol-gel technique in which an alkoxysilane is hydrolyzed in the presence of either nonreactive or reactive polymers.[671,672,673,674,675,676,677] This approach generally involves heterogeneous systems and therefore the control of the composite morphologies is very complicated. In addition, the composites prepared in this manner cannot be fabricated.

Another approach is based on the polymerization of monomers in the presence of surface-

---

[688] See, for example, the special issue "Nanostructured Materials": *Chem. Mater*. **1996**, *8*.
[689] Landry, C. J. T.; Coltrain, B. K.; Brady, B. K. *Polymer* **1992**, *33*, 1486.
[690] Landry, C. J. T.; Coltrain, B. K.; Teegarden, D. M.; Long, T. E.; Long, V. K. *Macromolecules* **1996**, *29*, 4712.
[691] Sun, C.-C.; Mark, J. E. *Polymer* **1989**, *30*, 104.
[692] Rodrigues, D. E.; Brennan, A. B.; Betrabet, C.; Wang, B.; Wilkes, G. L. *Chem. Mater*. **1992**, *4*, 1437.
[693] Noell, J. L.W.; Wilkes, G. L.; Mohanty, D. K.; McGrath, J. E. *J. Appl. Polym. Sci*. **1990**, *40*, 1177.
[694] Chen, Y.; Iroh, J. O. *Chem. Mater*. **1999**, *11*, 1218.
[695] (a) Spinu, M. *Ph.D. Thesis* Virginia Polytechnic Institute and State University: Blacksburg, VA, **1990**; (b) Spinu, M.; McGrath, J. E. *J. Org. Inorganomet. Chem. Polym*. **1992**, *2*, 103.
[696] Yano, K.; Arimitsu, U.; Okada, A.; Kurauchi, T.; Kamigaito, O. *J. Polym. Sci., Polym. Chem. Ed*. **1993**, *31*, 2493.
[697] Tyan, H-L; Liu, Y.-C.; Wei, K.-H. *Chem. Mater*. **1999**, *11*, 1942.
[698] Giannelis, E. P. *Adv. Mater*. **1996**, *8*, 29.
[699] Bagshaw, S. A.; Prouzet, E.; Pinnavaia, T. J. *Science* **1995**, *269*, 1242.
[700] Firouzi, A.; Atef, F.; Oertli, A. G.; Stucky, G. D.; Chmelka, B. F. *J. Am. Chem. Soc*. **1995**, *119*, 3596.
[701] Attard, G. S.; Glyde, J. C.; Goltner, C. G. *Nature* **1995**, *378*, 366.
[702] Melosh, N. A.; Lipic, P.; Bates, F. S.; Wudl, F.; Stucky, G. D.; Fredrickson, G. H.; Chmelka, B. F. *Macromolecules* **1999**, *32*, 4332.
[703] Templin, M.; Franck, A.; Du Chesne, A.; Leist, H.; Zhang, Y.; Ulrich, R.; Schadler, V.; Wiesner, U. *Science* **1997**,

functionalized silica.[678,679] The approach requires rigorous reaction condition to prevent the aggregation of the silica.

On other approach was developed by Giannelis *et al.*[698] In this approach, the silica surface was first modified and a mixture of the modified silica and the polymer were heated above the $T_g$ of the polymer. The process avoids using solvents and is environmentally friendly. However, modifying the silica surface is not a trivial issue. Generally, different surface treatment methods have to be found for different polymers.

In the past decade, many new phosphorus-containing high performance polymers including poly(arylene ether)s,[704] poly(arylene thioether)s,[705] polyimides,[706] and cyanate resins[707] have been synthesized. Many of these phosphorus-containing poly(arylene ether)s, poly(arylene thioether), and polyimides are miscible with bisphenol A poly(hydroxy ether), epoxies, and dimethacrylates.[708,709, 710] The driving force for the miscibility of the two components is hydrogen bonding interaction between hydroxyl groups and phosphonyl groups. This prompted our research on the possibility of making new nanocomposites by using silica and the phosphorus-containing high performance polymers by taking the advantage of hydrogen bonding. The major advantages of high performance polymers over common polymers include high $T_g$ and good mechanical properties of the former. In this paper, a new method for the preparation of polymer-silica composites is reported.

## *7.2 Experimental*

### 7.2.1 Materials

Silica colloid solution supplied by Nissan Chemical Co., is a silica colloid solution in

---

*278*, 5.

[704] (a) Smith, C.D. *Ph.D. Dissertation* Virginia Polytechnic Institute and State University: Blacksburg, VA, **1991**; (b) Smith, C.D.; Grubbs, H.J.; Webster, H. F.; Gungör, A.; Wightman, J. P.; McGrath, J. E. *High Perform. Polym.* **1991**, *4*, 211; (c) Riley, D.J.; Gungör, A.; Srinivasan, S. A; Sankarapandian, M.; Tchatchoua, C. N.; Muggli, M. W.; Ward, T. C.; McGrath, J. E.; Kashiwagi, T. *Polymer Eng. Sci.* **1997**, 37, 150.

[705] (a) Liu, Y. *Ph.D. Dissertation* Virginia Polytechnic Institute and State University: Blacksburg, VA, **1998**; (b) Liu, Y.; McGrath, J. E. *Polymer* **2000** (in press).

[706] (a) Tan, B.; Tchatchoua, C. N.; Dong, L.; McGrath, J. E. *Polym. Adv. Technol.* **1998**, *9*, 84; (b) Zhuang, H. *Ph.D. Dissertation* Virginia Polytechnic Institute and State University: Blacksburg, VA, **1998**.

[707] Abed, J.C.; Mercier, R.; McGrath, J. E. *J. Polym. Sci., Polym. Chem. Ed.* **1997**, *35*, 977.

[708] Srinivasan, S.; Kagumba, L.; McGrath, J. E. *Macromol. Symp.* **1997**, *122*, 95.

[709] Wang, S.; Ji, Q.; Chatchoua, C. N.; Shultz, A. R. *J. Polym. Sci., Polym. Phys. Ed.* **1999**, *37*, 1849.

[710] Wang, S.; Wang, J.; Ji, Q.; Shultz, A. R.; Ward, T. C.; McGrath, J. E. *Submitted to J. Polym. Sci., Polym. Phys. Ed.*

dimethylacetamide (DMAc) with 10-12 nm as the average size of the colloidal particles. Udel® (bisphenol A poly(arylene ether sulfone) is a commercial product produced by BP-AMOCO. Bisphenol A poly(arylene ether phenyl phosphine oxide) (BPA-PEPO) with $M_n$ = 39,000 and $M_w/M_n$ =1.9 was prepared in our laboratory via aromatic nucleophilic substitution polymerization.[704] The structures of the above polymers are:

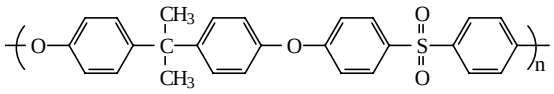

Udel® Bisphenol A Polysulfone

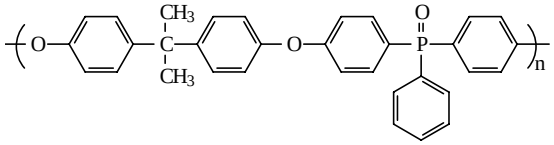

Bisphenol A Poly(arylene ether phenyl phosphine oxide) (BPA-PEPO)

### 7.2.2 Preparation of Silica/BPA-PEPO Nanocomposites

In a beaker was placed 5 g of silica colloid solution and various weights of polymer. DMAc was added to the solution until 100 g of the polymer-silica colloid solution was obtained. The solution was stirring for 24 h at room temperature. The solution was then filtered to remove any dirt particles and cast onto a glass surface in a nitrogen atmosphere. The solvent was slowly evaporated at about 65 °C using an infrared heat lamp or a hot plate to remove most of the solvent (about 12 h) until no obvious solvent was observed. The film was then peeled off the glass surface. It was further dried in a vacuum oven at ambient temperature for 4 h followed by slowly increasing the temperature to 120 °C. Finally, the film was heated to just below the $T_g$ of the unmodified BPA-PEPO polymer, and maintained there for 24 h to ensure the complete removal of any trapped solvent. TGA and NMR were used to verify the complete removal of trace amounts of the solvent DMAc.

Dry silica was prepared by the following procedure. The silica colloid solution was put into a small vial and most of the solvent was slowly evaporated. Then the concentrated fluid was cast onto a glass surface and dried in a nitrogen atmosphere at 65 °C for 24 h. The resulting solid mass was crushed and further dried in a vacuum oven under the same conditions as those used for drying the silica-polymer nanocomposites.

As a control, a composite of silica/Udel® ( 20:80 weight ratio) was also made employing

the same conditions as used for the silica/BPA-PEPO nanocomposites.

### 7.2.3 Characterization

Solid state $^{29}$Si CP-MAS NMR data for both the silica and the polymer-silica nanocomposites were obtained on a Bruker MSL 300 instrument. The $^{29}$Si NMR resonance was measured under a standard $^{29}$Si CP-MAS condition, with 2500 scans per FID using a spinning rate of 4.0 kHz, a relaxation delay of 4 s, and a contact time of 2 ms.

Thermogravimetric analysis (TGA) was conducted on a Perkin-Elmer TGA-7 instrument at a heating rate of 10 °C/min.

Dynamic mechanical analysis (DMA) was conducted at 1 Hz in a Perkin-Elmer DMA-7e instrument with an extension probe at a heating rate of 2 °C/min.

Transmission electron microscopy (TEM) was used to determine the morphologies of the cured polymer modified vinyl ester networks. The samples were imbedded in an epoxy resin in order to facilitate the cutting of small film sections. The imbedded samples were trimmed and ultramicrotomed with a Reichert-Jung Ultracut E equipped with a diamond knife. The sample thickness was about 700 Å. The electron micrographs were taken with a Philips 400T TEM instrument using an acceleration voltage of 100 kV.

X-ray photoelectron spectroscopy (XPS) analysis was performed using a Perkin-Elmer PHI 5400 x-ray photoelectron spectrometer with an achromatic Mg Kα X-ray source (91253.6 eV). All spectra were collected with the X-ray source operated at 15 kV and 400 W. The spot size used was 1 mm × 1 mm and the take-off angle was 45°. The spectrometer was typically run at a $10^{-8}$ torr vacuum range.

For each sample, a wide survey scan (0-1100 eV, 44.75 eV pass energy) was first carried out for element identification. Narrow multiple scans (ranging from 20 to 30 eV) were then taken for all the significant peaks for atomic concentration analysis and peak position examination. Data acquisition and analysis were performed with an Apollo 3500 series computer, using PHI software version 4.0. Binding energies were normalized to that of Au 4f at 83.7 eV.

## 7.3 Results and Discussion

### 7.3.1 Characterization of the Silica

The dry silica was made from silica colloid solution. Figure 7.3.1 shows the CP-MAS $^{29}$Si NMR of silica/BPA-PEPO. $^{29}$Si NMR qualitatively shows this silica contains quadrasiloxane (-112.1 ppm) and Si-OH (-102.1 ppm). The surface OH may be important for forming hydrogen bonding between hydroxyl groups and some proton acceptors. Figure 7.3.2 shows the TGA result for dry silica in air. Only slight weight loss was observed even when burnt at 900 °C in air. The slight weight loss may be due to the evaporation of trace amounts of solvent and water, elimination of surfactants, and the condensation of hydroxyl groups.

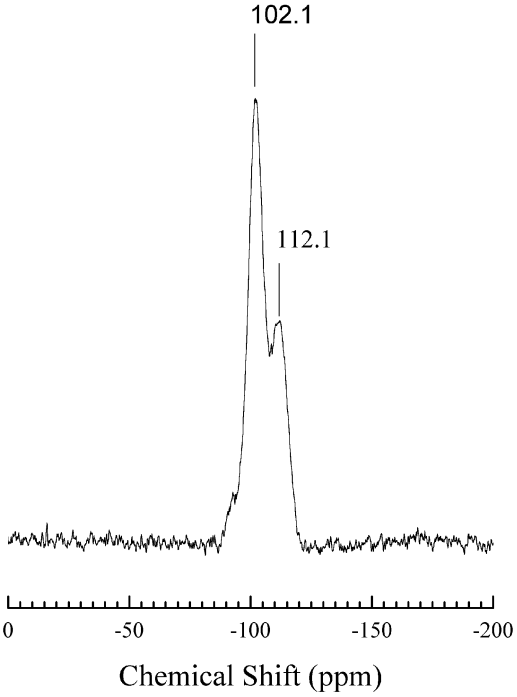


Figure 7.3.1 CP-MAS $^{29}$Si NMR spectrum of a dry silica (from silica colloid solution) recorded at room temperature.

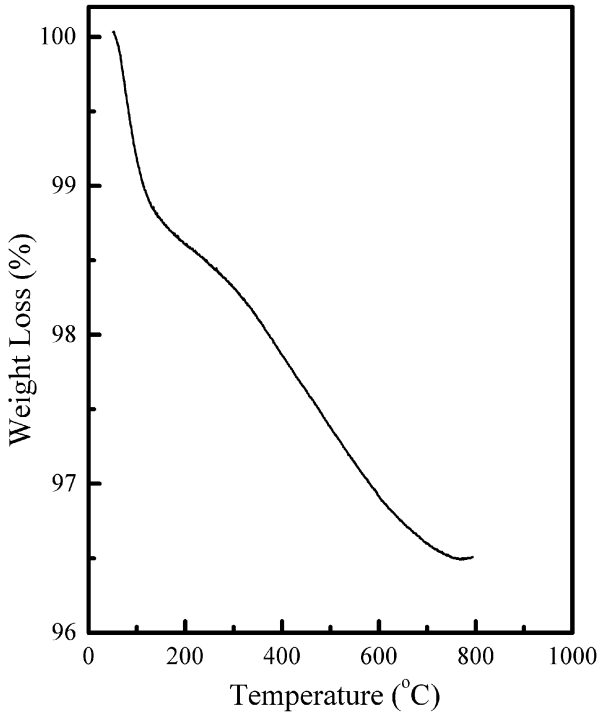


Figure 7.3.2 Thermogravimetric analysis of a dry silica at a heating rate of 10 °C/min in air.

### 7.3.2 Solubility of the Silica-Polymer Nanocomposites

The prepared films can be disintegrated in DMAc but with some small particles remain. The nanocomposite films are also soluble in chloroform with silica colloid up to 20 wt%. However, the film containing 40 wt% of silica colloid was no longer soluble in chloroform. After extraction by chloroform for 2 weeks, a film is left. Two reasons may explain these results: partial condensation of silica colloid particles and strong specific hydrogen bonding interactions between the silanol hydroxyl groups of the silica colloid and the phosphonyl groups of BPA-PEPO. Once the silica colloid particles are chemically bonded, they may not dissolve in solvent anymore. Certainly, small amounts of silica colloids are not enough to form silica networks. This explains why only high amounts of silica colloids generate a silica continuous phase.

### 7.3.3 Morphology

Tough, transparent silica/BPA-PEPO nanocomposite films containing up to 20 wt% of silica have been successfully made. The solution cast films can be subsequently melt fabricated into thin films. However, the nanocomposite with 40 wt% silica is quite brittle and

behaves more like an inorganic material film. No composites with silica concentrations higher that 40 wt% were made. In contrast, to the silica/BPA-PEPO films, the silica/Udel® composite films were opaque.

Figure 7.3.3 shows the TEM micrographs of silica/BPA-PEPO nanocomposites. These nanocomposites have very interesting morphologies. The silica colloid particles are evenly dispersed in the polymer matrix with the silica colloid content up to 20 wt%. Moreover, the silica particles dispersed in the polymer matrix have approximately the same size as in the silica colloid solution (12 nm). This result suggested that the silica colloid particles are not aggregated. Increasing the amount of silica colloid in the silica/BPA-PEPO increased the density of the particles in the polymer matrix, as expected. Further increasing the amounts of silica colloids to 40 wt% led to a bicontinuous morphology.

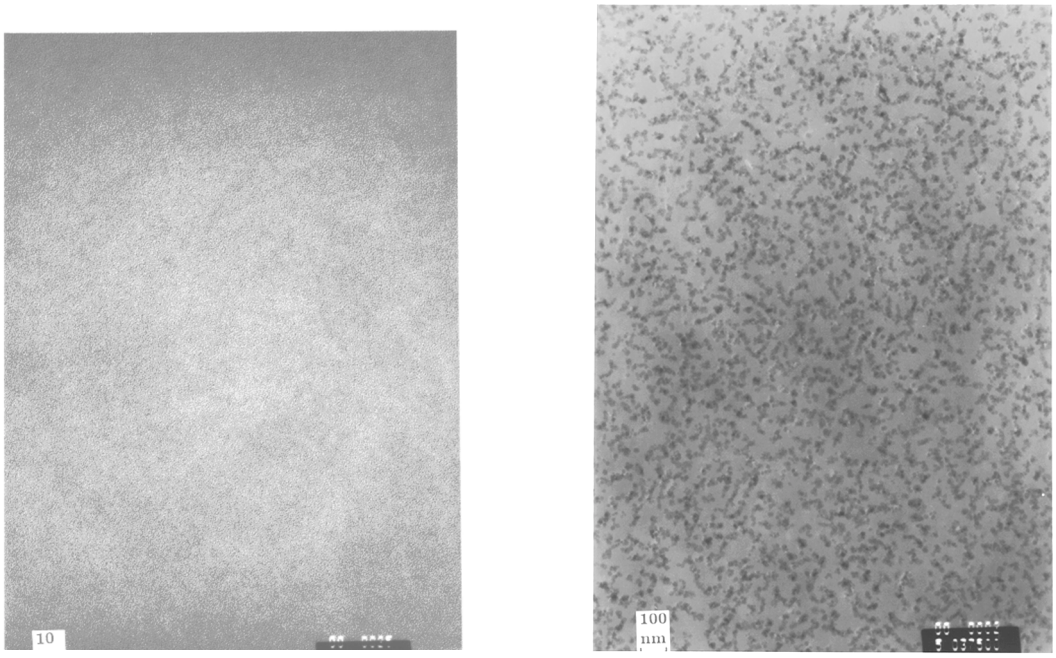


(A) (B)

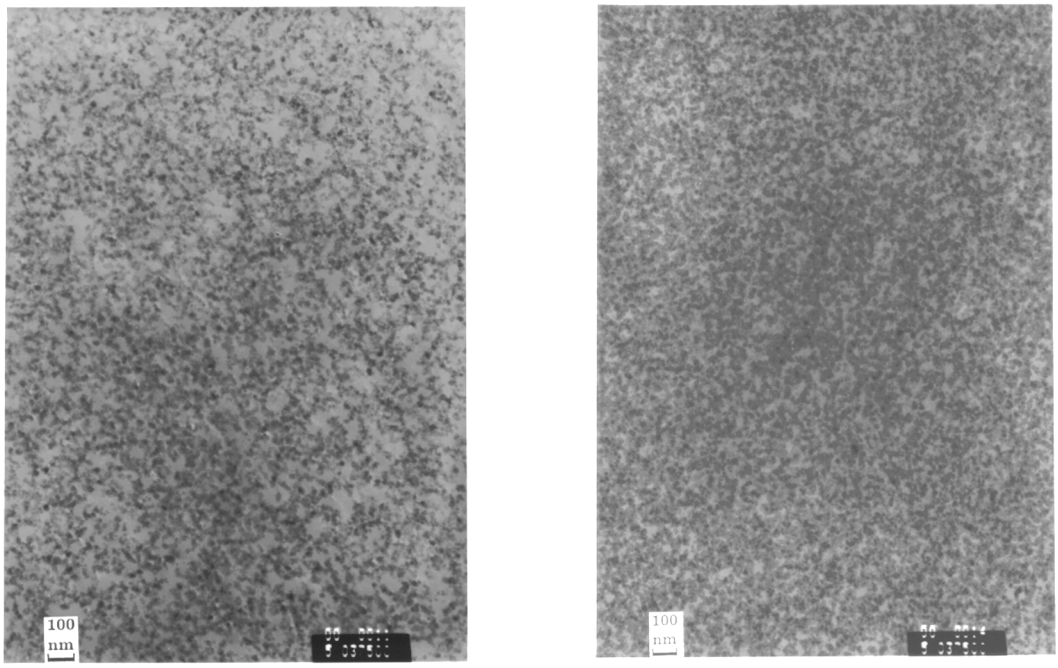


(C) (D)

Figure 7.3.3 TEM micrographs of silica/BPA-PEPO nanocomposites with (A) 10 wt %, (B) 20 wt %, and (C) 40 wt % silica colloids.

In comparison, the silica particles in the silica/Udel® composites tended to aggregate, leading to macrophase separation. Figure 7.3.4 shows the morphology of silica/Udel® composite with 20 wt % silica, indicating silica-enriched and polymer-enriched phases.

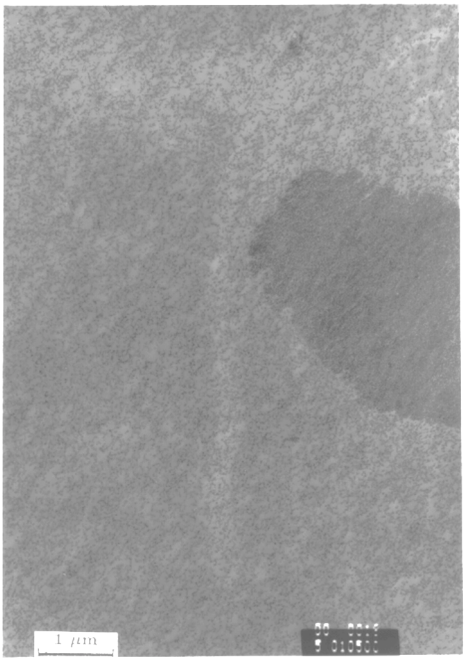


Figure 7.3.4 TEM micrograph of silica/Udel® hybrid composite with 20 wt % silica colloids

The different phase behavior is due to the different interactions between the silica particles and the polymer. The interactions between the two components of the hybrid composites can be Van der Waals forces and hydrogen bonding. Apparently, the interactions due to the Van der Waals forces should be approximately the same for both the silica/BPA-PEPO and the Silica/Udel® composites. The only difference arises from the hydrogen bonding interactions in the former mixtures.

In the silica/BPA-PEPO-100 nanocomposite system, FTIR and solid state NMR of $^{29}Si$ and $^{31}P$ did not give conclusive hydrogen bonding evidence. However, phosphonyl groups have been shown to have strong hydrogen bonding interactions with hydroxyl groups. Indeed, hydrogen bonding interactions have been widely recognized in triphenylphosphine oxide and small molecule complex systems.[711,712,713,714,715] Previous studies showed that phosphorus containing polymers are miscible with poly(hydroxy ether) or vinyl ester resin.[681,682,683] It is reasonable to assume a hydrogen bonding interaction between phosphonyl groups of the

[711] Hadzi, D. *J. Chem. Soc*. **1962**, 5128.
[712] Aksnes, G.; Gramstad, T. *Acta Chem. Scand*. **1960**, *14*, 1485.
[713] Gramstad, T. *Acta Chem. Scand*. **1961**, *15*, 1337.
[714] Maciel, G. E.; James, R. V. *Inorg. Chem*. **1964**, *3*, 1650.
[715] Hays, H. R.; Peterson, D. J. in *Organic Phosphorus Compounds, Vol. 3*. Kosolapoff, G. M.; Maier, L. Wiley-Interscience: New York, **1972**.

polymer and surface hydroxyl groups of the silica. Hydrogen bonding interactions between phosphonyl and hydroxyl groups stabilized the silica particles by retarding or even preventing the aggregation of silica particles in the silica/BPA-PEPO system.

In contrast, the hydrogen bonding interactions in the silica/Udel® composite system should be very weak if they even exist. Previous studies showed that bisphenol A polysulfone is not miscible with bisphenol A poly(hydroxy ether) or vinyl ester resin.[681,682,683] In a miscible polymer blend system poly(ether sulfone) (Victrex®), the hydrogen bonding between poly(ether sulfone) and bisphenol A poly(hydroxy ether) is very weak, as shown by the blue shift of the hydroxyl stretching vibration in infrared spectra.[716] All of these results suggest weak interactions between Udel® and the silica. Since weak or no strong specific interaction between bisphenol A polysulfone and silica is expected, the driving force of aggregation of silica particles results in phase separation. However, during the final drying stage the increased viscosity limited the silica particle aggregation. In this instance, the particle aggregation is kinetically controlled and a rapid drying process could prevent the silica particles from reaching an equilibrium aggregation state. Both factors lead to an incomplete aggregation with some amount of silica particles dispersed in the polymer matrix.

The silica/BPA-PEPO nanocomposite with 40 wt% silica showed a continuous silica morphology. This is probably because at such a high silica concentration the chance of condensation among silanol groups is greatly increased although the partially condensed particles may still have strong interaction with the polymer.

The continuous morphology of silica/BPA-PEPO can be also indirectly proved by the char of the composites. The composite char after heating in air to 900 °C is a translucent solid which maintains its physical integrity. Figure 7.3.5 is a TEM micrograph of this char, showing its porous structure. The result also suggests that this composite can be used to make highly porous glasses.

[716] Wang, S.; Zhuang, H.; Shobha, H. K.; Glass, T. E.; Sankarapandian, M.; Ji, Q.; Tchatchoua, C. N.; Shultz, A. R.; McGrath, J. E. *to be published*.

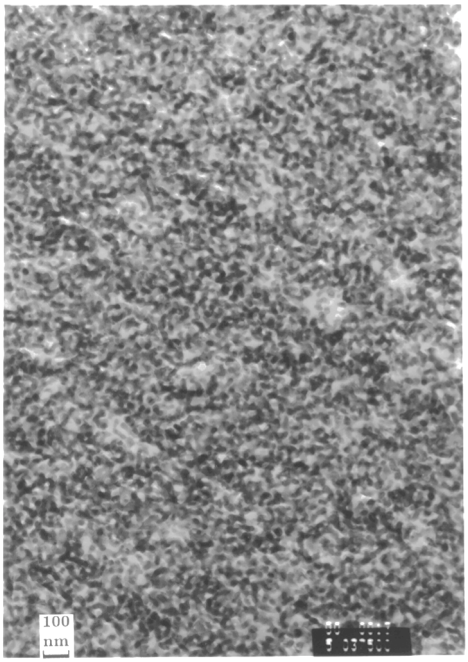


Figure 7.3.5 TEM micrograph of a char of silica/BPA-PEPO nanocomposite with 40 wt% silica colloids after dynamically burnt till 900 °C

### 7.3.4 Glass Transition Behavior

The incorporation of silica into BPA-PEPO did not significantly increase the polymer′s $T_g$. Figure 7.3.6 shows that the tan δ peak temperature values slightly increase and the peak becomes broader with increasing amounts of silica. DSC results did not show any obvious increase in $T_g$. These results suggest some interactions between the silica particles and the BPA-PEPO, but not sufficient to shift the polymer chain mobility in the glass.

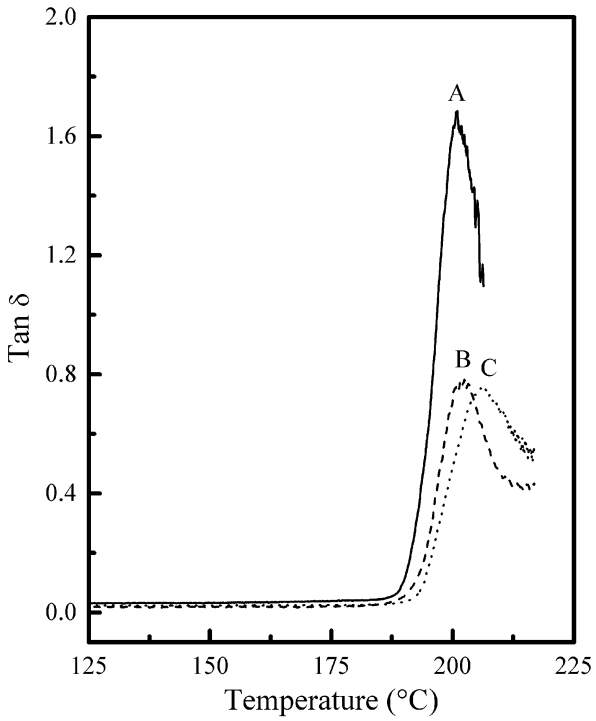


Figure 7.3.6 Mechanical loss tan δ of silica/BPA-PEPO nanocomposites with (A) 0 wt %, (B) 2.5 wt %, (C) 20 wt % of silica.

### 7.3.5 Thermal stability

Figure 7.3.7 shows thermogravimetric analysis results of BPA-PEPO and silica/BPA-PEPO in air. Incorporating silica colloids significantly increased the char yield at 800 °C. Introducing only 2.5 w t % of silica colloids increased the char yield by about 5 wt %. To the contrary, introducing silica colloid into Udel® did not improve the decomposition behavior. Figure 7.3.8 shows the char yield of silica/Udel® with 20 wt % silica heating in air to 800 °C. The result indicates that the amount of char is merely equal to the amount of silica colloid particles in the silica/Udel® particles. These results suggest that the formation of a nanocomposite plays an important role for the fire resistance of silica/polymer composites. High char yield suggests that incorporating the silica particles into the polymer can improve fire resistance. That incorporating nanoparticles increases the char yield and decreases the heat release rate has been reported in other systems.[717]

[717] (a) Gilman, J. W.; Kashiwagi, T.; Giannelis, E. P.; Manias, E.; Lomkin, S.; Lichtenhan, J. D.; Jones, P. *The 6th European Meeting on Fire Retardancy of Polymeric Materials* September 24-26, 1997. Proceedings. Special Publication No. 224; (b) Gilman, J. W.; Kashiwagi, T.; Brown, J. E. T.; Lomakin, S. *The 43th International SAMPE Symposium* **1998**, Vol. 43.

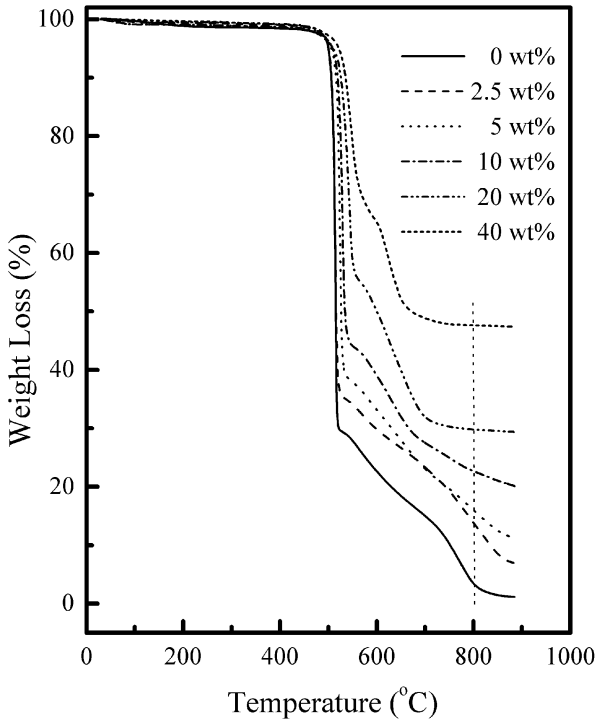


Figure 7.3.7 Thermogravimetric analysis of silica/BPA-PEPO nanocomposites with various wt % of silica at a heating rate of 10 °C/min in air.

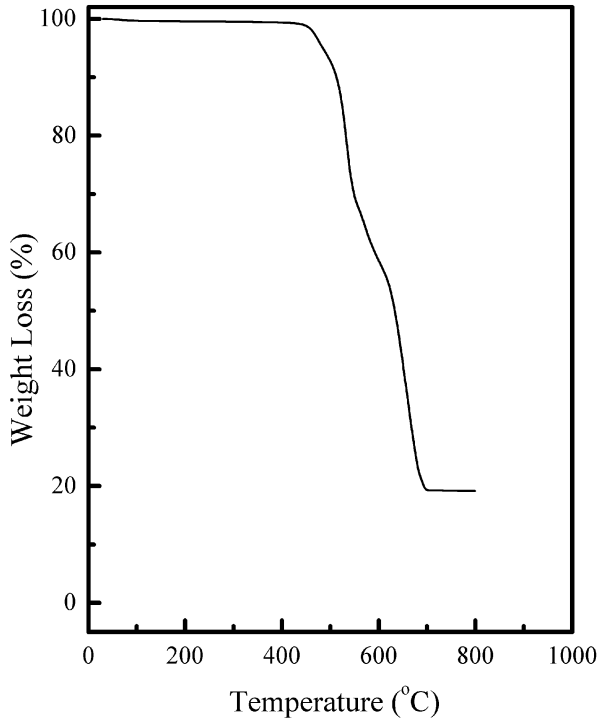


Figure 7.3.8 Thermogravimetric analysis of silica/Udel® hybrid composite with 20 wt % of silica at a heating rate of 10 °C/min in air.

The XPS results of the char of silica, BPA-PEPO, and silica/BPA-PEPO with 20 wt% silica heated in air to 900 °C showed a shift of binding energies of phosphorus, oxygen, and silicon. Table 7.3.1 lists the binding energies of the pristine materials and the chars. The alteration of binding energies of Si, P, and O for the nanocomposite chars may be due to the reaction of phosphorus and silicon and the resulting product may help increase the char yield. The formation of some compounds with Si and P may help prevent further burning of the polymer. Therefore, the char yield is increased.

Table 7.3.1 Binding Energies of related Atoms (XPS) of BPA-PEPO and Silica, and the Silica/BPA-PEPO Composites before and after Burnt till 900 °C.

| Sample | C1s | O1s | Si2p | P2p |
|---|---|---|---|---|
| BPA-PEPO | 285.0 | 532.3 | - | 132.6 |
| Char of BPA-PEPO | 284.9 | 533.3 | - | 134.2 |
| Silica | 285.0 | 532.8 | 103.4 | - |
| Char of Silica | 285.0 | 534.1 | 104.9 | - |
| Char of Silica/BPA-PEPO (20:80) | 285.0 | 533.5 | 104.3 | 135.2 |
| Char of Silica/BPA-PEPO (40:60) | 284.9 | 533.1 | 103.9 | 135.0 |

## *7.4 Conclusions*

A commercial silica colloid can be used to prepare silica/BPA-PEPO nanocomposites. The prepared nanoccomposites are transparent and contain silica colloidal particles evenly dispersed into the polymer matrix without change in particle size. These nanocomposites can be melt fabricated after their formation. The incorporation of silica particles also significantly increases the char yield in air. Moreover, high amounts of silica colloids in a composite may generate bicontinuous phases, suggesting they may be used as porous glasses after burning. In comparison, silica-Udel® hybrid films prepared by the same procedure are opaque due to the silica colloid aggregation. In these films there is no increase in the char yield. TEM showed a macrophase separated structure with both silica-enriched phase and silica depleted phases. The hydrogen bonding interactions between phosphonyl groups and silanol hydroxyl groups are assumed to be responsible for stabilizing silica/BPA-PEPO nanocomposites. By etching the silica or by dissolving or burning the polymer organic or inorganic materials may be

prepared from the silica/BPA-PEPO nanocomposites. Investigation of the properties of these new materials is ongoing.

# 8 Summary

Tough, film forming amorphous poly(arylene ether phenyl phosphine oxide/sulfone) homopolymers and copolymers with or without control of molecular weights have been successfully prepared via aromatic nucleophilic substitution polymerizations. Blends prepared via solution mixing of both these phosphorus-containing polymers with bisphenol A poly(hydroxy ether) (PHE) exhibited specific interaction (hydrogen bonding) between the phosphonyl groups of poly(arylene ether phosphine oxide) and hydroxyl groups of the phenoxy resin. This was confirmed by the observation of the band shift of the hydrogen-bonded hydroxyl group stretching mode from around 3445 $cm^{-1}$ to about 3300 $cm^{-1}$ for all the studied phosphorus-containing polymers and the $^{31}P$ chemical shift of solid state CP-MAS $^{31}P$ Nuclear Magnetic Resonance (NMR) from around 25 ppm to about 30 ppm. In comparison, the band due to the hydrogen-bonded hydroxyl group stretching mode in poly(ether sulfone)/PHE blends shifts to a higher wave number. This is because these miscible polymer blends are induced by different hydrogen-bonding interactions. The miscibility of the blends depends on the mole ratio of phosphine oxide to sulfone in the copolymer. Bisphenol A based copolymers form miscible blends with phenoxy resin even when the phosphine oxide monomer used to prepare copolymer is decreased to 20 mole%. However, further decrease of the amount of phosphine oxide in the copolymer to 10 mole% results in multi-phase blends. These results provided good evidence of the importance of hydrogen bonding on the miscibility of the polymer blends. Various empirical equations have been used to describe the composition dependency of the glass transition temperature ($T_g$). The increase of $T_g$ with increased phosphonyl group concentrations could be attributed to the hydrogen bonding specific interactions between the copolymer phosphonyl groups and the phenoxy resin hydroxyl groups. Replacement of bisphenol A by hydroquinone, biphenol, or hexafluorobisphenol A in the polymers did not significantly affect their miscibility with phenoxy resin, confirming the important role of phosphorus oxygen bond for this specific interaction.

Other phosphorus-containing polymers, such as poly(arylene thioether) (SS-PSPO), and polyimides (BPADA-DAMPO, BPADA-DAPPO) were also shown to be miscible with PHE

on the basis of optical clarity of the blends, and on DSC and DMA data. Both DSC and DMA results show single $T_g$s for the polymer blends. The glass transition temperatures of the polymer blends were intermediate between those of the pure components and varied monotonically with the blend compositions. It is suggested that the intermolecular hydrogen bonding of phosphonyl groups with hydroxyl groups is the driving force for the miscibility. As mentioned earlier, FTIR, solid state $^{31}$P CP-MAS NMR, and several other types of evidence supported the hydrogen bonding hypothesis. Furthermore, the band due to the hydrogen bonded hydroxyl stretching vibration shifted from about 3445 $cm^{-1}$ to about 3300 $cm^{-1}$ was observed in SS-PTPO (without an ether group)/PHE and in BPADA-DAMPO/PHE (no carbonyl stretching vibration band shift was observed). In addition, solid-state $^{31}$P CP-MAS NMR spectra showed a significant down field shift of the phosphorus resonance in phosphorus-containing polymer/PHE blends while no significant phosphorus chemical shift was observed in a miscible blend of BPA-PEPO/ERL 4421®.

In contrast, some polymers such as bisphenol A polysulfone and polyimides of BPADA-*m*PDA are not miscible with PHE, although they have similar structures to the ones used for this study, further suggesting the importance of hydrogen bonding interactions between the phosphonyl groups and the hydroxyl groups.

Evidence for miscibility in BPADA-DAMPO/PHE blends was also obtained from spin-lattice relaxation ($T_{1\rho(H)}$) measurements. From solid state NMR relaxation measurements the homogeneity scale of the different blends was evaluated and the proximity of different chains is approximately within 4 nm. These results further suggested that varying the main chain structural units of the phosphine oxide containing polymer does not significantly affect its miscibility with phenoxy resin.

These studies also suggested that these copolymers may be useful as interphase materials in several composite structures and in polymer blends.

The mixture of non-reactive bisphenol A based poly(arylene ether triphenyl phosphine oxide/diphenyl sulfone) copolymers of approximate number average molecular weight ($M_n$) 20k with a commercial vinyl ester resin exhibited increasing miscibility as the phosphine oxide content was increased. As in the thermoplastic blend systems, strong hydrogen bonding

between the hydroxyl groups of the vinyl ester and the phosphonyl groups of the copolymer was the driving force for the miscibility of the two components. Whereas the polysulfone control was insoluble, the copolymer mixed homogeneously in all proportions, provided the phosphonyl groups exceeded 50 mol%. The homopolymer also formed homogeneous mixtures with a commercial VE resin and the networks appeared to be transparent after curing. This suggests the possible use of the homopolymer or of phosphorus-containing copolymers as interphase materials between a VE resin matrix and glass, carbon, or aramide fibers.

The morphologies of cured poly(arylene ether triphenyl phosphine oxide/diphenyl sulfone) copolymer/VE resin mixtures depended both on the phosphine oxide content of the thermoplastic copolymer and on the weight fraction composition of the mixtures. In general, phase inversion appeared to generate a continuous thermoplastic phase reinforced by discrete microgel of VE resin particles. Although a similar phase inversion occurred during cures in systems having non-reactive thermoplastics mixed with step-growth network forming resins (e.g. epoxies), the phase inversion is greatly encouraged by the rapid, low conversion attainment of gel in the free radical cure system. This further points out the necessity to have reactive groups on the thermoplastic component of the latter systems, to assure that it is forced to form the internal toughening phase.

The fracture toughness of all the cured thermoplastic-modified VE resin materials exceeded that of the cured VE resin control. However, in most instances the materials were composed of the thermoplastic reinforced by high loadings of particulate VE resin. The improved fracture toughness does indicate good adhesion of the thermoplastic to the cured VE resin.

The incorporation of copolymer in the VE resin system did not significantly influence the 5% wt loss temperature. Also the observed $T_g$ of the cured VE resin remained about the same as that of the unmodified cured resin. However, due to the phase-inverted morphologies of most of the networks their solvent ("chemical") resistances were poor. The amorphous continuous thermoplastic phase was extracted from the samples and the materials disintegrated to yield the discrete microgel particles of the cured VE resin.

Bisphenol A poly(arylene ether phenyl phosphine oxide) and inorganic salts such as $CoCl_2$, $CuCl_2$ were successfully dissolved in DMAc and homogeneous solutions were obtained. Homogeneous, clear tough films were successfully made by solution casting these solutions onto glass plates and drying at high temperature. The film prepared with both salts at salt:BPA-PEPO-100 ≤ 20:100 (mole/mole) were quite stable in air or in water. All of the solution cast films could be redissolved in DMAc and melt molded. FTIR data showed a decrease in the intensity of the phosphonyl stretching vibration at 1197 $cm^{-1}$ and the appearance of a new band at 1145 $cm^{-1}$, suggesting a complexation between the metal ions and the phosphonyl groups. TEM results suggested that the inorganic salts were evenly dispersed in the system. Composites with mol ratios of salt:BPA-PEPO-100 ≤ 20:100 should have particle sizes smaller than 10 nm (if any particles exist) whereas composites with mol ratios of salt:BPA-PEPO-100 ≥ 50:100 afford particle sizes of about 300 nm. This is because most of the metal ions can complex with the phosphonyl groups with small amounts of the metal salts. The incorporation of $CoCl_2$ significantly increases both the $T_g$ and the char yield of poly(arylene ether phenyl phosphine oxide/sulfone) while incorporating $CuCl_2$ slightly decreases the $T_g$ of the same polymer. The inorganic salt/BPA-PEPOs show improved Young's modulus and tensile strength, although the percent elongation at break decreases. All of these results were explained according to specific interaction of the metal ions and the phosphonyl groups and to the different complexation modes.

A preliminary study shows $CoCl_2$/BPADA-DAMPO composites are also homogeneous with increased $T_g$, suggesting the specific interaction between Co(II) and phosphonyl group is the driving force for increasing $T_g$ of the composites.

Phosphorus-containing polymers can be also used to prepared silica/polymer nanocomposites. This has been demonstrated by incorporating a commercial silica colloid solution into BPA-PEPO-100. The prepared nanocomposites were transparent with silica colloids evenly dispersed into the polymer matrix. The nanocomposites with ≤ 20 wt% silica could be melt fabricated after their formation. TEM showed that the particle sizes were similar to those in silica colloid solution. The incorporation of silica also significantly increased the char yield in air. In addition, high amounts of silica colloid in the composites seemed to generate bicontinuous phases, suggesting that they may be used as porous glasses

after burning. In contrast, the silica/Udel hybrid films prepared by the same technique were opaque and their char yields did not increase. TEM showed a phase separated structure with both a silica-enriched phase and a silica sparsely dispersed phase. The hydrogen bonding interaction between phosphonyl groups and the silanol hydroxyl groups was assumed to have generated silica/BPA-PEPO-100 nanocomposites. Both inorganic and organic porous materials may be gnerated from silica/BPA-PEPO-100 nanocomposites. These can be achieved by etching the silica or burning the composites.